ADENOVIRUS-BASED EXOGENOUS GENE EXPRESSION IN MAMMALIAN CELLS

BY

MOHAMED A. EL-MOGY, B.Sc., M.Sc.

A Thesis

Submitted to the Department of Biological Sciences

in Partial Fulfillment of the Requirements for the Degree of

Doctor of Philosophy

October, 2009

Brock University

St. Catharines, Ontario, Canada

© Mohamed El-Mogy, 2009.

ABSTRACT

Adenoviruses have been used as a model system for understanding gene expression, DNA replication, gene delivery and other molecular biological phenomenon. In this project, adenovirus was used as a model to study exogenous gene expression in mammalian cells. More specifically, several adenoviral components were identified to enhance gene expression together with components needed for viral DNA replication. The adenoviral elements that enhance gene expression were assembled in an expression vector (pE1). These include the viral inverted terminal repeats (ITRs), the E1 region, the major late promoter (MLP) and the tripartite leader sequence (TPL). The green florescence protein (GFP) was used as a reporter gene. Various aspects of gene expression were examined including DNA delivery and stability inside the cells as well as mRNA transcription and protein expression.

First, the effect of DNA quality on its delivery, stability and expression in mammalian cells was studied. Five different conditions of the major DNA contaminants were used in this investigation including ethidium bromide (EtBr), cesium chloride (CsCl), EtBr/CsCl, endotoxins and ethanol. CsCl, EtBr/CsCl and endotoxins affected the delivery process while EtBr affected the expression process but not the delivery. The used EtOH had no significant effect on both. In addition, the effect of all the contaminants was reversible.

Next, we looked at the factors that enhance mRNA transcription and translation levels. Three approaches were tested, the first was the co-transfection of pE1 and a plasmid that contains adenoviral genes involved in replication (pE2: contains E2 and viral protease). The second was the establishment of a cell line expressing these adenoviral genes involved in replication and the third approach was the super-infection with the wild type adenovirus. The co-transfection did not show any significant increase in gene expression or vector stability. On the other hand, the construction of CHO-E2 cell lines yielded five cell lines but none of them showed expression of all the integrated adenoviral E2 genes or enhancement of stability.

Adenoviral super-infection enhanced gene expression. CHO cells showed higher enhancement in intensity and time than human embryonic kidney (HEK) 293 cells. In addition, such enhancement was dependent on the multiplicity of infection (MOI). Finally, this study emphasizes the importance of DNA quality on gene expression. However, the use of adenoviral elements to enhance exogenous gene expression is

successful only when the complementary viral proteins and sequences are present. Active expression of the adenoviral proteins does not depend on a few major elements, but depends on the combination of different elements that work in cis or trans to activate gene expression.

ACKNOWLEDGMENTS

It is difficult to overstate my gratitude to Dr. Yousef Haj-Ahmad for giving me the opportunity to pursue my doctorate studies under his supervision. His mentoring style gave me a vast degree of freedom in pursuing my research and the chance to investigate independent research ideas. He helped me throughout my thesis period with his enthusiasm, inspiration and encouragement.

I would also like to thank my committee members Dr. Robert Carlone and Dr. Debra Inglis for their invaluable input in my research project and also their careful review of this manuscript. The many suggestions they made helped to steer me in the right direction. I cannot express enough thanks for their contribution to this document.

My deepest gratitude goes to the Egyptian Government for allowing me the opportunity to attain my doctorate studies in Canada and to the Egyptian Cultural and Educational Bureau in Canada for their financial support and help throughout my doctorate studies.

I would like to extend my thanks to the staff of Norgen Biotek for their invaluable help throughout my research project. My warmest gratitude goes to all those persons whose comments, questions, criticism, support and encouragement, both personal and academic, have left a mark on this work. Thank you to: Ismail Aljourmi, Elisa Bibby, Christine Dobbin, Thomas Hunter, Dr. Won-Sik Kim, Dr. Bernard Lam, Nezar Rghei, Pam Roberts, Seema Shamim, Michele Tardif and Amy Whittard.

I am indebted to my many student colleagues for providing a stimulating and fun environment in which to learn and work. I am especially grateful to Moemen Abdalla, Taha Haj-Ahmad, Song Song Geng, Marcus Manocha, Hayam Mansour and Vanja Misic. Special thanks to Kamal Abubaker for his endless support and invaluable help and to Elisa Bibby and Vanja Misic for their valuable time and effort in proofreading and editing my thesis.

I would like to acknowledge my parents and sister for what I have become. I thank them for their love and support as well as their confidence. My parents guided me to put education as a first priority in life, and raised me to set high goals and standards for myself. They taught me to value honesty, courage, and humility above all other virtues. I dedicate this work to them, to honour their love, patience, and support.

TABLE OF CONTENTS

LIST OF TABLES

LIST OF FIGURES

LIST OF ABBREVIATIONS

Ad5	:	Adenovirus serotype 5
ADP	:	adenovirus death protein
ATF	:	Activating transcription factor
BHK	:	Baby hamster kidney
BSA	:	Bovine serum albumin
cDNA	:	Complementary DNA
CHO	:	*Chinese hamster* ovary
CMVie	:	Cytomegalovirus immediate early
COS	:	African green monkey kidney
CPE	:	Cytopathic effect
CsCl	:	Cesium chloride
DBP	:	DNA binding protein
DBS	:	Downstream binding site
DEAE-dextran	:	Diethylaminoethyl dextran
DHFR	:	Dihydrofolate reductase
DMSO	:	Dimethyl sulfoxide
dNTP	:	Deoxynucleotide trphosphate
DOTMA	:	*N*-(2,3-dioleyloxypropyl) *N, N, N*-trimethylamonium chloride
dsDNA	:	Double stranded DNA
DTT	:	Dithiothreitol
EDTA	:	Ethylene diamine tetra-acetic acid
eIF	:	Eukaryotic initiation factor
EtBr	:	Ethidium bromide
EtOH	:	Ethanol
EU	:	endotoxin unit
GFP	:	Green fluorescence protein
HAC	:	Human artificial chromosome
HEK 293	:	Human embryonic kidney 293
hGM-CSF	:	Granulocyte-macrophage colony-stimulating factor
HPV	:	Human papillomavirus
HSV	:	Herpes simplex virus

IRES	:	Internal ribosome entry site
ITR	:	inverted terminal repeat
LB	:	Luria-Bertani broth
MCS	:	Multi-cloning site
miRNA	:	Micro RNA
MLP	:	Major late promoter
MLTF	:	Major late transcription factor
MLTU	:	Major late transcription unit
MOI	:	Multiplicity of infection
NES	:	Nuclear export signal
NLS	:	Nuclear localization signal
NPC	:	Nuclear pore complexe
NS0	:	Mouse myeloma
orf	:	Open reading frame
PABP	:	Poly(A)-binding protein
PBS	:	Phosphate buffered saline
PCR	:	Polymerase chain reaction
pDNA	:	Plasmid DNA
PEI	:	Polyethyleneimine
PFU	:	Plaque forming units
PKR	:	Protein kinase RNA-activated
pTP	:	Precursor terminal protein
qPCR	:	Quantitative PCR
Rb	:	Retinoblastoma
rDNA	:	Recombinant DNA
RFU	:	Relative fluorescence units
RID	:	Receptor internalization and degradation
RNP	:	Ribonucleoprotein
RT	:	Reverse transcription
SDS	:	Sodium dodecyl sulfate
siRNA	:	Small interfering RNA
ssDBP	:	Single stranded DNA binding protein
ssDNA	:	Single stranded DNA
SV40	:	Simian virus 40

TBP	:	TATA-box binding protein
TFBS	:	Transcription factors binding site
Tm	:	Melting temperature
TP	:	Terminal protein
TPL	:	Tripartite leader sequence
USF	:	Upstream stimulatory factor
UV	:	Ultraviolet
VA RNA	:	Virus-associated RNA
X-gal	:	5-bromo-4-chloro-3-indolyl-beta-D-galactopyranoside

INTRODUCTION

Since the introduction of the central dogma of molecular biology by Crick (1958 and 1970), gene expression has gained increasing attention. Scientists have tried to understand the regulatory mechanisms of the different processes involved in gene expression as well as gene function. Modern recombinant DNA technology made it possible to clone, manipulate and deliver DNA constructs into various cells to study the expression of recombinant proteins out of their natural environment. This is called exogenous gene expression. The progress in this field has grown rapidly to match the scientific needs for recombinant proteins as tools not only for molecular biological research but also as tools in diagnostic and therapeutic applications.

It has been nearly forty years since Paul Berg and co-workers (Jackson *et al.*, 1972) reported the engineering of the first recombinant DNA molecule. It took nearly 10 years to produce the first recombinant human insulin (Humulin), the first genetically engineered human recombinant therapeutic protein used to treat diabetes (Goeddel *et al.*, 1979). Since that time, hundreds of genetically engineered human recombinant therapeutic proteins were developed in different gene expression systems. This introduction will discuss recombinant protein expression in mammalian cells with the main focus on the adenovirus serotype 5 (Ad5) genome and regulatory sequences and elements that control gene expression.

1.1- RECOMBINANT PROTEIN EXPRESSION

1.1.1- Ectopic gene expression in prokaryotes and in eukaryotes

Both prokaryotes and eukaryotes are used to express exogenous genes. Prokaryotes and eukaryotes differ in the physical separation of the expression process. In prokaryotes, transcription and translation are simultaneous, while the two processes are separated in the eukaryotes by the nuclear membrane. The prokaryotic expression machinery and its regulators are very simple relative to eukaryotes. They have only one RNA polymerase to transcribe all the RNA species and they lack the post-transcriptional modifications. Also, they do not facilitate many post-translational modifications that are important for imparting biological activity to many complex proteins (Lodish *et al.*, 2007).

Generally, prokaryotes are the preferred host for recombinant protein expression because they produce a high yield of protein in a short period of time and they are easy to manipulate. However, most of the post-translational modifications are not available in bacteria, making them unfavourable for the expression of many pharmaceutical proteins that require accurate protein structure (Verma *et al.*, 1998 and Hunt, 2005).

Eukaryotic organisms range in complexity from simple unicellular organisms, such as yeast, to multicellular complex organisms such as mammals. These organisms differ mainly in their growth rates and the complexity of their growth conditions. Also there is variability in their ability to perform complete and accurate post-translational modifications (Hunt, 2005 and Lodish *et al.*, 2007). Three RNA polymerases are involved in the transcription of their different RNA species. Most transgene constructs use promoters recognized by RNA polymerase II, responsible for mRNA transcription,

although some expression cassettes make use of promoters recognized by RNA polymerase III and these are used mainly for the expression of short mRNA or micro RNA (miRNA) (Lodish *et al.*, 2007).

1.1.2- Eukaryotic expression systems

Various eukaryotes have been used for transgene expression, including yeast, insect and mammalian cells. Generally, exogenous DNA is cloned in plasmids which can be delivered into these cells by different methods. *Pichia pastoris* is the most commonly used yeast strain for exogenous protein expression. Although it is harder to handle relative to bacteria, it is still more favourable than higher eukaryotes due to their expression yield (Boettner *et al.*, 2002). The *Pichia* system was used to express a variety of proteins from many different organisms, including humans. DNA topoisomerase I, Serum albumin and Granulocyte-macrophage colony-stimulating factor (hGM-CSF) are examples of human proteins that were successfully produced using this system (Bushell *et al.*, 2003, Wu *et al.*, 2003 and Yang *et al.*, 2004). However, they still have a major drawback with the glycosylation of their proteins. When used for immunization, glycosylated proteins expressed in *Pichia* can invoke an improper response, making them unsuitable for these applications (Macauley-Patrick *et al.*, 2005).

The most widely used insect cell expression system is the baculovirus-based system. Baculoviruses have a circular double stranded DNA and infects mainly insects, making them safer relative to other mammalian systems that use mammalian or human viral infections (Granados & Federici, 1986; Groner, 1986; Kang, 1988 and Luckow & Summers, 1988; Miller, 1988; Maeda, 1989 and Kost *et al.*, 2005). The virus produces

polyhedra which consist of the polyhedrin protein. The promoter of this protein is usually used to drive high transcription efficiency leading to high expression of the transgene (Miller, 1988 and Maeda, 1989). In addition, insect cells can recognise the secretion signal of mammalian proteins (Oker-Blom *et al.*, 1989).

Although insect cell expression systems have high efficiency of recombinant protein expression, they still have some drawbacks in the quality of the produced proteins. Insect cells, similar to yeast systems, have N-linked glycosylation problems. They can perform the N-linked glycosylation since they have the processing sites. However they cannot complete the process to same diversity of glycosylation as mammalian cells (Hseih & Robbins, 1984).

Mammalian cell lines are the most favourable host in the production of complex recombinant proteins because they can perform all the post-translational modifications and can recognize the correct signals for synthesis, processing and secretion. The major drawback of the mammalian systems remains their low protein yield and their complex handling procedures compared to the other systems (Wurm, 2004 and Hunt, 2005). The maximum protein amount produced in mammalian cells is about 5 g/L, which is almost one third of the production efficiency of bacteria or yeast (Anderson & Krummen, 2002; Gerngross, 2004 and Báez *et al.*, 2005). Mammalian cells can carry on complete proteolytic processing, phosphorylation, both O-linked and N-linked glycosylation and amino acid modifications.

1.1.3- Gene expression in cultured mammalian cells

Expression of transgenes in mammals has gained more attention than all the other expression systems due to the quality of the expressed proteins. Mammalian cells complete all the post-translational modifications and provide the correct folding of any protein molecule as their expression machinery is more advanced than the other eukaryotic expression systems (Makrides, 1999; Kaufman, 2000; Butler, 2005 and Hunt, 2005). The expression of protein with the right post-translational modifications and folding is important for the biological activity and hence the functionality of proteins.

The first step in designing a mammalian transgene expression system is the construction of the expression cassette. This includes choosing the appropriate promoter and poly(A) signal. Other elements might be included to fulfill specific functions that enhance the system stability or efficiency. Different methods are used to deliver the transgene into mammalian cells. These include the use of viral or non-viral vectors and will be discussed later.

Different mammalian cells are used, among them are: baby hamster kidney (BHK) (Wurm & Bernard, 1999), mouse myeloma (NS0) (Dinnis & James, 2005), African green monkey kidney (COS) (Blasey *et al.*, 1996), human embryonic kidney 293 (HEK 293) (Jordan *et al.*, 1998) and *Chinese hamster* ovary (CHO) cells (Preuss *et al.*, 2000). Cells can be grown as a monolayer by the cellular adhesion to the surface of culture plates or in suspension using special culture bottles or containers. Transgenes can be integrated in the genome of the cell to form a stable cell line expressing the recombinant protein. However, the process of mammalian cell line construction is both time consuming and

labour intensive. Another alternative method is to express the recombinant protein from a transient vector to obtain a good yield in a short period of time (Hunt, 2005).

CHO cells were the first mammalian cells used to express recombinant proteins, and they are currently being used to express the majority of therapeutic proteins expressed in mammalian cells (Wurm, 2004). They have been used to express many human recombinant proteins including the 21.5 kDa myelin basic protein and proteolipid protein (Jaśkiewicz *et al.*, 2005), the bone morphogenetic protein 2 (Zhang *et al.*, 2006) and the CD14 monoclonal antibody (Tang *et al.*, 2007).

Transgene expression in mammalian cells is characterized by its low protein yield. To enhance transgene expression levels, scientists make use of viral expression vectors. Among these systems is the poliovirus which uses its new genomic RNA molecules as templates for protein expression (Wimmer *et al.*, 1993 and Xiang *et al.*, 1997). The presence of different non-coding mRNA sequences in the viral mRNA increases its stability and enhances its translation. An example is the internal ribosome entry site (IRES), which was identified from poliovirus (Pelletier & Sonenberg, 1988; Jang *et al.*, 1989 and Molla *et al.*, 1992) and was used to enhance the binding of viral mRNA to the ribosomes. In addition, viruses use other regulatory elements that interfere with the cellular translational machinery to enhance viral translation.

1.2- Controlling Exogenous Gene Expression in Mammalian Cells

The control of gene expression in mammalian cells has been studied on different levels, from gene to protein. This includes transcription, post-transcription, translation

and post-translational levels. Two additional factors are involved only with exogenous genes: the first is the delivery of DNA and the second is the stability of exogenous DNA in the host cell.

1.2.1- Delivery of DNA

The first step in expressing any transgene is the successful transfer of the DNA into the nucleus of the host cell. Different methods are being used to deliver transgenes into mammalian cells. The efficiency of DNA delivery depends on the methods used as well as the type of cells. These methods have been classified according to the nature of the transfer process, either viral (infection) or non-viral (transfection). Non-viral DNA delivery has been further classified, according to the agent or technique used, into physical or chemical (Chou *et al.*, 2004 and Liu *et al.*, 2004).

1.2.1.1- Viral delivery

Viral delivery has the advantage of its high delivery efficiency and the ability to target specific cells or tissues and is being used intensively in gene therapy. Five major viral vectors are being used in the delivery of DNA both *in vitro* and *in vivo*, including adenovirus (Douglas, 2008), adeno-associated virus (Coura Rdos & Nardi, 2008), lentivirus (Philpott & Thrasher, 2008), herpes simplex virus (Burton *et al.*, 2002) and retrovirus (Tai & Kasahara, 2008). The pros and cons of these viral delivery vectors mentioned above are summarized in Table 1.1 and reviewed in Nuno-Gonzalez *et al.*, 2005 and Worgall, 2005.

Table 1.1: Characteristics of the most commonly used gene transfer vectors (modified from Worgall, 2005).

Vector type	Transgene capacity	Advantages	Disadvantages
Adenovirus	7.5 kb[a]	- Easy to produce at high titres - High expression levels - Almost all cell types transducible - Infects replicating and non-replicating cells - Cell targeting possible	- Host immune and inflammatory response - Transient expression - Instable genome
Adeno-associated virus	4.5 kb	- Almost no immunogenicity - Non-pathogenic in humans - Infects replicating and non-replicating cells - Site-specific, stable integration - Long-term expression	- Difficult to produce at high titres - Small transgenes - Late onset of expression
Retrovirus	8 kb	- Non-immunogenic - Stable integration in dividing cells - Cell type retargeting possible	- Insertion mutagenesis - Low titres - Infects only proliferating cells
Lentivirus	8 kb	- Non-immunogenic - Stable integration	- Safety concerns - Possible mutagenesis
Herpes simplex virus	10–40 kb[b]	- Good persistence in selected cell-types - Large expression cassette	- Toxicity and immunogenicity

[a] Capacity for helper-dependent (gutless) vectors containing no viral genes is approximately 36 kb.

[b] Herpes virus vectors 10 kb, herpes virus replicons 40 kb.

1.2.1.2- Non-viral delivery

Although they have lower efficiencies when compared to viral-based delivery, non-viral DNA transfer methods are immunologically safer with faster and easier DNA preparation (Zhang *et al.*, 2004). Non-viral transfer is performed either by using a physical transfer method or by a chemical agent although both have smaller gene size limitations. The physical methods are based on using physical forces to insert DNA into cells or tissues. On the other hand, the mechanism of the chemical delivery is based on

the interaction between the chemical compound and the DNA and their interaction with the cellular membrane. (Chou *et al.*, 2004).

1.2.1.2.1- Physical delivery

Physical methods can be used with a wide range of cells and tissues. One of the commonly used physical methods is electroporation, where an electrical pulse is being used to disturb the balance in the cellular membrane charge. This creates membrane pores through which the DNA can enter the cell. This method is being used with a variety of cells and tissues, both *in vitro* and *in vivo*, and also for single cell and adherent cells transfection (Olofsson *et al.*, 2003 & 2007 and Rabussay, 2008). Transgenes can also be delivered by capillary microinjection, where a single cell can be injected by the transgene (Graessmann & Graessmann, 1983 and Zhang & Yu, 2008).

Another method is the gene gun which bombards microscopic-size tungsten or gold particles carrying the transgene into the cytoplasm (Yang *et al.*, 2001 and Chou *et al.*, 2004). Finally, ultrasound has been used to enhance the chemical transfection by liposomes (Unger *et al.*, 1997 and Koch *et al.*, 2000). Ultrasound can be used on its own to deliver DNA into cells, although the delivery mechanism is still unknown (Frenkel *et al.*, 2002 and Deshpande & Prausnitz, 2007). Despite their efficiency and suitability to a wide range of cells and applications, physical methods are limited by their specific tools and apparatuses (Chou *et al.*, 2004). In addition, the application of physical force can reduce cell survival or damage them. For instance, electroporation at high voltages can increase cell death or induces apoptosis at lower voltages (Matsuki *et al.*, 2008).

1.2.1.2.2- Chemical delivery

Different chemical compounds are used in DNA transfection, including diethylaminoethyl dextran (DEAE-dextran), calcium phosphate and cationic polymers (Liu *et al.*, 2004). DEAE-dextran aggregates with DNA or RNA and forms a positive charged mixture that binds to the plasma membrane and is then internalized by endocytosis. The transfection efficiency is dependent on the cell type and can reach up to 80% (Onishi & Kikuchi, 2003; Liu *et al.*, 2004 and Onishi & Kikucchi, 2004).

Cationic polymers are another family of chemical reagents used in transfection and characterized by their high water solubility. Polyethyleneimine (PEI) is the most commonly used cationic polymer for gene transfer (Boussif *et al.*, 1995 and Abdallah *et al.*, 1996). PEI has two types, linear and branched, the latter is used in transfection and was used to transfect different cells *in vitro* and *in vivo* (Godbey *et al.*, 1999; Lemkine & Demeneix, 2001; Schatzlein, 2001; Aslan *et al.*, 2006 and Ahn *et al.*, 2008). When used in excess amounts, PEI forms a cationic complex with DNA that can bind to the cell surface and is internalized afterwards in an endosome from which it can break away into the cytoplasm (Boussif *et al.*, 1995; Kichler *et al.*, 1995; Behr, 1996 and Labatmoleur *et al.*, 1996). However, the high cytotoxicity of PEI is the major disadvantage that limits its use with several cell lines (Moghimi *et al.*, 2005).

Graham and van der Eb introduced the calcium phosphate transfection early in 1973 and since that time, the method has been used in the transfection of various cells. The transfection method is based on the precipitation of DNA as a calcium phosphate-DNA complex. The precipitate is then adsorbed on the cell surface and subsequently enters the cell by endocytosis (Loyter *et al.*, 1982 and Orrantia & Chang, 1990).

In 2002, Grosjean *et al.*, studied calcium phosphate transfection in CHO cells and found that the process is more efficient during cell division. Calcium phosphate transfection efficiency varies between the different cells and depends on the quality and size of the formed precipitate and can reach 50% of the initial used cell count (Liu *et al.*, 2004).

Cationic lipids are another family of transfection reagents and was introduced by Felgner *et al.* (1987) when they used *N*-(2,3-dioleyloxypropyl) *N, N, N*-trimethylammonium chloride (DOTMA) in a lipofection process to transfect DNA. In 1989, the same reagent was used to transfect RNA into different cells including mouse, rat and human (Malone *et al.*, 1989). Many different cationic lipids are being used today for transfection and all have the same basic structure that consists of a head, a linker and an anchor. The head contains nitrogen atoms to give the head its positive charge and hydrophilic nature, while the anchor is hydrophobic since it consists of one to three hydrocarbon chains. Both the head and the anchor are essential for the mechanism of transfection mediated by cationic lipids (Gao & Huang, 1995; Dalby *et al.*, 2004 and Liu *et al.*, 2004). The major classes of cationic lipids are reviewed by Balaban & Ilies (2001).

Due to their amphiphilic nature, cationic lipids form liposomes in aqueous solutions. DNA interacts with the positively charged head and forms complexes called lipoplexes, which can then interact with the negatively charged cell membrane and deliver the DNA into the cell (Liu *et al.*, 2004). Lipofection is used for DNA, RNA and small interfering RNA (siRNA) delivery both *in vitro* and *in vivo* (Felgner & Ringold, 1998 and Pautz *et al.*, 1993). Although the transfection efficiency depends mainly on the structure of the cationic lipid, there are other factors that affect the efficiency including

the cell type, DNA size and the ratio between the cationic lipid and DNA (Liu *et al.*, 2004 and Recillas-Targa, 2004).

1.2.2- Transgene stability

The physical presence of the transgene and its activity directly affects gene expression efficiency. After the delivery of the transgene into the nucleus of the host cell, two possible pathways can take place. The first is the episomal presence of the exogenous DNA with no integration into the genome of the host cell and is called transient transfection. However in the second pathway, the transgene integrates into the genome to form stable transfected cells.

1.2.2.1- Transient transfection

The transgene is present in an episomal form, with no integration in the genome, and will last for a period of time that depends on its degradation rate and its ability to replicate. Usually, high degradation levels are common in transient transfection and about 50% of plasmid DNA is degraded within one to two days post-transfection (Recillas-Targa, 2004). For this reason, various attempts have been carried out to increase the stability of episomal transgenes inside the cell by using viral replication elements. Among these viral replication origins are: the SV40 (Stillman, 2005), the bovine papillomavirus (BPV) and the human papillomavirus (HPV) (Chow & Broker, 1994).

The introduction of the first human artificial chromosome (HAC) in 1997 was a promising step to enhance the stability of gene expression from episomal DNA (Harrington *et al.*, 1997). HACs can be obtained by two techniques; the first method is

the top-down and is based on the use of a complete chromosome and its size reduction (Farr *et al.*, 1992). The second is the bottom-up method where the chromosome is a combination of different DNA fragments (Basu & Willard, 2005). The utilization of HACs is limited due to their low stability and their high integration probability into the cellular genome (Lipps *et al.*, 2003; Conese *et al.*, 2004 and Basu & Willard, 2005 and Glover *et al.*, 2005).

1.2.2.2- Stable transfection

The integration of the transgene into the host cell genome will generate a stable cell line which can express the integrated transgene. The establishment of stable cell lines is a time consuming and labour intensive process. In addition, different factors affect the expression of the transgene from the new cell lines. The integration site and the integrity of the transgene together with its copy number are the most important factors (Recillas-Targa, 2004).

The integration site of the transgene in a stable cell line has a major effect on its gene expression efficiency (Grosveld *et al.*, 1987; Phi-Van *et al.*, 1990 and Chung *et al.*, 1993). Upon transfection, the transgene integrates either in the euchromatin or the heterochromatin. Since the majority of the genomic DNA is heterochromatin, transgene integration most likely will lead to its silencing and transcription repression. Alternatively, an integration site within the euchromatin will guarantee the active transcription of the transgene (Dillon & Festenstein, 2002 and Dillon, 2004). Various methods have been attempted to protect transgene against the epigenetic effects that can repress transgene expression. The two main strategies used for such protection are

modifications performed on histones or by incorporating protective sequences into the transgene.

Transgene copy number is a very important factor in enhancing its expression. To increase the copy number, a classical method based on the tandem cloning of multiple copies of the transgene in the same vector can be used, however this strategy leads to transgene silencing upon integration (Garrick *et al.*, 1998). Another more sophisticated strategy is based on gene amplification which can be described simply as *in vivo* PCR. The dihydrofolate reductase (DHFR)/methotrexate system is the most well understood and used method for gene amplification and has been used to express different proteins (Monaco *et al.*, 1996; Peroni *et al.*, 2002 and Chung *et al.*, 2003).

1.2.3- Transcription

Choosing an active and appropriate promoter is essential for maximizing gene expression. In addition, the incorporation of enhancers and transcription factors can further improve expression levels.

1.2.3.1- Promoters

Promoters are DNA sequences where the different transcriptional elements, including the enhancers, transcription factors and RNA polymerase interact to initiate the transcription process (Huang *et al.*, 1996; Goodrich *et al.*, 1996 and Novina & Roy, 1996). Promoters recognized by eukaryotic RNA polymerase II are predominantly used in transgene expression since this polymerase is responsible for mRNA transcription. The TATA box, in addition to an upstream element, such as a CAAT box or GC boxes, are the essential components of most eukaryotic promoters although some promoters do

not have a TATA box (Kollmar *et al.*, 1994 and Boam *et al.*, 1995). Transgenes designed for expression in mammalian cells should include a promoter compatible with the eukaryotic transcription machinery (Kaufman, 1990 and Kriegler, 1990). Promoter strength has a direct effect on ultimate protein production (Yew *et al.*, 1997). Both viral and eukaryotic promoters can be used, however viral promoters are characterized by their high efficiency due to the nature of the viral infection. Active and high levels of viral protein production are required for the completion of the viral life cycle. Therefore, the most commonly used promoters in transgene expression are of viral origin and these include the cytomegalovirus immediate early (CMVie) promoter, the Ad5 major late promoter (MLP), the SV40 promoter, Rous Sarcoma virus promoters and the murine 3-phosphoglycerate kinase promoter (Markrides, 1999 and Papadakis *et al.*, 2004).

Some promoters show different efficiencies, either lower or higher activity, in different tissues. For instance, the CMV promoter, which is known for its high efficiency, has lower activity in hepatocytes (Najjar & Lewis, 1999). Other promoters exert their activity in a tissue-specific manner and are particularly important in gene therapy to control the site where the therapeutic protein will be expressed. The major difficulty in achieving high and localized transgene expression is the weakness of tissue-specific promoters. For that reason, efforts are being made to enhance the promoter strength by different methods including the positive feedback loop (Nettelbeck *et al.*, 1998), the two step amplification method (Iyer *et al.*, 2001) and the Cre-loxP method (Kaczmarczyk & Green, 2001 and Nakamura *et al.*, 2008).

1.2.3.2- Enhancers

Enhancers are DNA sequences that increase mRNA transcription regardless of their distance or orientation. Their activity can be limited by insulators which were first defined as enhancer blockers. The first enhancer was found in the SV40 virus while the immunoglobulin heavy-chain locus contained the first identified human enhancer (Banerji *et al.*, 1981; Banerji *et al.*, 1983; Atchison, 1988 and Lee & Young, 2000). Enhancers contain transcription factors binding sites (TFBSs) that allow the interaction with transcription factors to enhance the transcription process. They are similar in their function to the upstream promoter elements that also contain TFBSs and enhance transcription. However, enhancers are more flexible in both distance and orientation (Maston *et al.*, 2006). They can work from a long distance through DNA looping to bring both the promoter and the enhancer close to each other. This action will allow the recruitment of the general transcription factors at the TFBSs and the creation of the transcription pre-initiation complex (Szutorisz *et al.*, 2005 and Vilar & Saiz, 2005).

The incorporation of enhancers in the integrated transgene prevents its silencing, however rapid decrease and loss of expression from integrated transgenes was reported when the enhancers were deleted (Walters *et al.*, 1995 & 1996 and Sutherland *et al.*, 1997). This anti-silencing effect is mediated by the ability of enhancers to guide the transgene to integrate away from heterochromatin. This prevents its silencing and maintains the active transcription state (Francastel *et al.*, 1999).

1.2.3.3- Transcription factors

Transcription factors are proteins that interact with RNA polymerase to initiate or enhance the transcription process. Factors related to the RNA polymerase II can be subdivided into two types; general factors and promoter-specific factors. General factors are essential for transcription initiation; they interact with the TATA box and the RNA polymerase. Promoter-specific factors vary between the different promoters; they interact with specific DNA sequences in the promoter to enhance the transcription process (Weaver & Hedrick, 1992).

Although not essential for transcription initiation, promoter-specific transcription factors play a role in enhancing transgene expression. Similar to enhancers, the incorporation of a transcription factor in the transgene is determined by the degree of enhancement and the spacing considerations. However, transcription factors differ from enhancers in that they are proteins that interact with cis-acting DNA motifs of about 10 bp. The coding genes of these factors can be placed, if their expression is required, either in *cis* or in *trans* from the transgene. Therefore, the presence of these small motifs in the promoter used for transgene expression has an additional enhancing effect. They can normally be present in the promoter or they can be inserted during promoter design and construction (Papadakis *et al.*, 2004). Examples of these transcription factors are the zinc finger proteins, homeodomains and leucine zippers. While the majority of transcription factors perform their function by protein-DNA interaction, some factors, such as the Ad5 E1A protein, do not interact directly with these DNA motifs but instead interact with other proteins that can bind specific DNA (Liu *et al.*, 1994).

When their binding DNA motifs are engineered correctly in a transgene, over-expression of transcription factors can efficiently increase transgene expression. Over-expression of the zinc finger transcription factors MAZ and Sp1 increased expression from the adenovirus MLP in HeLa cells. This expression was increased to about 200-fold in the presence of adenovirus E1A proteins (Parks & Shenk, 1997).

1.2.4- Post-transcription

The control of transgene expression on the post-transcriptional level includes different events. Since the nuclear envelop acts as a physical barrier between the nuclear and cytoplasmic environments, scientists have divided these post-transcriptional control events into post-transcriptional modifications, mRNA transport and mRNA stability.

1.2.4.1- Post-transcriptional modifications

The majority of mRNA transcripts in eukaryotes undergo a capping process to protect the 5' end from cellular exonucleases (Furuichi *et al.*, 1977 and Shatkin, 1985). In addition, this capping enhances the transport of mRNA from the nucleus to the cytoplasm and is essential for the interaction between the mRNA molecule and the ribosomes in the first step of the translation process (Banerjee, 1980; Rhoads, 1988; Hamm & Mattaj, 1990 and Ullu & Tschudi, 1991). These modifications can be done *in vitro* through the incorporation of an mRNA cap using modified cap nucleotides (Stepinski *et al.*, 2001). However, no cap modifications have been applied on transgene mRNA capping since no DNA sequence can alter the process.

Polyadenylation is the addition of a non-coding poly(A) tail to the 3' end of the mRNA molecule, a process that takes place mostly in the nucleus (Birnstiel *et al.*, 1985

and Carter *et al.*, 1993). The length of the tail varies between different organisms, ranging from 70-90 nucleotides in yeast and 200-250 nucleotides in mammalian cells (Jacobson, 1996). The polyadenylation process includes two steps, first a clipping enzyme cleaves the newly synthesized premature mRNA molecule at a specific site, and then the poly(A) polymerase starts to add the tail (Wahle & Ruegsegger, 1999; Zhao *et al.*, 1999; Edmonds, 2002; Hall, 2002; Wu & Alwine, 2004 and Clark, 2005). This tail protects the 3' end from degradation by an exonuclease and is also involved in the regulation of the translation (Brawermann, 1981; Bernstein & Ross, 1989 and Gallie *et al.*, 1991). Both the poly(A) tail and the cap are needed for mRNA transport and they efficiently enhance gene expression (Bechler, 1997). In addition, longer poly(A) tails are translated more efficiently than shorter tails and yield more protein (Mockey *et al.*, 2006).

Therefore, the incorporation of a suitable polyadenylation signal downstream of the gene in transgene design is very important for accurate mRNA production and processing. In fact, the signal specifies the cleavage site for the clipping enzyme. This signal should be recognizable by the transcription machinery of the used cell or organism. In mammalians, the polyadenylation signal has three elements in its core sequence, starting with a highly conserved AAUAAA sequence, then the cleavage site (downstream by 10-30 nucleotides) and ending with a conserved region rich in GU or U nucleotides (Chou *et al.*, 1994; Chen *et al.*, 1995; Graber *et al.*, 1999 and Hans & Alwine, 2000).

1.2.4.2- mRNA transport

After the post transcriptional modifications, mRNA is transported to the cytoplasm where the translation can start. While still in the nucleus, mRNA interacts with proteins to form mRNA-protein complexes called ribonucleoproteins (RNPs). These complexes are then exported through the nuclear pore complexes (NPCs) in a process that requires energy and is regulated by transport factors-mediated recognition (Mattaj & Englmeier, 1998; Görlich & Kutay, 1999; Conti & Izaurralde, 2001; Reed & Magni, 2001 and Reed & Hurt, 2002).

The mRNA transcribed from transgenes is being transported under the same conditions and mechanism as cellular mRNAs. No reported sequences or genes encoding nuclear localization signals (NLSs) and/or nuclear export signals (NESs) were incorporated into transgenes to facilitate the transport process. On the other hand, a few viruses have a more complicated system since some of their proteins can act as NLSs and/or NESs. These proteins interact specifically with viral mRNAs and guide them through the transport process. One example is the active transport of the adenovirus late mRNA mediated by the interaction between the E1B 55k protein and the E4 orf6 proteins with viral mRNA (Horridge & Leppard, 1998).

1.2.4.3- mRNA stability

The net balance between rates of mRNA synthesis and degradation determines mRNA accumulation. One side of the balanced equation is more controllable on the transgene design level and contains all the aforementioned factors that affect the transcription efficiency. The other side of the equation contains the factors that affect

mRNA stability and unfortunately are less controllable. In general, mRNA stability is determined by the different elements that confer resistance to degradation and it plays an important role in gene expression regulation (Coller & Parker, 2004).

The degradation of mRNA starts with poly(A) deadenylation which indicates the importance of the tail in protecting the molecule (Fort *et al.*, 1987; Peppel & Baglioni, 1991; Shyu *et al.*, 1991; Bernstein *et al.*, 1992; Lieberman *et al.*, 1992 and Parker & Song, 2004). The length of the poly(A) tail is another stability determinant. Since poly(A)-binding protein (PABP) has a high affinity in binding poly(A), longer poly(A) tails allow the binding of more PABP which protects the tail from the degradation by exonucleases or by other complex interactions (Bernstein *et al.*, 1992; Görlach *et al.*, 1994 and Rowlett *et al.*, 2008). The presence of a stable poly(A) tail will not only increase the accumulation of mRNA in the cytoplasm, but will also enhance mRNA translation (Bernstein & Ross, 1989; Sachs, 1990; Patel & Butler, 1992; Peltz & Jacobson, 1992 and Sachs, 1993).

The presence of the 3' untranslated region is another element to determine mRNA stability since this region commonly contains signals for mRNA decay (Chen *et al.*, 2001; Wang & Kiledjian, 2001 and Mukherjee *et al.*, 2002). Examples of these regions are the Histone mRNA 3'-terminal stem-loop (Marzluff & Pandey, 1988 and Schumperli, 1988) and the AU-rich elements (Caput, *et al.*, 1986 and Shaw & Kamen, 1986). Some proteins bind to the 3' untranslated region to cover and shield their mRNA decay signals (Caput, *et al.*, 1986; Shaw & Kamen, 1986 and Ross, 1995). The endonuclease site within the 3' C-rich sequence of the globin mRNA is used for regulating mRNA decay and therefore globin gene expression. The poly(C)-binding protein can shield this

endonuclease site and is believed to be regulated by a cellular signalling pathway that controls the binding affinity of the poly(C)-binding protein to the C-rich sequence (Wang *et al.*, 1995; Weiss & Liebhaber, 1995 and Waggoner & Liebhaber, 2003).

As previously mentioned, the 5' cap protects the mRNA and is important for its translation initiation. Decapping of the mRNA might add another regulatory pathway since cap-containing mRNAs are at least four times more stable than cap-lacking mRNAs (Furuichi *et al.*, 1977; Shimotohno *et al.*, 1977; McCrae & Woodland, 1981 and Peltz *et al.*, 1987). In addition, some 5' untranslated regions can enhance mRNA stability several fold and control its localization and translation efficiencies (Pesole *et al.*, 2001). For instance, the tripartite leader sequence (TPL) in adenovirus mRNA increases its stability by five folds (Moore & Shenk, 1988).

1.2.5- Translation

The final destination of the mRNA molecule is to bind to the ribosomes and then initiation of the translation. The process is regulated by different mechanisms during the initiation and the elongation steps (Jefferson & Kimball, 2003). The initiation step starts with the formation of the pre-initiation complex by the assembly of three main components; the mRNA, 40S ribosomal subunit and the methionine-tRNA. The formation of this complex is mediated by different factors called the eukaryotic initiation factors (e.g. eIF4F). The different factors interact with the three main components and bring them into close proximity to form the initiation complex (Klann & Dever, 2004).

The control of the translation initiation step is mediated mainly by the phosphorylation performed on some of the eukaryotic initiation factors or their binding

proteins. Translation is suppressed by the phosphorylation of eIF2, which can be controlled by different stimuli of cellular kinases. This includes the stimulation of the double-stranded protein kinase RNA-activated (PKR) by viral double-stranded RNA (dsRNA) (Kaufman, 1999 and Hinnebusch, 2000), dimerization disruption (Lee *et al.*, 1994 and Gale *et al.*, 1997, 1998 and 1999) and blocking the interaction between PKR and its substrate (Beattie *et al.*, 1991; McMillan *et al.*, 1995; Brand *et al.*, 1997 and Kawagishi-Kobayashi *et al.*, 1997). Similarly, phosphorylation of eIF4E binding protein-1 will prevent binding the eIF4E which then allows its function in the initiation step to occur (Ptushkina *et al.*, 1999). On the contrary, phosphorylation of eIF4G enhances its binding potential to the initiation complex (Bolster *et al.*, 2004).

Transgene translation usually undergoes the same cellular regulatory mechanisms that are based on the cap binding and the formation of the pre-initiation complex. However, some mRNA sequences can enhance the translation process and they can be incorporated or optimized during the transgene design and construction. This includes the kozak sequence, the stop codon, the codon usage and the IRESs.

1.2.5.1- Kozak sequence

The sequence that flanks the AUG initiation codon is defined as a consensus sequence of CC(A/G)CCAUGG and was named as the Kozak sequence. In addition to the AUG, A/G at the -3 position and the G at the +4 are the most important two nucleotides in the sequence. The presence of this sequence enhances the recognition of the translation initiation codon by eukaryotic ribosomes (Kozak, 1987 and 1997). The

incorporation of the Kozak sequence upstream of the gene was found to increase gene expression.

In vitro expression of the human serum albumin gene in different horse cells was enhanced by the kozak sequence (Olafsdottir *et al.*, 2008). Du *et al.* (2008) investigated the effect of A or G nucleotide at the +4 position of the kozak sequence on green fluorescence protein (GFP) expression in HEK 293 cells. They reported that using G at +4 enhances GFP expression by 4 fold providing that the -3 nucleotide is a purine (A/G). This +4 G enhancement effect is more related to the presence of alanine (GCN) and glycine (GGN) in the second amino acid position (Xia, 2007).

1.2.5.2- Codon usage

Codon usage and optimization can enhance translation since mammals have more than one codon for each amino acid and some organisms favour one codon over the others (Ikemura, 1985 and Nagata *et al.*, 1999). Some poorly translated poxvirus and human papillomavirus genes, expressed transiently in mammalian cells, showed improved translation efficiencies upon codon optimization (Disbrow *et al.*, 2003; Mossadegh *et al.*, 2004 and Barrett *et al.*, 2006). The optimization of *Aequorea victoria* GFP (AvGFP) increased its expression in mammalian cells by four to ten fold and also enhanced its fluorescence (Yang *et al.*, 1996 and Zolotukhin *et al.*, 1996). Similarly, expression of human erythropoietin in mammalian cells was enhanced by more than 13 fold after codon optimization (Kim *et al.*, 1997). Even the choice of the stop codon (UAA, UGA or UAG) and the adjacent nucleotides affects the translation termination efficiency (Cassan & Rousset 2001, Namy *et al.*, 2001 and Sun *et al.*, 2005).

1.2.5.3- IRES

The expression of some viral proteins under cellular translation suppression attracted scientists to investigate the mechanisms and sequences used to escape from the cellular translation regulation. One interesting sequence is the IRES, used by the ribosomes to bind within the mRNA molecule, although not from the 5' end, and start the recognition and subsequent translation from the AUG codon downstream from the IRES. It was first identified from poliovirus (Pelletier & Sonenberg, 1988) and named by Jang *et al.* (1989) after a study on encephalomyocarditis virus RNA and confirmed from poliovirus by Molla *et al.* (1992).

Different viral and cellular IRESs have been isolated and function to allow the ribosomal attachment and translation of an internal gene without the need of the cap-binding initiation mechanism (Jang *et al.*, 1988; Pelletier & Sonenberg, 1988, Jackson & Kaminski, 1995 and reviewed in Baird *et al.*, 2006 and Martínez-Salas *et al.*, 2008). This mechanism, together with the absence of tissue specificity, allowed the incorporation of IRES sequences in transgenes design to transcribe bicistronic mRNA. Expression from this mRNA occurs with cap-dependent translation of the first gene and IRES-mediated translation of the second gene (Lucas *et al.*, 1996 and Shaw-Jackson & Michiels, 1999).

1.2.6- Post-translation

Although some sequences can be incorporated in a transgene to guide the protein secretion, other elements are less controllable and rely on the cellular ability to perform accurate post-translational modifications. As mentioned earlier in this chapter, transgene

expression was upgraded from simple prokaryotes to complex mammalian cells to match the increased requirement for efficient and accurate post-translational cellular machinery.

Various post-translational modifications are performed on the primary polypeptide chain to form the final protein molecule in its active form. Among these modification reactions are acetylation, acylation, adenosine diphosphate-ribosylation, amidation, γ-carboxylation, β-hydroxylation, disulfide bond formation, folding, glycosylation, phosphorylation, proteolytic processing and sulfation (Walsh & Jefferis, 2006). Despite the fact that mammalian cells can perform all of these modifications, the efficiency and accuracy of these processes is encountered by other reactions or drawbacks such as glycosylation variation, methionine oxidation, asparagine and glutamine deamidation and protein misfolding and aggregation (Jenkins *et al.*, 2008).

Viral expression systems are used as a model to understand gene expression in mammalian cells. In this study, different genes and sequences that are thought to enhance gene expression were used from the Ad5 genome to study gene expression in mammalian cells.

1.3- ADENOVIRUS

The adenovirus, named after its first isolation from adenoidal tissue in 1953 (Rowe *et al.*, 1953; Hillemann & Werner, 1954), is considered the most extensively used viral model for gene delivery and expression studies. The virus is widely used in molecular biology research and is well understood on both the structural and genetic levels. The adenovirus was used the research model where RNA splicing was first established. Among the different isolated types of adenoviruses, human serotype 5 remains the workhorse in the majority of research and applications. The virus does not induce human cancer, which makes it the most favourable viral gene delivery vector for mammalian cells, especially in gene therapy.

1.3.1- Classification

Adenoviruses belong to class I viruses (double stranded DNA viruses) according to the Baltimore classification system. They are grouped in the family *Adenoviridae* and subdivided, according to their host, into four different genera: *Atadenovirus*, *Aviadenovirus*, *Mastadenovirus*, and *Siadenovirus* (Figure 1.1). Human adenoviruses are members of the genus *Mastadenovirus*, and they are sub-grouped, according to different properties including their nucleotide sequence and hemagglutination, into six subgroups (A to F). The types of the different groups are distinguished by their serological differences and are known as serotypes. The collective serotype numbers in the six groups of human adenoviruses is fifty-one (Benko *et al.*, 1999 and Lichtenstein & Wold, 2004).

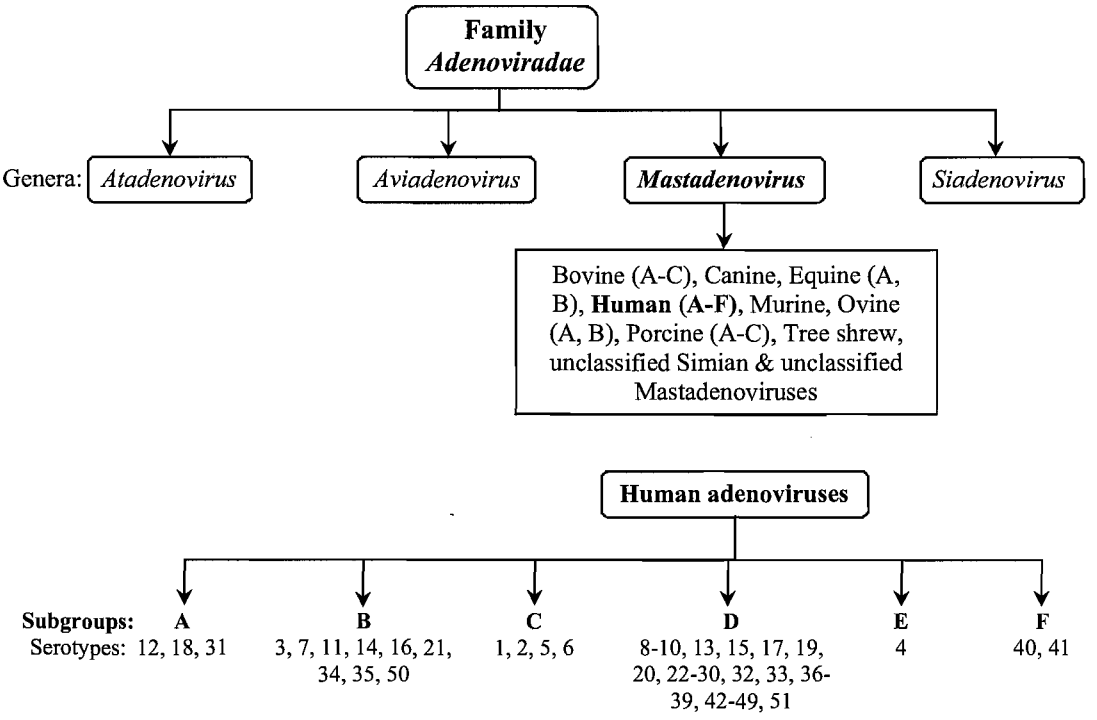

Figure 1.1: Taxonomic structure of the family *Adenoviridae* (reproduced from the National Center for Biotechnology Information (NCBI) taxonomy browser: http://www.ncbi.nlm.nih.gov/Taxonomy/Browser/wwwtax.cgi?id=10508).

1.3.2- Genome

Human adenoviruses have a linear double stranded genome of 35-38 kbp. The genome is characterized by its inverted terminal repeats (ITRs) and the 5' terminal protein which are essential for viral genome replication (Rekosh *et al.*, 1977 and Hay *et al.*, 1995). Adenovirus genes are divided into early and late genes according to the stage of their transcription within the viral life cycle. All the adenoviral mRNAs are transcribed by RNA polymerase II except the virus-associated RNA (VA RNA) which is an RNA polymerase III transcript (Shenk, 2001). Viral transcripts and their protein products are shown in Figure 1.2.

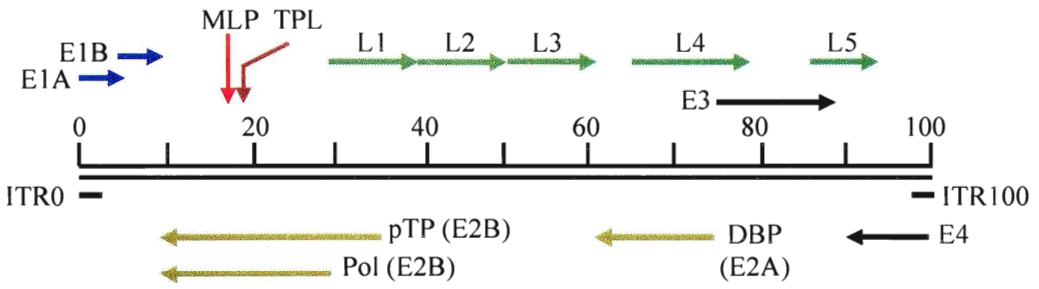

Figure 1.2: Transcription of the Ad5 genome. Early and late transcripts and their direction are indicated by arrows. The major late promoter (MLP) and the tripartite leader sequence (TPL) are indicated.

1.3.3- Life Cycle

A copious amount of information is available on every gene and the relationship to the other viral and cellular genes. This review will be limited to those genes directly related to this study. Adenovirus life cycle can be divided into two distinct phases: early and late. The early phase starts upon the entry of the virus into the cell and ends just before viral DNA replication starts. Then, the late phase begins and lasts until cell lysis and the release of the new viruses.

1.3.4- Early region

Early genes are the first genes transcribed and expressed during viral infection, after the delivery of the viral genome into the nucleus. Early genes include four cassettes and are subdivided into immediate early (E1A) genes, and early genes that include E1B, E2 (E2A and E2B), E3 and E4. All these genes have mainly a regulatory function in the viral cell cycle and viral-host interaction.

1.3.4.1- The Immediate Early Genes (E1A)

Gene products of the E1 region are divided into E1A and E1B. Two major mRNA transcripts are produced from E1A early after infection, the 13S and 12S which are named according to their sedimentation coefficient or 289 and 243, according to the length of their amino acid residues (Shenk, 2001). An additional three mRNA transcripts of 9S, 10S and 11S are produced from E1A in the later stages, however their function is unknown (Stephens & Harlow, 1987 and Ulfendahl *et al.*, 1987). Transcription of these mRNAs is driven by a common promoter and they share the same 5' and 3' terminal sequences since they are produced by differential splicing. The E1A regions of most of the human adenoviruses share three conserved regions (CR1, CR2 and CR3) (Figure 1.3).

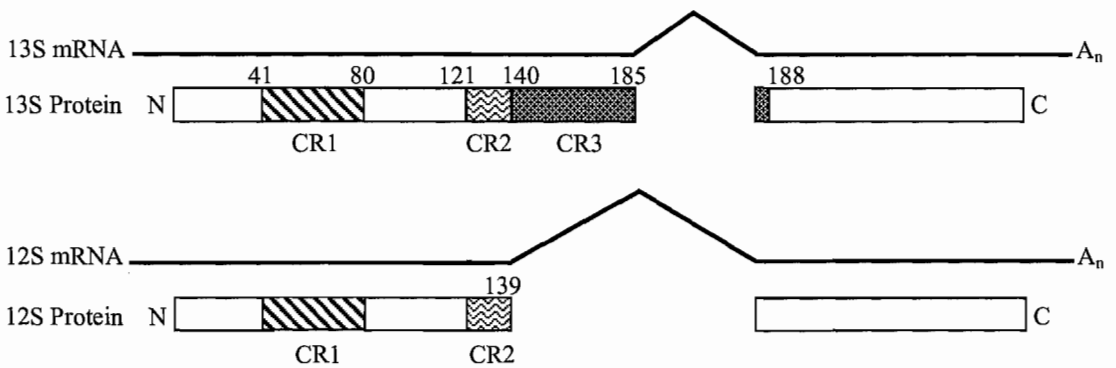

Figure 1.3: E1A major mRNAs and their encoded polypeptides. 13S and 12S mRNAs are represented in lines; exons are represented by horizontal lines and introns are the caret symbols and (A_n) is the poly A sequence. Polypeptides are represented by triangles, conserved regions 1 to 3 (CR1, CR2 and CR3) are shown on the Figure (Shenk, 2001).

E1A protein products have different functions. They regulate the expression of the other adenoviral proteins (early and late). Viruses with a mutated or deleted E1A region are replication incompetent since they cannot activate the expression of viral proteins (Berk *et al.*, 1979; Jones & Shenk, 1979 and Shenk *et al.*, 1980). The HEK 293 cell line, which contains the integrated adenovirus E1 region, can be used to grow these replication incompetent viruses (Graham *et al.*, 1977).

Other functions of the E1A 12S and 13S protein products include the stimulation of cell division and growth (Keblusek *et al.*, 1999). They play an important role in activating the expression of adenoviral E2 proteins and other cellular S-phase proteins. E1A proteins also have the ability to bind and inactivate the retinoblastoma (Rb) tumour suppressor proteins. This binding will release the E2F which is the transcription factor of E2 and S-phase protein expression (Brehm *et al.*, 1998). The release of E2F will stabilize the p53 tumour suppressor protein. This action is mediated by the induction of the human $p14^{ARF}$ which in turn will bind the mdm2 oncogene and alter its ability to bind and inactivate p53 (Lowe & Ruley, 1993; Querido *et al.*, 1997b; Bates *et al.*, 1998; Prives, 1998 and Zhang *et al.*, 1998).

In spite of the unique presence of CR3 in the 13S, the lack of this region in the 12S does not affect its ability to mediate cellular transformation. Only CR1 and CR2 are responsible for cellular transformation (Whyte *et al.*, 1989 and Stein *et al.*, 1990). However, the CR3 region has its own functions. CR3 has the binding site of the TATA-box binding protein (TBP), thus it has an advantage in transcription regulation. The CR3 also contains a zinc finger domain involved in its binding site with TBP (Culp *et al.*, 1988; Horkoshi *et al.*, 1991; Lee *et al.*, 1991; Webster & Ricciardi, 1991 and Webster *et*

al., 1991). It also mediates transactivation of the activating transcription factor (ATF) family of proteins. The interaction of CR3 with ATF-2 and ATF-a is through their leucine zipper-dependent activation (Chatton *et al.*, 1993 and Liu & Green, 1994) or a CR3-dependent activation (Flint & Jones, 1991).

Zinc finger domains of E1A 13S and its ability to interact with the TBP are important to increase the late protein expression. E1A increases the expression from the adenovirus MLP 4 to 10 fold. On the other hand, MLP activity increases 200 folds when both E1A and either MAZ or Sp1 transcription factors are present (Parks & Shenk, 1997).

1.3.4.2- E1B

Unlike E1A which activates p53-mediated apoptosis, E1B proteins inhibit apoptosis and antagonize the effect of E1A. Two major protein products are expressed from E1B, 19k and 55k, and both function as apoptosis repressors to reverse the action of E1A, but via different methods (Rao *et al.*, 1992; Debbas & White, 1993 and Acheson, 2007). Both proteins share a single mRNA which is 22S, but they have different AUG codons for their translation initiation. Despite the overlap in their mRNA sequence, there is no homology in the amino acid sequence of both proteins due to the different codon positions (Esche *et al.*, 1980; Bos *et al.*, 1981 and Montell *et al.*, 1984).

E1B 55k blocks the p53-dependent apoptotic pathway by the direct binding of p53 (Sarnow *et al.*, 1982 and Roth *et al.*, 1998). The complex of E1B 55K-p53 is co-localized in the cytoplasm (Grand *et al.*, 1999). This interaction is important for viral mRNA transport and viral replication (Ridgway *et al.*, 1997 and Horridge & Leppard, 1998). E4

orf6 protein has a similar function in binding and inactivating p53 (Dobner *et al.*, 1996 and Nevels *et al.*, 1997). The presence of both 55k and E4 orf6 proteins cause a marked reduction in p53 production (Querido *et al.*, 1997a and Steegenga *et al.*, 1998).

The 55k protein also has important functions during the late phases of the viral cell cycle. It binds to the E4 orf6 protein product and the new complex plays the main role in active transport of the TPL-containing mRNA from the nucleus to the cytoplasm (Babiss & Ginsberg, 1984; Babiss *et al.*, 1985; Halbert *et al.*, 1985; Pilder *et al.*, 1986a,b; Williams *et al.*, 1986; Leppard & Shenk, 1989 and Bridge & Ketner, 1990).

The complex of E1B 55k and E4 orf6 is present in the viral transcription sites in the nucleus (Gonzalez & Flint, 2002 and Ornelles & Shenk, 1991). Evidence suggests that viral mRNA interacts with this complex through the ability of E1B 55k to bind RNA (Horridge & Leppard, 1998) and facilitates its transport to the cytoplasm using the E4 orf6 proteins nuclear localization and transport signals (Dobbelstein *et al.*, 1997). This complex also enhances late viral mRNA accumulation in the cytoplasm and its subsequent translation (Imperiale *et al.*, 1995). Cellular mRNA transport to the cytoplasm and synthesis of cellular proteins are blocked by the same complex (Beltz & Flint 1979 and Flint & Gonzalez, 2003).

The smaller E1B protein, the 19K, is more efficient than the 55k in repressing apoptosis (Rao *et al.*, 1992) and it is a member of the BCL-2 death antagonists family (Chao and Korsmeyer, 1998). The 19k protein represses apoptosis by binding to Bax and inhibiting the activation of caspases (Han *et al.,* 1996 and Sabbattini *et al.,* 1997). E1B 19k viral mutants have several viral DNA and host cell degradation and low viral production (Pilder *et al.*; 1984 and white *et al.*, 1984).

1.3.4.3- E2

The expression of the E1A genes activates expression of E2 proteins as well as the S-phase cell cycle proteins and this prepares the cell for viral DNA replication (Hay *et al.*, 1995). E2 gene products are related directly to genome replication and are subdivided into E2A and E2B. Three proteins are produced from the entire E2; DNA binding protein (DBP) from E2A in addition to viral DNA polymerase and precursor terminal protein (pTP) from E2B.

Two promoters drive expression from the E2 region; one during the early phase of the cell cycle (E2 early promoter) and the second is active during the late events (E2 late promoter) (Swaminathan &Thimmapaya, 1995). The E2 early promoter has two sites for transcription factors, one for ATF-2 and the second is for E2F. Activation of both sites is mediated by E1A proteins (Shenk & Flint, 1991; Swaminathan &Thimmapaya, 1995 and Brehm *et al.*, 1998). The binding of E2F on the E2 early promoter is enhanced by the E4 orf6/7 19k protein (Neill *et al.*, 1990 and Helin & Harlow, 1994).

The DBP is a 59k protein that has a high binding affinity for DNA and fulfile different functions (van Breukelen *et al.*, 2003). It protects against *in vitro* DNA degradation by inhibiting the DNase-mediated hydrolysis (Nass and Frenkel, 1980). It binds cooperatively and non-cooperatively with single stranded DNAs and double stranded DNAs, respectively (Dekker *et al.*, 1997). DBP has a major role during viral replication to unwind DNA and to stabilize the single stranded DNA during elongation (Brenkman *et al.*, 2001) and its flexibility is important for its unwinding function (van Breukelen *et al.*, 2000). In addition, it has an important role in replication initiation by

enhancing the binding of the viral DNA polymerase to the origin of replication (van Breukelen *et al.*, 2003).

DBP enhances transcription, mRNA stability and assembly of the new viral particles (Nicolas *et al.*, 1983; Cleghon *et al.*, 1989 and Zijderveld *et al.*, 1994). Transcription from most of the adenoviral promoters, except the E4 promoters, is activated by DBP (Chang and Shenk, 1990). In addition, the binding of the upstream stimulatory factor 1 (USF1) to the MLP is enhanced by the DBP (Zijderveld *et al.*, 1994).

Adenovirus DNA polymerase and pTP are produced from E2B and together initiate viral DNA replication through a protein-priming mechanism (Parker *et al.*, 1998). Adenoviruses cannot use cellular DNA polymerase for its genome replication and instead use the viral DNA polymerase, since it has the ability to interact with pTP and initiate the process. Adenovirus polymerase works in the 5' to 3' direction and it has 3' to 5' exonuclease activity which is important for proofreading during the replication process. Both the polymerase and exonuclease activities decrease upon their binding to pTP (Field *et al.*, 1984 and King *et al.*, 1997a,b).

The adenovirus replicates its genome through a strand displacement mechanism. ITRs are about 100 bp at the left and right ends of the viral genome and they serve as an origin of replication. Only the terminal 20 bp from each ITR are needed to initiate the process (Brenkman *et al.*, 2002). The first step is the binding of pTP to the viral polymerase to form the pTP-polymerase complex which binds to nucleotides 9 to 18 on the replication origin site (Temperley & Hay, 1992). pTP contains a serine residue which

binds to a dCTP and plays a key role in the priming activity of the protein (Lichy *et al.*, 1981 and King *et al.*, 1994).

Some cellular transcription factors are involved in the process, such as nuclear factor I (NFI) and Oct-1 (also called nuclear factor III). They enhance viral replication by binding to specific regions on the ITRs and then function to guide and stabilize the pTP-polymerase complex at the ITRs (O'Neill *et al.*, 1988; Bosher *et al.*, 1990; Mul *et al.*, 1990 and Berk, 2007). A specific protein-protein interaction appears between NFI or Oct-1 and the pTP-polymerase complex. NFI is activated by DBP and it binds to the polymerase, however Oct-1 binds to the pTP part of the complex (Cleat & hay, 1989; Chen *et al.*, 1990; Stuiver & van der Vliet, 1990; Mul & van der Vliet, 1992; van Leeuwen *et al.*, 1997 and Botting & Hay, 1999). The presence of these two transcription factors is not essential to initiate the replication process, however they increase the replication activity by 200 fold (Hay *et al.*, 1995; van der Vliet, 1995 and de Jong & van der Vliet, 1999).

The sequence of the first four nucleotides of the 3' end of both the adenoviral genome strands is 3' $G^1T^2A^3G^4$ 5'. The fourth nucleotide on the viral template (G) directs the binding between pTP and the dCTP in a reaction activated by the viral DNA polymerase. The polymerase will continue to add another two nucleotides to form an intermediate of three nucleotides (CAT) bound to the pTP-polymerase complex. Then, the 3' end of the viral template pairs with the intermediate nucleotides to form the primers and the viral DNA polymerase dissociates from the pTP-CAT. This process continues to the elongation step and a new complementary strand is synthesized (King & van der Vliet, 1994 and King *et al.*, 1997a).

According to the different probabilities in the initiation of the replication process, there are two types of adenoviral replication as illustrated in Figure 1.4, both types will end up with the formation of two viral genome copies. Type I replication is the synchronized replication at both ends of the viral genome yielding two genome copies, or the one end replication initiation to yield one genome copy and one single stranded DNA (ssDNA) copy. However, type II is the replication of the ssDNA templates to form the complete double stranded genome (Shenk, 2001).

In type II replication, the presence of ITRs allows the ssDNA to form a panhandle structure that is stabilized by DBP. ITRs of the panhandle structure function as the origin of replication for the synthesis of the complementary strand (Lechner & Kelly, 1977 and Berk, 2007). Then, the viral protease cleaves the pTP while attached to the genome, yielding its mature TP form (Smart & Stillman, 1982).

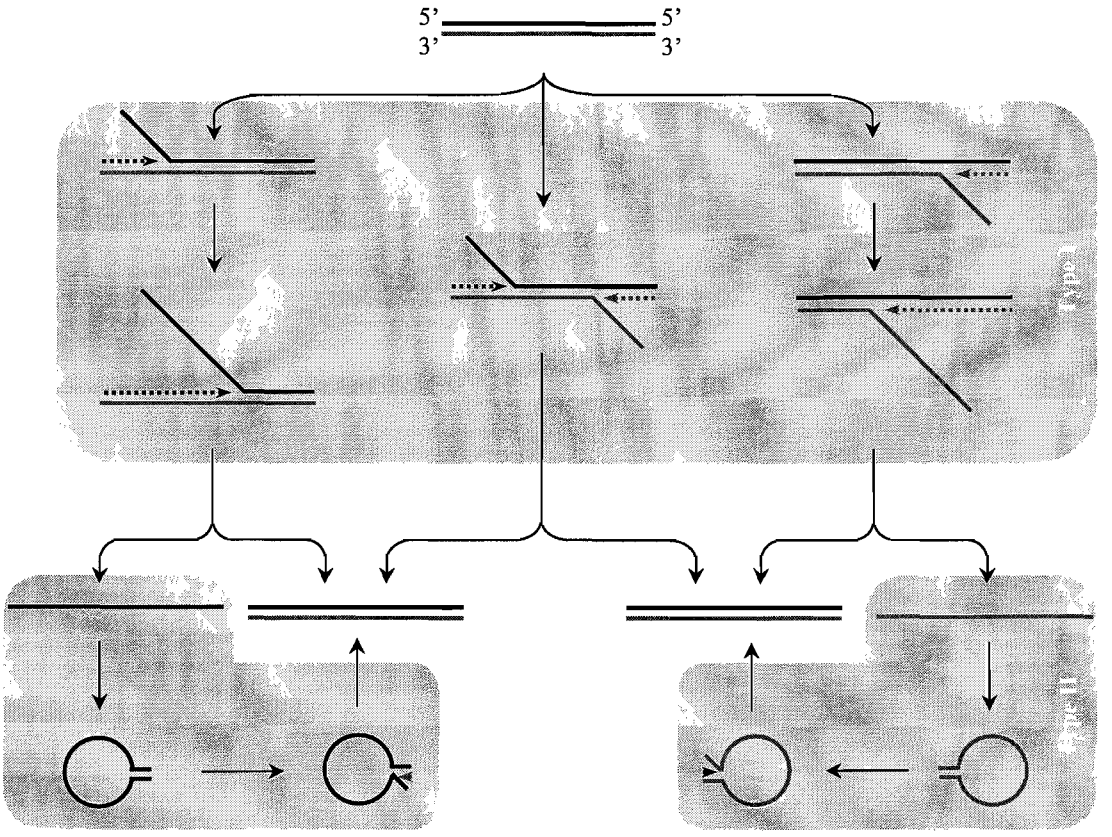

Figure 1.4: Adenovirus genome replication (reproduced from Shenk, 2001).

1.3.4.4- E3

The control of the various host immune responses is the main function of the E3 genes (Horwitz, 2001). This region is not important for viral growth in cell culture and is deleted in most adenoviral vectors. E3 encodes for several proteins including adenovirus death protein (ADP), gp19K, receptor internalization and degradation (RID)α, RIDβ and 14.7k proteins. It also encodes for another two proteins with unknown function referred to as 12.5k and 6.7k (Russell, 2000).

1.3.4.5- E4

The E4 region encodes several proteins that are named according to their open reading frame (orf) position within the region. Different E4 orfs were found in the Ad5 including orf1 to orf4, orf6 and orf6/7. Early studies on adenovirus 2 revealed that E4 products are generated from a single mRNA of about 2800 nucleotides, driven by the E4 promoter which undergoes differential splicing to generate about 18 mRNAs with common 5' and 3' terminal sequences (Hérissé *et al.*, 1981; Freyer *et al.*, 1984; Virtanen *et al.*, 1984; Gilardi & Perricaudet, 1986 and Watanabe *et al.*, 1988). Protein products of the multiple orfs have different functions, mainly auxiliary to other proteins such as the E1B 55k protein. These proteins work during the different stages of the viral life cycle including early events and replication as well as late protein expression and inhibition of cellular expression (Halbert *et al.*, 1985).

1.3.5- The major late transcriptional unit

The major late transcription unit (MLTU) contains five families, called L1 to L5, that are expressed under the control of one promoter, the MLP (Figure 1.5). The MLTU contains all of the structural proteins that are needed for the assembly of the new viral capsids with a primary transcript length of about 29 kbp (Evans *et al.*, 1977; Ziff & Evans, 1978 and Nevins & Darnell, 1978). Five different poly(A) sites are present inside the MLTU and they are used to subdivide the unit into the five families. About 18 proteins are being produced from the MLTU by differential splicing (Chow *et al.*, 1977; Nevins & Darnell, 1978 and Ziff & Fraser, 1978). During the early phase of viral infection, transcription from the MLTU is weak as the MLP is not fully active and it

drives low levels, mainly from the L1 (Shaw & Ziff, 1980 and Nevins & Wilson, 1981). Once replication is initiated, MLP and hence the MLTU gains its full activity and expression proceeds from L1 to L5.

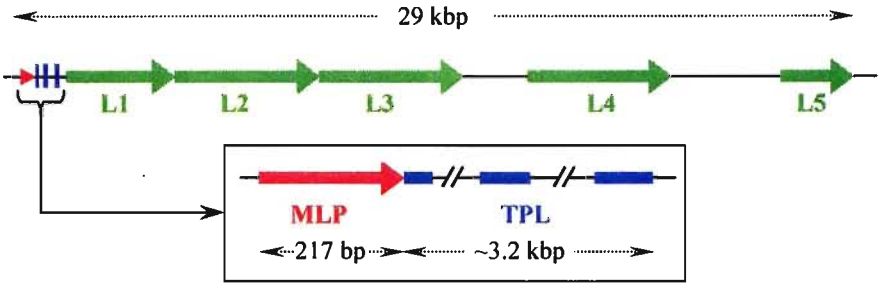

Figure 1.5: Ad5 major late transcription unit. L1 to L5 are the late adenoviral genes. MLP is the major late promoter and TPL is the tripartite leader sequence.

Late protein expression in adenovirus infection is very efficient. The production of the viral proteins is accompanied with an increase in the cell dry weight and cell size; HEK 293 cell diameter increases 13% after infection (Nadeau *et al.*, 2000a,b). The plaque assay determined that 7000 to 12000 plaque forming units (PFU) were formed per cell from adherent cells, and 5000 PFU/cell from cells growing in suspension (Nadeau *et al.*, 2001 and Nadeau & Kamen, 2003). This indicates the abundant amount of production particularly when considering that the plaque assay measures only the infectious particles not all the produced particles and that the protein content of each particle is 87% (Russell, 2000).

Two main components within the MLTU are responsible for the efficient adenovirus protein production; the first is the promoter (MLP) and the second is the TPL. Both are located at the beginning of the transcription unit and work together to ensure high transcription and translation levels of the viral late proteins (Figure 1.4).

1.3.5.1- MLP

The major late promoter gains its full activity during the late phase of infection (Ziff & Evans, 1978). This activity is the driving force of transcription from the five late families (L1 to L5) and at the same time, efficient transcription levels. The MLP of Ad5 is 217 bp in length and is recognized by the cellular RNA polymerase II. The activity of this promoter can be understood by examining its structure as well as the viral and cellular proteins that contribute to its activity.

Promoters recognized by the RNA polymerase II have a typical structure consisting of the TATA box in addition to one or more upstream elements. Both of these are very important for the activity of the promoter since they act as recognition sites involved in the direct interaction with the transcription factors and/or the RNA polymerase II itself. In the SV40 early promoter, the upstream element consists of three pairs of GC boxes located between -103 and -40 and each pair is about 21 bp. Another pattern for the upstream elements appears with the herpes simplex virus (HSV) thymidine kinase promoter which has a CAAT box flanked with two GC boxes (Weaver & Hedrick, 1992).

MLP has an interesting structure that is believed to be related to its high activity. It has a TATA box from -31 to -25, a CAAT box at -70, and a binding site for an USF called the major late transcription factor (MLTF) at -50. The MLP also has a downstream binding site (DBS) that binds to a complex of cellular and viral proteins. The structure around the TATA box is unique, since it is flanked with two GC-rich sequences located at -36 and -18 (Figure 1.6) (Shenk, 1996; Song *et al.*, 1996, Parks & Shenk, 1997 and young, 2003).

The presence of these different elements in the MLP enables its interaction with different viral and cellular proteins. MAZ and Sp1 are examples of cellular transcription factors that interact with and enhance the activity of MLP. Among the different sites within the promoter region, MAZ binds strongly to both -36 and -18 GC-rich regions located around the TATA box and close to the transcription initiation, and increases the MLP activity by 40-50 folds. However, Sp1 binds only to the -18 GC-rich region and provides four to ten folds increase in MLP activity (Parks & Shenk, 1997). Another cellular factor that activates MLP is the major late transcription factor which binds to the -50 site (Miyamoto *et al.*, 1985).

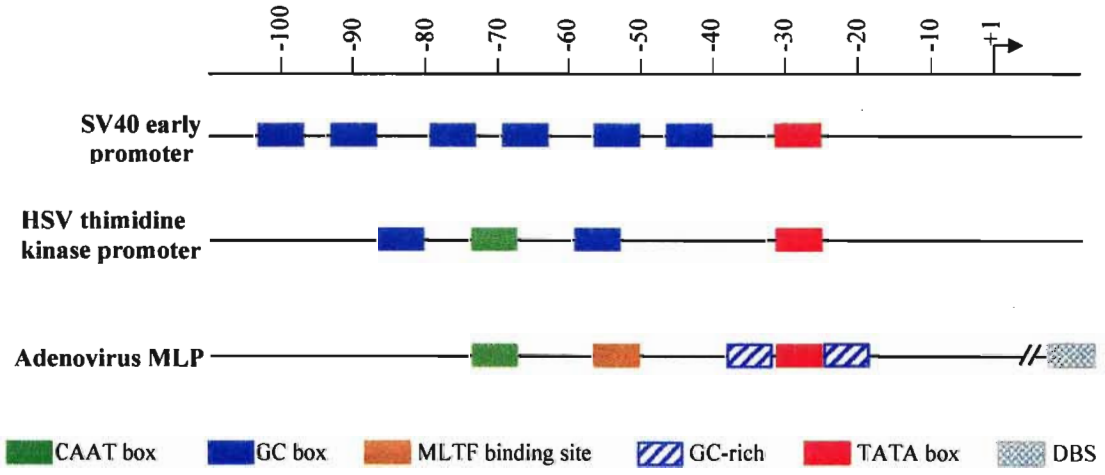

Figure 1.6: Architectural elements of SV40 early promoter, HSV thimidine kinase promoter and the adenovirus MLP (Weaver & Hedrick, 1992, Parks & Shenk, 1997 and Young, 2003).

Different viral proteins have a positive effect on MLP activity. The E1A 13S protein product activates the MLP through its zinc finger domain and enhances its activity by four fold, this activity increases 200 folds in the presence of either MAZ or Sp1 (Parks & Shenk, 1997). Protein IX and protein IVa2 are expressed in large amounts during the events of MLP activation after initiation of viral genome replication to induce

the activity of MLP (Lutz & Kendinger, 1996 and Lutz *et al.*, 1997). IVa2 forms a protein complex with cellular proteins; this complex can bind to the DBS of the MLP (Shenk, 1996).

1.3.5.2 TPL

The TPL is a 5' end untranslated RNA sequence of 201 nucleotides present in all the late viral mRNA. As indicated from its name, the TPL originates from three exons on the adenoviral genome (Berget *et al.*, 1977). The primary TPL transcript is 3685 bp, since it contains two introns of 1021 bp and 2461 bp (Alignment of the TPL sequence obtained from Zhang *et al.* (1989) and Ad5 genome obtained from the National Center for Biotechnology Information (NCBI) genome browser, accession number: AC_000008). During the post-transcriptional modifications on the viral late mRNAs, the two introns are removed and only 201 bp, resembling the exons, are joined together to form the mature TPL (Figure 1.7). The TPL introns are not important for its function however, they are important for the MLP activity since the first intron contains the majority of the DBS (Mansour *et al.*, 1986).

The TPL facilitates late mRNA transport and accumulation in the cytoplasm and is responsible for the selective translation of the late viral proteins instead of the cellular proteins (Logan & Shenk, 1984; Berkner & Sharp, 1985 and Zhang *et al.*, 1994). Adenovirus E1B 55k and E4 orf6 play the main role in the active transport of viral late mRNA, containing the TPL, from the nucleus to the cytoplasm (Babiss *et al.*, 1985; Halbert *et al.*, 1985; Pilder *et al.*, 1986a,b; Williams *et al.*, 1986; Leppard & Shenk, 1989 and Bridge & Ketner, 1990). The viral transcription sites in the nucleus contain a

complex of E1B 55k and E4 orf6 (Ornelles & Shenk, 1991 and Gonzalez & Flint, 2002). Viral mRNA interacts with this complex through the ability of E1B 55k to bind mRNA through the TPL (Horridge & Leppard, 1998) and facilitate its transport to the cytoplasm using the E4 orf6 proteins' nuclear localization and transport signals (Dobbelstein *et al.*, 1997). Cellular mRNA transport is blocked by the same complex (Flint & Gonzalez, 2003).

During the late phase, viral mRNA is translated with high efficiency while the translation of cellular genes is shut off (Beltz & Flint, 1979; Babiss & Ginsberg, 1984 and Halbert *et al.*, 1985). The adenovirus exerts this regulatory effect by giving translation priority to its structural genes. The cap-binding protein complex (eIF-4F), needed for mRNA binding to the ribosomes and hence translation, is inactivated through blocking its phosphorylation. Dephosphorylation of the eIF-4F appears with the activation of the MLP at the beginning of the late phase.

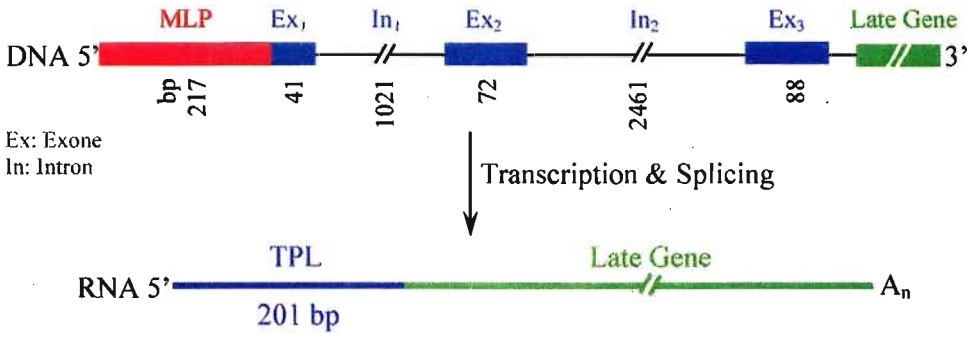

Figure 1.7: TPL architecture on genomic DNA and late viral mRNA. Size and location of the exons and introns were determined by aligning TPL sequence obtained by Zhang *et al.* (1989) with that of human Ad5 obtained from the National Center for Biotechnology Information (NCBI) genome browser (accession number: AC_000008). Ex: exon and In: intron

The viral regulatory element that mediates eIF-4F phosphorylation inhibition is the 100k late protein. It is encoded by L4 and produced at the beginning of the late phase (Bablanian & Russell, 1974 and Oosterom-Dragon & Ginsberg, 1980). This protein binds and blocks a site on the eIF-4G that is needed for the kinase MnK1 to bind to and start its function in phosphorylating the cap-binding protein (Cuesta *et al.*, 2000). In addition, the 100k protein has an RNA-binding domain that interacts with the cytoplasmic mRNA, specially the TPL sequence (Adam & Dreyfuss, 1987 and Riley & Flint, 1993). The formation of the 100K-TPL complex and then its binding to the eIF-4G will facilitate ribosome shunting and hence translation of the late viral mRNAs (Xi *et al.*, 2004 and 2005).

Upon inactivation of the eIF-4F, cellular mRNAs are unable to attach to ribosomes and therefore, cannot initiate translation. However, only late viral mRNAs will be able to initiate translation, since the TPL binding to the ribosomes is eIF-4F-independent (Dolph *et al.*, 1988). The relaxed secondary structure of the TPL facilitates its function in translation initiation even when eIF-4F is inhibited (Dolph *et al.*, 1990). The TPL allows ribosome shunting, in a similar manner to the IRES recognition, which avoids the scanning mechanism that is needed for cellular mRNAs and the required cap-binding (Yueh & Schneider, 1996 and 2000).

AIM OF THE STUDY

The aim of this study was to investigate the effect of various factors on gene expression in mammalian cells. The following four factors were examined:

1- The effect of DNA quality on DNA uptake and gene expression. More specifically, the effect of Ethidium bromide, Cesium Chloride, endotoxins and Ethanol on calcium phosphate-mediated transfection into CHO cells and the expression of LacZ gene.

2- The effect of adenoviral major late promoter and tripartite leader sequence exons on gene expression. Also, the effect of the adenoviral E1 genes and the cellular background was studied.

3- The effect of adenoviral DNA replication genes on the copy number and the expression efficiency of the transgene. This involves the construction of a cell line expressing these viral replication genes and allows the replication of the ITRs-containing expression vector.

4- The effect of wild type adenoviral super-infection at different multiplicity of infections (MOIs) on exogenous gene expression in mammalian cells. This involves the study of the expression under super-infection in CHO and HEK 293 cells.

MATERIALS AND METHODS

2.1- BACTERIAL CULTURE

2.1.1- Bacterial strain

Plasmid DNA cloning and propagation was carried out in *Escherichia coli* DH5α, with the following genotype: F^-, Φ80, δ*lac*Z, ΔM15, Δ(*lac*ZYA-*arg*F), U169, *deo*R, *rec*A1, *end*A1, *hsd*R17(rk^-, mk^+), *pho*A, *sup*E44, *thi*-1, λ^-, *gry*A96, *rel*A1 (Woodcock *et al.*, 1989).

2.1.2- Bacterial culture and colonies maintenance

Bacterial cultures were grown and maintained at 37°C in Luria-Bertani broth (LB: 1% (w/v) bacto-tryptone, 0.5% (w/v) bacto-yeast extract, 1% (w/v) NaCl, sterilized by autoclaving). For growing bacterial colonies, LB-agar plates were prepared by adding 2% (w/v) agar to LB. After autoclaving, the solution was cooled down to 45°C and 0.1 mg/mL ampicillin was added for selection purposes. Twenty millilitres of the LB-agar solution was poured into 10 mm Petri dishes then let stand to solidify and stored at 4°C.

2.1.3- Competent cells

Competent cells were prepared from a stock cell population (New England Biolabs), according to Inoue *et al.* (1990). A single colony was obtained from an antibiotic-free LB-agar plate and inoculated into 2 mL of antibiotic-free LB. After an overnight incubation at 37°C in a shaking water bath, the inoculum was transferred to

250 mL of SOB medium (2% (w/v) bacto-tryptone, 0.5% (w/v) bacto-yeast extract, 10 mM NaCl, 2.5 mM KCl, 10 mM $MgCl_2$, 10 mM $MgSO_4$, 20 mM glucose) in a 2 L flask and grown with vigorous shaking (250 rpm) at 18°C, to mid-log phase (OD_{600}=0.6). The culture was then placed on ice for 10 minutes and centrifuged at 3000 x g in a Beckman GPR centrifuge for 10 minutes at 4°C. The supernatant was discarded and the pellet was resuspended in 80mL of ice-cold transformation buffer (TB: 10 mM Pipes (or Hepes), 55 mM $MnCl_2$, 15 mM $CaCl_2$, 250 mM KCl, pH 6.7) and placed on ice for 10 minutes. Cells were centrifuged again at 3000 x g for 10 minutes at 4°C. The supernatant was discarded and the pellet was resuspended in 12-15 mL of ice-cold TB. Dimethyl sulfoxide (DMSO) was added with gentle swirling on ice to a final concentration of 7% and then kept on ice for 10 minutes. Competent cells were then aliquoted and frozen immediately in liquid nitrogen. Cells were transferred to -80°C for long-term storage.

2.1.4- Transformation

Plasmid DNA was resuspended into a 20 µL volume of water or TE buffer (1mM ethylene diamine tetra-acetic acid (EDTA), 10mM Tris-HCl), prior to transformation into competent cells. Frozen competent cells were thawed on ice and then used to inoculate the plasmid DNA. The mixture was incubated on ice for 30 minutes and then subjected to a heat shock at 42°C for 45 seconds. After the heat shock, the cells were put immediately on ice for 2 minutes and 700 µL of antibiotic-free LB was added to the transformation mixture and incubated with shaking at 37°C for 45 minutes.

2.1.5- Bacterial selection

The ampicillin gene was used as a selection marker in all the constructed plasmids, therefore LB-agar plates with 2X ampicillin (0.1 mg/mL) were used to grow and select the positively transformed colonies. Plates were incubated overnight at 37°C and the selected colonies were picked and inoculated into 2 mL of LB with 2X ampicillin and shaken overnight at 37°C. In addition, X-gal (5-bromo-4-chloro-3-indolyl-beta-D-galactopyranoside) was used for blue and white screening when cloning was performed inside the β-galactosidase gene. When used, 0.8 mg (40 μL from a stock of 20 mg/mL) of X-gal was added to the surface of an LB-agar plate prior to the spreading of transformed bacteria.

2.1.6- Small-scale plasmid DNA preparation

Small-scale plasmid DNA isolation and preparation was carried out either by the alkaline lysis procedures (Cohen *et al.*, 1972 and Sambrook *et al.*, 1989), or by the Plasmid DNA MiniPrep Kit (Norgen Biotek Corp.) according to the manufacturer's instructions. The obtained plasmid DNA was stored at -20°C.

2.1.7- Endotoxin-free plasmid DNA preparation

Endotoxin-free plasmid DNA preparation for cell culture experiments was carried out using the Endotoxin-free DNA MaxiPrep Kit (Norgen Biotek Corp.), according to the manufacturer's instructions.

2.1.8- Large-scale plasmid DNA preparation

The preparation of large-scale plasmid DNA starts with the pre-inoculation of 10 µL of the desired frozen plasmid culture into 10 mL of LB medium supplemented with 2X ampicillin (0.1 mg/mL) and incubated at 37°C with shaking. When the OD_{600} of the growing culture reached 0.4 to 0.6, the pre-inoculated culture was inoculated into 1 L of LB medium supplemented with 2X ampicillin and incubated overnight (16 h) with shaking at 250 rpm. The growing culture was harvested by centrifugation in 1L centrifugation bottles at 4,560 x g for 1 hour at 4°C in a JS-4.2 rotor using a Beckman J-6B centrifuge.

After decanting the supernatant and drying the bacterial pellet for 5 minutes, the cells were resuspended by gentle vortexing in 50 mL of resuspension solution (50mM Tris, 10 mM EDTA pH 8.0 and 0.1 mg/mL RNase A) and incubated at room temperature for 5 minutes. The resuspended cells were lysed by adding 50 mL of lysis solution (1% sodium dodecyl sulfate (SDS) and 0.4 M NaOH) and mixing by inversion 10 times and incubated at room temperature for no more than 5 minutes. Fifty millilitres of the neutralization solution (3M Sodium Acetate pH 4.8) was added immediately and mixed by inversion 10 times followed with incubation at 4°C for a minimum of 30 minutes.

The bacterial lysate was then transferred to 250 mL centrifugation bottles and centrifuged at 30,100 x g for 30 minutes at 4°C in a JA-14 rotor using a Beckman J2-MI centrifuge. The supernatant was filtered into a clean 1L bottle using eight-micron filter paper (Whatman). The filtrate was treated with 5 units/mL RNase T1 (Cedarlane Laboratories Ltd., Worthington) and incubated at 55°C for 30 minutes. Then, 2.5

volumes of ice-cold 95% ethanol was added to the filtrate and incubated overnight at -20°C or -70°C.

The next day, the precipitated plasmid DNA was harvested by transferring the 1L bottle contents into several 250 mL centrifugation bottles and centrifuging at 30,100 x g for 20 minutes at 4°C. The supernatant was discarded and the bottles were dried, after which the precipitated DNA in the 3 or 4 bottles used was dissolved in 5 mL of TE buffer (10 mM Tris-HCl and 1 mM EDTA, pH 7.5). The harvested DNA was confirmed by restriction enzyme digestion before proceeding to cesium chloride banding.

2.1.9- Cesium chloride gradient

The density of the harvested large-scale plasmid DNA was adjusted to 1.57-1.59 g/mL using CsCl (about 1.01 g of CsCl is used per 1 mL of plasmid DNA). The harvested and density-adjusted DNA from 1 L culture was adjusted to 8.7 mL using TE-CsCl (density of 1.59 g/mL). Two mg ethidium bromide was added (200 µL from a stock of 10 mg/mL) and mixed by inversion. The contents were transferred into 8.9 mL Beckman OptiSeal ultracentrifuge tubes and sealed with the tube stopper. The tubes were then placed in a type 70.1 Ti rotor and centrifuged in a Beckman L8-80M ultracentrifuge at 246,960 x g for 22 hours at 22°C.

The resultant lower supercoiled plasmid DNA band was extracted from the banding tube using an 18 gauge needle assembled to a 1 mL syringe and transferred into a 15 mL Falcon tube. The extracted DNA was then cleaned to remove the ethidium bromide by repetitive mixing with isoamyl alcohol saturated with CsCl. To enhance the phase separation, the well-mixed contents were centrifuged for 5 minutes at 2,000 x g in a

Beckman GPR centrifuge equipped with a JS-42 rotor. After centrifugation, the upper isoamyl alcohol layer was aspirated from the tube. This was repeated several times until the pink color disappeared. The cleaned DNA liquid phase was then transferred into Spectra/Por 7 dialysis tubing (Spectrum Laboratories, Inc.), pre-heated at 65°C for 10 minutes and sealed with clips. The filled dialysis tube was dialyzed against 10 L of TE buffer at 4°C, with continual changing of the buffer every 16-24 hours for three times (a total of 30 L). Plasmid DNA was collected afterwards and stored at -20°C.

2.2- MAMMALIAN CELL CULTURE

2.2.1- Cell lines and maintenance

The *Chinese hamster* ovary (CHO) cells utilized in this study were the subclone K1 (ATCC CCL-61) derived from the parental cell line initiated by Puck *et al.* (1958) and were obtained from Dr. Andrew Rainbow (McMaster University, Ontario, Canada). Cells were maintained as a monolayer in Petri cell culture dishes and cultured in advanced Dulbecco's Modified Eagle Medium (Advanced D-MEM: Invitrogen Corp., Gibco), containing 5% (v/v) fetal bovine serum (FBS, PAA Laboratories Inc.), 1% (v/v) penicillin/streptomycin (Invitrogen Corp., Gibco) and 1% (v/v) glutamine (Invitrogen Corp., Gibco). Growing cells were incubated in a water-jacketed incubator (Fisher Scientific, Pittsburgh PA) at 37 °C with 96% relative humidity and 5% CO_2.

At 90% confluencey, cells were passaged by using EDTA-trypsin solution (0.53 mM tetrasodium EDTA, 0.05% (v/v) Trypsin). The used volume is determined by the size of the cell culture plate, for a 150 mm plate, a 4 mL volume was used. After

aspirating the media, cells were washed with 6 mL phosphate buffered saline (PBS), pH 7.4. Upon removal of the wash by aspiration, EDTA-trypsin was added to the monolayer for two minutes, and then cells were lifted by gentle tapping of the side of the dish. Six millilitres of the culture medium was then added to the cell suspension with pipetting to split the cells. Four milliliters of the cell suspension was added to a new culture plate and the volume was completed to 20 mL with new culture medium and the cells were incubated at 37°C.

Maintenance of human embryonic kidney (HEK) 293 cells (Graham *et al.*, 1977; Microbix Inc., ATCC CRL-1573) was done using similar handling to the CHO cells but with different media components and solutions. The medium used was autoclavable MEM (Invitrogen Corp., Gibco) supplemented with 3% (v/v) sodium bicarbonate (Invitrogen Corp., Gibco), 1% L-glutamine (Invitrogen Corp., Gibco), 10% (v/v) FBS (PAA Laboratories Inc.) and 1% (v/v) Antibiotic-Antimycotic (10,000 units/mL penicillin G sodium, 25 μg/mL amphotericin B, and 10,000 units/mL streptomycin sulphate, Invitrogen Corp., Gibco). Saline citrate was used to wash and lift the cells and 5 minutes of incubation at 37°C was used for the lifting step.

2.2.2- Cell freezing and thawing

Cells were grown to the late log phase (about 90% confluencey) and then lifted using EDTA-trypsin for CHO cells or Saline citrate for HEK 293 cells. Cells were centrifuged at 670 x g for 5 minutes at 4°C (Beckman Spinchron Centrifuge). The medium was aspirated and the CHO cell pellet was resuspended in 4 mL of ice cold new growth medium with 10% (v/v) DMSO, however the HEK 293 cell pellet was

resuspended in FBS with 10% (v/v) DMSO. Cells were then transferred to 1 mL sterile cryogenic tubes (Sarstedt), and frozen slowly by wrapping them with insulating paper towel in a Styrofoam container and stored in a -70°C freezer.

Cell thawing was done by hand rubbing the frozen cryogenic vial and pouring the contents into 150 mm cell culture dish containing 20 mL of preheated (37°C) growth medium. The medium was changed within 24 hours to remove DMSO and changed every other day thereafter.

2.2.3- Cell counting

Cells were lifted from the plate and transferred to a microcentrifuge tube. A 20 µL volume of the sample was placed on the notch of a hemocytometer covered with a cover slip. A light microscope was used to visualize and count the average cell number in the defined fields of the hemocytometer. The total number of cells could then be calculated in the original sample.

2.2.4- Calcium phosphate transfection

Calcium phosphate transfection was carried out according to the optimized protocol done by Jordan *et al.* (1996) based on the method created by Graham & Van der Eb (1973). On the day prior to transfection, cells were split in a 6-well plate and allowed to attach overnight. The amount of cells used was optimized so that the confluencey would be 60-70% at the transfection time. Two hours before transfection, the medium was replaced with 2 mL fresh medium. Transfection solutions were warmed up to room temperature prior to use. The transfection mixture was made by diluting 5 µg plasmid

DNA into 90 µL TE buffer (pH 7.6). A 10 µL volume of 2.5 M $CaCl_2$ (filter sterilized) was added to the DNA-TE slowly with swirling followed by gentle vortexing for complete mixing of components. Next, 2X HEPES (140 mM NaCl, 1.5 mM Na_2HPO_4, 50 mM HEPES, pH 7.05, filter sterilized) was placed in a 1.5 mL Eppendorf tube and vigorously shaken on a vortex while adding the DNA-TE-$CaCl_2$ slowly and dropwise. This mixture was let stand for 30 seconds and then mixed well by pipetting to split the aggregates. The solution was added evenly and dropwise on the medium surface. Cells were then incubated at 37°C and the medium changed 6 hours post-transfection to reduce cytotoxicity. The transfection efficiency was tested 21 hours post-transfection.

2.2.5- Lipofectamine 2000 transfection

Lipofectamine 2000 (Invitrogen) was used to transfect plasmids DNA into mammalian cells. The confluencey of the monolayer was ensured to be at least 70% at the transfection time. The culture medium was replaced prior the transfection with 2 mL of antibiotic-free medium. The transfection mix for each well (of a 6-well plate) was prepared in 500 µL by mixing plasmid DNA and Lipofectamine 2000. First, 5 µg plasmid DNA was diluted in a total volume of 250 µL using Opti-MEM I Reduced Serum Medium (Invitrogen Corp., Gibco). Similarly, 5 µL Lipofectamine 2000 was diluted in 250 µL total volume by using Opti-MEM. Both the diluted DNA and Lipofectamine 2000 were incubated at room temperature for 5 minutes then mixed together and incubated at room temperature for additional 20 minutes. The 500 µL transfection mixture was added dropwise onto the well and shaken to distribute the

mixture evenly. Finally, the plate was incubated at 37°C for 6 hours before changing the medium with the regular, antibiotic-containing, medium.

2.2.6- LacZ activity assay

Positive LacZ transfected cells were stained and visualized under a light microscope. The medium was aspirated 21 hours post-transfection from the 6-well plate followed by 2 washes with 1 mL PBS. A 1 mL volume of 4% paraformaldehyde (pH 7.2) was added to each well and incubated at 37°C for 2 minutes. The cells were then washed twice with 1 mL PBS. A 2 mL volume of X-gal stain (35 mM $K_3Fe(CN)_6$, 35 mM $K_4Fe(CN)_6$, 1 mM $MgCl_2$, in PBS; pH 7.4, supplemented with 1 mg/mL of X-gal) was added and the cells were incubated overnight at 37°C with 96% relative humidity. The next day, the number of blue cells was counted to determine the transfection efficiency.

2.2.7- G418 selection

G418 (Bioshop Canada) was used for selecting or maintaining mammalian foci positively transfected with the neomycin resistance gene. A concentration of 0.5 mg/mL of the culture medium was mixed freshly and added to the cells under-selection. The G418-containing medium was replaced every other day during the selection period (about two weeks).

2.2.8- Adenovirus infection

The adenoviral infection of mammalian cells was carried out in 6-well plates by using a volume of the viral stock equivalent for the required multiplicity of infection (MOI). This viral volume was mixed with PBS^{++} (0.01% $CaCl_2.2H_2O$ and 0.01%

$MgCl_2.6H_2O$ dissolved in PBS) in a total volume of 500 µL/well and then added to the cell monolayer (after aspirating the medium). The 6-well plate was then incubated for 1 hour at 37 °C with 96% relative humidity and 5% CO_2, with swirling the plate every 15 minutes. After that, 2 mL of the culture medium were added to each well and the plate was returned to the incubator.

2.2.9- Trypan blue staining

Cell vitality was investigated by using trypan blue staining. First, cells were collected by centrifugation at 2000 rpm for 5 minutes and resuspended in PBS. Then, 10 µL of cells were mixed with 10 µL of trypan blue and counted under a light microscope using a hemocytometer. Live cells appear bright under the microscope while dead cells appear blue.

2.3- DNA MANIPULATION

2.3.1- RNA/DNA isolation

DNA and RNA were isolated, all from the same sample, using the RNA/DNA/Protein Purification Kit (Norgen Biotek Corp.), according to the manufacturer's instructions.

2.3.2- DNA quantification

DNA was quantified using a spectrophotometer after dilution with water. The absorbances were measured at wavelengths 260 nm (A_{260}) and 280 nm (A_{280}) and the

DNA concentration was then calculated according to the following formula (Sambrook *et al.*, 1989):

$$[\text{DNA}]\ (\mu g/\ \mu L) = \frac{(A_{260}) \times (\text{dilution factor}) \times (50\ ng/\ \mu L)}{1000}$$

The value A_{260}/A_{280} was used to determine sample purity. If the value was between 1.8 and 2.1, the samples were considered pure.

2.3.3- Endotoxin preparation and quantification

A freshly prepared *E. coli* culture, grown overnight, was centrifuged at 3000 x g in a Beckman GPR centrifuge for 30 minutes. The supernatant was then filtered through a sterile Acrodisc® 25mm syringe filter with 0.2 µm HT Tuffryn® membrane (PALL, Life Sciences) to eliminate any bacteria left from the centrifugation step and the collected supernatant was used as a source of endotoxin. The level of endotoxin in the supernatant was quantified by measuring the endotoxin units (EU) per mL using the Limulus Amebocyte Lysate (LAL) Endochrome Kit (Charles River Laboratories), according to the manufacturer's instructions.

2.3.4- DNA cleaning

DNA was cleaned using the CleanAll Kit (Norgen Biotek Corp.), according to the manufacturer's instructions.

2.3.5- DNA extraction from agarose gel

After excision from an agarose gel, DNA was cleaned using the DNA Gel Extraction Kit (Norgen Biotek Corp.), according to the manufacturer's instructions.

2.3.6- Cleaning of PCR amplification Product

PCR amplification products were cleaned using the PCR Purification Kit (Norgen Biotek Corp.), according to the manufacturer's instructions.

2.3.7- Restriction enzymes digestion

All of the restriction enzymes that were used were obtained from either New England Biolabs (NEB) or MBI Fermentas. Digestion and heat inactivation were carried out according to the manufacturer's instructions. In digestion preparations used for agarose gel electrophoresis, 0.5 to 5 μg of DNA was digested using one to ten units of restriction enzyme in a 20 μL reaction volume for two hours. However, larger volumes or longer incubation times were used for other digestion applications. When needed, enzyme inactivation was performed by heating up the reaction to 70°C or higher for 20 minutes, if recommended by the manufacturer.

Multiple restriction enzyme digestion was required to obtain some fragments needed for downstream cloning purposes. In most cases, a one step digestion with multiple enzymes was used with the most suitable buffer, with attention to the enzymes' activity. Equal amounts of restriction enzymes were used and the extent of digestion was determined with agarose gel electrophoresis. When incomplete digestion was encountered, the enzyme amount and digestion time were adjusted. In some cases, sequential digestion was used with incompatible restriction enzymes.

2.3.8- DNA ligation

DNA fragments were ligated in a 20 μL reaction using 400 units of T4 DNA ligase (New England Biolabs), according to the manufacturer's instructions. The reaction was performed at room temperature for 2 hours when ligating sticky ends and 8 hours for blunt end ligation. If necessary, heat inactivation was carried out at 65°C for 20 minutes.

2.3.9- Oligonucleotides phosphorylation

An amount of 150 pmol of each of the oligonucleotides was phosphorylated in a 25 μL reaction using five units of T4 polynucleotide kinase (New England Biolabs), according to the manufacturer's instructions. The reaction was at room temperature for 30 minutes followed by heat inactivation at 65°C for 20 minutes.

2.3.10- Oligonucleotides annealing

Oligonucleotides that were used for generating multi-cloning sites or constructing DNA fragments were mixed and annealed by using the iCycler PCR machine (Bio-Rad). The oligonucleotide mixture was heated to 94°C followed by lowering the temperature in decrements of 0.5°C every 10 seconds. When the temperature reached 18°C, the mixture was cooled down directly to 4°C.

2.3.11- Adjacent oligonucleotides ligation

Ligation of the annealed adjacent oligonucleotides is carried out to form a phosphodiester bond between the neighbouring 5' phosphate and 3' hydroxyl terminal ends, in a process similar to nick-closing. The reaction was performed in a 20 μL

volume, using 40 units of *Taq* DNA ligase (New England Biolabs), according to the manufacturer's instructions.

2.3.12- DNA sequencing

DNA sequencing was performed at York University Core Molecular Biology and DNA Sequencing Facility. Cycle sequencing reactions were carried out with Bigdye Terminator chemistry on the Applied Biosystems 337 DNA Sequencer, using the appropriate primers.

2.3.13- PCR

Polymerase chain reaction (PCR) (Mullis *et al.*, 1986) was carried out according to the polymerase manufacturer's instructions. The used of forward (F) and reverse (R) primers, ordered from Sigma Genosys, for all of the PCR reactions are listed in Table 2.1. Primers were dissolved to a concentration of 50 µM using dH_2O and stored as aliquots at -20°C. The iCycler PCR machine (Bio-Rad) was used to perform the reactions. A 20 µL reaction mixture was made as follows: 1 ng of less of DNA template, 0.12 µL of each primer (50 µM stock), 0.2 µL deoxynucleotide triphosphates (dNTPs) (10 mM), 2 µL of the supplied 10X PCR buffer (100mM Tris-HCl (pH 9.0), 500 mM KCl, 1% Triton X-100, and with or without 15mM $MgCl_2$) and 0.1 µL (5 units/µL) *EconoTaq* DNA polymerase (Lucigen). When using *Pfu* polymerase, 0.2 µL (2.5 unit/µL) enzyme was used with 2 µL of 10X reaction buffer (200 mM Tris-HCl (pH 8.8 at 25°C), 100 mM $(NH_4)_2SO_4$, 100 mM KCl, 1% (v/v) Triton X-100, 1 mg/ml bovine serum albumin (BSA)). The reaction volume was completed with dH_2O.

The reaction program was started with 3 minutes at 94°C to dissociate the DNA template. Annealing was applied for 15 seconds at 5°C lower than the primers' melting temperature (Tm), followed by an extension time of 1 minute per 1 kbp or 2 minutes per 1 kbp at 72°C with *Taq* or *Pfu* DNA polymerases, respectively, then a denaturation step for 15 seconds at 94°C. Thirty to thirty-five cycles (annealing-extension-denaturation) were used, with holding the reaction for 5 minutes at 72°C and a final incubation at 4°C.

Table 2.1: Names, sequences and amplicon sizes of the different PCR primers. Tm can be obtained by for each primer by using Sigma Genosys's online DNA calculator (http://www.sigma-genosys.com/calc/DNACalc.asp). Parentheses indicate nucleotides added as linkers.

Name	Sequence	Amplicon size (bp)
DBP-F	5' ACCATGGAGGACGTGTCG 3'	489
DBP-R	5' AGCCTCCATGCCCTTCTC 3'	
E1A-13S-F	5' CTGGCTGATAATCTTCCACCTC 3'	479
E1A-13S-R	5' (CACAGG)ACTGTAGACAAACATGC 3'	
E1B-55k-F	5' GGAGGATAGGGTGGCCTTTA 3'	867
E1B-55k-R	5' (GCGGCTG)CTCAATCTGTATC 3'	
E2RB-F	5' CGGCTATTACCACCACACCT 3'	558
E2RB-R	5' AGTGGACCAGGTGTTTCAGG 3'	
GA-F	5' (GGGCCC)TGTTGCCTTTACTTC 3'	969
GA-R	5' (GACGTC)CCTCCCACACCTCC 3'	
GFP-F	5' ATCCTGATCGAGCTGAATGG 3'	484
GFP-R	5' TGCCATCCTCGATGTTGTG 3'	
MT-F1	5' ATAAGAGCCAAGTTCCAGCGTCC 3'	493
MT-R1	5' AATACCTGTGGCTTGCGATACCG 3'	
pCMVβ-F	5' TCGCTACCATTACCAGTTGGTC 3'	677
pCMVβ-R	5' GAGTTAGCTCACTCA-TTAGGCACC 3'	
pE2F-F	5' TTGTACTGAGAGTGCACCATACATG 3'	743
pE2F-R	5' AACTGTCCTAACCTTGGATTACATCAAG 3'	
pTP-F	5' ATGGCCAACTGCACTTACACC 3'	565
pTP-R	5' ACCTGAGCGAGTCCGCATC 3'	
TPL1,2-F	5' GTGACCGGGTGTTCC 3'	183
TPL1,2-R	5' (GATACCATGG)TACCGTTCGGAGGCC 3'	
VPol-F	5' TCTTGCAAGCCATCGACG 3'	701
VPol-R	5' TTCCCAGCGGTCCCATC 3'	
VPro-F	5' AGCCATTGTCAAAGATCTTGGTTG 3'	562
VPro-R	5' AGTGGCGCTCCTAATCTGC 3'	
TPLate1-F	5' CGAGGGCCAGCTGTTGG 3'	160, 219 & 332
GFPlate-R	5' TGCCGTAGGTGGCATCG 3'	

2.3.14- Agarose gel electrophoresis

Agarose gel electrophoresis was carried out according to Sambrook *et al.* (1989). AlphaImager 2200 (Alpha Innotech) was used to capture gel pictures under ultraviolet (UV) light exposure.

2.3.15- Quantitative PCR

Quantitative PCR (qPCR) was performed on a known concentration of template DNA (4 to 10 ng) or complementary DNA (cDNA) (volume equivalent to 20-100 ng of initial RNA used in a reverse transcription reaction), using the Bio-Rad iCycler thermal cycler. The reaction mixture contained 10 µL of 2X SYBR GREEN master mix (Bio-Rad), and 1.2 µL of each primer (5 mM stock). The total volume of the reaction was completed with dH_2O to 20 µL. A 15 minutes heating at 95°C was used to activate the hotstart enzyme. Forty amplification cycles were performed as follow: 15 seconds at 95°C, 30 second at 59°C and 1 minute at 72°C. The reaction was kept at 57°C for 1 minute before starting a melting curve analysis by a 0.5°C increment every 10 sec over 80 rounds. A standard curve of known plasmid concentration (10 fg to 1 ng) was used to determine the initial concentration of plasmid in each sample.

2.4- RNA MANIPULATION

2.4.1- Total RNA isolation

Total RNA was extracted using the Total RNA Purification Kit (Norgen Biotek Corp.), according to the manufacturer's instructions.

2.4.2- Cytoplasmic and nuclear RNA isolation

Both cytoplasmic and nuclear RNA were isolated using Cytoplasmic & Nuclear RNA Purification Kit (Norgen Biotek Corp.), according to the manufacturer's instructions.

2.4.5- DNase treatment of RNA

The digestion of residual DNA in the isolated RNA samples was performed by using TURBO DNase (Ambion). Each 50 µL of sample was digested in a 100 µL reaction mixture containing the provided buffer and four units of TURBO DNase, with incubation at 37°C for 30 minutes.

2.4.3- RNA cleaning

All cleaned RNA samples were carried out by using the RNA CleanUp and Concentration Kit (Norgen Biotek Corp.), according to the manufacturer's instructions.

2.4.4- RNA quantification

RNA was quantified using a spectrophotometer after dilution with RNase-free water. Then absorbances were measured at wavelengths 260 nm (A_{260}) and 280 nm (A_{280}). RNA concentration was then calculated according to the following formula (Sambrook *et al.*, 1989):

$$[\text{RNA}]\ (\mu g/\ \mu L) = \frac{(A_{260}) \times (\text{dilution factor}) \times (40\ ng/\ \mu L)}{1000}$$

2.4.6- Formaldehyde agarose gel electrophoresis

RNA integrity was determined by using formaldehyde agarose gel electrophoresis, prepared according to Sambrook *et al.* (1989). AlphaImager 2200 (Alpha Innotech) was used to capture gel pictures under UV light exposure.

2.4.7- Reverse transcription

Two to five hundred nanograms of total RNA was used in reverse transcription (RT) reactions. RNA was mixed with 0.5 µL of 100 mM oligo$(dT)_{18}$ primer (Sigma), and completed to a final volume of 5 µL using RNase/DNase-free water (Ambion). This mixture was heated up for 5 minutes at 70°C, then chilled to 4°C. During the cooling step, 15 µL of the RT reaction solution is added to the mixture. The added RT reaction solution contains 4 µL of 5X First Strand Buffer (250 mM Tris-HCl pH 8.3, 375 mM KCl and 15 mM $MgCl_2$), 2 µL of 0.1 M Dithiothreitol (DTT), 1 µL of 10 mM dNTPs, 0.1 µL Superscript III reverse transcriptase (Invitrogen) and 7.9 µL RNase/DNase-free water (Ambion). The reaction was continued by an incubation step at 25°C for 5 minutes, followed with 90 minutes incubation at 42°C and 15 minutes incubation at 70°C before finally holding the reaction at 4°C.

2.5- GFP Fluorescence Intensity Quantification

The fluorescence intensity of green fluorescence protein (GFP) was quantified directly from mammalian cells by measuring the relative fluorescence units (RFU) using the BioTek Synergy HT Multi-Mode Microplate Reader. Transfected cells were washed twice with PBS, lifted from the plate and counted. Fifty thousand cells per well were then

transferred to a black rounded-bottom 96-well plate (Costar) in a total volume of 200 µL of PBS. The RFU was then measured at an excitation wavelength of 485 nm and an emission wavelength of 528 nm, using non-transfected cells as a blank.

2.6- DATA GRAPHING AND ANALYSIS

The obtained data was graphed by using OriginPro version 8.0724 (Origin Lab, Northampton, MA, USA). The same software was used for statistical analysis of the data. The significance of all values were attested at $P<0.05$ using the two sample t-Test for comparing the means of two samples and the one or two way ANOVA using Tukey's test when comparing the means of more than two samples at the same time.

RESULTS

3.1- Effect of DNA Contaminants on Transfection Efficiency and Mutation Frequency

Contamination is a major problem that is encountered when using different methods of DNA preparation. The purity of a DNA preparation is important and often an overlooked parameter when studying transfection efficiency and DNA stability. Since DNA preparation involves many different steps, the risk of having DNA contamination is high. These contaminants include ethidium bromide (EtBr), cesium chloride (CsCl), endotoxin and ethanol (EtOH). In this section, the effect of these contaminants on transfection efficiency, gene expression and mutation frequency in mammalian cells was investigated. Experiments were carried out in *Chinese hamster* ovary (CHO) cells using calcium phosphate transfection of DNA, after spiking with varying concentrations of contaminants.

3.1.1- Ethidium bromide

Different concentrations of EtBr (0, 2.5, 25 and 250 nM) were used to spike the plasmid pCMVβ. After spiking, plasmid DNA was incubated for 10 minutes at room temperature and then transfected into CHO cells using calcium phosphate in 6-well plates. Samples were done in two groups as one was used for staining and the second for DNA isolation. In each group, triplicate wells were used for each concentration. Twenty-one hours post-transfection, cells were stained by X-gal and the numbers of cells which

developed the blue color were counted under a light microscope. Records were calculated as a percentage from the control value (Figure 3.1-A).

Quantitative polymerase chain reaction (qPCR) was performed to determine the exact transfection efficiency by using equal amounts (10 ng) from the isolated DNA. A standard curve of known plasmid concentration was used to determine the initial plasmid concentration. Duplicate measurements were carried out for each of the triplicate samples. Since the amount of DNA per CHO cell is 3.1 pg (Gregory, 2005), and 10 ng of DNA was used per reaction, it was possible to calculate the average plasmid copy number per cell (Figure 3.1-B).

All the results were analyzed by a one-way ANOVA using Tukey's test at a significance level of 0.05. Significant reduction in LacZ expressing cells was obtained with EtBr concentrations of 25 and 250 nM (Figure 3.1-A). However no significant differences were obtained with the DNA delivery at any used concentration (Figure 3.1-B).

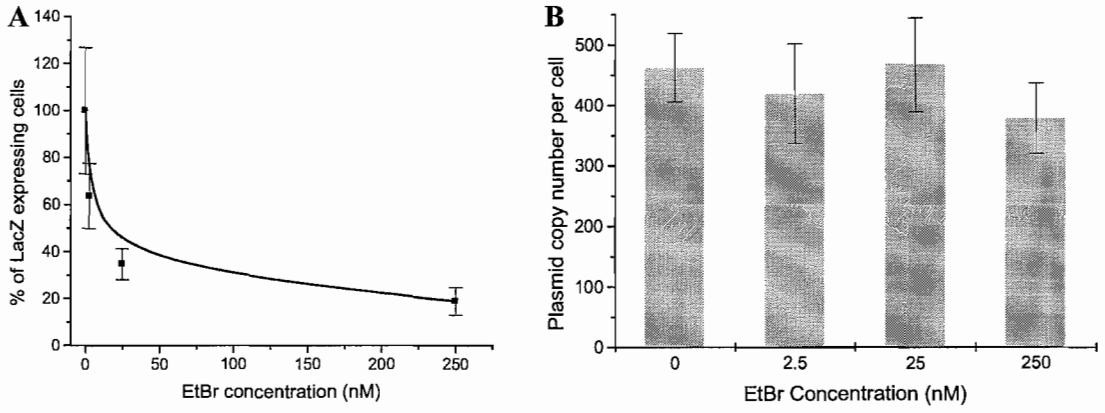

Figure 3.1: Effect of EtBr on gene expression and delivery. (A) Number of cells expressing LacZ and (B) Plasmid copy number per cell.

3.1.2- Cesium chloride

After spiking the plasmid pCMVβ with different concentrations of CsCl (0, 0.56, 5.6 and 56 μM), DNA was transfected into CHO cells as outlined above for EtBr. Significant reduction in the number of LacZ expressing cells was found with the higher two concentrations of 5.6 μM and 56 μM (Figure 3.2-A). On the other hand, a significant decrease in plasmid copy number per cell was observed in all of the higher CsCl concentrations (Figure 3.2-B).

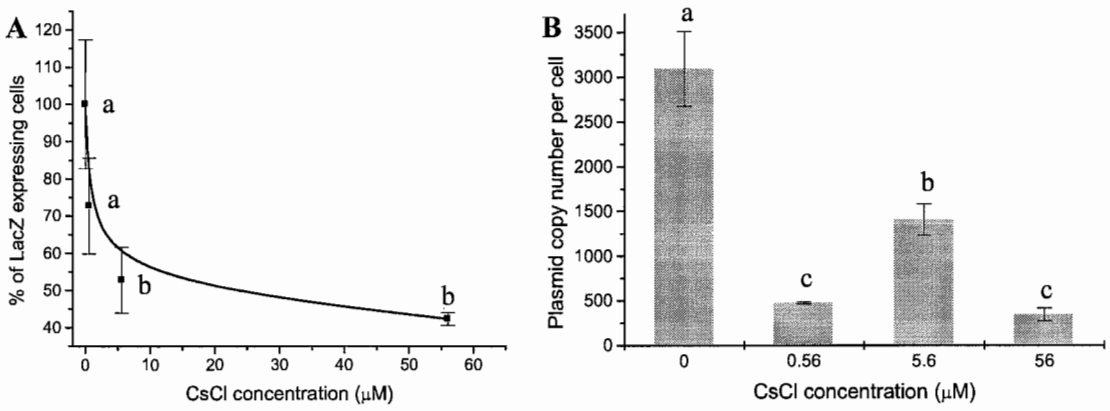

Figure 3.2: Effect of CsCl on gene expression and delivery. (A) Number of cells expressing LacZ and (B) Plasmid copy number per cell.

3.1.3- Ethidium bromide/Cesium cloride

Spiking was carried out by using a combination of EtBr and CsCl (0/0, 2.2/0.51, 22/5.1 and 220nM/51μM). The same transfection and collection procedures were followed according to part 3.1.1. Significant reduction in the number of LacZ expressing cells (Figure 3.3-A) was found in the highest used concentrations. The reduction in plasmid copy number per cell (Figure 3.3-B) was significant with all the used concentrations.

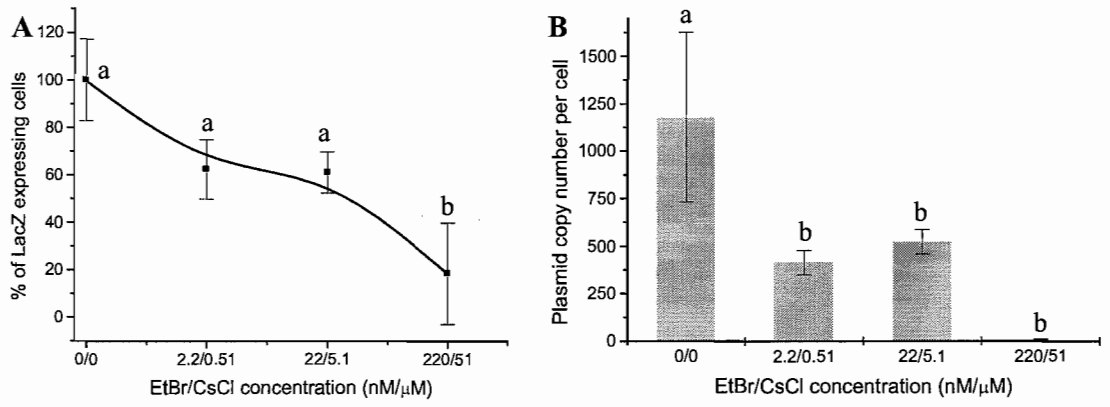

Figure 3.3: Effect of EtBr/CsCl on gene expression and delivery. (A) Number of cells expressing LacZ and (B) Plasmid copy number per cell.

3.1.4- Endotoxin

Spiking was carried out by using a combination of endotoxin (0.32, 4, 40 and 400 EU/μg DNA). Same transfection and collection procedures performed previously were followed. Significant reduction in the number of LacZ expressing cells (Figure 3.4-A) as well as the plasmid copy number per cell (Figure 3.4-B) was found in all the used concentrations, with a steady state between the middle two concentrations.

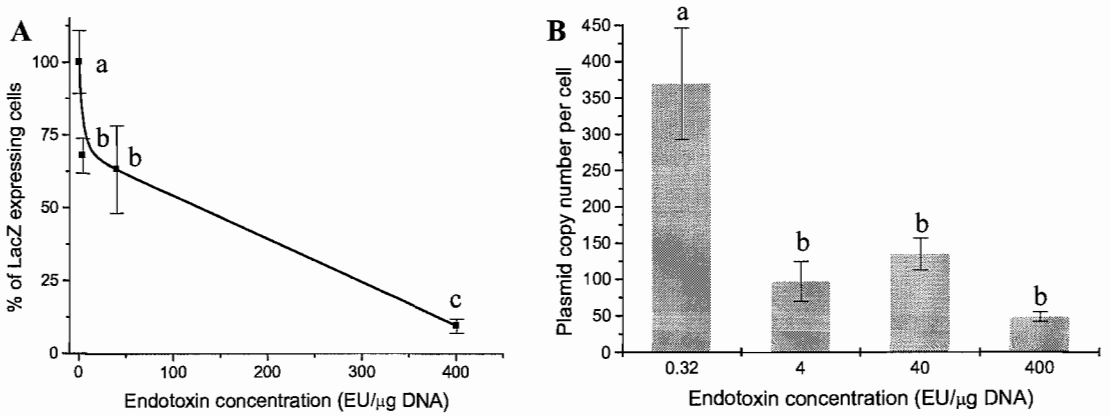

Figure 3.4: Effect of endotoxin on gene expression and delivery. (A) Number of cells expressing LacZ and (B) Plasmid copy number per cell.

3.1.5- Ethanol

EtOH spiking of pCMVβ was carried out by using different concentrations (0, 0.1, 0.5 and 1%). The same transfection and collection procedures performed earlier were followed. Significant reduction in the number of LacZ expressing cells (Figure 3.5-A) was observed only in the 0.5% concentration. On the other hand, no significant differences were obtained with the DNA delivery at any used concentration (Figure 3.5-B).

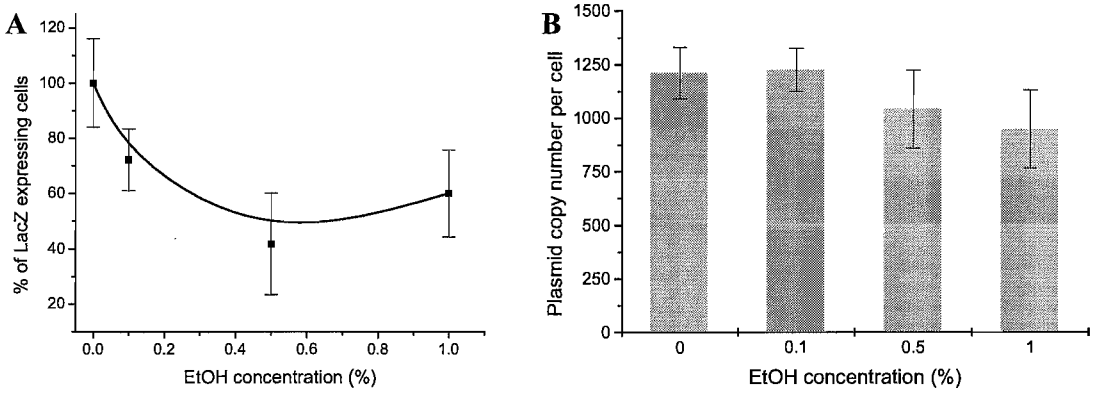

Figure 3.5: Effect of EtOH on gene expression and delivery. (A) Number of cells expressing LacZ and (B) Plasmid copy number per cell.

3.1.6- Reversibility of the spiking effect

To study the reversibility of contaminant interaction with DNA, a spiking followed by DNA cleaning and transfection was carried out. The highest concentration of each contaminant was used to spike the same amount of DNA. Following the incubation time at room temperature, spiked DNA as well as the control DNA was cleaned. DNA was then quantified to transfect cells with consistent amounts of DNA. Twenty-one hours post-transfection, the LacZ activity assay and DNA isolation were performed (triplicate samples for each).

Blue cells expressing LacZ were counted under a light microscope and the percentage of cells expressing the gene was calculated from the control value that was set at 100% (Figure 3.6). Three of the conditions (EtBr, CsCl and endotoxin) had values over 70%. The two other conditions (EtBr/CsCl and EtOH) had a lower value of expressing cells. The effect of cleaning was compared to direct spiking (no cleaning), with respect to the number of cells expressing LacZ (Figure 3.6). The data was analysed statistically by a Student's t-test at a significance level of 0.05. Significant improvement (at $P<0.05$) in the expression of LacZ was noted in three of the cleaned conditions (EtBr, CsCl and endotoxin). The percentage of cells expressing the LacZ gene increased from 18.9±5.8% to 73.9±6.1% with EtBr and 42.3±1.7% to 70.6±6.7% with CsCl (Figure 3.6). The improvement was dramatic with endotoxin, increasing from 9.4±2.4% to 98.5±4.1%. Insignificant improvement was obtained with EtBr/CsCl and EtOH.

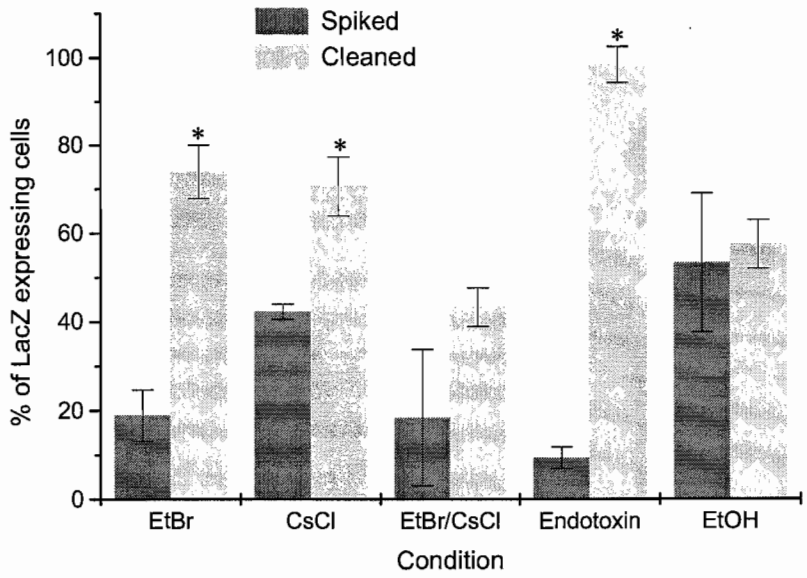

Figure 3.6: Effect of contaminants on the number of cells expressing LacZ. Numbers were calculated as a percentage from the control value. The used contaminant concentrations were: 250 nM (EtBr), 56 μM (CsCl), 220 nM/51 mM (EtBr/CsCl), 400 EU/μg DNA (endotoxin) and 1% (EtOH).

The percentage of transfection efficiency of cleaned and uncleaned conditions, relative to their controls, is shown in Figure 3.7. No significant change in transfection efficiency was obtained in both EtBr and EtOH. On the other hand, significant improvement in transfection efficiency of the cleaned CsCl, EtBr/CsCl and endotoxin was achieved. Transfection efficiency improved from the uncleaned to the cleaned of these three conditions by 5, 67 and 7.7 folds, respectively.

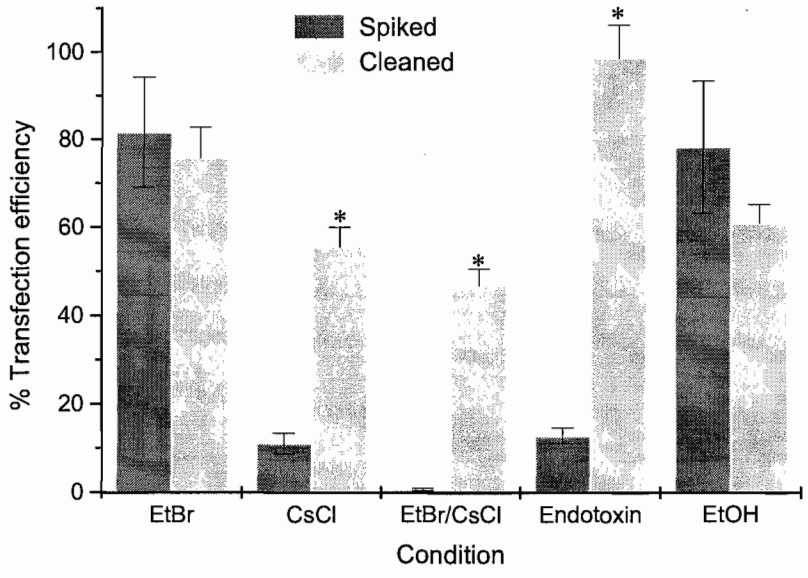

Figure 3.7: Transfection efficiencies of Spiked and cleaned DNA. The used contaminant concentrations were: 250 nM (EtBr), 56 μM (CsCl), 220 nM/51 mM (EtBr/CsCl), 400 EU/μg DNA (endotoxin) and 1% (EtOH).

3.1.7- Effect of contaminants on mutation frequency

In order to evaluate the effect of these contaminants on mutation frequency, pCMVβ was spiked with various contaminant concentrations. To screen for the mutation rate after spiking and transfection into mammalian cells, an ultrasensitive mutation detection method was developed (Figure 3.8) based on the use of restriction enzyme

digestion followed by polymerase chain reaction (PCR) amplification with two primers flanking the restriction site. Briefly, any mutation within the recognition sequence of this enzyme would prevent the plasmid digestion and that in turn will allow the PCR amplification to take place. In contrast, the lack of mutations would allow the proper recognition and subsequently digestion of the plasmid (Figure 3.8).

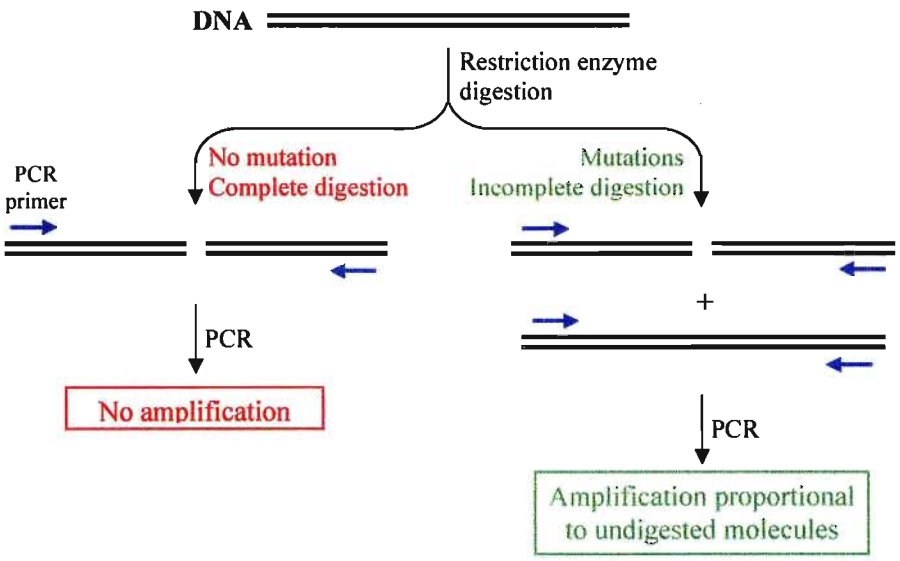

Figure 3.8: Strategy of ultrasensitive mutation detection. Restriction endonuclease digestion is followed by PCR amplification using primers flanking the digestion sites.

In this study, 40 ng of DNA isolated from CHO cells was digested with 10 units of *Hin*dIII in an overnight reaction (20 µL) at 37°C and then the enzyme was heat inactivated at 70°C for 20 minutes. Five microlitres (10 ng DNA) from this reaction and 10 ng from the undigested template were used for the PCR reactions. This allowed the recognition of the PCR amplification profile before and after *Hin*dIII digestion. Amplification was obtained with all the undigested conditions. However, amplification from the digested templates was positive only with the highest concentrations of EtBr (Figure 3.9). No amplification was noted with any of the other conditions (See the

appendix). The same PCR reactions were performed on pre-transfected cleaned DNA that was spiked with the separate highest contaminants concentrations. No amplification occurred in the digested templates, including the cleaned DNA that was spiked with EtBr (See the appendix).

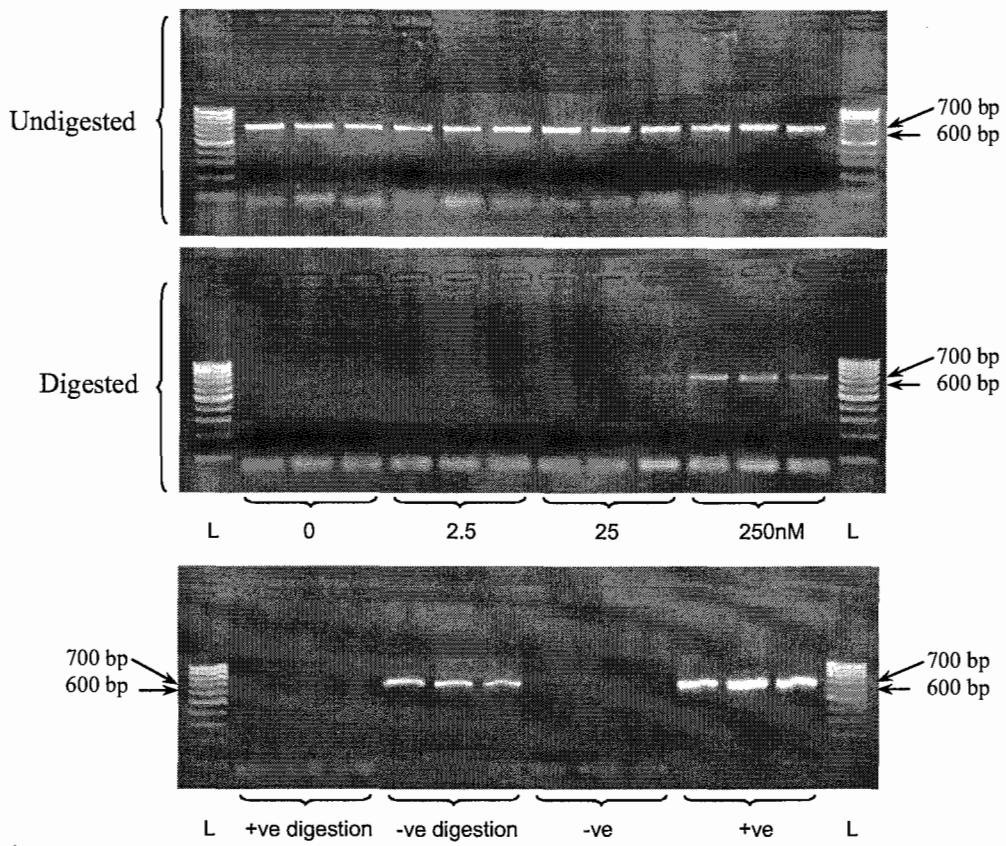

Figure 3.9: PCR amplification before and after *Hin*dIII digestion of DNA isolated from cells transfected with pCMVβ spiked with EtBr. The amplicon size of 677 bp and EtBr spiking concentrations are shown on the Figure. *Hin*dIII digestion of 0.4 ng of the plasmid (+ve digestion) and same plasmid amount with no *Hin*dIII added (-ve digestion). (-ve) and (+ve) are the direct negative and positive controls, respectively. The DNA ladder (L) used is Norgen's PCRSizer.

*Hin*dIII digested and undigested EtBr-spiked DNA (isolated from CHO cells after transfection) was used in a qPCR reaction to quantify the number of mutated AAGCTT recognition sequence. Ten nanograms of DNA was used per reaction (either digested or undigested DNA). The percentage of mutations in the *Hin*dIII site was determined from a standard curve of known initial concentration of plasmid DNA using the following equation:

> % of molecules which lost *Hin*dIII sites= (Plasmid copy number of digested sample/Plasmid copy number of undigested DNA sample) x 100

Figure 3.10 shows the relation between the percentage of molecules with lost *Hin*dIII sites and EtBr spiking concentration. No significant changes were obtained between the lower EtBr concentrations (2.5 and 25 nM) and the control sample without spiking. The percentage of molecules with lost *Hin*dIII sites with the 0, 2.5 and 25 nM concentrations were 0.037, 1.37 and 1.56%, respectively. The number of lost sites increased significantly (at $P<0.05$) over all the EtBr concentrations when using a spiking concentration of 250 nM, with 9.8% lost sites.

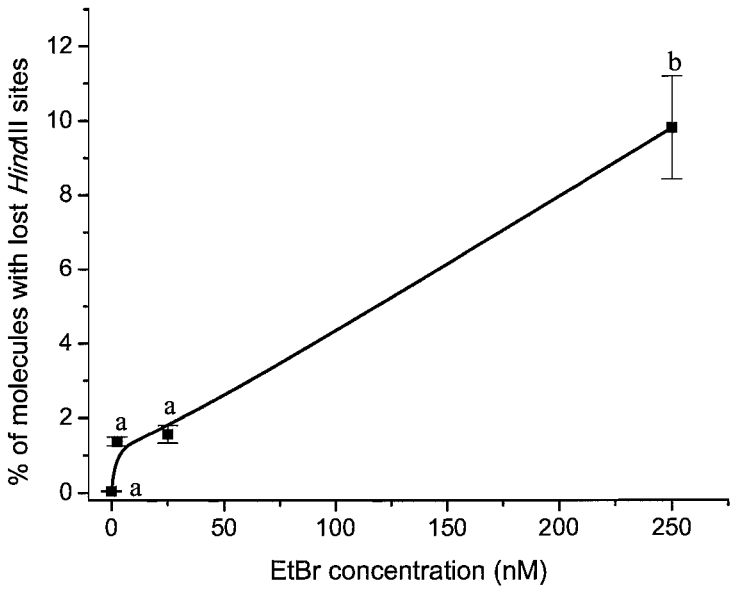

Figure 3.10: Percentage of pCMVβ molecules with lost *Hin*dIII sites. Values were determined through qPCR of EtBr-spiked DNA (concentrations: 0, 2.5, 25 & 250 nM), before and after *Hin*dIII digestion.

3.2- EFFECT OF ADENOVIRAL TRIPARTITE LEADER SEQUENCE AND E1 ON GENE EXPRESSION

Adenoviruses have different elements that may affect gene expression. These elements include the activity of the major late promoter (MLP) and the presence of complete or incomplete tripartite leader sequence (TPL). The E1 region and cell type are also other elements that affect the MLP as well as the TPL. Experiments in this section were done by *in vitro* transfection and transient gene expression and all of the plasmids used were engineered for this study.

3.2.1- Plasmid construction

The expression vector pE1 is a shuttle plasmid that was engineered to contain the expression cassette in addition to the adenovirus serotype 5 (Ad5) E1 region and both the left and right inverted terminal repeats (ITRs). The expression cassette contains the adenovirus MLP and the TPL with green florescence protein (GFP) as a reporter gene and simian virus 40 poly(A) signal (SV40 poly(A)) and is based on pUC19 backbone (see the appendix for a detailed engineering strategy). In addition, another four plasmids (pMGA, pMT_1GA, $pMT_{1,2}GA$ and pMTGA) were constructed with E1 deletion and sequential addition of TPL exons. These plasmids were engineered through an extensive series of cloning steps utilizing various cloning strategies and techniques (see the appendix for a detailed engineering strategy). The final engineered plasmids needed for this study are shown in Figure 3.11.

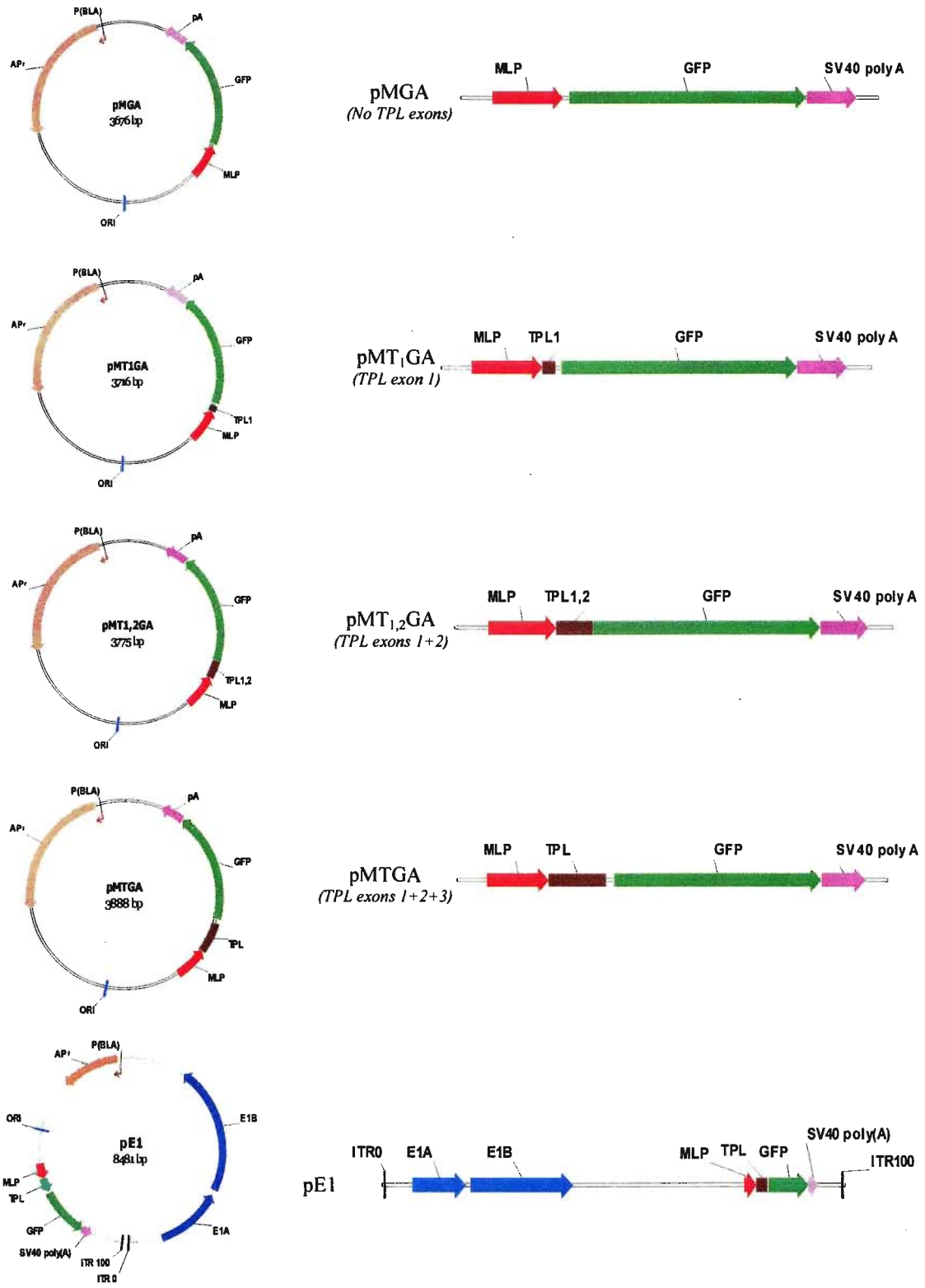

Figure 3.11: Schematic diagrams of the constructed plasmids and their expression cassettes.

3.2.2- Transcription of pE1 genes

To confirm that the various cloned genes and the two promoters are biologically active, it was necessary to examine the transcription of these genes in CHO cells. Briefly, plasmid pE1 was transfected into CHO cells using the calcium phosphate method and cells were harvested 24 hours post-transfection. Total RNA was isolated and treated with DNase to digest any plasmid DNA background. The transcription of three pE1 genes was evaluated by RT-PCR using specific primers. These genes include: GFP driven by the MLP and the E1A and E1B transcripts driven by the E1 promoter. Primers used to detect GFP mRNA were GFP-F and GFP-R, while those used for E1A 13S and E1B 55K mRNAs detection were E1A-13S-F, E1A-13S-R, E1B-55k-F and E1B-55k-R, respectively. The agarose gel of the amplification products shows positive transcription of the three genes (Figure 3.12). The gel indicates that both the MLP and the E1 promoters are active and the genes under their control are being transcribed successfully.

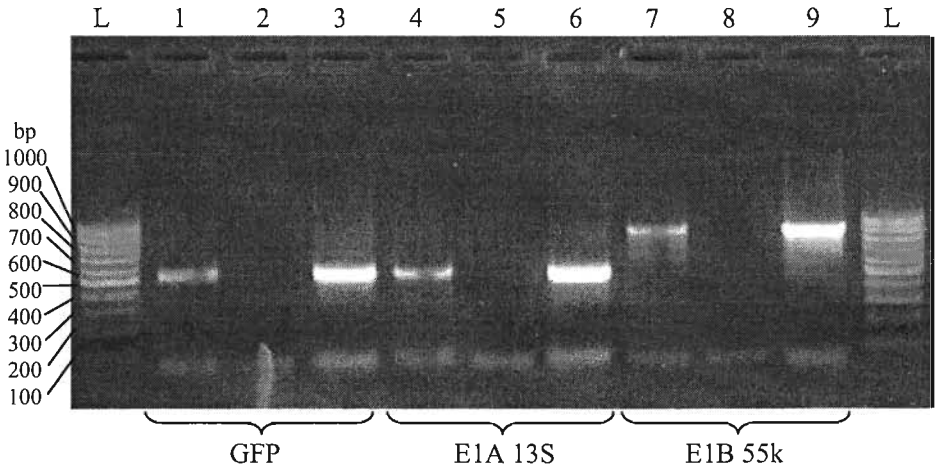

Figure 3.12: Transcription of pE1 genes 24 hours post-transfection in CHO cells. RT-PCR on mRNAs of GFP, E1A 13S and E1B 55k are shown in lanes 1, 4 and 7, with amplification products of 484 bp, 479 bp and 867 bp, respectively. RT-PCR negative controls (water) of the three genes are shown in lanes 2, 5 and 8 with their PCR positive controls in lanes 3, 6 and 9, respectively. The bp size of each ladder band is shown on the left side (Norgen's PCRSizer).

3.2.3- Effect of Ad5 TPL exons on GFP gene expression

The effect of TPL exons sequences on GFP gene expression was evaluated using three parameters: plasmid stability, transcription efficiency and transport rate. Equal amounts from each of the four plasmids (pMGA, pMT_1GA, $pMT_{1,2}GA$ and pMTGA) were transfected into CHO cells using the calcium phosphate method. Transfection was done in triplicate wells in 6-well plates and the medium was replaced 6 hours post-transfection. Transfected cells in each of the triplicate wells were divided into two isolation procedures. The first was used to isolate cytoplasmic and nuclear RNA and the second was used to isolate DNA and total RNA. Samples were collected after 0, 12 and 24 hours post-transfection and processed for further analysis.

3.2.3.1- Plasmids stability

Quantitative PCR was performed on equal amounts of the isolated DNA using the GFP specific primers. A standard curve of known plasmid concentration was used to determine the copy number of each plasmid per cell, at each collection point. Maximum plasmid copy number was reached at 12 hours post-transfection. This starts to decline thereafter with all plasmids in a very similar decay rate. In spite of the fast drop in plasmid copy number at 24 hours, the plasmid copies are still significantly (at $P<0.05$) more than that of the starting copy number at 0 hour (Figure 3.13). Plasmid DNA copy numbers would be used to normalize the mRNA results and obtain the transcription efficiency from each cassette.

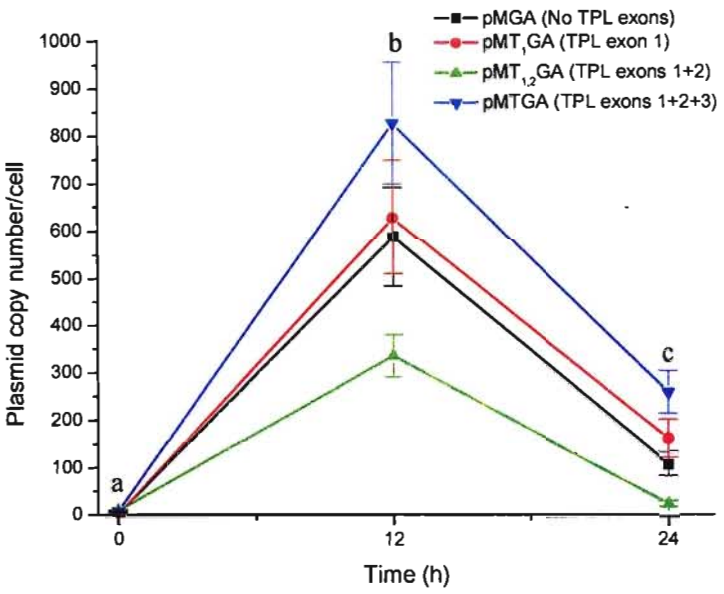

Figure 3.13: Copy numbers of plasmids containing incomplete or complete TPL over 24 hours post-transfection in CHO cells. Copy numbers were obtained by qPCR using a standard curve of known plasmid DNA concentration.

3.2.3.2- GFP mRNA transcription

All isolated RNAs were treated with DNase to digest any residual DNA background and were then cleaned to remove the DNase. A specific PCR for the GFP fragment was used to check the success of the digestion step. The different cleaned RNA samples (total, cytoplasmic and nuclear) in addition to the isolated DNA were quantified to determine their concentration. Equal amounts of total RNA were used as templates of the RT reaction followed by qPCR to measure copy numbers of GFP mRNA using the GFP specific primers and a standard curve of known plasmid concentration (Figure

3.14). The data obtained was statistically analysed by the two-way ANOVA using Tukey's test. The mRNA copy numbers were increasing significantly by 24 hours post-transfection, not by 12 hours, with all of the different cassettes. By 24 hours, higher GFP mRNA copy numbers per cell were obtained from cassettes with no TPL exons or with the complete TPL (three exons). The cassette with the first TPL exon showed non-significant increase in mRNA levels, however, the cassette with the first and second exons showed significant decrease in GFP mRNA content when compared to the control cassette that does not contain any TPL exons.

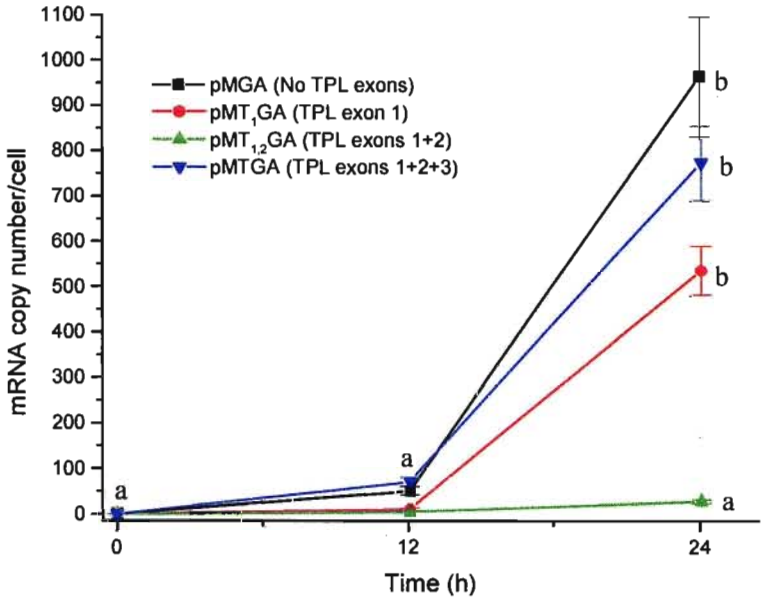

Figure 3.14: GFP mRNA transcripts from cassettes with complete and incomplete TPL exons, over 24 hours post-transfection in CHO cells. Copy numbers were obtained by qPCR using a standard curve of known plasmid DNA concentration.

3.2.3.3- GFP Transcription efficiency

Transcription efficiency was measured from the data obtained for plasmid copy number per cell and GFP mRNA copy number per cell. Values of transcription efficiency

were calculated by dividing the copy number of mRNA by that of their plasmid copies per cell, and are illustrated in Figure 3.15. No significant changes were found in transcription efficiency from all the different plasmids at 12 hours post-transfection, however, at 24 hours the efficiency increased significantly (at $P<0.05$). The highest efficiency was obtained in the absence of TPL exons and the lowest was found when the first and second exons were incorporated. Similar values resulted from using only the first TPL exon or the complete three exons. The differences between the three different cassettes that contain TPL exons were insignificant.

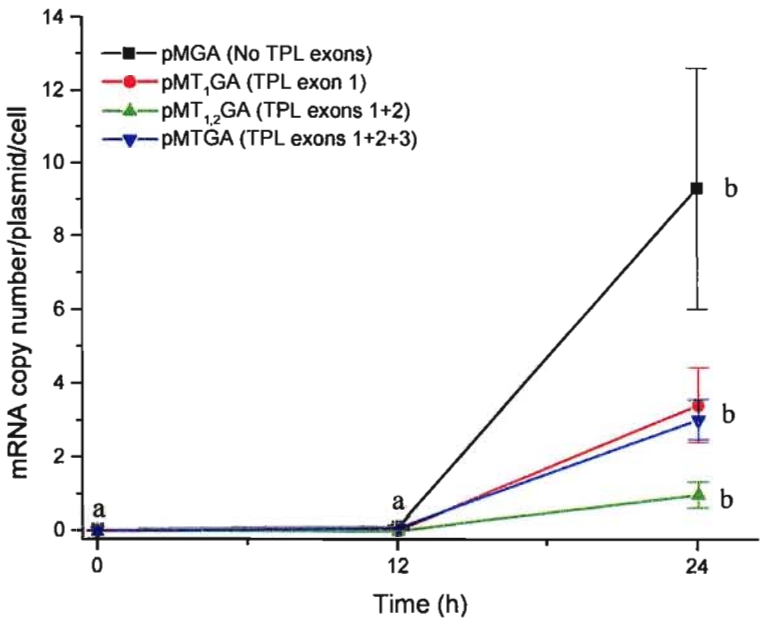

Figure 3.15: Transcription efficiency of GFP mRNA over 24 hours post-transfection in CHO cells, from cassettes with complete and incomplete TPL exons. Efficiency was defined as GFP mRNA copy numbers per plasmid per cell.

3.2.3.4- GFP mRNA transport rate

Both cytoplasmic and nuclear RNA were isolated from the same sample, and they were treated with DNase and then cleaned. RT-qPCR was used in the same way as previously described with total RNA. GFP mRNA copy numbers were quantified by the RT-qPCR using a standard curve and was then calculated per cell. The significant increment (at $P<0.05$) in mRNA copy numbers in both cytoplasmic (Figure 3.16) and nuclear (Figure 3.17) samples was found at 24 hours post-transfection.

In cytoplasmic RNA samples, higher mRNA copy numbers resulted with the lack of TPL exons (pMGA) or the presence of the entire TPL (pMTGA) and minor increments were obtained with the other two plasmids. However, statistical analysis of the data (at $P<0.05$) showed significant changes only between pMGA and $pMT_{1,2}GA$. The trend of GFP mRNA over time in nuclear RNA samples can be placed in a descending order, from higher to lower increment levels, as follows: pMGA, pMTGA, pMT_1GA and $pMT_{1,2}GA$. Similar to cytoplasmic mRNA, statistical significance (at $P<0.05$) was found only between pMGA and $pMT_{1,2}GA$.

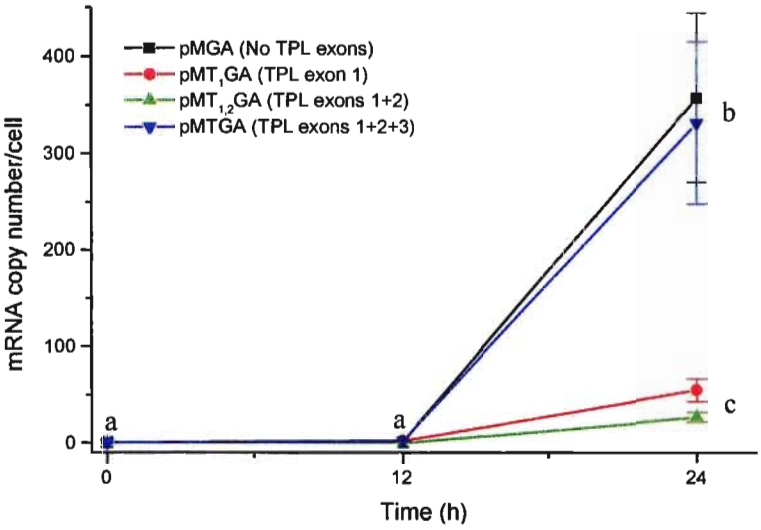

Figure 3.16: Cytoplasmic GFP mRNA transcribed from cassettes with complete and incomplete TPL exons, over 24 hours post-transfection in CHO cells. Copy numbers were obtained by qPCR using a standard curve of known plasmid DNA concentration.

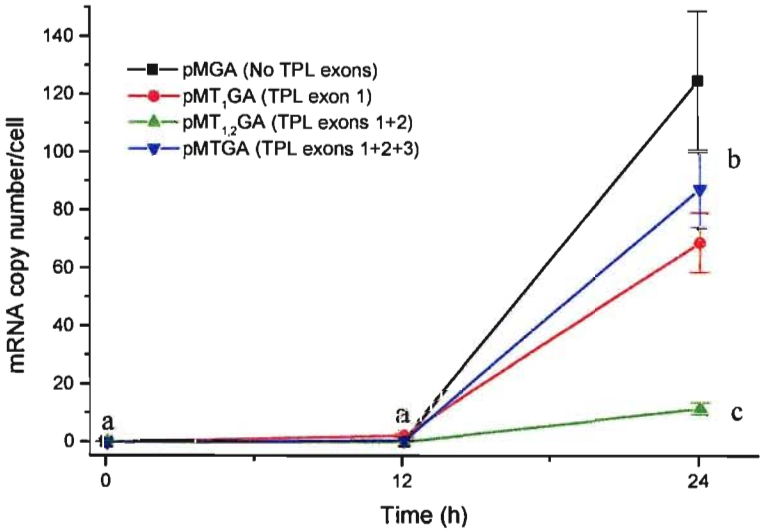

Figure 3.17: Nuclear GFP mRNA transcribed from cassettes with complete and incomplete TPL exons, over 24 hours post-transfection in CHO cells. Copy numbers were obtained by qPCR using a standard curve of known plasmid DNA concentration.

The rate of GFP mRNA transport from the nucleus to the cytoplasm was calculated from the data obtained from cytoplasmic and nuclear GFP mRNA quantification. The percentage of transport rate at each time point was calculated according to the following equation:

$$\%T = \frac{mRNA_t^C}{mRNA_t^C + mRNA_t^N} X100$$

where T is the transport rate, C and N stands for cytoplasmic and nuclear RNAs at time t. mRNA was measured in our experiment as copy number per cell. The data is illustrated in Figure 3.18 and statistical analysis was performed by the two-way ANOVA using Tukey's test. No significant change (at $P<0.05$) was noted in the transport rate between 12 hours and 24 hours post-transfection, with all the used plasmids. Significantly lower transport rate was observed with mRNA transcribed from pMT_1GA (only the first TPL exon), when compared to the other three plasmids.

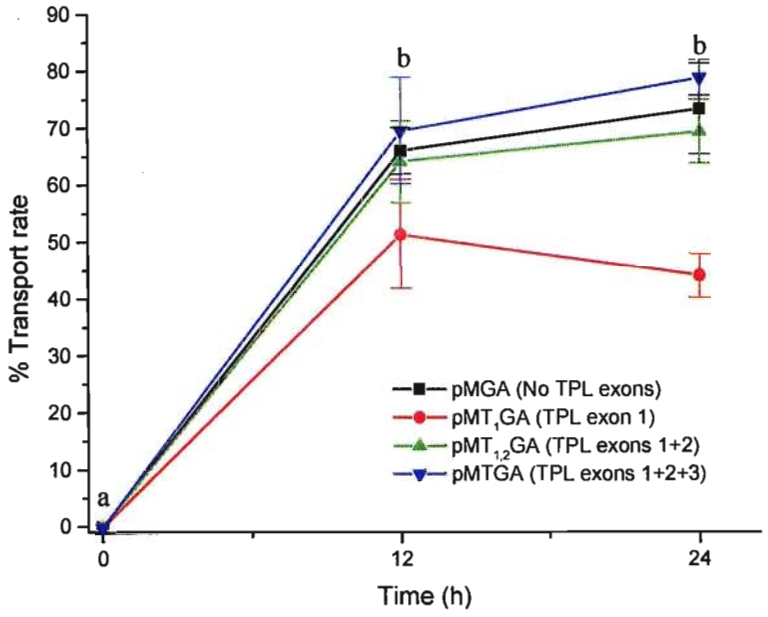

Figure 3.18: GFP mRNA percentage transport rate after transcription from cassettes with complete and incomplete TPL exons, over 24 hours post-transfection in CHO cells. Percentage transport rate was calculated from data obtained after estimating mRNA copy numbers in the cytoplasm and nucleus by RT-qPCR.

3.2.3.5- Integrity of the GFP mRNA transcripts

RT-PCR was used to ensure the presence of the incomplete and complete TPL in the 5' end, upstream to the GFP mRNA. Specific primers (TPLate1-F & GFPlate-R) were designed in both the first TPL exon as well as the GFP sequence. The amplicon size of these primers varies according to the incorporated TPL exons (Figure 3.19). Reverse transcription was performed on DNase treated and cleaned RNA samples isolated 24 hours post-transfection. Then, the RT products together with negative and positive RT controls were used in PCRs performed using *Taq* polymerase and the amplification products were visualized by agarose gel electrophoresis (Figure 3.20).

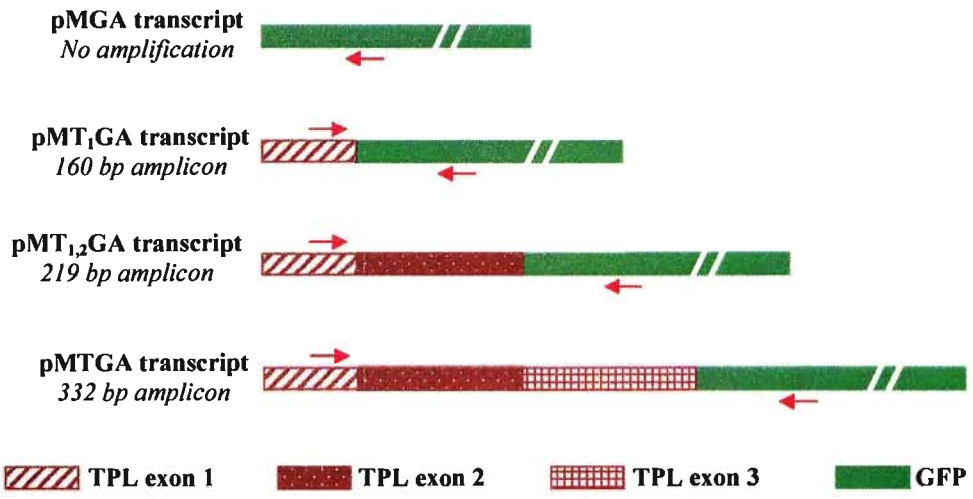

Figure 3.19: Schematic diagrams of the GFP mRNA transcripts with the different TPL constructs. The red arrow refers to the position of the PCR primers and the amplicon size from each transcript is shown.

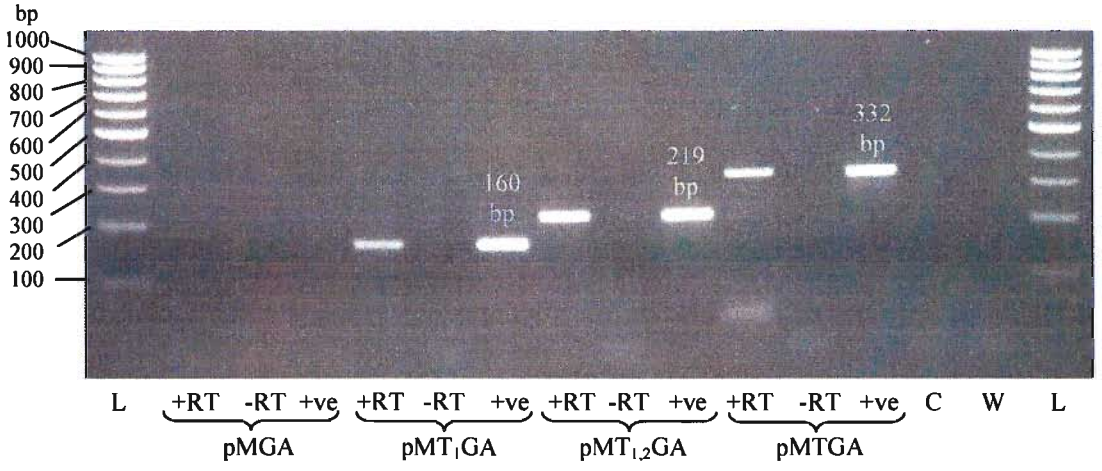

Figure 3.20: RT-PCR amplification of the incomplete and complete TPL attached to GFP mRNA. The different samples were collected at 24 hours post-transfection in CHO cells. The used conditions for each plasmid are: RNA with RT (+RT), RNA with no RT (-RT) and the template plasmid DNA (+ve). CHO DNA (C) as well as water (W) was used as negative controls. Plasmids names and amplicon size are shown on the Figure. Lanes L are Norgen's PCRSizer DNA ladder. The bp size of each ladder band is shown on the left side of the picture.

3.2.4- Effect of the adenoviral E1 on plasmid stability and MLP activity in CHO cells

The two plasmids, pE1 and pMTGA have exactly the same GFP expression cassette in identical plasmid, except for the Ad5 E1 region that is missing in pMTGA. This allows us to look at the effect of the E1 region on plasmid stability as well as the expression from the MLP. The two plasmids were transfected into CHO cells, triplicate wells for each plasmid, using Lipofectamine 2000. Following transfection, cells were collected from the transfected wells over 14 days (0, 1, 2, 3, 5, 8, 11 & 14 days) post-transfection. CHO cells transfected with pUC19 were included as a negative control. Samples were processed to isolate DNA and RNA, both from same sample, and were then used afterwards in the different analyses. DNA was quantified and used to investigate plasmid stability, transcription and translation over the experimental time.

3.2.4.1- Plasmid stability

Equal amounts of DNA were used in the qPCR reaction with the GFP specific primers. Plasmids copy numbers were determined from a standard curve of a known plasmid concentration and then converted to copy number per CHO cell and illustrated in Figure 3.21. A two-way ANOVA using Tukey's test was used to analyze the data. Plasmid copy number reaches its highest concentration one day post-transfection and starts to decline after this to reach insignificant values (at $P<0.05$) from the starting copy numbers in day 0. The plasmid pMTGA shows significantly higher copy number (at $P<0.05$) after one day post-transfection than pE1.

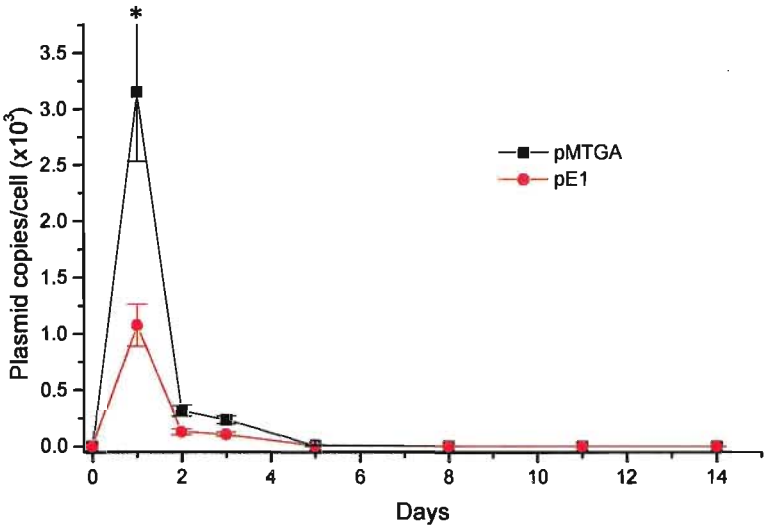

Figure 3.21: Copy numbers of pMTGA and pE1 over 14 days post-transfection in CHO cells. Copy numbers were obtained by qPCR using a standard curve of known plasmid DNA concentration.

3.2.4.2- GFP transcription efficiency

MLP activity in the presence of E1 was investigated by looking at GFP mRNA transcription from both plasmids over time. RNA samples were treated with DNase and cleaned afterwards. The samples were quantified and run in an RT reaction to generate the first strand complementary DNA (cDNA) that was later used as a template for qPCR with specific GFP primers. Figure 3.22 shows the GFP mRNA copy number in each sample as quantified using a standard curve. The results were analysed statistically by the two-way ANOVA using Tukey's test. The mRNA transcription was found to be significantly increasing (at $P<0.05$) on the second and third days post-transfection, but started to decline until the baseline was almost reached by day five. pE1 showed significant higher levels of GFP mRNA per cell within the period between day one and day three post-transfection.

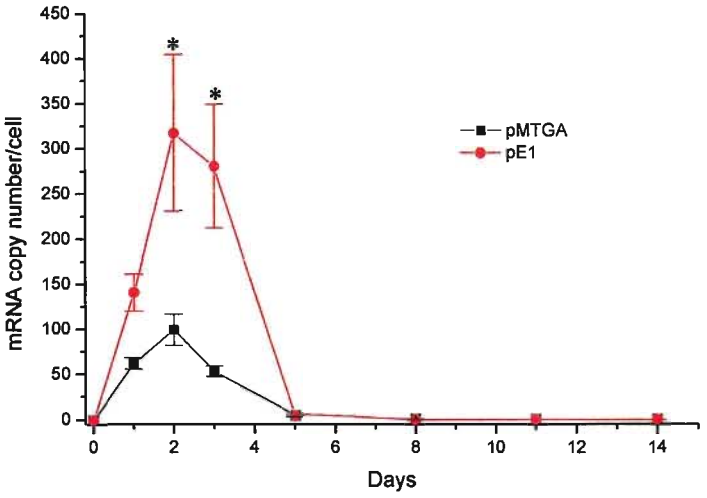

Figure 3.22: GFP mRNA transcripts from pMTGA and pE1 over 14 days post-transfection in CHO cells. Copy numbers were obtained by qPCR using a standard curve of known plasmid concentration.

The transcription efficiency was calculated as the copy number of GFP mRNA produced from each plasmid per cell (Figure 3.23). The efficiency from the pE1 plasmid was higher than pMTGA after day one and until day eight post-transfection. The results were analysed statistically by the two-way ANOVA using Tukey's test (at $P<0.05$) and the difference between the efficiencies from the two plasmids was significant at the peak period. However, from day eight on, the efficiencies were close to the baseline.

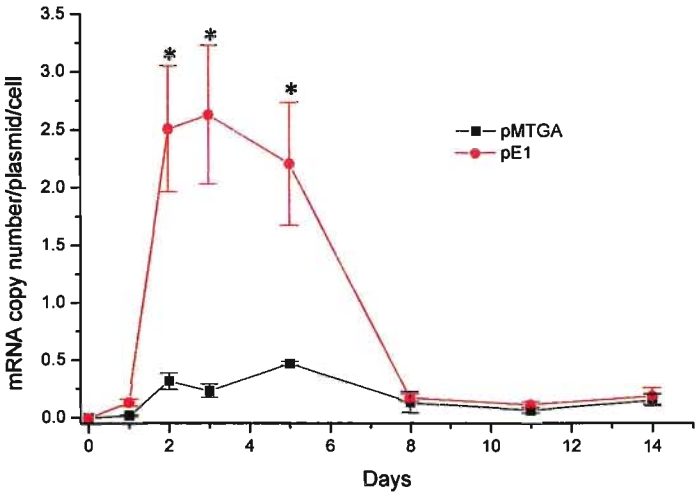

Figure 3.23: Transcription efficiency of GFP mRNA over 14 days post-transfection of pMTGA and pE1 in CHO cells. Efficiency was defined as GFP mRNA copy numbers per plasmid per cell. Copy numbers per cell of plasmid DNA and GFP mRNA were estimated by qPCR using a standard curve of a known plasmid concentration.

3.2.4.3- GFP translation

The GFP was quantified from its fluorescence intensity by measuring the relative fluorescence units (RFU) in 50,000 cell. The data obtained was graphed and analyzed statistically at a significance level of less than 0.05 (Figure 3.24). The results show a significant increase in protein expression from the pE1 plasmid over pMTGA after the second day and up until the eighth day post-transfection. The values reached almost the baseline on day 11 post-transfection.

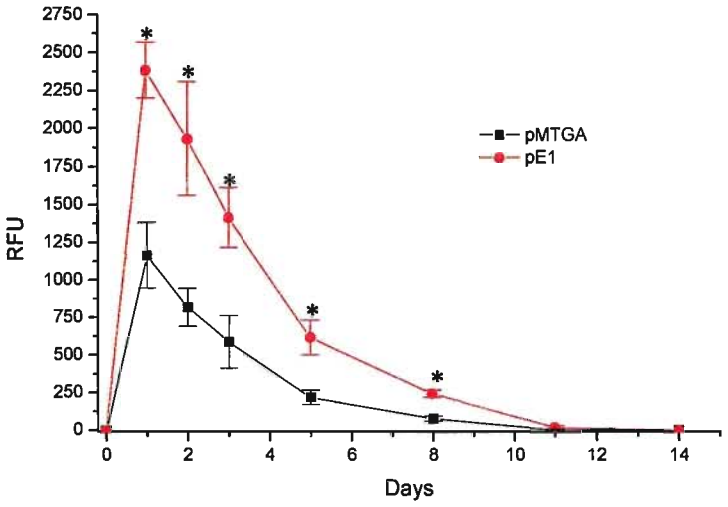

Figure 3.24: GFP fluorescence intensity over 14 days post-transfection of pMTGA and pE1 in CHO cells. Fluorescence intensity was measured by the relative fluorescence units (RFU) of equal cell counts.

3.2.5- Plasmid pE1 stability, transcription and translation in CHO and HEK 293 cells

To evaluate MLP activity in the presence of pre-existing Ad5 E1 gene products, HEK 293 and CHO cells were transfected with pE1 using Lipofectamine 2000 and various parameters were evaluated including plasmid stability, GFP transcription and translation. Negative controls for each cell line transfected with pUC19 were included. DNA and RNA were isolated over time, both from the same sample and used for downstream analysis. Collection times were as follow: 0, 1, 2, 3, 5, 8, 12 and 14 days post-transfection.

3.2.5.1- Plasmid stability

DNA was quantified and equal amounts were used in a qPCR reaction using GFP specific primers. A standard curve of known pE1 concentration was used to determine the plasmid copy number per cell for each collection time, since the amount of genomic DNA per HEK 293 cells and CHO cell is 3.5 pg and 3.1 pg, respectively (Gregory, 2005). The data obtained is illustrated in Figure 3.25. A two-way ANOVA using Tukey's test was used in statistical analysis, at a significance level of 0.05. Both cell lines showed significant high levels of plasmid copy numbers only on day one post-transfection. Plasmid copies started to drop after this to reach insignificant levels compared to the baseline. When looking at the differences between both cell lines, CHO cells showed significant higher ability (at $P<0.05$) in uptaking plasmid DNA than HEK 293. This is observed in the first two days post-transfection. However, the trend of plasmid stability seems to be identical in both cell lines.

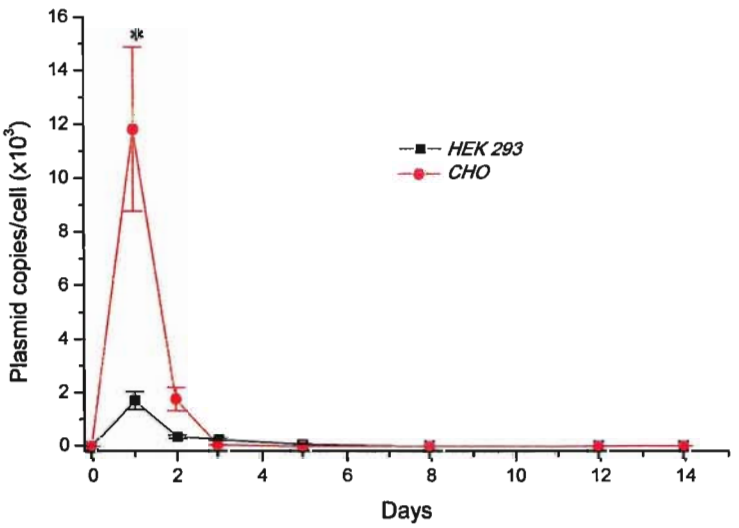

Figure 3.25: Copy numbers of pE1 over 14 days post-transfection in HEK 293 and CHO cells. Copy numbers were obtained by qPCR using a standard curve of known plasmid concentration.

3.2.5.2- GFP transcription efficiency

DNA residues in the isolated RNA were digested by DNase treatment followed by RNA cleaning. After quantification, equal amounts of RNA were used in an RT reaction to synthesise the first strand cDNAs. Following this, equal volumes of the RT product were used in a qPCR reaction using the GFP specific primers. A standard curve of known pE1 concentration was used to determine the GFP mRNA copy number. The amount of total mRNA per HEK 293 cell and CHO cell is 8.88 pg and 8.17 pg, respectively (determined by total RNA isolation and spectrophotometric quantification). These numbers were used to determine the copy number of GFP mRNA per cell (Figure 3.26). A significant (at $P<0.05$) increase in GFP mRNA was obtained on the second and third days post-transfection. HEK 293 cells showed significantly more GFP mRNA transcripts per cell than CHO cells, especially on the third day post-transfection. Both cell lines show no significant differences from each other or the baseline over days eight to 14 post-transfection.

Transcription efficiency was calculated from the plasmid copy number and GFP mRNA copy number per cell. Figure 3.27 shows the transcription efficiencies in both cell lines over the 14 day time period. The statistical analysis of the data at the significance level of 0.05 showed overall significant higher transcription efficiency in HEK 293 cells over CHO cells.

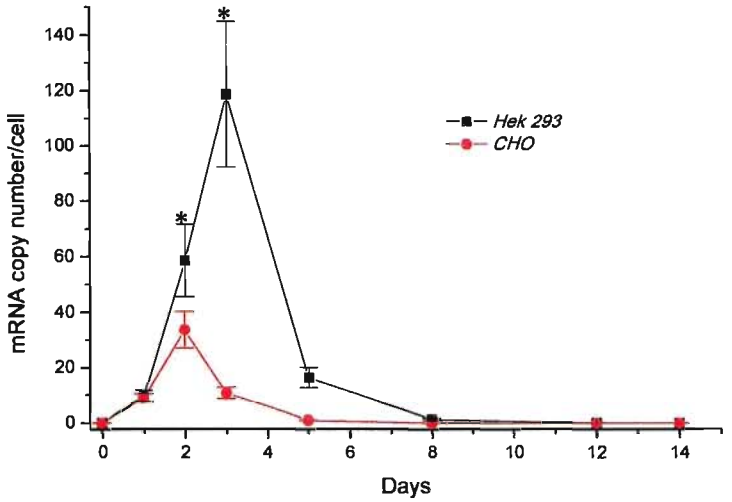

Figure 3.26: GFP mRNA transcripts from pE1 over 14 days post-transfection in HEK 293 and CHO cells. Copy numbers were obtained by qPCR using a standard curve of known plasmid DNA concentration.

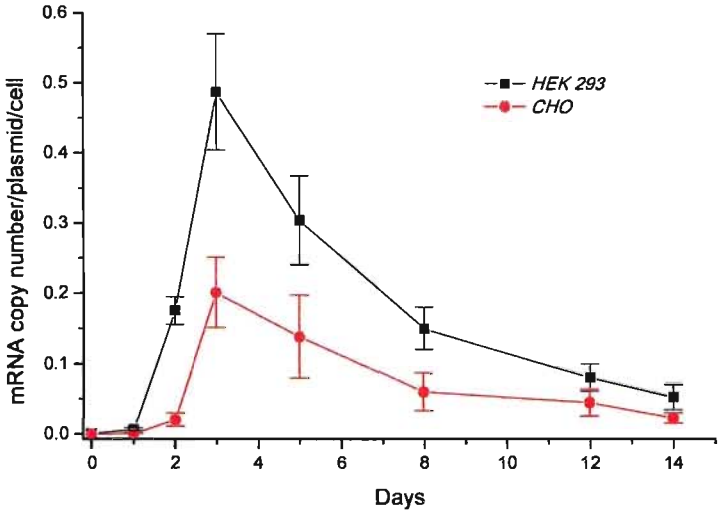

Figure 3.27: Transcription efficiency of GFP mRNA over 14 days post-transfection of pE1 into HEK 293 and CHO cells. Efficiency was defined as GFP mRNA copy numbers per plasmid per cell. Copy numbers per cell of plasmid DNA and GFP mRNA were estimated by qPCR using a standard curve of a known plasmid concentration.

3.2.5.3- GFP translation

The expressed GFP in both cell lines was measured by its fluorescence intensity and was significantly (at $P<0.05$) increased in both cell lines from day one to day eight post-transfection. The GFP fluorescence intensity detected in HEK 293 cells over this period of time was significantly higher than that obtained from CHO cells. Fluorescence intensity remained close to the baseline after day eight post-transfection in both cell lines (Figure 3.28).

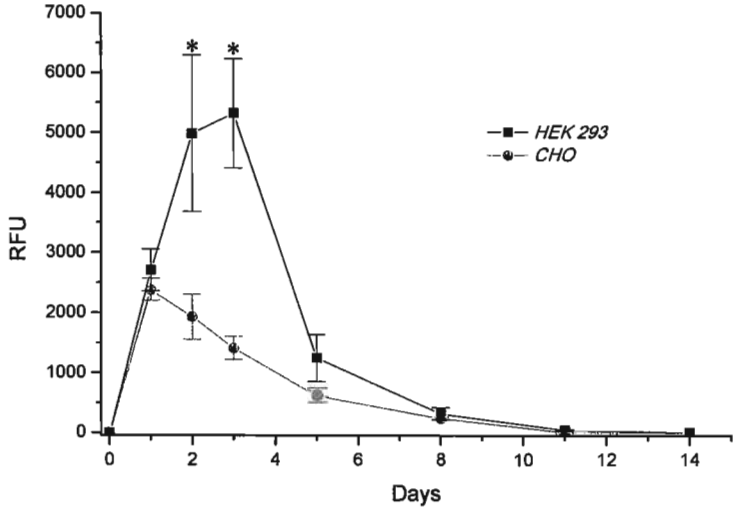

Figure 3.28: GFP fluorescence intensity over 14 days post-transfection of pE1 in HEK 293 and CHO cells. Fluorescence intensity was measured by the relative fluorescence units (RFU) of equal cell counts.

3.3- Construction of a Cell Line Expressing the Ad5 E2 and Protease Genes

3.3.1- pE2 construction

Engineering a plasmid containing the Ad5 E2 and viral protease genes is essential for the establishment of a cell line that expresses these genes, constitutively or upon induction by the Ad5 E1 genes. For this purpose, the pE2 plasmid was engineered to contain all the needed sequences for the cell line construction and selection. We used pUC19neo as a backbone plasmid which contains the neomycin resistance cassette for selection in mammalian cells. The construction of pE2 (Figure 3.29) involved the cloning of E2 (E2A and E2B), the E2 promoter and viral protease. E2A encodes for the single stranded DNA binding protein (ssDBP), whereas E2B encodes for viral polymerase and precursor terminal protein (pTP) and all are driven by the E2 promoters. Expression of the viral protease is driven by the MLP which is located on the complementary strand of the E2B region. All of the viral fragments of this construction were obtained from the plasmid pBHGfrtdel1,3FLP, which contains the adenoviral backbone with deleted E1 and E3 regions (see the appendix for a detailed engineering strategy).

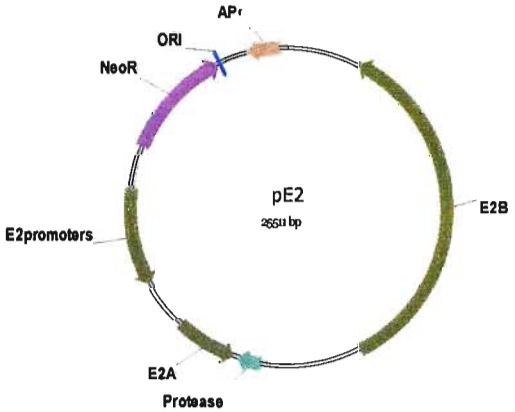

Figure 3.29: Schematic diagrams of pE2.

3.3.2- Evaluation of pE2 gene transcription in HEK 293 cells and CHO cells

The basic expression levels from the pE2 plasmid were performed by calcium phosphate transfection of the cesium chloride banded preparation of the plasmid into both HEK 293 and CHO cells. Samples were collected and handled as previously described with pE1 transfection. RT-PCR was used to detect the transcription of the different pE2 genes in the two cell lines. Four genes were tested including three in the E2 region in addition to the viral protease. E2 promoters drive the transcription of the three E2 genes, which are the ssDBP, viral polymerase and pTP. The expression of the viral protease is driven by the MLP located on the complementary strand of the E2B region. The specific primers used were DBP-F and DBP-R for ssDBP, VPol-F and VPol-R for viral polymerase, pTP-F and pTP-R for the pTP and VPro-F and VPro-R for the viral polymerase. The gel picture of the PCR product shows positive amplification of all genes in HEK 293 cells (Figure 3.30). On the other hand, viral protease was the only transcribed gene in CHO cells (Figure 3.31).

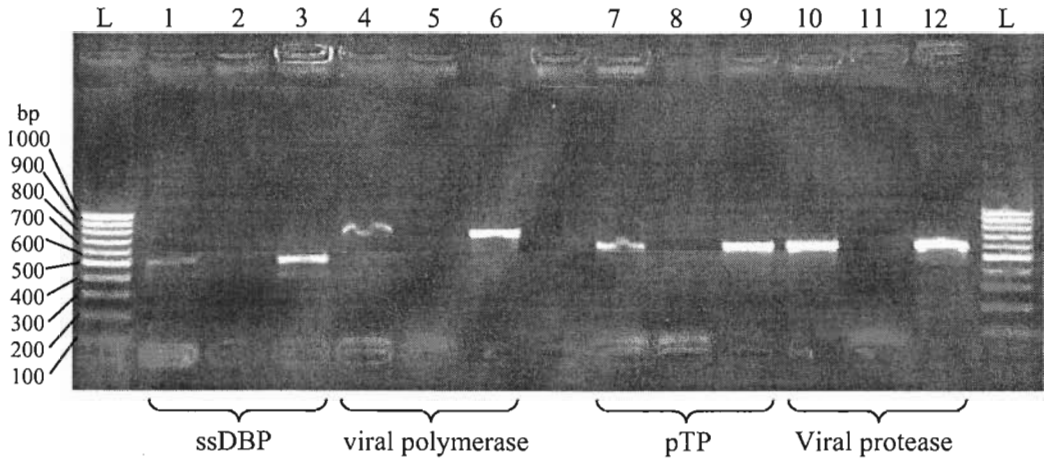

Figure 3.30: Transcription of pE2 genes 24 hours post-transfection in HEK 293 cells. RT-PCR on mRNAs of ssDBP, viral polymerase, pTP and viral protease are shown in lanes 1, 4, 7 and 10, with amplification products of 489 bp, 701 bp, 565 bp and 562 bp, respectively. RT-PCR negative controls (water) of the four genes are shown in lanes 2, 5, 8 and 11 with their PCR positive controls in lanes 3, 6, 9 and 12, respectively. The bp size of each ladder band (Norgen's PCRSizer) is shown on the left side.

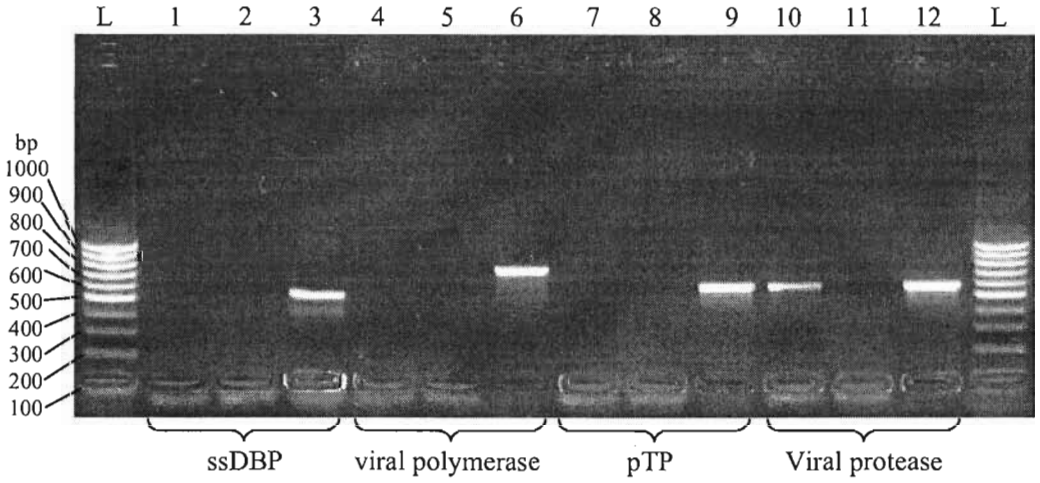

Figure 3.31: Transcription of pE2 genes 24 hours post-transfection in CHO cells. RT-PCR on mRNAs of ssDBP, viral polymerase, pTP and viral protease are shown in lanes 1, 4, 7 and 10. RT-PCR negative controls (water) of the four genes are shown in same order in lanes 2, 5, 8 and 11 with their PCR positive controls in lanes 3, 6, 9 and 12, with amplification products of 489 bp, 701 bp, 565 bp and 562 bp, respectively. The bp size of each ladder band (Norgen's PCRSizer) is shown on the left side.

3.3.3- Co-transfection and evaluation of pE1 and pE2 stability and expression in CHO cells

pE1 and pE2 plasmids were co-transfected into CHO cells using Lipofectamine 2000, to guarantee high levels of co-transfection. Different molar ratios were used from each plasmid to verify their effect on gene expression over 15 days. The used pE1:pE2 molar ratios were: 0:0, 1:0, 0:1, 1:1, 1:3, 1:6, 1:9, 3:1, 6:1 and 9:1. Samples were collected at days 0, 1, 3, 5, 8, 12 and 15 post-transfection. RNA, DNA and protein were all isolated from the same samples and used for analysis of plasmid stability and gene expression.

3.3.3.1- Plasmid stability

Stability of both pE1 and pE2 were investigated over time using the isolated DNA of the different samples. After the spectrophotometric quantification of DNA, the GFP primers and the pTP primers were used in a PCR reaction with the same starting amount of DNA template. The agarose gel electrophoresis of the GFP PCR product (Figure 3.32) showed positive amplification in almost all of days 1 and 3. No observed changes in pE1 stability were obtained with the different molar ratios of either pE1 or pE2. A similar profile was resulted from pTP PCR (Figure 3.33). Neither of the plasmids was affected by the presence of the other plasmid or by the different molar ratios.

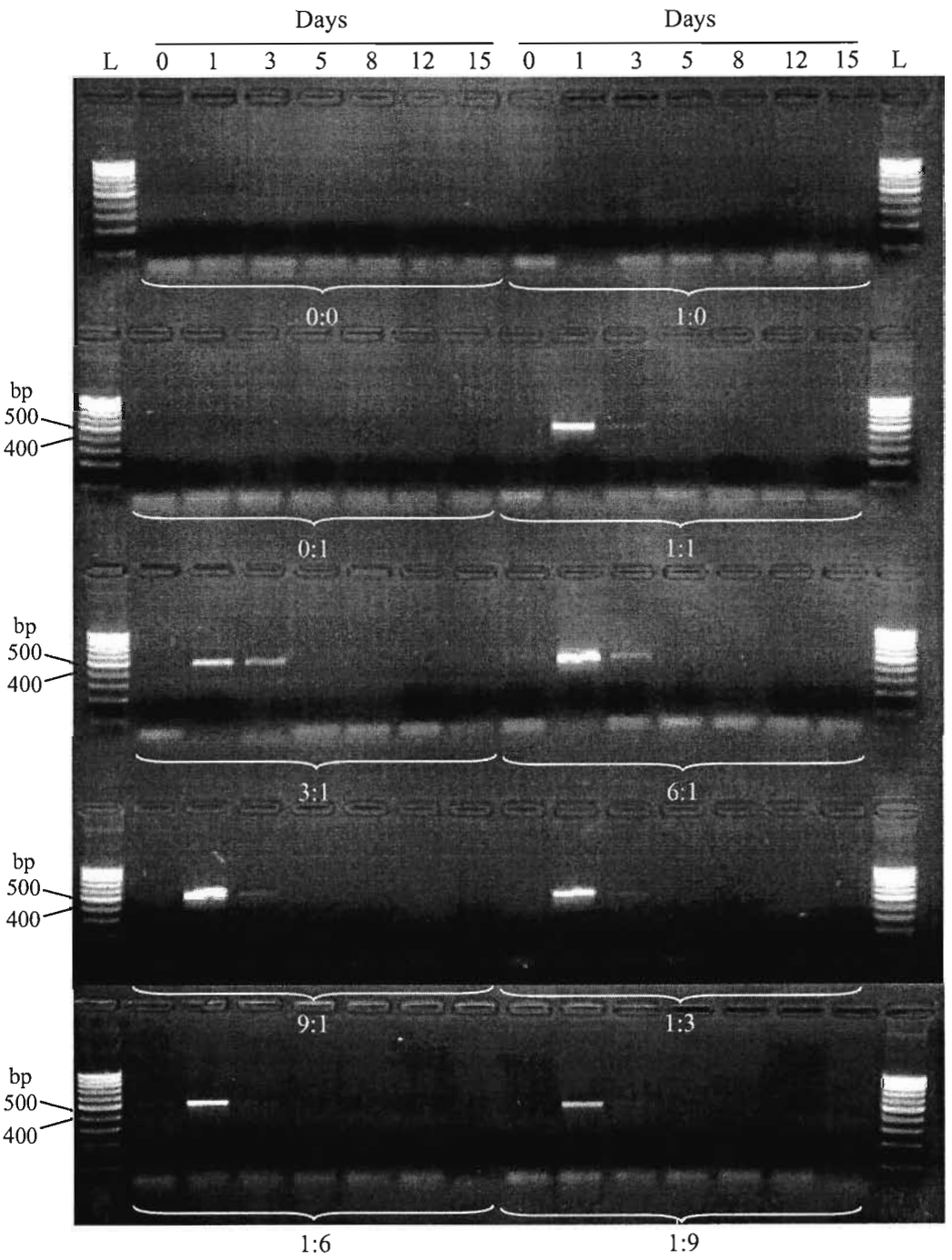

Figure 3.32: pE1 stability in CHO cells, over 15 days, after co-transfection with different molar ratios of pE1 and pE2. Post-transfection sample collection times are shown on the top of the Figure. The molar ratio of pE1:pE2 is written underneath its collection set, after performing PCR amplification with a product size of 484 bp. Lanes L are Norgen's PCRSizer DNA ladder.

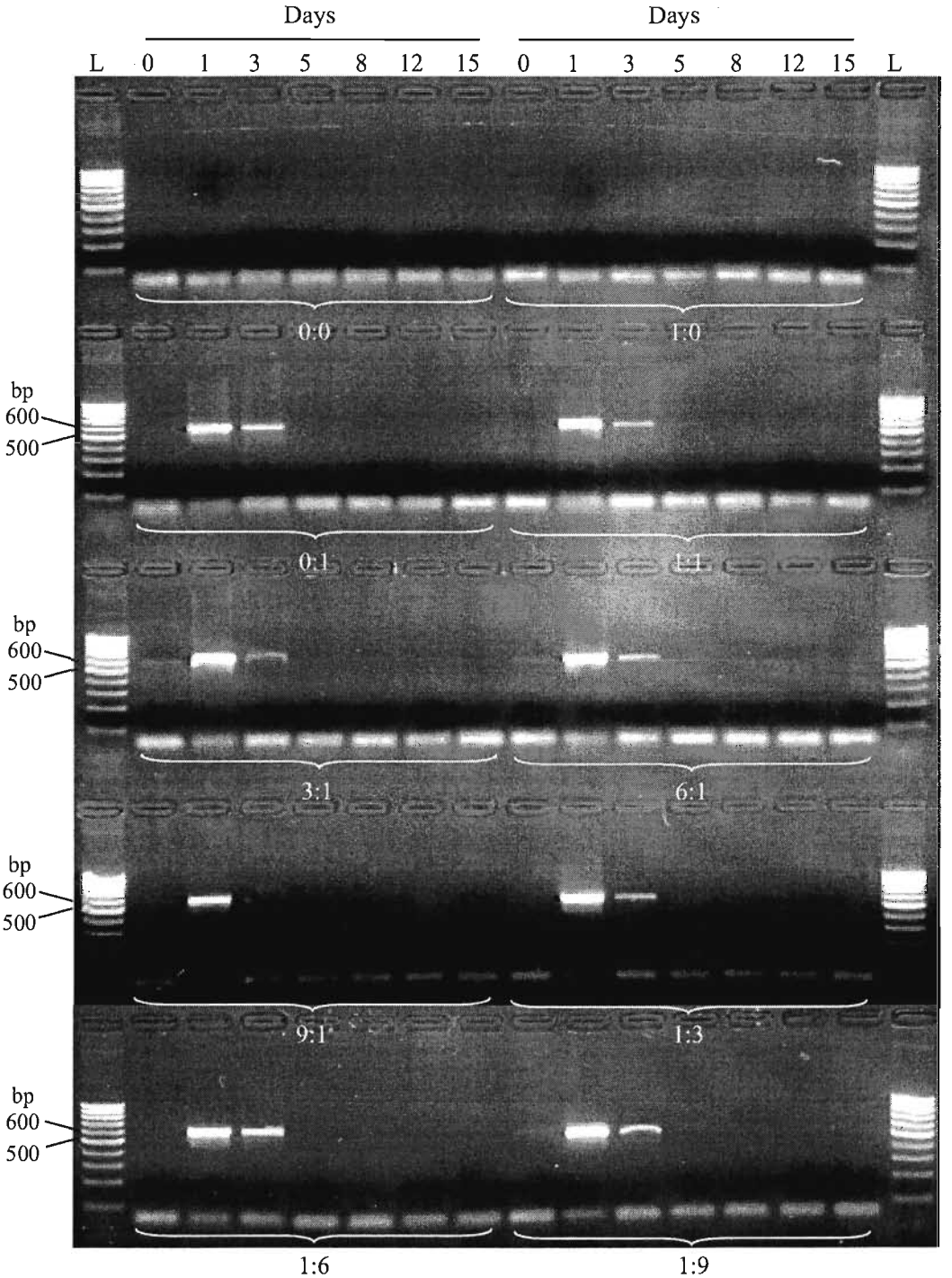

Figure 3.33: pE2 stability in CHO cells, over 15 days, after co-transfection with different molar ratios of pE1 and pE2. Post-transfection sample collection times are shown on the top of the Figure. The molar ratio of pE1:pE2 is written underneath its collection set, after performing PCR amplification with a product size of 565 bp. Lanes L are Norgen's PCRSizer DNA ladder.

3.3.3.2- Transcription levels

Transcription of GFP mRNA (pE1) and both pTP and viral protease (pE2) were investigated by RT-PCR. First, isolated RNA was treated with DNase to digest any plasmid DNA contamination. RNA was then cleaned and quantified. Equal amounts of RNA were used in an RT reaction to synthesize the first strand cDNA of the different mRNAs. Equal volumes were used from the RT product to perform a PCR reaction using specific primers for GFP, pTP and viral protease (VPro). Agarose gel electrophoresis was used to identify the PCR products of the different reactions. Positive amplification from GFP mRNA was obtained only in day 1 and days 1-3 of co-transfected pE1:pE2 molar ratios of 6:1 and 9:1, respectively (Figure 3.34). No amplification was obtained with any of the different co-transfection ratios after performing RT-PCR on pTP mRNA (data not shown). However, positive amplification from viral protease mRNA was obtained only in day 1 of co-transfected pE1:pE2 molar ratios of 1:6 and 1:9 (Figure 3.35).

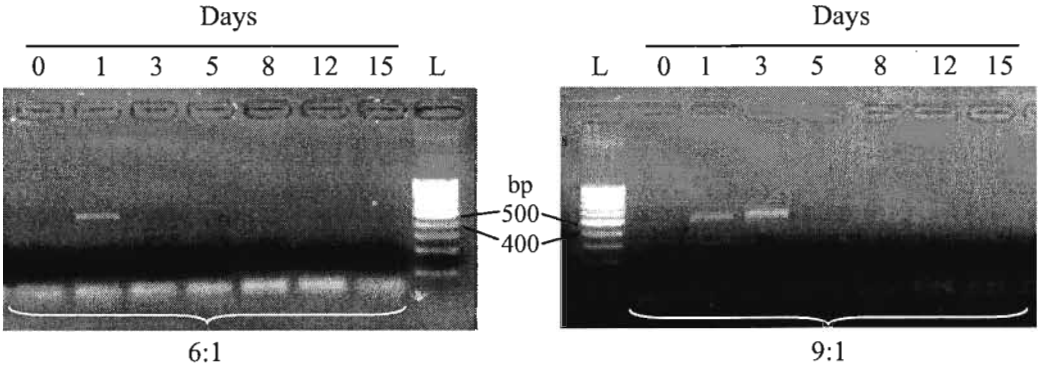

Figure 3.34: GFP mRNA transcription in CHO cells over 15 days, after co-transfection with pE1 and pE2. Post-transfection sample collection times are shown on the top of the Figure. The molar ratio of pE1:pE2 is written underneath its collection set, after performing RT-PCR amplification with a product size of 484 bp. Lanes L are Norgen's PCRSizer DNA ladder.

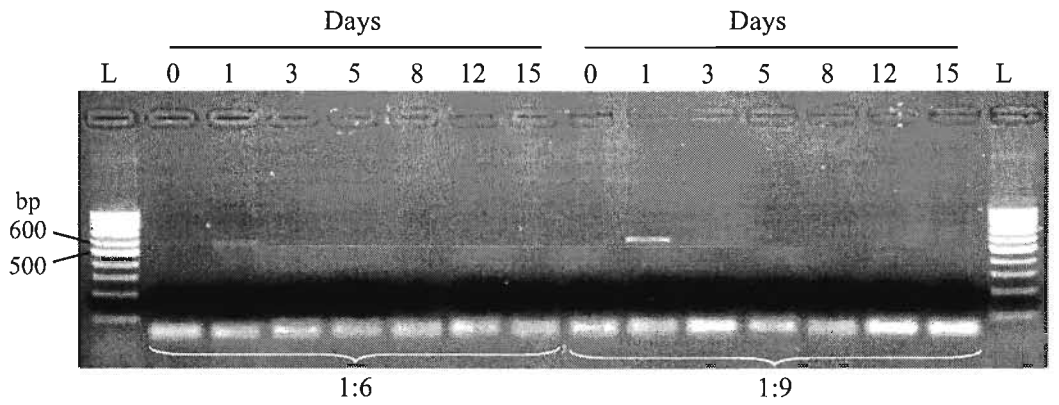

Figure 3.35: Viral protease mRNA transcription in CHO cells over 15 days, after co-transfection with pE1 and pE2. Post-transfection sample collection times are shown on the top of the Figure. The molar ratio of pE1:pE2 is written underneath its collection set, after performing RT-PCR amplification with a product size of 562 bp. Lanes L are Norgen's PCRSizer DNA ladder.

3.3.4- Transfection and selection of CHO cell line

The construction of CHO-E2 cell line is based on the transfection of CHO cells with the pE2 plasmid followed by the specific selection of positively transfected cells using G418. Cells that have the pE2 plasmid will resist the G418 selection due to the presence of the neomycin resistant cassette. The selection will force the cells to retain the plasmid as well as force its integration into the genomic DNA. The integration of this circular plasmid is completely random with regards to both the site of plasmid linearization as well as genomic integration site. Therefore, the restriction enzyme *NdeI* was used to linearize the plasmid with heat inactivation after the complete digestion, prior to plasmid transfection into CHO cells. Only one restriction site of *NdeI* is present in the pE2 plasmid and it does not interfere with any of the regulatory or coding sequences of the different cassettes (Figure 3.36).

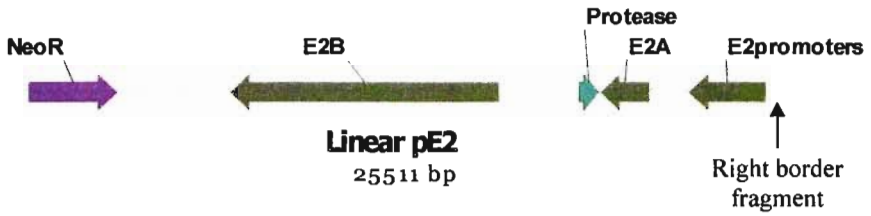

Figure 3.36: Map of *NdeI* linearized pE2.

After calcium phosphate transfection and G418 selection, cells were kept under the selection pressure for 14 days till the small resistant foci started to form. After that, 96 foci were picked under a light microscope and grown in separate wells in four of 24-well plates. The picked foci were kept for an additional three days under the selection pressure of G418. Fifty-six of the picked foci continued to grow afterwards and were split with replating half of each well and harvesting the other half for DNA isolation.

PCR amplification of the right border of the linear plasmid was used to screen for the presence of the full size linear pE2, since the left borders already contain the neomycin resistant cassette. Two specific primers were used in the amplification reaction, named E2RB-F and E2RB-R. Amplification was obtained only in five foci and they were designated CHO-E2-1 to CHO-E2-5 (Figure 3.37). These five foci were transferred into larger plate and kept under G418 selection for an additional 40 days.

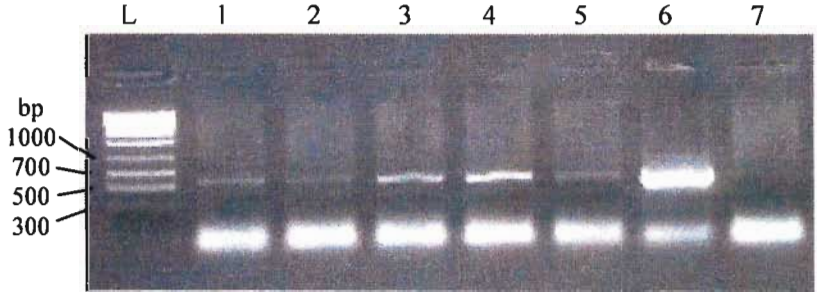

Figure 3.37: Amplification of linear pE2 right borders from foci CHO-E2-1 to CHO-E2-5. DNA isolated from the different foci was used in a PCR reaction of an amplicon size of 558 bp. Lanes 1-5 shows the amplification from the five foci, respectively. Lane 6 is the positive control, lane 7 is CHO DNA and lane L is Norgen's MidRanger DNA ladder.

3.3.5- Detection of the different pE2 genes in the constructed CHO-E2 cell lines

The four main genes of pE2 were detected in the newly constructed cell lines that were kept under the selection pressure for two months. Primers that have been used to test the basic transcription levels of the different pE2 genes were used to screen for the presence of these genes in the foci. All of the foci showed positive amplification of ssDBP, viral polymerase, pTP and the viral protease (Figures 3.38-3.41). Two negative controls were used, the first is DNA isolated from CHO cells and the second is water. The used positive control was the pE2 plasmid.

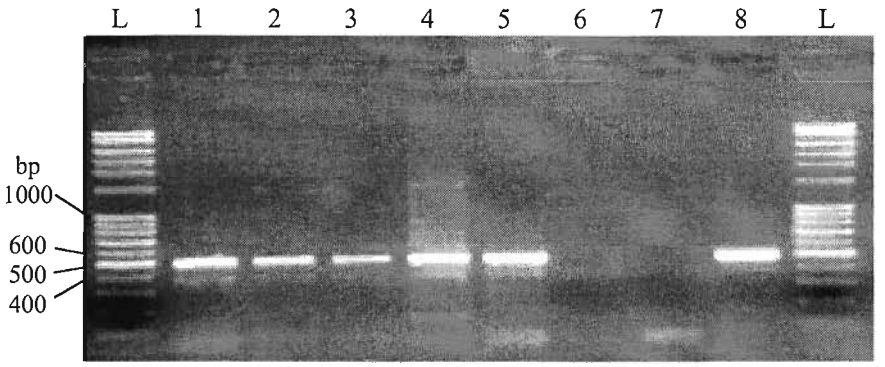

Figure 3.38: PCR amplification of ssDBP fragment from cell lines CHO-E2-1 to CHO-E2-5. DNA isolated from the different cell lines was used in a PCR reaction of an amplicon size of 489 bp. Lanes 1-5 shows the amplification from the five cell lines, respectively. Lane 6 is CHO DNA, lane 7 is the negative control (water), lane 8 is the positive control and lanes L are Norgen's FullRanger DNA ladder.

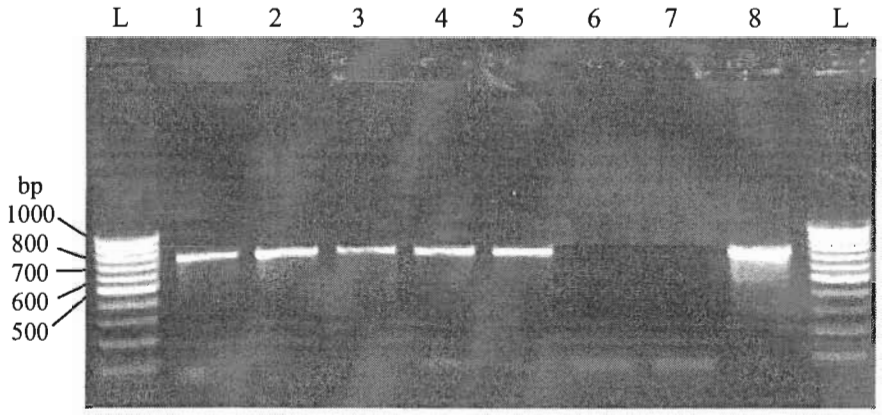

Figure 3.39: PCR amplification of viral DNA polymerase fragment from cell lines CHO-E2-1 to CHO-E2-5. DNA isolated from the different cell lines was used in a PCR reaction of an amplicon size of 701 bp. Lanes 1-5 shows the amplification from the five cell lines, respectively. Lane 6 is CHO DNA, lane 7 is the negative control (water), lane 8 is the positive control and lanes L are Norgen's PCRSizer DNA ladder.

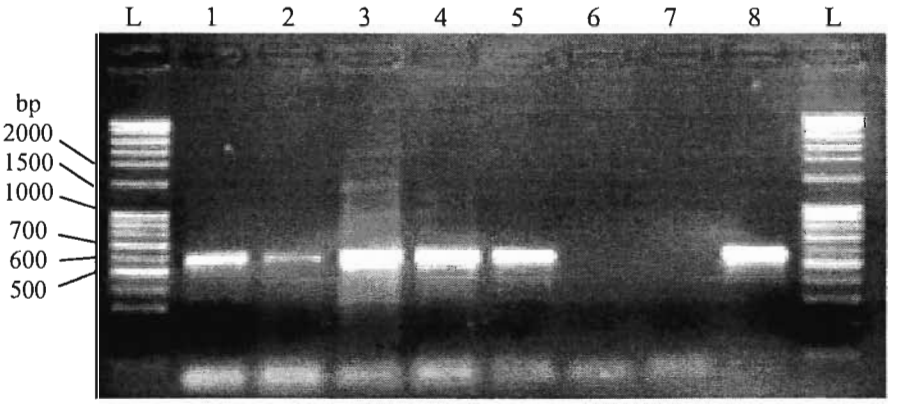

Figure 3.40: PCR amplification of pTP fragment from cell lines CHO-E2-1 to CHO-E2-5. DNA isolated from the different cell lines was used in a PCR reaction of an amplicon size of 565 bp. Lanes 1-5 shows the amplification from the five cell lines, respectively. Lane 6 is CHO DNA, lane 7 is the negative control (water), lane 8 is the positive control and lanes L are Norgen's FullRanger DNA ladder.

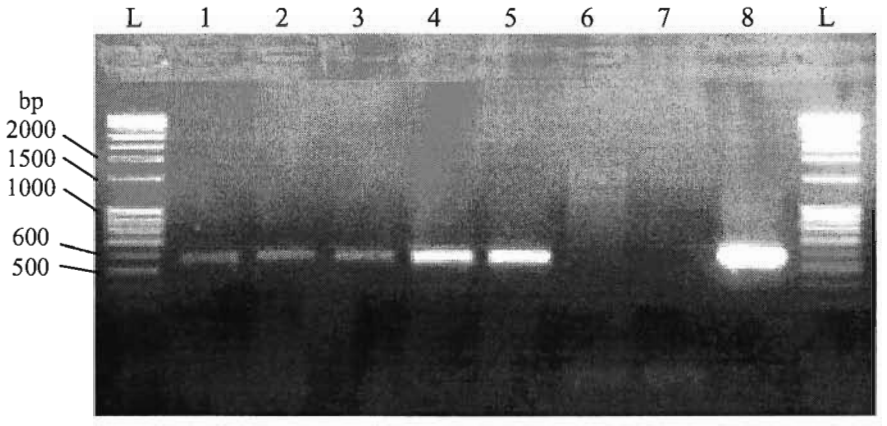

Figure 3.41: PCR amplification of viral protease fragment from cell lines CHO-E2-1 to CHO-E2-5. DNA isolated from the different cell lines was used in a PCR reaction of an amplicon size of 562 bp. Lanes 1-5 shows the amplification from the five cell lines, respectively. Lane 6 is CHO DNA, lane 7 is the negative control (water), lane 8 is the positive control and lanes L are Norgen's FullRanger DNA ladder.

3.3.6- Detection of the ligated pE2 terminal ends in the new cell lines

Linearized pE2 was used for cell line construction. However to test the probability of plasmid ligation after transfection, we used specific PCR primers (pE2F primer set) that lie at both terminal ends of the *NdeI*-linearized plasmid. Positive PCR amplification would be obtained only if the linearized plasmid ends were ligated to each other. PCR was performed on DNA isolated from the five cell lines. Negative controls included DNA isolated from CHO cells and water. In addition, PCR was performed on 100 ng of the transfection stock of *NdeI*-linearized pE2. Positive amplification was obtained with CHO-E2-2, CHO-E2-4 and CHO-E2-5 cell lines and no amplification was obtained with CHO-E2-1, CHO-E2-3, negative controls or the *NdeI*-linearized pE2 transfection stock. The agarose gel picture of the PCR result is shown in Figure 3.42.

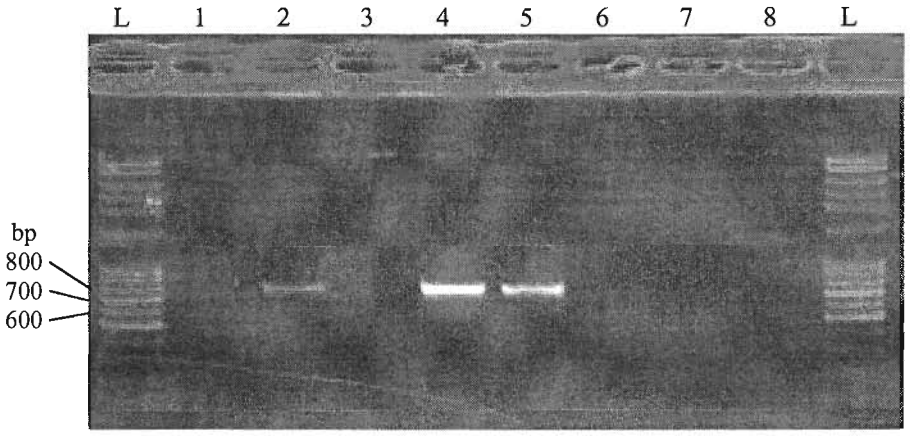

Figure 3.42: PCR amplification of the ligated terminal ends of pE2 in the five cell lines. DNA isolated from the different cell lines was used in a PCR reaction of an amplicon size of 743 bp. Lanes 1-5 shows the amplification from the five cell lines, respectively. Lane 6 is CHO DNA and lane 7 is the negative control (water). Lane 8 is the product of PCR performed on 100 ng of the transfection stock of *NdeI*-linearized pE2. Lanes L are Norgen's FullRanger DNA ladder.

3.3.7- pE1 expression and stability in CHO-E2 cell lines

Having established CHO cell lines containing the Ad5 E2 and protease genes, it was anticipated that the transfection of these cell lines with a plasmid carrying the Ad5 E1 would lead to the induction of the integrated genes and would in turn increase gene expression. Therefore, pE1 was transfected into the five CHO-E2 cell lines in addition to CHO cells performed by Lipofectamine 2000 in a 6-well plate. One day post-transfection, monolayer cells were washed with PBS and visualized under the confocal microscope directly from the 6-well plate, without lifting the cells. Images of the transfected cells were acquired by monitoring GFP expression with a 4X objective lens. All the different cell lines showed almost the same fluorescence intensity (Figure 3.43).

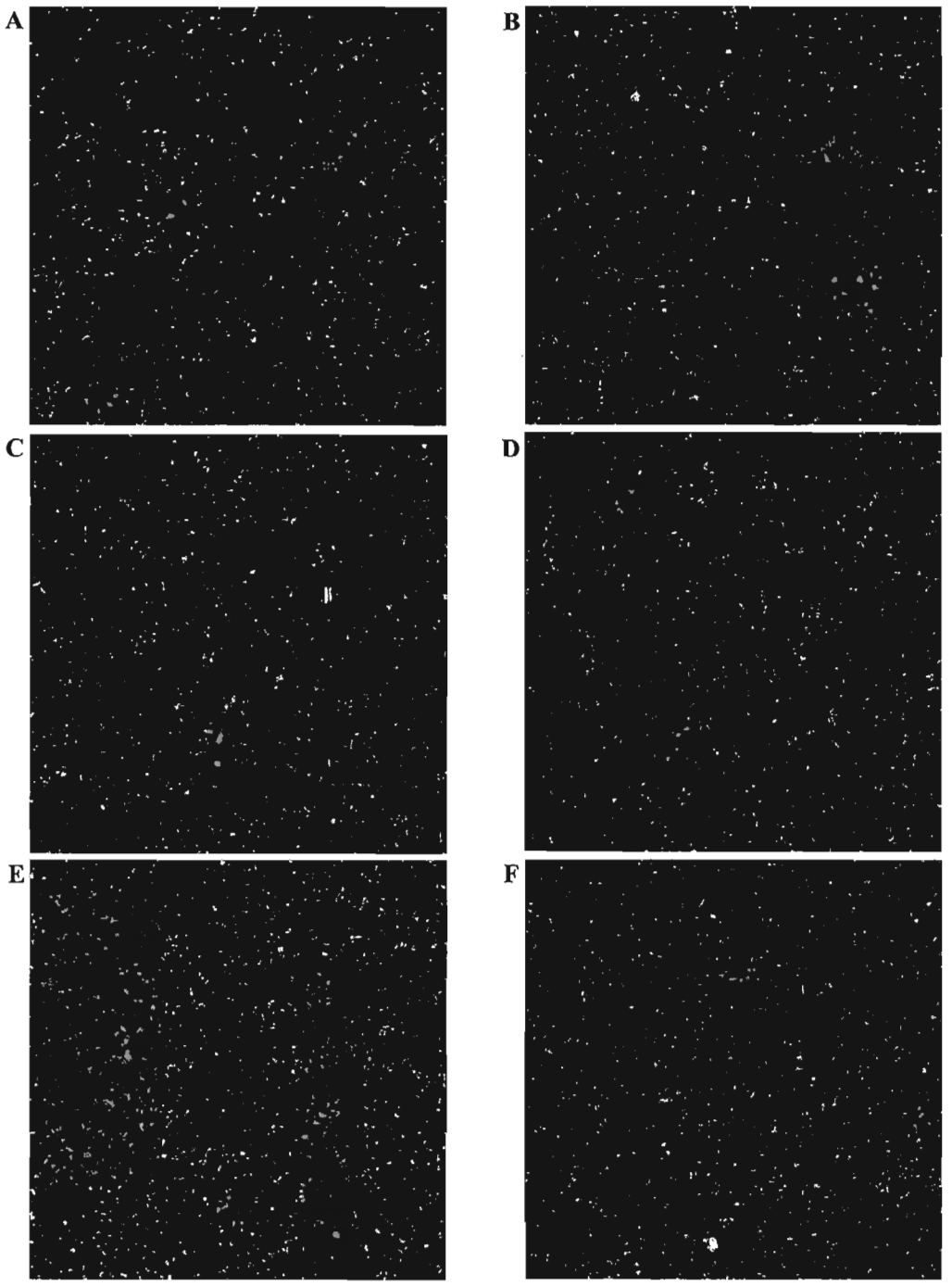

Figure 3.43: Confocal microscope pictures of GFP expression in monolayers of the different CHO-E2 cell lines. Images were processes 24 hours post-transfection of pE1 using Lipofectamine 2000. CHO-E2-1 (A), CHO-E2-2 (B), CHO-E2-3 (C), CHO-E2-4 (D), CHO-E2-5 (E) and CHO (F). Fluorescence was visualized by Nikon's confocal microscopy and images were acquired with a 4X objective lens.

3.3.7.1- pE1 stability in the different cell lines

Next, it was anticipated that the transfected plasmid will replicate inside the established cell lines. Therefore, the stability of pE1 in the different CHO cell lines, in addition to CHO cells, was monitored over time using PCR amplification performed on DNA isolated from cells transfected with pE1. Transfection was performed by the calcium phosphate method and samples were collected at times 0, 2, 6, 12, 24, 48 and 72 hours post-transfection. RNA was isolated along with DNA, both from the same sample. The GFP primer set were used in the PCR amplification, with an amplicon size of 484 bp. Agarose gel electrophoresis was used to run the PCR products. The amplification results revealed plasmid stability in all the different cell lines over the first 24 hours. Plasmid starts to be lost from the cells at 48 and 72 hours post-transfection. CHO-E2-3 and CHO cells retained more plasmids at 48 and 72 hours post-transfection than the other CHO-E2 cell lines (Figure 3.44).

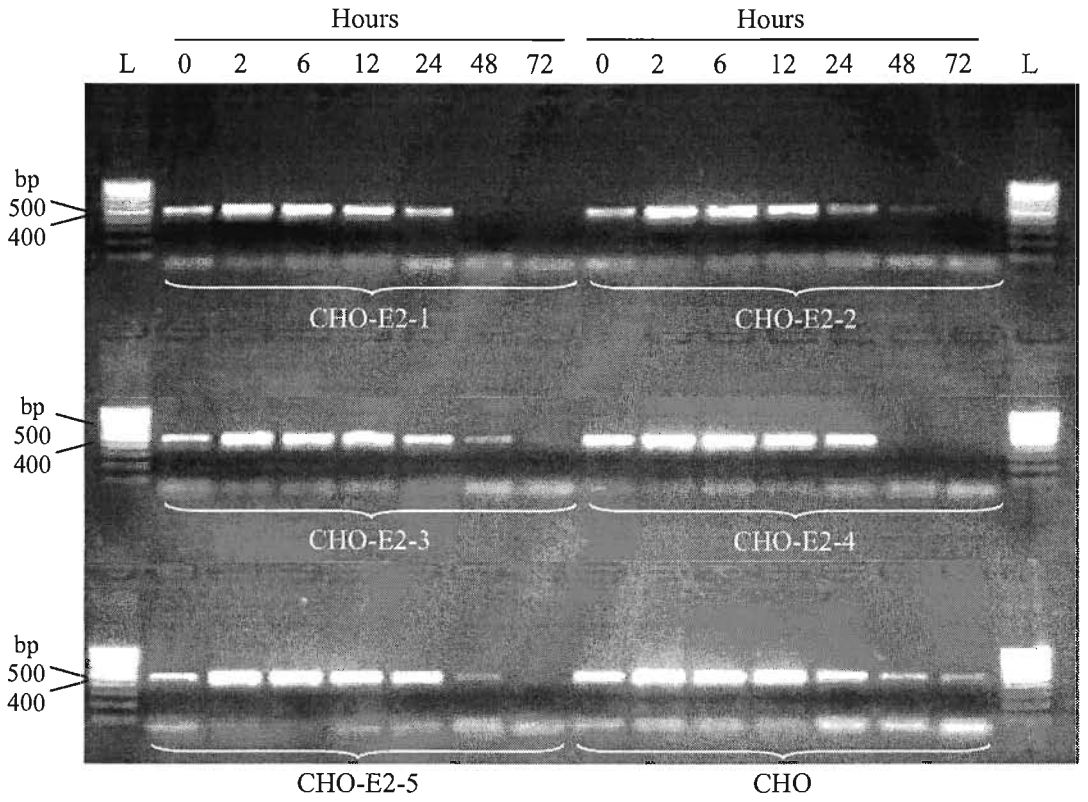

Figure 3.44: pE1 stability in CHO-E2 cell lines and CHO cells, over 72 hours post-transfection. Post-transfection sample collection times are shown on the top of the Figure. The name of each cell line is written underneath its collection set, after performing GFP PCR amplification with a product size of 484 bp. Lanes L are Norgen's PCRSizer DNA ladder.

3.3.7.2- Transcription from the different genes of pE1 and pE2 in CHO-E2 cell lines

Lastly, it was anticipated that the transcription of the various genes encoded in pE1 and pE2 may be affected in the established cell lines. Therefore, RNA samples from the different pE1 transfected cell lines were isolated along with the DNA, over 72 hours, as in the previous step. Samples were subjected to DNase treatment to digest any DNA background. RNA was cleaned afterwards to completely remove residual DNase. The success of the DNA digestion was checked by running PCR reactions on the treated

RNA and using the GFP specific primer set. Negative amplification was obtained with all the samples indicating the success of the background digestion. RT was performed on the same amount of treated RNA samples to create the first strand cDNA of the different mRNA templates. Subsequently, PCR was performed on the same volume of RT product to amplify the first strand cDNA, using specific primers of the target mRNA. Different mRNAs were checked for their transcription including both pE1 genes (GFP, E1A and E1B: Figures 3.45 – 3.47) and pE2 genes (ssDBP, viral polymerase, pTP and viral protease). The RT-PCR on the E2 genes mRNA resulted in negative amplification with all the CHO-E2 cell lines (data not shown). However, minor amplification was obtained from viral protease mRNA, 48 hours post-transfection, only with three cell lines: CHO-E2-1, CHO-E2-3 and CHO-E2-5 (Figure 3.48).

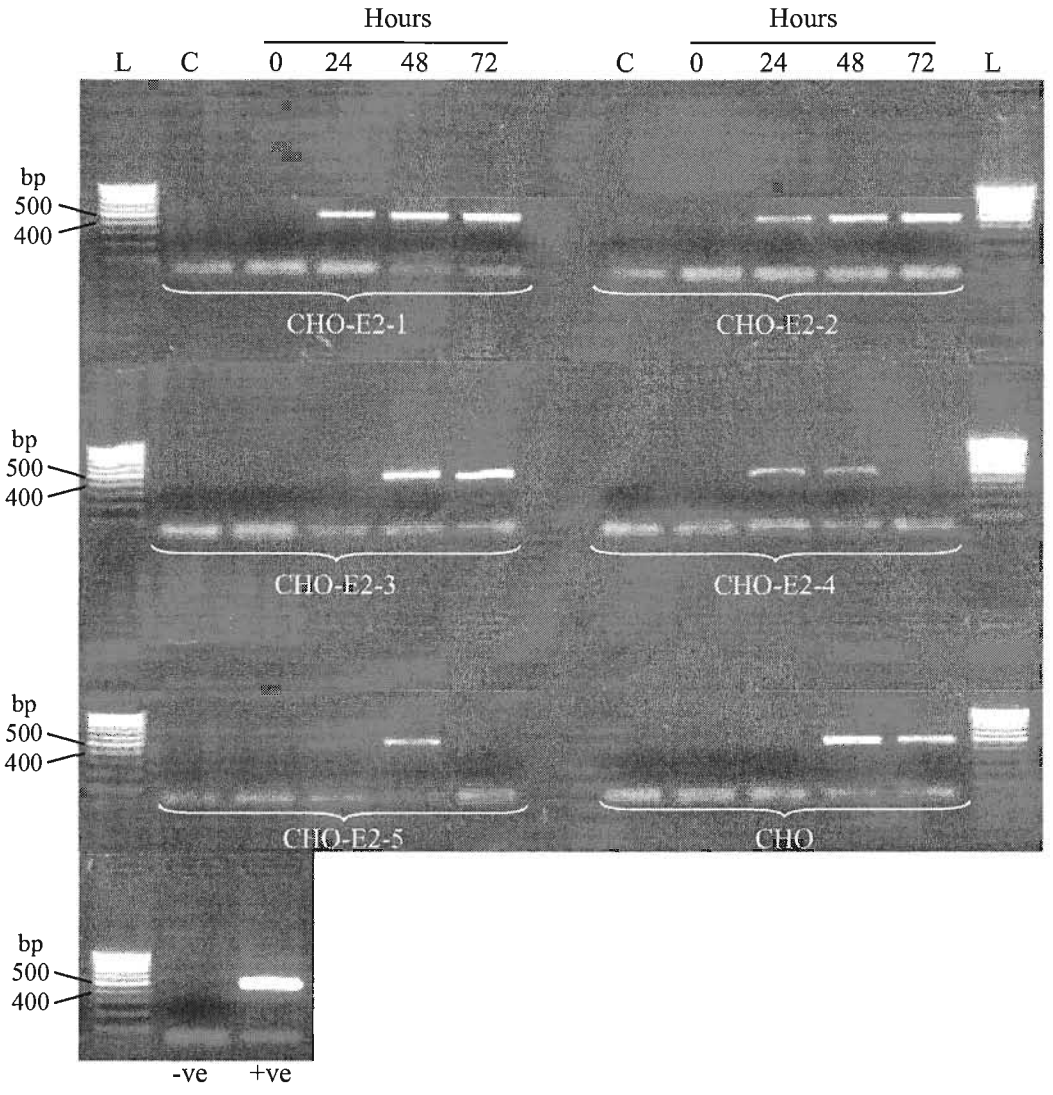

Figure 3.45: GFP mRNA transcription in CHO-E2 cell lines and CHO cells, over 72 hours post-transfection with pE1. Post-transfection sample collection times are shown on the top of the Figure. The name of each cell line is written underneath its collection set, after performing PCR amplification with a product size of 484 bp. C is non-transfected cells, –ve and +ve are the negative and positive controls, respectively and lanes L are Norgen's PCRSizer DNA ladder.

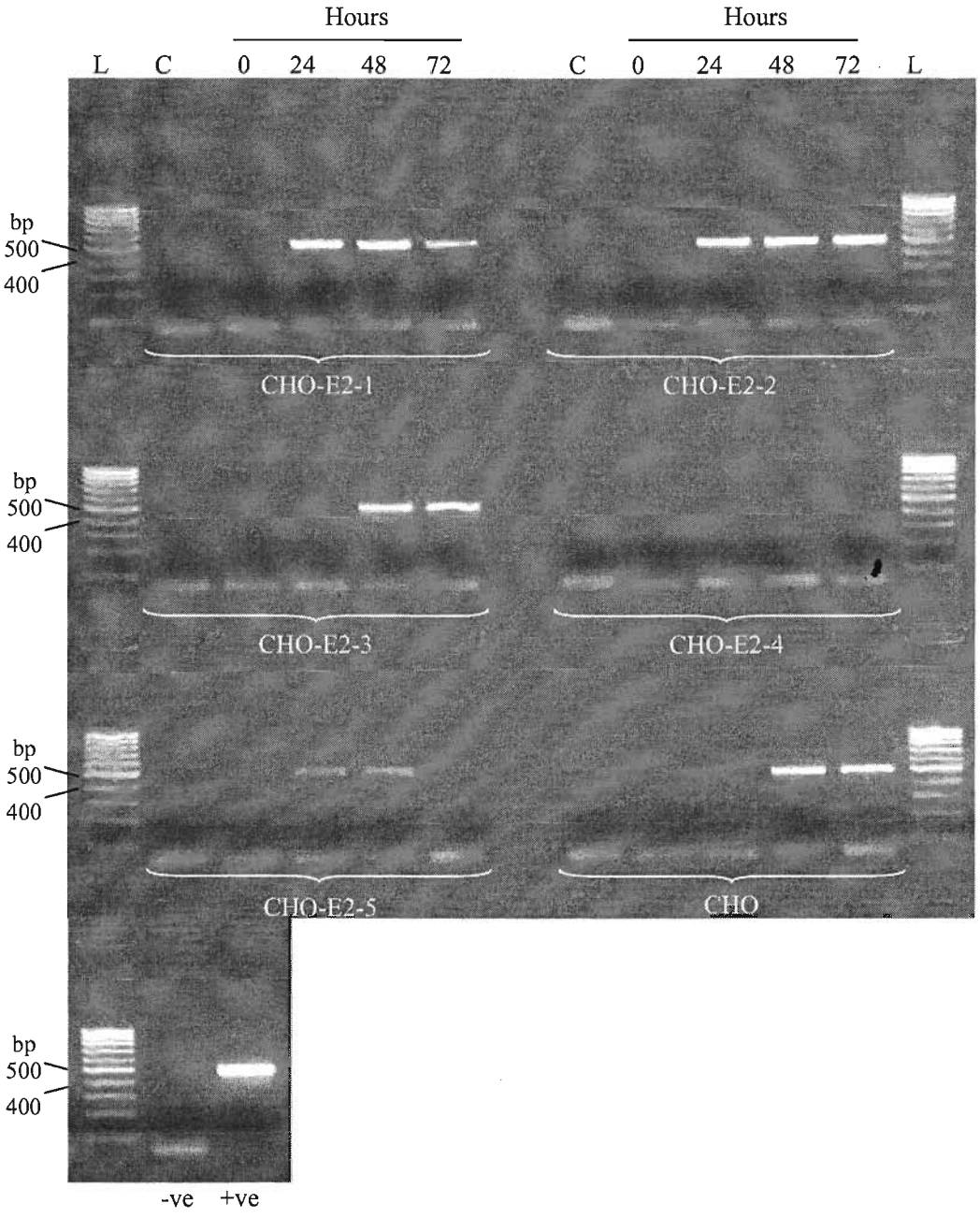

Figure 3.46: E1A-13S mRNA transcription in CHO-E2 cell lines and CHO cells, over 72 hours post-transfection with pE1. Post-transfection sample collection times are shown on the top of the Figure. The name of each cell line is written underneath its collection set, after performing RT-PCR amplification with a product size of 479 bp. C is non-transfected cells, –ve & +ve are the negative and positive controls, respectively and lanes L are Norgen's PCRSizer DNA ladder.

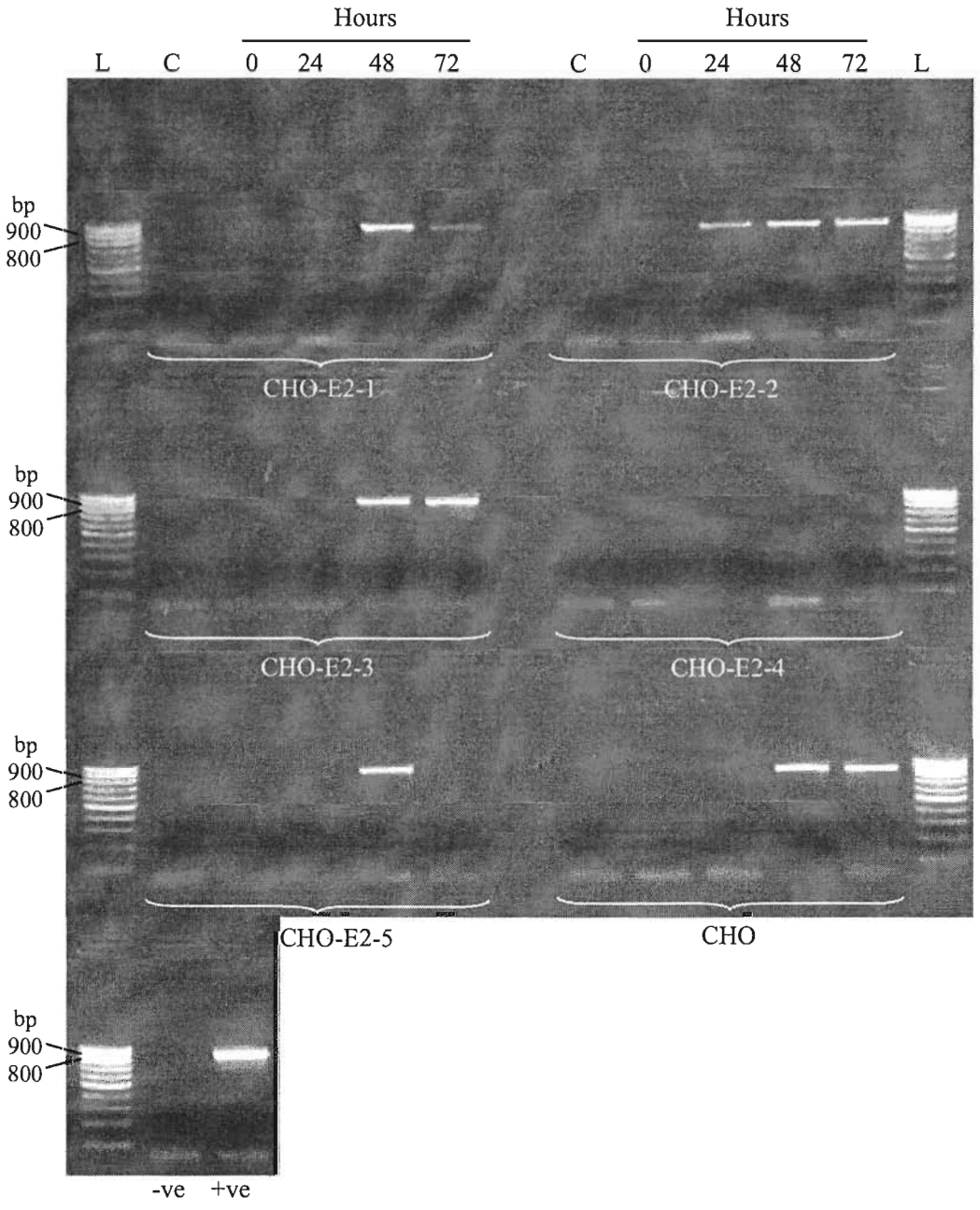

Figure 3.47: E1B 55k mRNA transcription in CHO-E2 cell lines and CHO cells, over 72 hours post-transfection with pE1. Post-transfection sample collection times are shown on the top of the Figure. The name of each cell line is written underneath its collection set, after performing RT-PCR amplification with a product size of 867 bp. C is non-transfected cells, –ve & +ve are the negative and positive controls, respectively and lanes L are Norgen's PCRSizer DNA ladder.

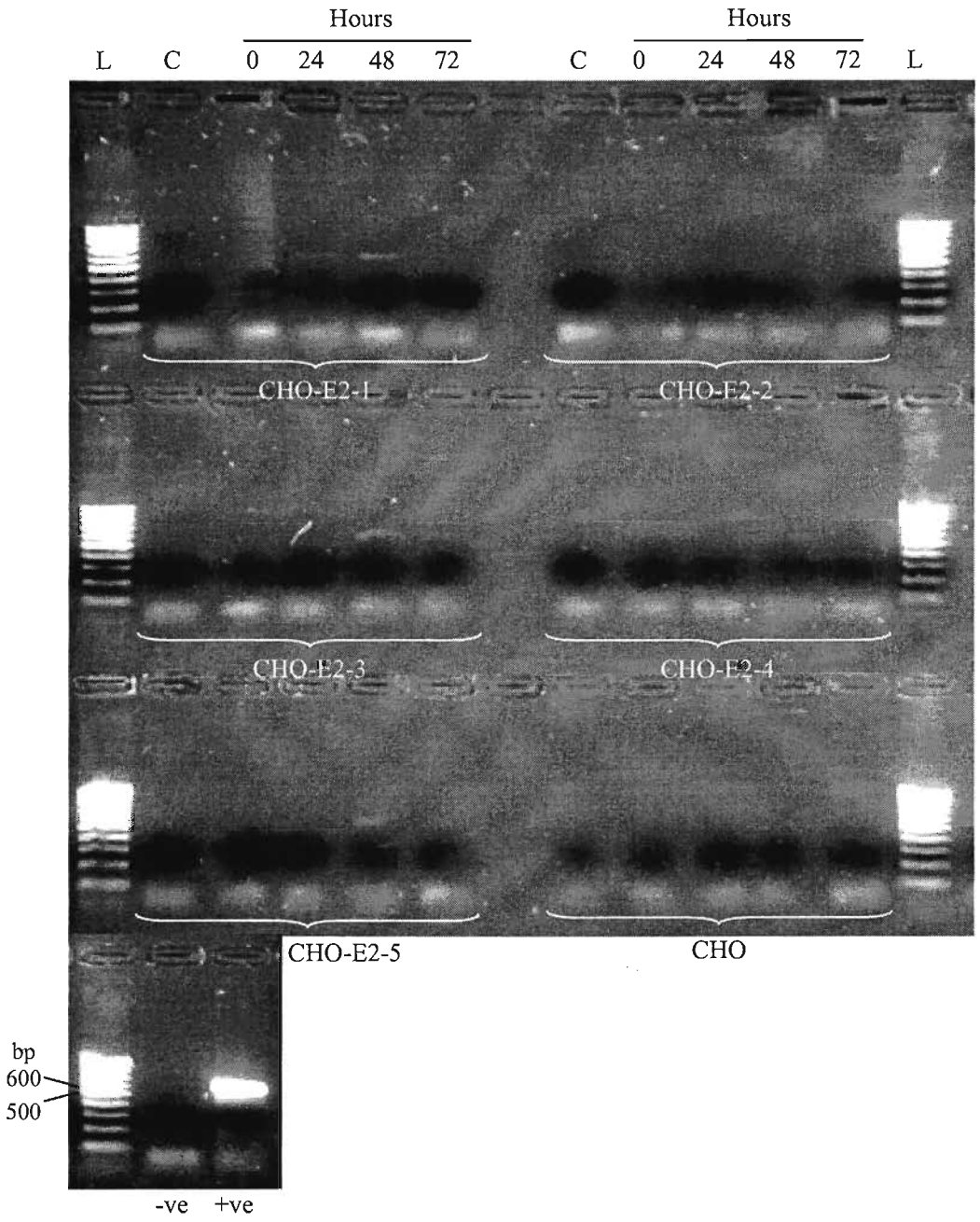

Figure 3.48: Viral protease mRNA transcription in the different CHO-E2 cell lines and CHO cells, over 72 hours post-transfection with pE1. Post-transfection sample collection times are shown on the top of the Figure. The name of each cell line is written underneath its collection set, after performing RT-PCR amplification with a product size of 562 bp. C is non-transfected cells, –ve & +ve are the negative and positive controls, respectively and lanes L are Norgen's PCRSizer DNA ladder.

3.4- Induction of Gene Expression by Adenovirus Super-Infection

This section focuses primarily on the effect of adenovirus super-infection on gene expression under the control of the Ad5 MLP with incomplete or complete TPL and in the presence of Ad5 ITRs and E1 region. It was anticipated that super-infection of cells (CHO or HEK 293) harbouring plasmids would lead to measurable effect on plasmid copy number, transcription and translation.

3.4.1- Stability and transcription from pMTGA in HEK 293 and CHO cells super-infected with adenovirus

Two groups of triplicate wells for each cell line were transfected with pMTGA using Lipofectamine 2000. The growth medium was replaced 6 hours post-transfection to remove the transfection reagent and allow the cells to recover. At 12 hours post-transfection, one of the two groups of each cell line was super-infected with adenovirus at a multiplicity of infection (MOI) of 10 plaque forming units (PFU) per cell. Samples were collected from the transfected and super-infected groups at: 0, 0.5, 1.5, 2.5, 3.5 and 4.5 days post-transfection. Two negative controls were included for each cell line; the first is transfected with pUC19 and used as a control for transfected cells, while the second is pUC19 transfected and super-infected with the wild type virus. An additional group of viral infection into both cell lines was included as a negative control. DNA and RNA were isolated, both from same sample, and used for downstream analysis.

3.4.1.1- Plasmid stability

DNA samples were quantified and equal amounts were used in a qPCR with specific primers for GFP. The copy number of the plasmid DNA was obtained using a standard curve of known plasmid concentration. Figures 3.49 and 3.50 show the plasmid copy number per cell in HEK 293 and CHO cells respectively, over the collection period. Data was statistically analyzed by the two way ANOVA using Tukey's test. Both cell lines showed significantly (at $P<0.05$) higher plasmid copies after 12 hours and 1.5 days post-transfection (zero and one day after super-infection). No significant changes were observed in the trends of plasmid stability with the transfection and super-infection conditions. The lysis of HEK 293 cells was observed after 2.5 days post-transfection. In contrast, CHO cells did not lyse upon super-infection, although they showed a large amount of detached cells after 3.5 days post-transfection.

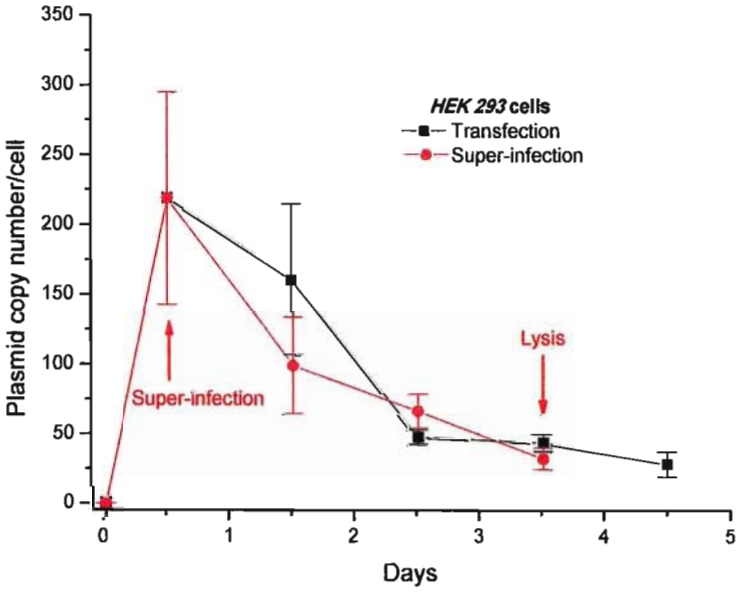

Figure 3.49: Copy numbers of pMTGA over 4.5 days post-transfection in HEK 293 cells with transfection and super-infection conditions. Copy numbers were obtained by qPCR using a standard curve of known plasmid DNA concentration.

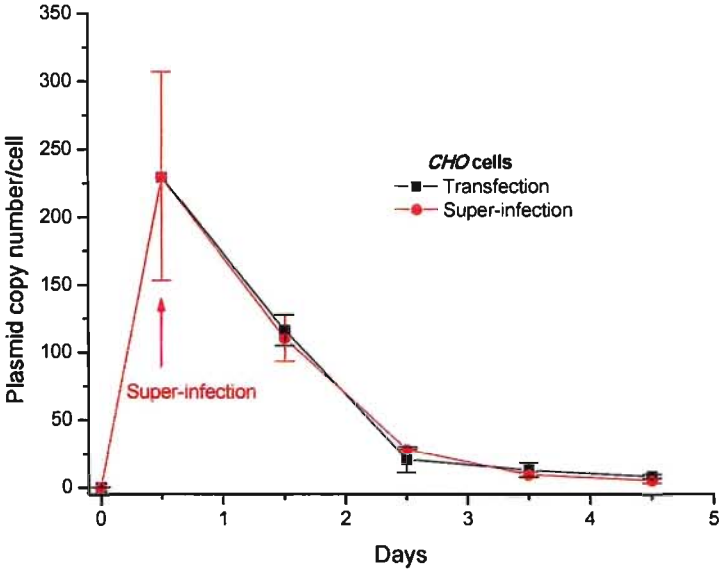

Figure 3.50: Copy numbers of pMTGA over 4.5 days post-transfection in CHO cells, with transfection and super-infection conditions. Copy numbers were obtained by qPCR using a standard curve of known plasmid DNA concentration.

3.4.1.2- GFP transcription efficiency

DNase was used to digest any residual DNA in the RNA samples, followed by cleaning and quantification. Equal amounts of RNA were used in an RT reaction to synthesize the first strand cDNA of the different mRNAs. After this, a qPCR was performed on equal volumes of the RT product using the GFP specific primer set. GFP mRNA copy numbers were quantified using a standard curve and then were calculated per cell. The data obtained from the different samples collected over time from both HEK 293 and CHO cells are shown in Figures 3.51 and 3.52, respectively. Statistical analysis of the data at a significance level of 0.05 showed no significant increase in GFP mRNA from the super-infected HEK 293 cells over the transfected ones. Only at 2.5 days post-transfection was a change noted as cell lysis started to occur. However, in

CHO cells, the increment in GFP mRNA was significant after the super-infection, particularly on 1.5 days post-transfection.

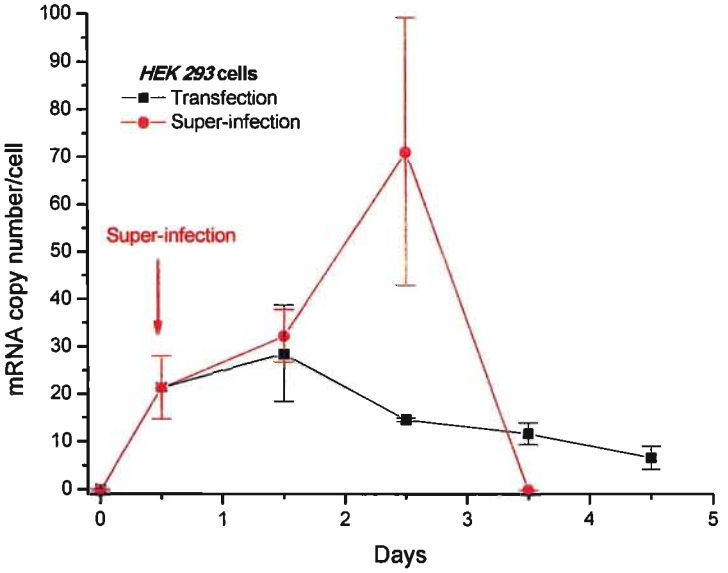

Figure 3.51: GFP mRNA transcripts from pMTGA over 4.5 days post-transfection in HEK 293 cells with transfection and super-infection conditions. Copy numbers were obtained by qPCR using a standard curve of known plasmid DNA concentration.

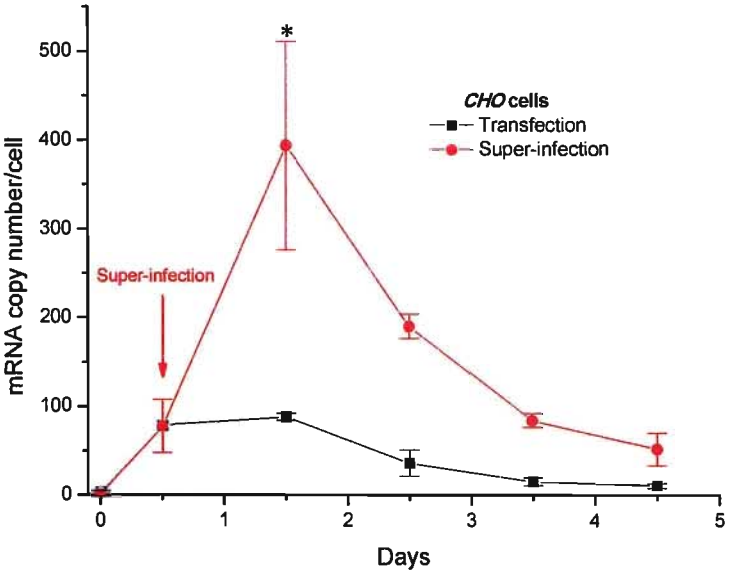

Figure 3.52: GFP mRNA transcripts from pMTGA over 4.5 days post-transfection in CHO cells, with transfection and super-infection conditions. Copy numbers were obtained by qPCR using a standard curve of known plasmid DNA concentration.

Transcription efficiency was calculated from the obtained copy numbers of both plasmid DNA and GFP mRNA. Figures 3.53 and 3.54 illustrate the transcription efficiency over time in both HEK 293 and CHO cells. The statistical analysis of the data (at $P<0.05$) demonstrated insignificant increase of GFP transcription efficiency upon super-infection of HEK 293 cells, with elevated efficiency 2.5 days post-transfection. On the other hand, super-infection of CHO cells showed significant (at $P<0.05$) increase in GFP transcription efficiency over time relative to non-infected. The fold increase in transfection efficiency of the super-infected samples over the corresponding transfected ones is shown in Figure 3.55. CHO cells have a higher relative increase in transfection efficiency with time over HEK 293 cells. Up to an eight fold increase was obtained from super-infected CHO cells at 4.5 days post-transfection.

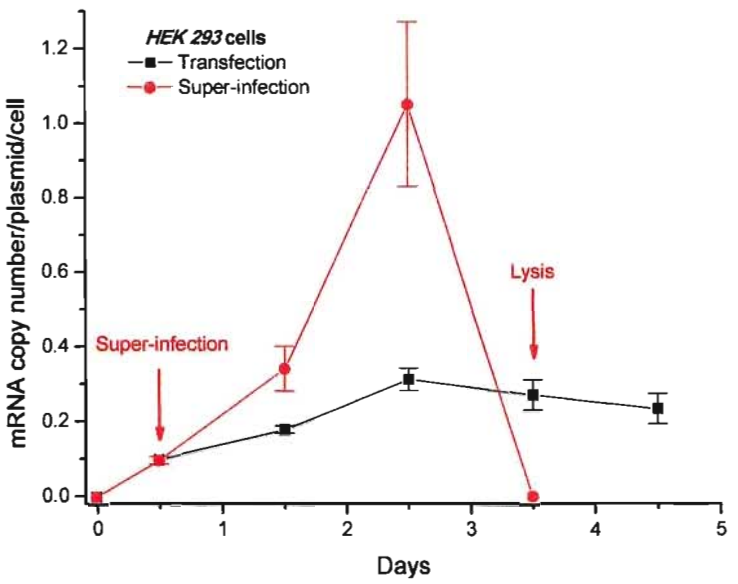

Figure 3.53: Transcription efficiency of GFP mRNA over 4.5 days post-transfection in HEK 293 cells, with transfection and super-infection conditions. Efficiency was defined as GFP mRNA copy number per plasmid per cell and. Copy numbers per cell of plasmid DNA and GFP mRNA were estimated by qPCR using a standard curve of a known plasmid concentration.

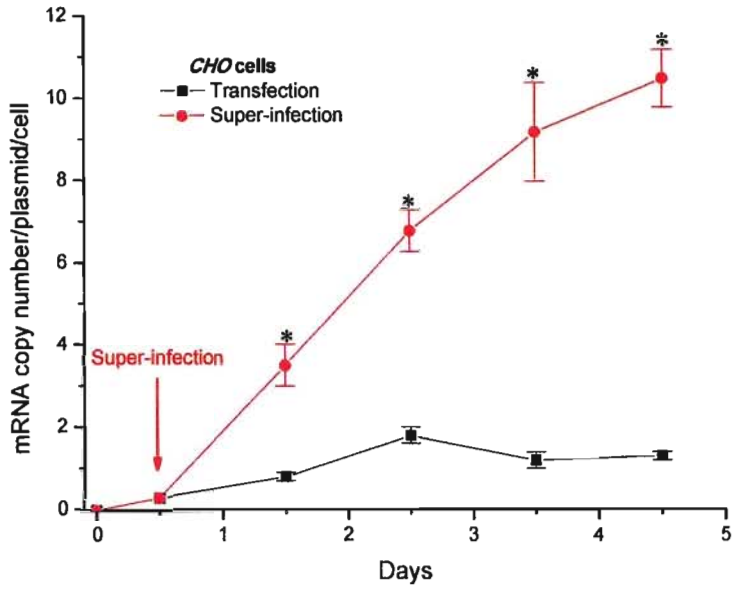

Figure 3.54: Transcription efficiency of GFP mRNA over 4.5 days post-transfection in CHO cells, with transfection and super-infection conditions. Efficiency was defined as GFP mRNA copy number per plasmid per cell. Copy numbers per cell of plasmid DNA and GFP mRNA were estimated by qPCR using a standard curve of a known plasmid concentration.

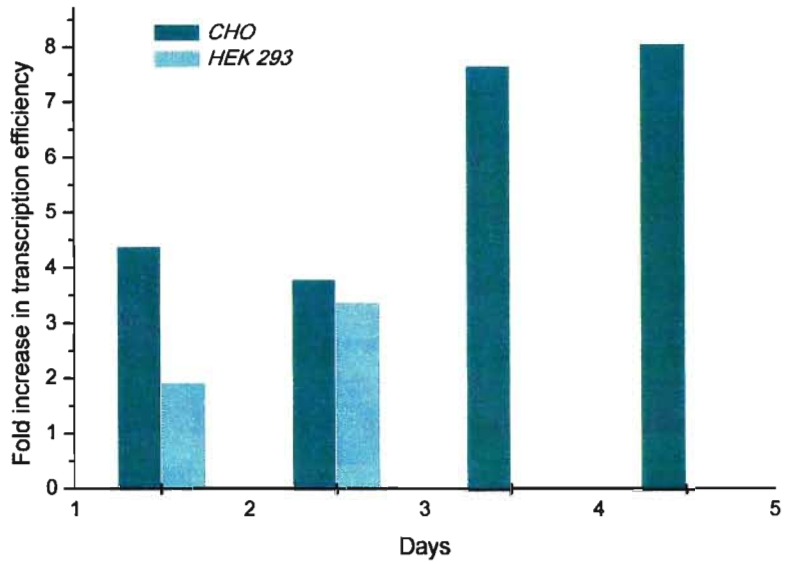

Figure 3.55: Fold increase in transcription efficiency in HEK 293 and CHO cells, after super-infection with adenovirus. HEK 293 cells underwent lysis after 2.5 days post-transfection.

3.4.2- Gene expression from different plasmids in CHO cells super-infected with adenovirus at MOI of 10 PFU/cell

The following five plasmids were used in this experiment: pMGA, pMT_1GA, $pMT_{1,2}GA$, pMTGA and pE1. All of these plasmids contain the MLP and GFP in their expression cassette with partial or complete TPL. pMGA has no TPL however pE1 contains the complete TPL in addition to the adenovirus ITRs-E1 fragment. The maps of the different GFP expression cassettes are shown in Figure 3.11.

Plasmids were transfected into CHO cells using Lipofectamine 2000 in two triplicate groups for each plasmid. The medium was changed 6 hours post-transfection. Twelve hours after transfection, Super-infection was carried out on one group of each plasmid. In addition to the zero and 12 hours collection times, samples were collected at 1.5 and 3.5 days and then every 3 days thereafter. Two negative controls were included; the first is the CHO cells transfected with pUC19 and used as a control for the transfected cells, while the second is pUC19 transfected and super-infected with the wild type virus. DNA and RNA were isolated from the same collected samples.

3.4.2.1- Plasmid stability

After quantifying the isolated DNA, it was used in a qPCR reaction to determine the copy number of each plasmid. A GFP primers set was used with all the plasmids since they all contain the GFP gene. A standard curve was used as previously mentioned, and the copy numbers per cell for transfection and super-infection conditions of each plasmid were calculated and illustrated in Figure 3.56. The obtained data was statistically analyzed by the two way ANOVA using Tukey's test at a significance level of 0.05. All

of the plasmids, with the exception of pE1, share the same stability trend over time in CHO cells with both transfection and super-infection. The maximum plasmid copy numbers in the cell were at 12 hours post-transfection, followed with a significant (at $P<0.05$) decrease in the copy number over the next two collection points (1.5 and 3.5 days, post-transfection) to reach very close to the baseline on day 3.5. Super-infection of the pE1 showed different stability, with significantly (at $P<0.05$) increased copy number on day 1.5 post-transfection. A dramatic drop in pE1 copy number was observed on day 3.5 post-transfection.

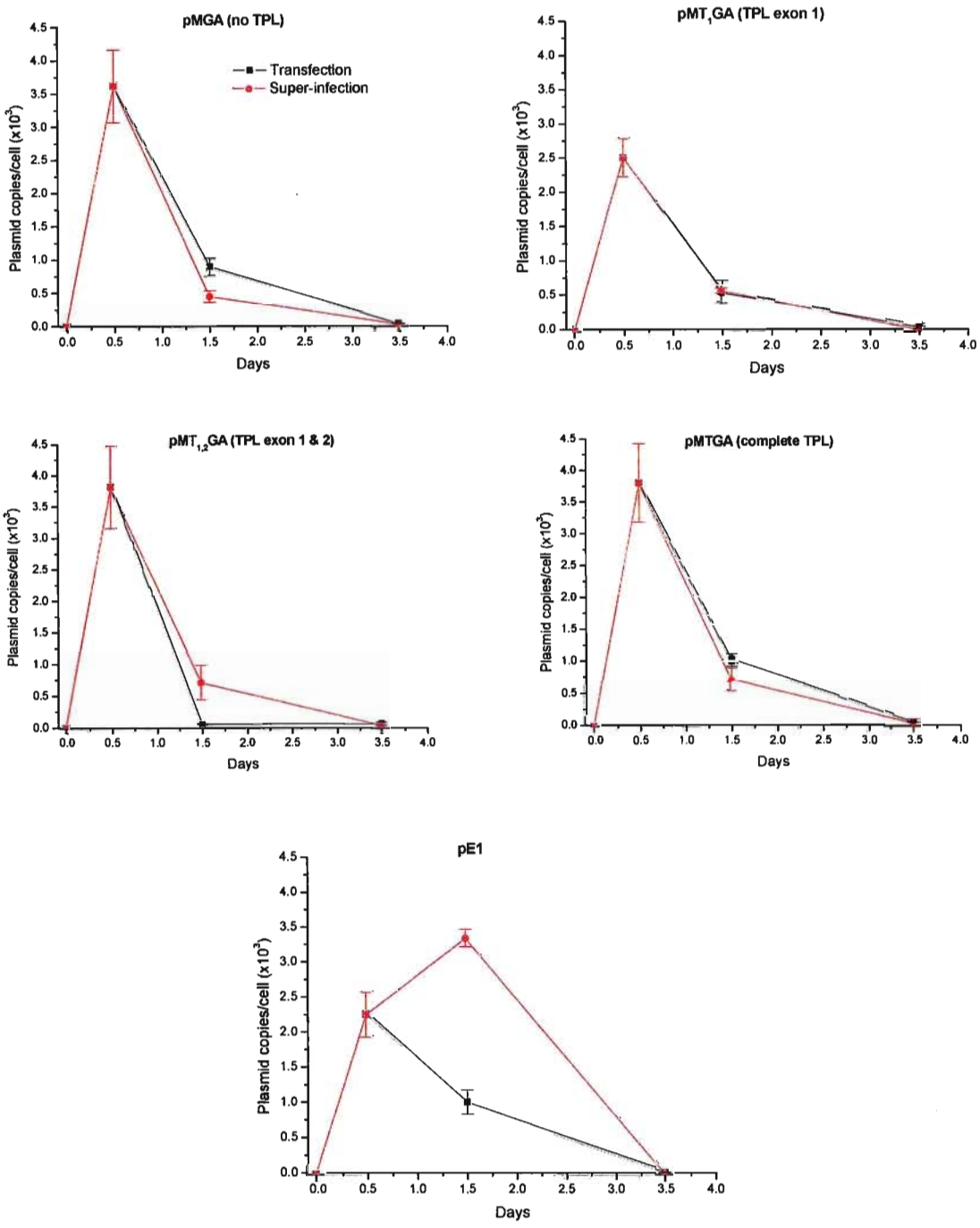

Figure 3.56: Copy numbers of the different plasmids over 3.5 days post-transfection in CHO cells, with transfection and super-infection (at MOI of 10 PFU/cell) conditions. Copy numbers were obtained by qPCR using a standard curve of known plasmid DNA concentration.

3.4.2.2- GFP transcription efficiency

As done in the previous experiments, RNA was treated with DNase, cleaned then quantified and used in an RT reaction followed by qPCR using the GFP specific primers. The GFP mRNA copy numbers, transcribed from the different plasmids in both transfection and super-infection conditions, were then quantified using a standard curve. RNA was then calculated per cell and illustrated for each plasmid in both the transfection and super-infection conditions (Figure 3.57). Statistical analysis was done as described with the DNA data. The mRNA of all the transfection conditions showed almost same trend, with a significant (at $P<0.05$) peak on day 1.5 post-transfection followed by a decline in levels. The effect of super-infection on mRNA levels varies with the different plasmids. An insignificant (at $P<0.05$) increase in mRNA levels was observed upon super-infection of pMGA, pMT_1GA and pE1. In contrast, significant increase was noted with $pMT_{1,2}GA$ and pMTGA.

The transcription efficiency was calculated as the copy number of GFP transcripts per plasmid per CHO cell. Efficiencies from the transfection and super-infection conditions of each plasmid are shown in Figure 3.58. Statistical analysis of the data obtained was performed as previously mentioned. Increased transcription efficiency levels were observed in the super-infected conditions of pMGA and pMT_1GA compared to their transfection conditions on day 1.5 post-transfection. Efficiencies from both plasmids declined on day 3.5 post-transfection of the super-infection conditions while the transfection conditions continued to increase. However, the overall difference was not significant when analyzed at $P<0.05$. The plasmid pE1 showed no significant increase in

transcription efficiency over time when comparing the transfected to the super-infected conditions. In addition, the transcription efficiency of the super-infection condition of $pMT_{1,2}GA$ was insignificantly increasing over time when compared to the efficiencies of the transfection conditions. Only pMTGA showed a significant (at $P<0.05$) increase in transcription efficiency over time within the super-infection condition than that of transfection.

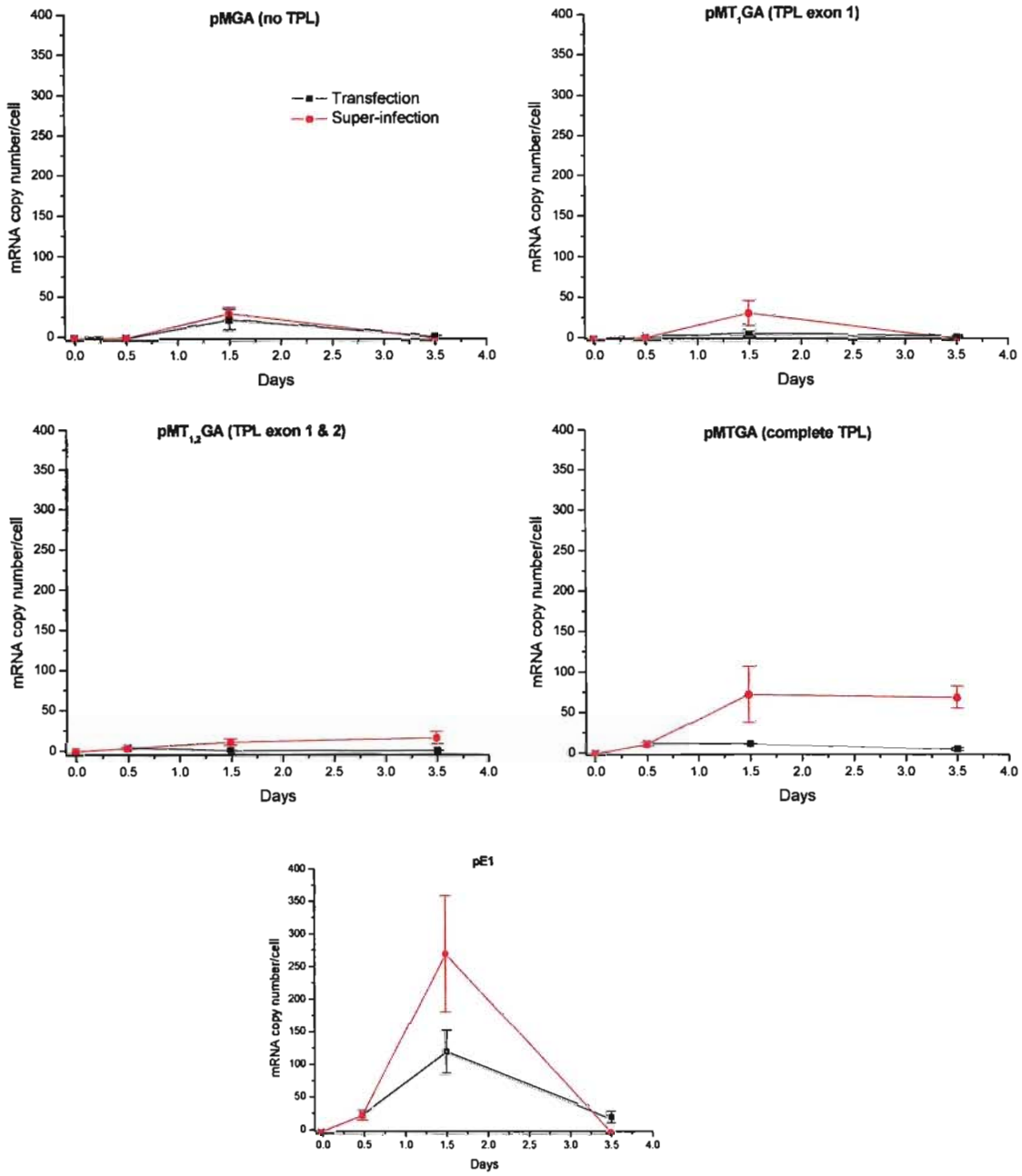

Figure 3.57: GFP mRNA transcripts from the different plasmids over 3.5 days post-transfection in CHO cells, with transfection and super-infection (at MOI of 10 PFU/cell) conditions. Copy numbers were obtained by qPCR using a standard curve of known plasmid DNA concentration.

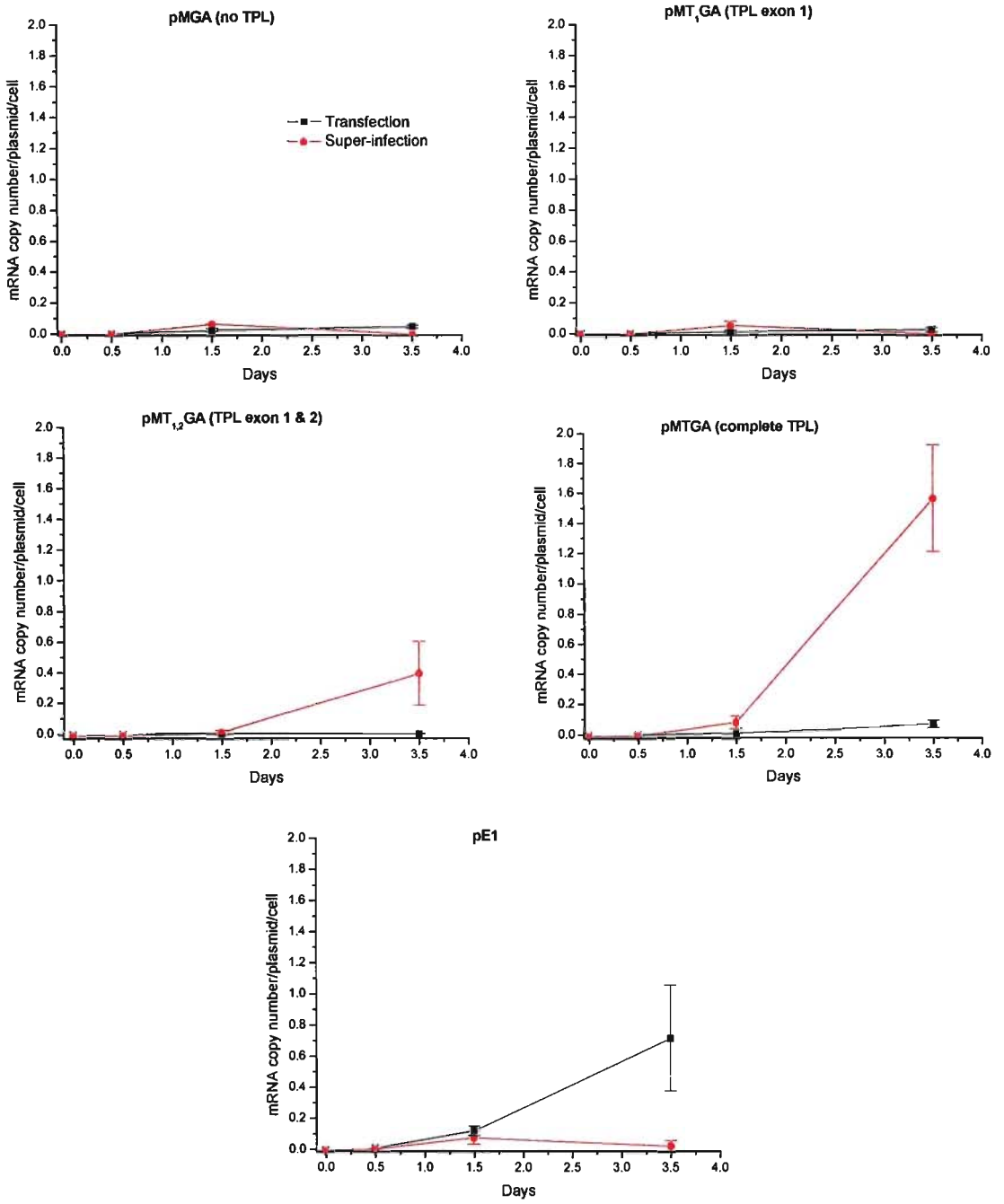

Figure 3.58: Transcription efficiency of GFP mRNA over 3.5 days post-transfection in CHO cells, with transfection and super-infection (at MOI of 10 PFU/cell) conditions. Efficiency was defined as GFP mRNA copy number per plasmid per cell. Copy numbers per cell of plasmid DNA and GFP mRNA were estimated by qPCR using a standard curve of a known plasmid concentration.

3.4.2.3- GFP translation

Fluorescence intensity was used to measure GFP level in equal cell counts from the different samples. CHO cells were used as a blank and the two negative controls (pUC19-transfected and pUC19-transfected/super-infected CHO cell) were included. The fluorescence intensity from the transfection and the super-infection conditions of each plasmid are shown in Figure 3.59. Statistical analysis of the data obtained was performed as previously mentioned. All of the plasmids showed significant (at $P<0.05$) increase in GFP fluorescence intensity after 12 hours post-transfection, in both the transfection and the super-infection conditions. On the other hand, all of the plasmids used showed similar or insignificant change in their GFP expression on day 3.5 of both conditions. At this time point, there were still significantly elevated GFP levels. However, on day 1.5, the differences between the two conditions were clearly observed. Only pMGA showed significantly higher GFP in the transfected condition over the super-infected one. The opposite was seen with $pMT_{1,2}GA$; it had significantly elevated GFP on day 1.5 of the super-infected over the transfected conditions. The remaining plasmids showed minor, non-significant differences between their expressed GFP in the two conditions.

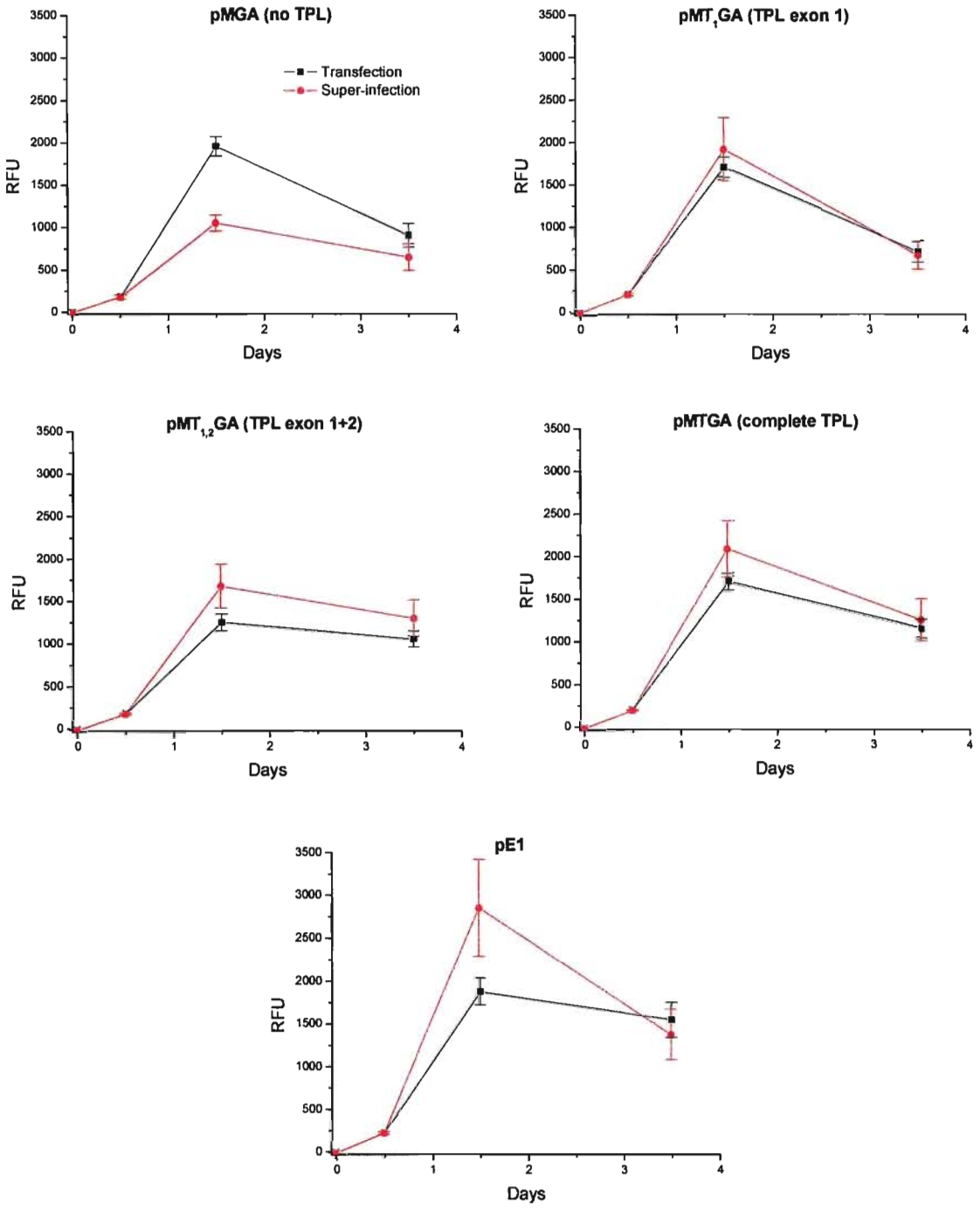

Figure 3.59: GFP fluorescence intensity over 3.5 days post-transfection in CHO cells, with transfection and super-infection (at MOI of 10 PFU/cell) conditions. Fluorescence intensity was measured by the relative fluorescence units (RFU) of equal cell counts.

Although the experimental aim was to investigate gene expression over longer periods of time, this was not possible due to cell detachment. Detachment started after day 3.5 and about 95% of the cells detached after 5.5 days of the super-infection. The cell monolayers of all of the transfected conditions remained attached with few cells detaching. The question that arose was if these detached cells were viable or dead.

Therefore, detached cells on day 3.5 were collected from the pE1 super-infected samples and cell vitality was determined using trypan blue. The dye penetrates and stains dead cells but not viable cells. Most of the detached cells were still alive (81.3±41.7%) and small number of cells were dead (18.8±5.3%).

The plasmid copy number and GFP mRNA transcripts per cell were measured in detached cells, using qPCR and RT-qPCR, respectively. In addition, transcription efficiency was also calculated. Figure 3.60 shows the number of plasmids copies, mRNA transcripts and transcription efficiency in both attached and detached cells of the pE1 super-infected condition. A two sample t-test (at $P<0.05$) showed significant increase in plasmid copies and transcription efficiency in detached cells.

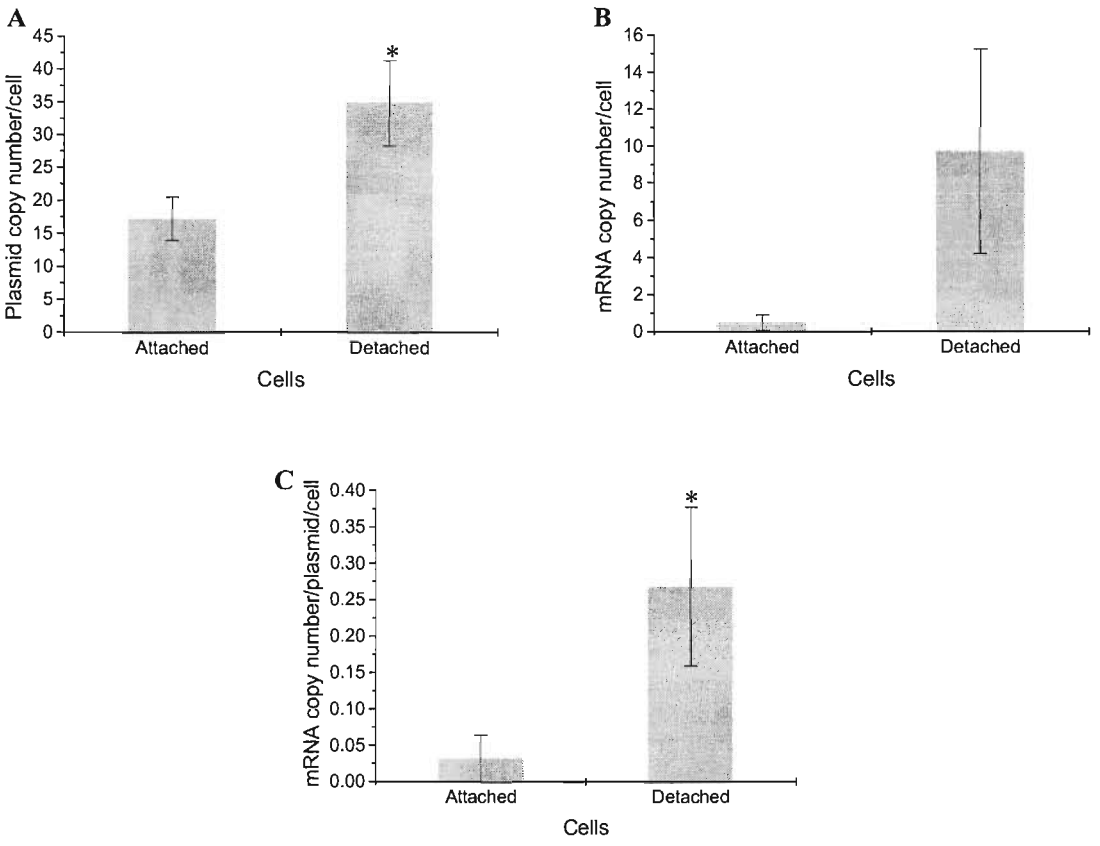

Figure 3.60: Plasmid copies, transcripts copies and transcription efficiency in attached and detached cells of the pE1 super-infection (at MOI of 10 PFU/cell) condition on 3.5 days post-transfection. (A) pE1 copy number per cell, (B) GFP mRNA copy number per cell and (C) GFP transcription efficiency.

3.4.3- Effect of adenovirus super-infection on gene expression in CHO cells at different MOIs

In the previous super-infection experiments, an MOI of 10 PFU/cell was used. The high MOI may be the reason for the cell detachment after 3.5 days post-transfection in the super-infected conditions of the last experiment. Therefore, lower MOIs were used to super-infect CHO cells that have been transfected with pE1 and examined gene expression as well as cell adhesion. Four groups of triplicate wells of CHO cells were first transfected with pE1, using Lipofectamine 2000. The transfection medium was changed 6 hours after transfection and cells were allowed to recover from the transfection for another 6 hours. Then, three groups were super-infected with the wild type virus dl309 at MOIs of 0, 1, 5 and 10 PFU/cell. Samples were collected over time (0, 0.5, 1.5, 4.5, 9.5 and 14.5 days post-transfection) and DNA and RNA were isolated from the same samples, and used for gene expression analysis. Two negative controls were included; the first is CHO cells transfected with pUC19 and used as a control for transfected cells, while the second is pUC19 transfected and super-infected with the wild type virus. Statistical analysis of all the data obtained was performed by two way ANOVA using Tukey's test, at a significance level of <0.05.

The cells remained attached in monolayers with MOIs of 0 and 1 PFU/cell, while cell detachment was observed with MOIs of 5 and 10 PFU/cell. The confluencey of detached cells, on day 5 post-transfection, was estimated to be 40-50% with MOI 5 PFU/cell and 80-90% with MOI 10 PFU/cell using a light microscope. Cell detachment seems to be proportional to the MOI.

3.4.3.1- Plasmid stability

Equal amounts of DNA were used in a qPCR reaction, using the specific GFP primers set, to determine the plasmid copy number per cell, within the different collected samples (Figure 3.61). A significant (at $P<0.05$) increase in plasmid copy number was observed at 12 hours post-transfection, then it decreases significantly on day 1.5 post-transfection but is still significantly higher than the baseline. Insignificant increase from the baseline was reached on day 4.5 and afterwards. The same trend was observed for plasmid stability with all of the MOIs.

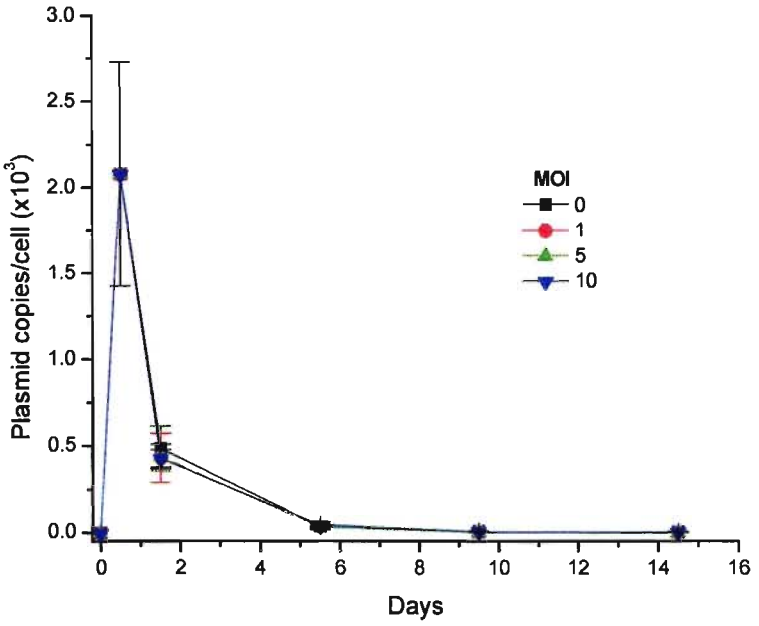

Figure 3.61: Copy numbers of pE1 over 14.5 days post-transfection in CHO cells, with super-infection using different MOIs. Copy numbers were obtained by qPCR using a standard curve of known plasmid DNA concentration.

3.4.3.2- GFP transcription efficiency

RNA samples were treated with DNase, cleaned and then equal amounts were used in an RT reaction. Equal volumes of the RT product were used in a qPCR reaction (using the GFP primers set) to quantify GFP mRNA copy numbers. Figure 3.62 shows the GFP mRNA transcripts per cell. Statistical analysis of the data revealed significant (at $P<0.05$) elevation in GFP mRNA transcripts on day 1.5 post-transfection. An insignificant increase from the baseline was observed after this time point. The same mRNA transcription trend was observed with all of the MOIs used.

The obtained plasmid and GFP mRNA copy numbers for each sample were used to calculate the transcription efficiency over time (Figure 3.63). A significant (at $P<0.05$) increase in transcription efficiency was obtained from day 4.5 post-transfection with all of the used MOIs except with an MOI of 10 PFU/cell. The MOIs of 1 and 5 PFU/cell were significantly higher than the MOI of 10 PFU/cell, with a lower effect on cell attachment, particularly when using MOI of 10 PFU/cell.

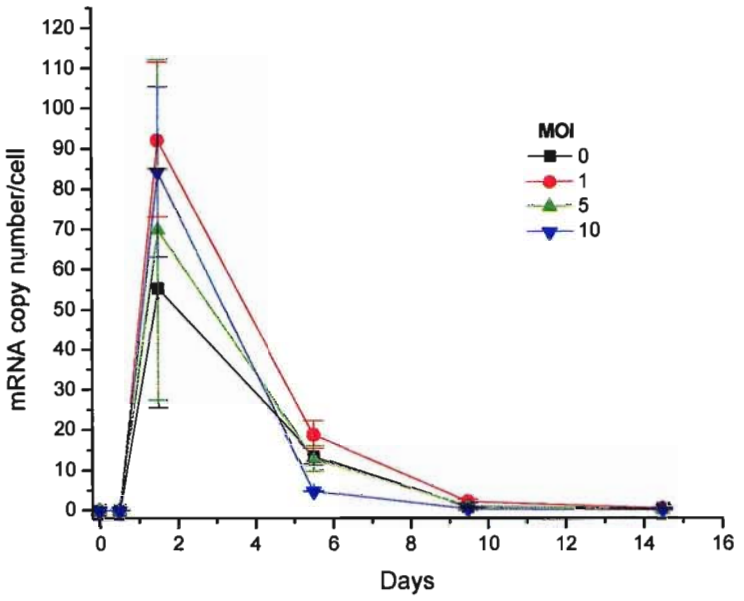

Figure 3.62: GFP mRNA transcripts from pE1 over 14.5 days post-transfection in CHO cells, with super-infection using different MOIs. Copy numbers were obtained by qPCR using a standard curve of known plasmid DNA concentration.

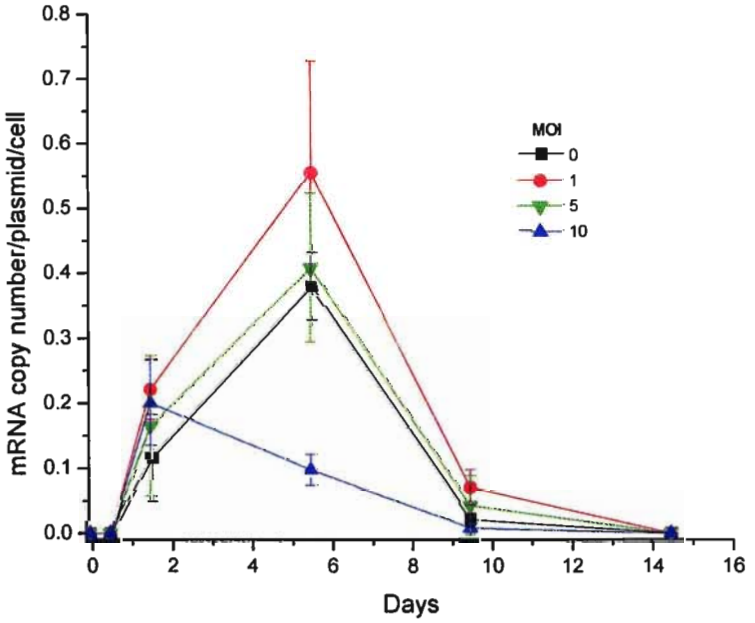

Figure 3.63: Transcription efficiency of GFP mRNA over 14.5 days post-transfection in CHO cells, with super-infection using different MOIs. Efficiency was defined as GFP mRNA copy number per plasmid per cell. Copy numbers per cell of plasmid DNA and GFP mRNA were estimated by qPCR using a standard curve of a known plasmid concentration.

3.4.3.3- GFP translation

The GFP intensity was determined in equal cell counts from each sample by measuring the RFU (Figure 3.64). A significant (at $P<0.05$) increase in fluorescence intensity was obtained over days 1.5 to 5.5 post-transfection with all of the MOIs used and reached the baseline on day 9.5 and thereafter. Super-infection at an MOI of 1 PFU has significantly higher expressed GFP than MOIs of 0 and 10 PFU and insignificantly higher than the expression with an MOI of 5 PFU.

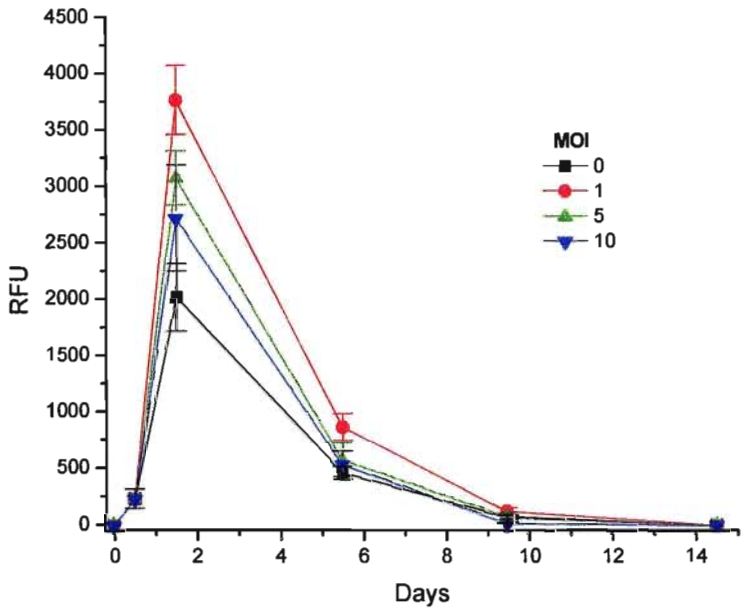

Figure 3.64: GFP fluorescence intensity over 14.5 days post-transfection in CHO cells, with super-infection using different MOIs. Fluorescence intensity was measured by the relative fluorescence units (RFU) of equal cell counts.

3.4.4- Gene expression from different plasmids in CHO cells super-infected with adenovirus at MOI of 1 PFU/cell

Expression from the different plasmid constructs was investigated with wild type super-infection at MOI 1 PFU/cell. The lower MOI allows the side effects encountered at MOI 10 PFU/cell to be overcome, which is the massive cellular detachment from the monolayer. The same experimental conditions for transfection (as in part 3.4.2) were performed, with the exception of the super-infection step that was done at an MOI of 1 PFU/cell. Triplicate samples were collected on 0, 0.5, 1.5, 3.5, 7.5, 11.5 and 15.5 days post-transfection, in which the super-infection was performed at 12 hours post-transfection. Two negative controls were included; the first is CHO cells transfected with pUC19 and used as a control for transfected cells, while the second is pUC19 transfected and super-infected with the wild type virus. DNA and RNA were isolated from the same collected samples.

3.4.4.1- Plasmid stability

The isolated DNA was quantified spectrophotometrically and equal amounts were used in a qPCR reaction to determine the copy number of each plasmid, using the GFP primer set. Plasmid copy number per cell was quantified in the transfected and super-infected conditions, using a standard curve and the results are illustrated in Figure 3.65. The statistical analysis was performed on the data by the two way ANOVA using Tukey's test at a significance level of lees than 0.05. All of the plasmids have an insignificant change in their stability in CHO cells with the transfection and the super-infection conditions. The maximum plasmid copy number was obtained at 12 hours post-

transfection with all of the plasmids used and the two conditions. The plasmids' copy numbers remain significantly elevated on day 1.5 post-transfection and reach the baseline on day 7.5 post-transfection.

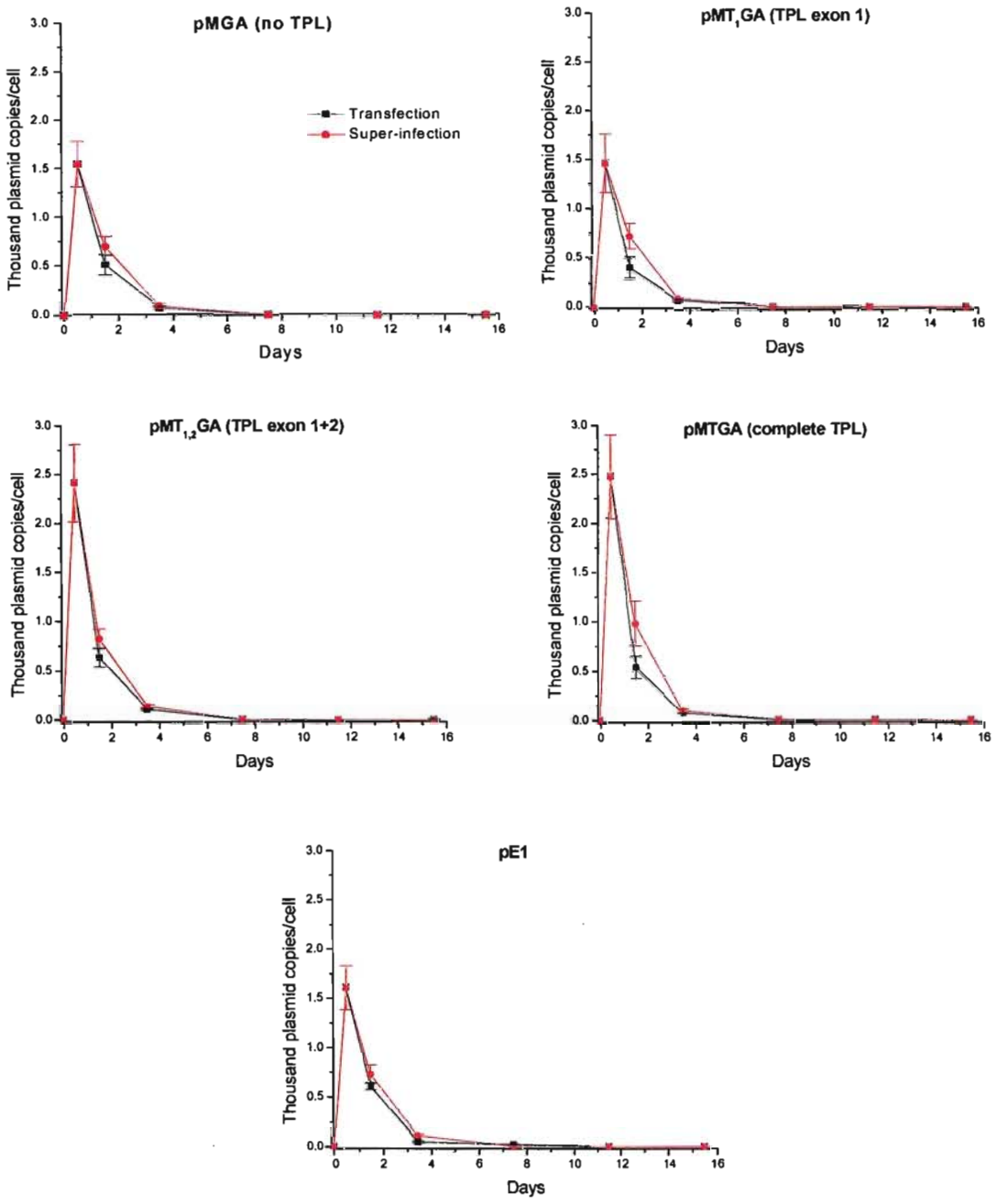

Figure 3.65: Copy numbers of the different plasmids over 15.5 days post-transfection in CHO cells, with transfection and super-infection (at MOI of 1 PFU/cell) conditions. Copy numbers were obtained by qPCR using a standard curve of known plasmid DNA concentration.

3.4.4.2- GFP transcription efficiency

The DNase treated and cleaned RNA was used in an RT reaction followed by qPCR using the specific GFP primer set. The copy numbers of GFP mRNA transcripts from each plasmid in the transfection and the super-infection conditions were calculated per cell, using a standard curve. The obtained data for each plasmid in the two conditions are illustrated in Figure 3.66. The statistical analysis of the data obtained was performed as described earlier in the plasmid quantification. The trend for mRNA transcripts produced from the different plasmids over time in both the transfection and the super-infection conditions was similar, with a significant increase in days 1.5 to 3.5. The transcripts' levels almost reached the baseline in day 7.5 and thereafter. Despite having the same trend, the increment with the super-infected conditions was significantly higher than that of the transfected conditions in the five plasmids, especially over the peak period (days 1.5 to 3.5). On the other hand, more mRNA transcripts were produced from pE1 over any of the other plasmids in both the transfection and super-infection conditions.

Transcription efficiency was calculated using the data obtained from the qPCRs performed on both DNA and RNA. Copy numbers of mRNA per plasmid per cell were estimated for each plasmid in the two conditions and illustrated in Figure 3.67. The data obtained was analyzed statistically by the two way ANOVA using Tukey's test at a significance level of 0.05. The overall trend for transcription efficiency in transfected and super-infected conditions of pMGA, pMT_1GA, $pMT_{1,2}GA$ and pMTGA showed insignificant changes over time. However, pE1 showed a significant increase in its super-

infected conditions compared with the transfected ones. The comparison between transfection efficiency of the different plasmids within the same condition revealed superiority of pE1 over all the other plasmids. The increased efficiency from pE1 over the other plasmids was more dramatic in the super-infected conditions than that of the transfected conditions.

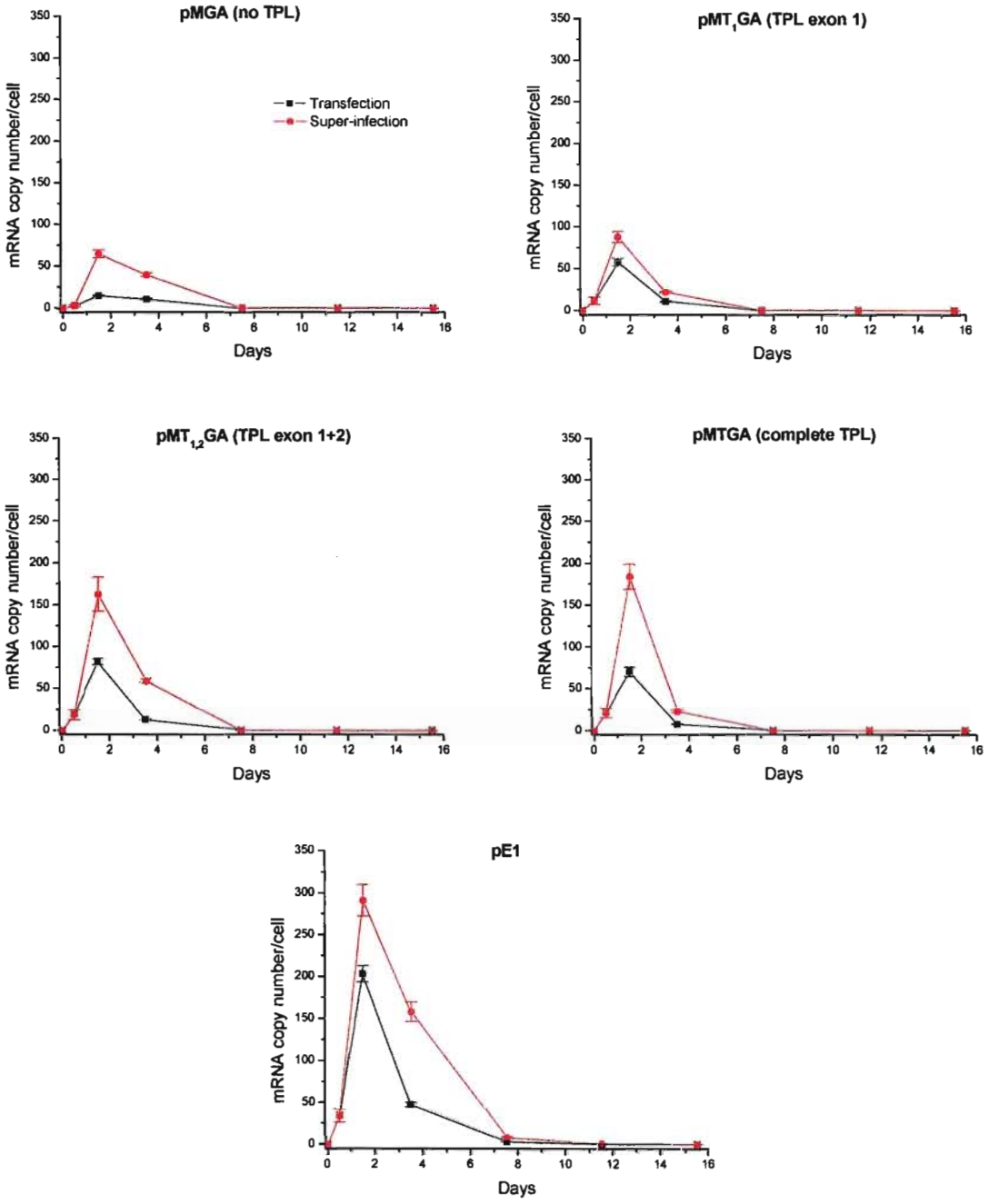

Figure 3.66: GFP mRNA transcripts from the different plasmids over 15.5 days post-transfection in CHO cells, with transfection and super-infection (at MOI of 1 PFU/cell) conditions. Copy numbers were obtained by qPCR using a standard curve of known plasmid DNA concentration.

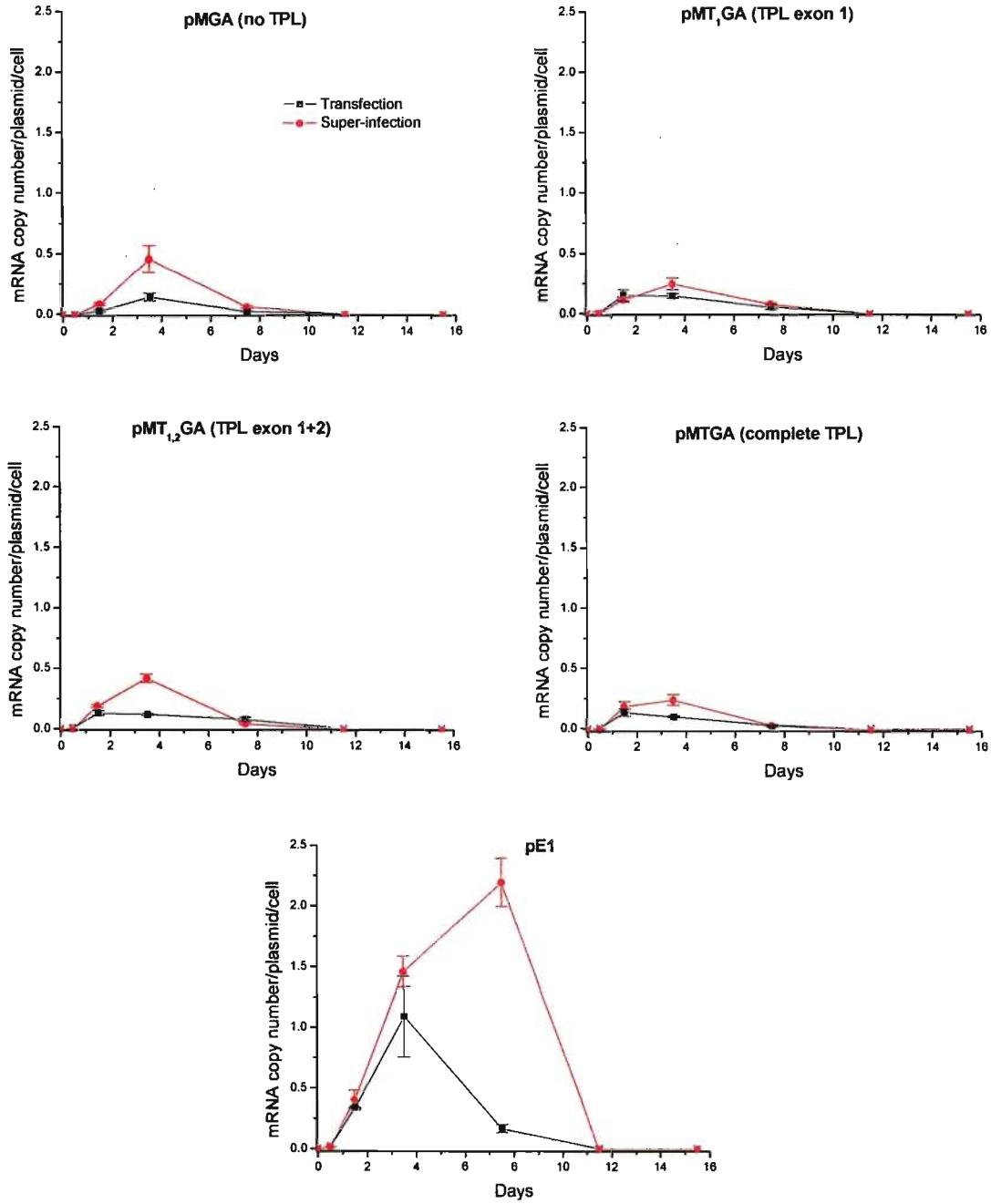

Figure 3.67: Transcription efficiency of GFP mRNA over 15.5 days post-transfection in CHO cells, with transfection and super-infection (at MOI of 1 PFU/cell) conditions. Efficiency was defined as GFP mRNA copy number per plasmid per cell. Copy numbers per cell of plasmid DNA and GFP mRNA were estimated by qPCR using a standard curve of a known plasmid concentration.

3.4.4.3- GFP translation

GFP was estimated by its fluorescence intensity and measured as the RFU in the equal cell counts from the different samples. CHO cells were used as a blank and the two negative controls (pUC19-transfected and pUC19-transfected/super-infected CHO cell) were included. The RFUs of GFP expressed in each plasmid with both conditions are shown in Figure 3.68. Statistical analysis of the data obtained was performed as mentioned earlier. All of the plasmids showed significant (at $P<0.05$) increase in GFP fluorescence intensity after 12 hours post-transfection, in both the transfection and the super-infection conditions, and last until day 7.5 post-transfection. Only pMGA showed almost identical expression levels of GFP in both the transfected and the super-infected conditions. The rest of the plasmids showed significantly higher GFP intensity with the super-infection over the transfection conditions.

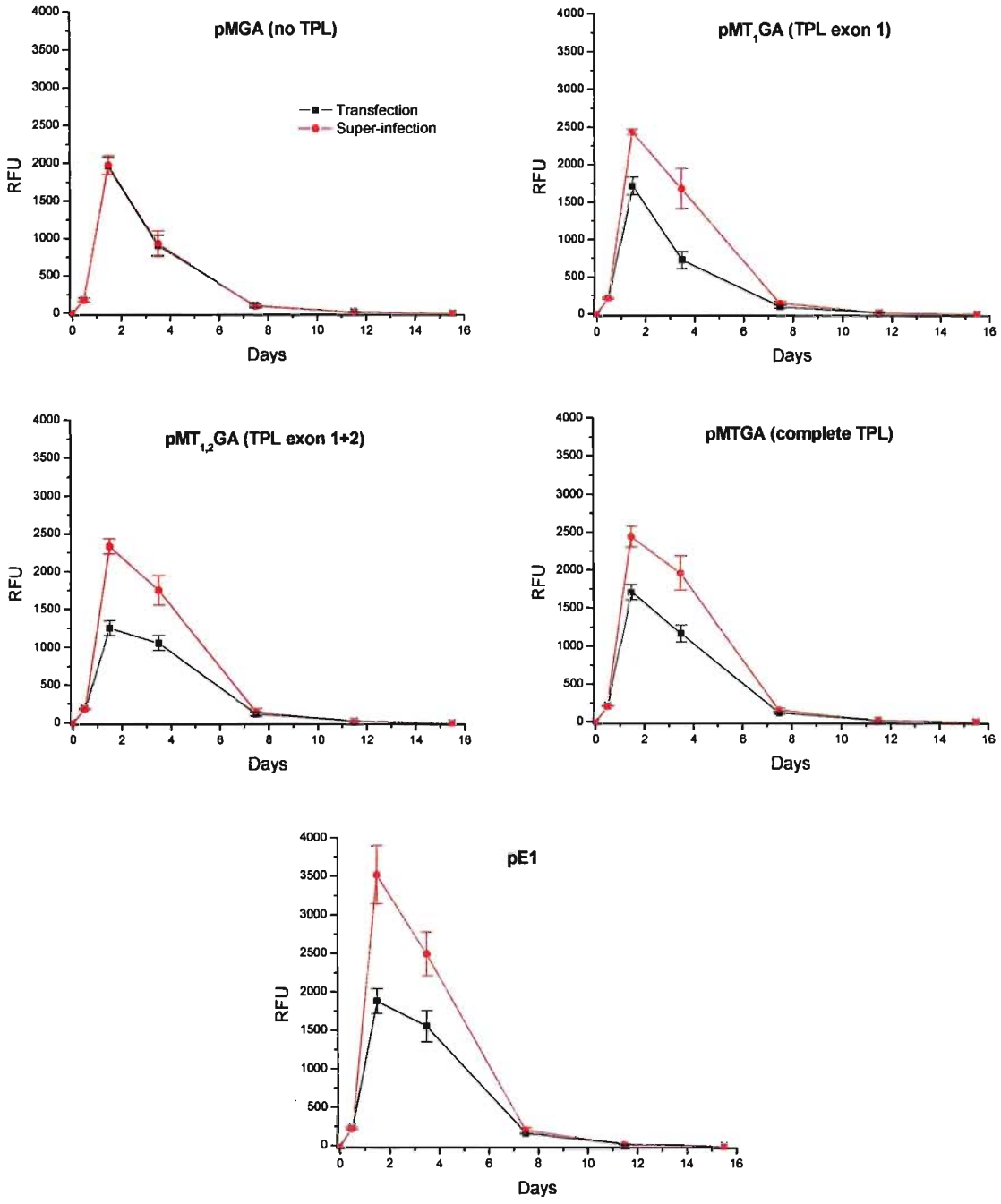

Figure 3.68: GFP fluorescence intensity over 15.5 days post-transfection in CHO cells, with transfection and super-infection (at MOI of 1 PFU/cell) conditions. Fluorescence intensity was measured by the relative fluorescence units (RFU) of equal cell counts.

DISCUSSION

Exogenous gene expression is a promising research field that has a number of downstream applications including gene therapy, vaccination and therapeutic protein production. Various organisms, ranging from simple prokaryotes to complex mammalian cells, are exploited for heterologous protein expression. Expression systems that utilize mammalian cells are favoured over other systems because these cells are capable of expressing complex proteins of high quality which are suitable for various applications. However, the major drawback of exogenous gene expression in mammalian cells is their characteristic inefficient recombinant protein expression relative to bacterial or yeast systems.

The study of viral infections, particularly the study of viral gene expression, has changed our views on the perceived inefficiency of mammalian cells as exogenous gene expression hosts. After infection, the completion of the viral life cycle results in the expression of many proteins in quantities that far exceed the observed expression levels of most non-viral transgenes. Hence, the inefficiency of mammalian recombinant gene expression is hypothesized to be the result of a limited understanding of the factors that govern gene expression in mammalian cells, rather than being a reflection on the protein-producing ability of these cells. As previously mentioned; some viruses achieve extremely high levels of viral gene expression once they enter the cell and exert control over the various cellular regulatory processes. The key players that act on these processes are viral regulatory elements, which are made up of mostly proteins.

The present study was designed with the purpose of increasing our understanding of the various factors that influence exogenous gene expression in mammalian cells. Since viruses are the ultimate exploiters of intracellular expression of foreign genes, adenovirus was used as a model virus. It contains multiple elements that exert their effect at different regulatory levels to enhance or control the cellular expression of viral genes. Adenoviruses have already been used as model systems for understanding gene expression, as well as oncogenic transformation, DNA replication, gene delivery, gene therapy and other molecular biological phenomena. The accumulated knowledge on adenoviruses was essential for further investigations of gene expression regulation.

We investigated exogenous gene expression at different levels; starting from the quality of the transgene (focusing on its delivery, stability and mutation rate) to evaluating adenoviral regulatory elements, including the major late promoter (MLP), the tripartite leader sequence (TPL), the E1 genes (cellular regulation and promoter transactivation) and the inverted terminal repeats (ITRs) (replication). In addition, we sought to enhance transgene expression in mammalian cells using these elements, along with other adenoviral components, and employing a number of different strategies.

4.1- DNA QUALITY

Two of the major considerations in molecular biology research that pertain to transgene expression are DNA purity and base pair accuracy. Contamination of DNA by chemical impurities and sequence mutations interferes with most downstream applications, including *in vitro* transfections and expression of transgenes, as well as *in vivo* administration of DNA for gene therapy or vaccination. Several techniques, such as

column-based chromatographic DNA isolation or cesium chloride gradients, have been developed to ensure high DNA purity and sequence accuracy. However, both of these methods have the potential to add even more impurities to the DNA. This is because the chemical reagents that are used as part of the isolation/purification procedures can contaminate the DNA. In this part of the study, we evaluated the effect of the major DNA contaminants, which are introduced to the DNA through bacterial culturing or DNA preparation, on transgene delivery and expression. The contaminants evaluated include: ethidium bromide (EtBr), cesium chloride (CsCl) and a combination of the later two, as well as endotoxin and ethanol (EtOH).

The effect of these different contaminants on the delivery of pCMVβ and the expression of the LacZ gene (encoded by the plasmid) was evaluated using *Chinese hamster* ovary (CHO) cells. The LacZ activity assay is widely used to determine the transfection efficiency of most cell culture transfection methods. However, this assay is only an indicator, rather than a direct measurement of transfection efficiency. To expand, LacZ activity is a measure of transgene (LacZ) expression efficiency, rather than the efficiency of transgene uptake by the cells. As such, the accuracy of this assay is subject to mutations within the coding sequence of the LacZ gene that may disrupt its expression or function but does not affect transgene uptake negatively. All of the contaminants, except EtOH, significantly reduced the number of cells that expressed LacZ. However, they did not all act to lower transfection efficiency, but some impaired transgene expression without affecting the efficiency of its delivery.

The use of qPCR allowed for a precise determination of the plasmid copy number per cell. This is an accurate measurement of transfection efficiency, as qPCR measures

the physical presence of the DNA molecule and not the expression of the genes encoded in the plasmid. The stability of the DNA molecule is also directly measured by this method, in contrast to the LacZ assay which measures an enzyme that is a downstream product of the transfected DNA, which differs in stability relative to the transfected DNA itself. The data obtained by the qPCR method indicated that spiking with CsCl, a combination of EtBr/CsCl or endotoxin lowered the transfection efficiency which accounts for the observed low expression of LacZ when spiking with these contaminants. However, spiking with EtBr and EtOH did not interfere with the transfection efficiency (the copy number of pCMVβ), as measured by qPCR. Therefore, the decreased expression levels of LacZ, which were observed after spiking with EtBr, were not the result of low plasmid copy numbers.

In addition, spiking with EtBr caused mutations in the DNA molecules which accounted for the lower expression of LacZ in cells that have been transfected with the contaminated DNA. EtBr intercalation with DNA introduces frame-shift mutations that inhibit transcription and subsequently, translation (Tripathi & Kumar, 1986 and Hurley, 2002). When spiking with the highest concentration of EtBr used in this experiment (250 nM), the number of cells expressing functional LacZ decreased by 80% relative to the non-spiked control. Hayashi and Harada (2007) reported that at a concentration of 1 mM of EtBr, 57% of base pairs will be occupied with the chemical in a single 500bp DNA molecule.

These results were confirmed by the restriction enzyme-PCR mediated mutation detection method which was first introduced in this work (Figure 3.8). The premise of this mutation detection method is that the digestion of plasmid DNA (pDNA) by a

restriction enzyme prevents its subsequent PCR amplification (when using primers that flank the digestion site), unless the restriction site is masked by a mutation in its sequence. It is already known that EtBr inhibits *in vitro* digestion with restriction endonucleases. This inhibition occurs wherever EtBr is bound to the restriction enzyme recognition site itself or 2-3 base pairs far from the site, with favourable binding to the G-C base pairs (Krugh & Reinhardt, 1975 and Hardwick *et al.*, 1984). However, in this study, spiked DNA was transfected into mammalian cells and re-isolated after 21 hours post-transfection. During this time, the DNA repair mechanism will introduce frame-shift mutations in the DNA sequence (Tripathi & Kumar, 1986).

The restriction enzyme *Hin*dIII, which recognizes a six base pair restriction site, was used for the purpose of our experiment. The plasmid pCMVβ has one *Hin*dIII site which represents 0.084% of the whole plasmid length. Using agarose gel electrophoresis, the products of endpoint PCR amplification were observed for the samples spiked with high EtBr concentrations. This observation indicated that EtBr spiking caused an incomplete digestion of pCMVβ by *Hin*dIII, allowing the amplification to occur. *Hin*dIII digestion of the pDNA spiked with other contaminants, even when EtBr was combined with CsCl, prevented subsequent PCR amplifications (as no bands were visible on the gel). This indicated that these contaminants do not compromise the sequence accuracy of the delivered DNA.

To quantify the occurrence of mutations introduced by EtBr, we carried out qPCR on the same EtBr-spiked samples before and after digestion (Figure 3.10). EtBr spiking induced mutations in 9.8% of *Hin*dIII recognition sites. This is a very high proportion considering that the screening was based on only 0.084% of the total plasmid length. As

previously mentioned, EtBr accumulates on 57% of base pairs in a single DNA molecule at a concentration of 1 mM EtBr (Hayashi & Harada, 2007). This experiment validated the accuracy and sensitivity of the mutation detection method through high-throughput screening.

CsCl reduced the transfection efficiency by interfering with the interaction of pDNA and calcium phosphate, while endotoxin spiking reduced the ability of the cells to take up pDNA. We used the calcium phosphate transfection method, first introduced by Graham & Van der Eb in 1973 and later optimized by Jordan *et al.* in 1996, where pDNA co-precipitates with calcium phosphate. Jordan *et al.* (1996) tested the effect of phosphate and calcium concentrations on DNA transfections and showed the importance of these parameters on this process. The high salt concentration, which results from spiking with CsCl, may be the main reason for the decreased transfection efficiency.

Cesium is very reactive and is the highest electropositive metal, even more positive than sodium or potassium (Patnaik, 2003). The presence of cesium in the transfection reaction may lead to a side reaction that reduces the amount of precipitated DNA or disrupts the optimal transfection pH. CsCl may also reduce DNA transfection efficiency by directly interacting with the DNA and thus protecting it against the mutagenic effect of EtBr when a combination of EtBr and CsCl was used for spiking DNA. CsCl shielded the DNA molecule from interacting with the mutagen EtBr.

It is generally accepted that transfection efficiency is negatively affected by the presence of an endotoxin in the transfection mixture (Sambrook *et al.*, 1989). This was confirmed when we spiked the DNA with different concentrations of endotoxin. Although we did not have a completely endotoxin-free DNA, as our control contained

0.32 EU/μg DNA, increasing endotoxin concentrations caused a significant drop in transfection efficiency. We cannot refer to any cellular effect that might directly cause such a reduction since mammalian cells are not sensitive to endotoxin (Wright *et al.*, 2003). Endotoxin interaction with DNA and/or the cell membrane may reduce transfection. The presence of endotoxin in the transfection mixture may decrease DNA precipitation which in turn will decrease transfection efficiency. Also, the lipopolysaccharide nature of an endotoxin may increase the cellular resistance to transfection by interacting with the cellular membrane.

The interactions of the contaminants used in this study with pDNA are reversible, as demonstrated by the DNA cleaning procedures that restored transfection efficiencies and transgene expression rates that were comparable to that of non-spiked controls (Figures 3.6 & 3.7). Cleaning of pDNA spiked with CsCl, EtBr/CsCl and endotoxin improved transfection efficiency (increased copy number), verifying that these contaminants acted to lower the efficiency of transgene delivery to the cells. The cleaning of EtBr spiked samples did not have an effect on the efficiency of transfection, nevertheless, an improved transgene (LacZ) expression was observed. This indicated that EtBr affects the DNA structure and function inside the cell and does not interfere with the efficiency of transgene delivery.

All of the investigated contaminants, except EtOH, had reversible, negative effects on DNA delivery or expression. EtBr affected expression through its mutagenic effect. In contrast, CsCl and endotoxins affected the efficiency of DNA transfection by calcium phosphate, with no mutagenesis. More studies are needed to understand the nature and

the mechanisms of the interactions between CsCl and the transfection process or endotoxin with the DNA and the cell membrane.

4.2- ADENOVIRAL TPL EXONS AND E1 REGION

To achieve active gene expression from exogenous DNA, we tried to mimic the late viral protein production of the adenovirus. The different elements that were incorporated in the plasmid pE1, such as the MLP and the TPL, are either directly related to gene expression or, as in the case of adenoviral E1 genes, they act indirectly to enhance and regulate the expression process. ITRs were incorporated to serve as origins of replication and provide plasmid stability by preventing the dilution of pDNA by mitosis.

4.2.1- TPL exons

The TPL used in the plasmid construction was based on joined exon sequences without introns. The plasmid stability in CHO cells was not affected by the presence of different TPL exon combinations (exon 1, exons 1+2 and the complete TPL). Plasmid DNA reached its highest concentration inside the cells 12 hours post-transfection, the first point to be measured after transfection. Plasmid copy number decreased after this point, reaching less than half of the copy numbers at 24 hours post-transfection. Plasmid DNA can be diluted by mitotic division (Pauletti *et al.*, 1990) and degradation by nucleases (Wilson *et al.*, 1992) or by integrating into the cellular genome by homologous recombination (Bollag *et al.*, 1989). Dilution and degradation are the most likely mechanisms by which the plasmid copy numbers decreased in our experiment, as plasmid integration may be excluded due to the short time period of the experiments. Cellular division by mitosis was the main cause of plasmid dilution, since the average

CHO doubling time in some reports is 12 hours (Chang & Little, 1991) and 19.1 hours in other papers (Parham *et al.*, 1998). The average plasmid copy numbers per cell varied between different transfections due to the inconsistency of the calcium phosphate transfection method (Liu *et al.*, 2004).

Transgene mRNA transcription rates are directly subject to transgene copy numbers and therefore, variations in transfection efficiencies introduced bias in the assessments of transgene expression. To minimize the transfection efficiency bias, transgene transcription was measured and reported as mRNA copy number per plasmid per cell. The transcription of the different TPL exon combinations, including the complete TPL, cloned in the 5' untranslated region (UTR) upstream of the green fluorescence protein (GFP) mRNA, was confirmed for all plasmid constructs. The maximum amount of expressed GFP mRNA was measured 24 hours post-transfection. This result did not coincide with the maximum plasmid copy numbers which were observed 12 hours post-transfection, reflecting the time required for transgene transcription and the accumulation of mRNA. Inclusions of TPL exon 1 or the complete TPL in the 5' UTR did not affect transgene transcription, while the inclusions of both exons 1 and 2 significantly reduced GFP transcription. These results indicate that different TPL exons and even the complete TPL do not enhance mRNA transcription. This finding is in accordance with Mansour *et al.* (1986) who reported that transcription enhancement from the MLP by the TPL occurred through the downstream binding site (DBS) present within the first intron, but not through the TPL exons themselves.

The effect of TPL exon 1 was more pronounced on transgene mRNA transport (from the nucleus to the cytoplasm) than on transgene transcription because its inclusion

in the transcript significantly decreased the accumulation of GFP mRNA in the cytoplasm. Based on the observed nuclear accumulation of GFP mRNA, it suggests that TPL exon 1, the shortest TPL exon, could not form the secondary structure required for TPL functionality.

The inclusions of TPL exons 1 and 2 and even the complete TPL sequence did not have an effect on the transport of GFP mRNA from the nucleus to the cytoplasm. While the addition of these sequences did not decrease mRNA transport, as was the case when only TPL exon 1 was used, it is clear that the activity of the TPL was severely diminished by the absence of viral proteins, specifically the E1B 55k (Horridge & Leppard, 1998) and the E4 orf6 (Dobbelstein *et al.*, 1997) proteins, which interact with the TPL. Once this occurs, the TPL serves as a linker for the viral mRNA, rather than a leader, while the E1B 55k and the E4-ofr6 are the actual "leaders" of the mRNA.

4.2.2- ITRs-E1

The presence of ITRs and E1 in the pE1 plasmid did not have any effect on plasmid stability relative to the pMTGA plasmid (Figure 3.21). The difference in copy numbers (average number of plasmids per cell) between the two plasmids was a consequence of their different molecular weights, since equal masses were transfected into CHO cells. Twenty-four hours post-transfection, the ratio between their copy numbers (pE1 : pMTGA = 1 : 2.8) was close to the ratio between their sizes (8481 bp : 3716 bp = 2.3 : 1, respectively). As expected, the copy number of pE1 did not increase because the ITRs cannot function as an origin of replication in the absence of adenoviral E2 proteins (Rekosh *et al.*, 1977 and Hay *et al.*, 1995). Without the ability to replicate, pE1 was not

maintained in transfected cells. The increase in GFP mRNA transcripts and GFP intensity in the presence of ITRs and E1 was likely a result of the transactivation of the MLP by the E1 proteins (Parks & Shenk, 1997).

4.2.3- Cellular background

In order to investigate the effect of cellular background on MLP activity and the functionality of adenoviral elements that are used to enhance the expression from the MLP, we studied the stability and activity of the pE1 plasmid in both CHO and human embryonic kidney (HEK) 293 cells. The results show that CHO cells exhibited seven folds higher transfection efficiency than HEK 293 cells. The difference in transfection efficiencies can be attributed to the transfection agent that was used in this experiment (Lipofectamine 2000) as well as the growth rates of these two cell lines. Transfection with Lipofectamine 2000 is cell cycle dependent and is more efficient with dividing than non-dividing cells. Thus, the transfection efficiency with cells in the S or G2 phase is up to 500 fold greater than with cells in the G1 phase (Brunner *et al.*, 2000). Since CHO cells have approximately two and a half fold faster doubling time than HEK 293 cells (Parham *et al.*, 1998), more CHO cells will be dividing during the transfection period and hence, take up the plasmid more efficiently. Although Preuss *et al.* (1999) reported that HEK 293 cells exhibited higher transfection efficiencies than CHO cells, they used the calcium phosphate transfection method in their experiments, which accounts for the contradictory data.

Despite their lower transfection efficiency, HEK 293 cells produced significantly more GFP transcripts than CHO cells. Therefore, HEK 293 cells exhibited higher

transcription efficiency than CHO cells, since on-average, they produced more GFP mRNA copies per plasmid DNA per cell than CHO cells. Liu *et al.* (2008), who investigated and optimized the factors that affect transient transfection in HEK 293 and CHO cells, showed that both cell lines exhibited similar GFP productivities. Since cellular background did not directly influence GFP production, our data demonstrated that the difference in transgene mRNA expression between the two cell lines was due to the cell line-dependent differential activity of the MLP. Namely, HEK 293 cells offer a more favourable environment for the activity of the MLP promoter. They have more adenoviral E1 proteins, which are continually expressed from their integrated E1 genes, and they are a cell line derived from the natural host of Adenovirus serotype 5 (Ad5) (human) (Aiello *et al.*, 1979). CHO cells have a similar reduction of MLP activity as human cells which were previously reported for adenovirus 12 late RNAs in CHO cells expressing Ad5 E1 genes (Klimkait & Doerfler, 1985 and 1987).

4.3- Cell Line Construction

The low stability of the pE1 plasmid and the relatively low expression of the transgene (GFP) led to the conclusion that the elements encoded on pE1 were not enough to attain high expression levels in CHO cells. In the next step of the study, the effects of introducing additional adenoviral components (to complement the elements that were already encoded on the plasmid) on plasmid stability and GFP expression were investigated. Three different methods were devised and implemented for this purpose. The first method was co-transfection with another plasmid, pE2; the second required the

development of a specific cell line which enhanced pE1 stability and expression; and the third method was adenoviral super-infection.

4.3.1- Co-transfection

The pE2 plasmid encodes Ad5 E2 genes and the MLP-driven viral protease gene, all of which were successfully transcribed post-transfection in HEK 293 cells. However, transfection of the same plasmid into CHO cells resulted in the expression of only the viral protease. Transactivation of the E2 promoter in HEK 293 cells was facilitated by the expression of Ad5 E1 genes that are integrated into the host cell genome. CHO cells lack these E1 genes and could not activate the E2 promoter. Therefore, transcription did not take place. However, the viral protease was expressed in CHO cells, as its transcription was driven by the MLP present on the strand complementary to the E2 genes, and did not require primary activation.

Co-transfection of various molar ratios of pE1 and pE2 into CHO cells did not result in the cellular retention of either of the two plasmids. Neither of the plasmids was affected by the presence of the other and both were lost from the cells three days after the transfection. According to Shenk & Flint, 1991; Swaminathan & Thimmapaya, 1995 and Brehm *et al.*, 1998, the expected interaction between the two plasmids and their products would predict that the expression of E1A would activate the E2 promoter to express E2 proteins, and the presence of E2 proteins would allow the replication at the circular ITRs (Graham *et al.*, 1989). However, as mentioned previously, none of the obtained results suggested that pE2 co-transfection facilitated pE1 replication.

The transcription of GFP from pE1 was detected only when the highest amount of pE1 was transfected into CHO cells. The fast growth rate of these cells may, in part, be responsible for the lack of any detectable transgene transcription with lower plasmid concentrations. This is because episomal DNA is quickly diluted out by mitosis. Transcription of any of the E2 genes from pE2 was undetectable, even when the highest amount of pE2 was transfected into the cells. The only detected transcription from pE2 was the viral protease and, similarly to GFP, was only observed with the highest amount of plasmid used. There are two possible explanations for this result. First, the amount of expressed E1 genes was not enough to transactivate the E2 promoter in CHO cells, unlike in the HEK 293 cells where the E1 genes are integrated and continually expressed. Second, the success of co-transfections depends mainly on the coexistence of both plasmids in the same cell. Although both plasmids were detected after transfection, the simultaneous presence of both plasmids inside the same cell remains unknown.

4.3.2- CHO cell lines

As neither pE1 nor pE2 plasmids were maintained after their co-transfection into CHO cells, the next step was to construct a new CHO cell line with integrated Ad5 E2 and viral protease genes (CHO-E2 cell line). After transfecting linearized pE2 into CHO cells, followed by selection procedures, five different foci with G418 resistance (left end of the linearized plasmid) were isolated and that were confirmed to carry the right end of the linearized pE2. Linearized pE2 was used because the integration of linearized DNA is more probable than the integration of circular forms (Brinster *et al.*, 1985) and it is also used to control the linearization site so that it does not interfere with coding or regulatory sequences or their order within the DNA construct (Nagy *et al.*, 2003).

The presence of the four viral genes encoded on pE2 was confirmed by PCR performed on DNA isolated from all five cell line constructs. Although this is not the ideal selection or detection method, it was the only feasible way to select for the presence of these genes. A better selection method should have focused on the expression of these genes, so that foci that actively express all of the genes could be discriminated from foci with integrated, but inactive genes. This selection method is suited for genes whose expression is driven by constitutive or simple inducible promoters, however, the adenoviral E2 promoter is transactivated only in the presence of E1A proteins (Shenk & Flint, 1991; Swaminathan & Thimmapaya, 1995 and Brehm *et al.*, 1998).

The circular form of the plasmid was detected in three of these five CHO-E2 cell lines (CHO-E2-2, CHO-E2-4 and CHO-E2-5) (Figure 3.42). These are interesting results, since the stock linearized plasmid that was used for the construction of all the cell lines was confirmed by PCR (detecting for the circular form) to be linearized completely. A possible explanation for this finding is that the linearized plasmids re-ligated inside the cells after the transfection. Mammalian cells are able to ligate linear DNA, especially when its ends are cohesive. The detection of circular forms of the adenoviral genome early after infection and before the initiation of viral genome replication, supports this assumption (Ruben *et al.*, 1983 and Graham, 1984). Additionally, non-homologous end-joining ligation, detected between co-transfected plasmids, can occur as a result of double strand breaks in the foreign DNA (Ishikawa *et al.*, 2004). The ends of two DNA molecules can be ligated in the cells, regardless of the degree of homology between them (Wake *et al.*, 1984). Thus, non-homologous end-joining was the mechanism by which

circularization of linear plasmids occurred, after transfection (Kabotyanski *et al.*, 1998 and Smith *et al.*, 2003).

All five CHO-E2 cell lines were transfected with pE1 and expressed GFP, detected by confocal microscopy (Figure 3.43), twenty-four hours post-transfection. However, there were no major differences in expression efficiency between the cell lines. In addition, pE1 was not maintained in any of the new cell lines, as it was lost two days post-transfection in four of the five cell lines and after three days in the fifth one (CHO-E2-3). Unaltered CHO cells retained the pE1 plasmid for three days. The stability of pE1 was dependent on the initial transfection efficiency, as the starting plasmid copy number dictated the amount of time it took for any given cell line to lose the plasmid by DNA degradation or dilution by mitosis. None of the constructed CHO-E2 cell lines were able to maintain pE1 because replication from the ITRs did not occur. This finding also indicated that E2 proteins, which are essential for replication initiation from the ITRs, were lacking or present in insufficient amounts (Flint & Shenk, 1997).

The transfection of pE1 into the constructed CHO-E2 cell lines was supposed to provide the E1 proteins required for the transactivation of the E2 promoters (Shenk & Flint, 1991; Swaminathan & Thimmapaya, 1995 and Brehm *et al.*, 1998). However, expression of any of the E2 genes was not detected. In three of the five cell lines, the viral protease gene, which is under the control of the MLP and encoded on the complementary strand of the E2 genes, was expressed, as detected by qPCR. The MLP promoter is constitutive and does not require transactivation to initiate the expression of the viral protease. This explains why the viral protease was expressed and the E2 genes were not, despite being encoded on the same DNA molecule, but on opposite strands.

As stated above, only three cell lines (CHO-E2-1, CHO-E2-3 and CHO-E2-5) transcribed the viral protease gene. The other two cell lines (CHO-E2-2 and CHO-E2-4) did not express detectable amounts of the viral protease mRNA. Interestingly both of these cell lines screened positive for the presence of the circular form of pE2. As it is highly unlikely that these cells maintained pE2 as an episome, it was assumed that in these cells, the linearized pE2 was initially re-ligated (circularised) and subsequently linearized at a different site prior to integration into the host genome. This reorganization may have separated the viral protease gene from its promoter, accounting for the complete absence of viral protease expression in these cell lines. Although the cell line CHO-E2-5 tested positive for the presence of the circular form of pE2, it was able to express the viral protease gene. This indicated that pE2 most likely linearized at a site that did not interfere with the viral protease cassette. The lack of transcription of the E2 genes in the three cell lines where the circular forms of the plasmid were detected may also be the result of disrupting the order of the E2 cassette (which constitutes 69.5% of plasmid length).

In summary, the constructed cell lines did not express E2 genes, neither constitutively nor upon induction, and thus, were unable to facilitate the replication of episomal DNA. Furthermore, the lack of a complete genome sequence of CHO cells made it impossible to precisely determine the sites of integration of pE2. This also prevented the screening of homologous sequences (possibly present in the plasmids) that may have influenced the sites of integration. These findings emphasize the suggestion made by Griffin *et al.* (2007) that the availability of such genome sequence data will

enable the development of other tools such as microarrays that are useful in the genomic and transcriptomic analysis of the newly constructed CHO cell lines.

4.4- Induction of Gene Expression by Adenovirus Super-Infection

4.4.1- Stability and transcription from pMTGA in HEK 293 and CHO cells super-infected with adenovirus

Initially, the super-infection experiments were performed in both HEK 293 and CHO cells. The pMTGA plasmid, which encodes the complete TPL upstream of the GFP transgene, was transfected into both cell lines and then super-infected with the wild type adenovirus dl309. Adenoviral infection did not enhance the stability of the transgenes despite the presence of the viral DNA binding protein (DBP), whose function is to protect single and double-stranded DNA from cellular DNases (Nass & Frenkel, 1978 and 1980 and Frenkel & Horan, 1983). Therefore, it was assumed that dilution by mitosis, rather than DNA degradation by DNases, was the main force determining the stability or instability of the plasmid.

The observed differences in transgene expression efficiencies between CHO cells and HEK 293 cells (Figures 3.53 & 3.54) can be explained by examining the progression of the adenoviral life cycle in each of them. HEK 293 cells were lysed early after the super-infection, while CHO cells appeared unaffected. Although the adenoviral genome is replicated with equivalent efficiencies in CHO and HeLa cell lines, adenovirus-infected CHO cells produce approximately 6,000 fold fewer virions than adenovirus-infected HeLa cells (Longiaru & Horwitz, 1981). However, the adenovirus infection of CHO cells resulted in the synthesis of most viral proteins as well as active replication of

the viral genome, but not in complete virions. Similarly, studies that investigated infections of BHK21 hamster cells by adenovirus serotype 12 reported that these cells did not support the completion of the adenoviral life cycle (Doerfler, 1991). Although supplementing adenovirus 12 with the E1 region of Ad5 resulted in the replication of the viral genome and the transcription of late genes, virion production still did not occur. Adenoviruses are unable to complete their life cycles in hamster cells because the hexon and fibre proteins, which are essential for virion assembly, are not produced in these cells (Schiedner *et al.*, 1994 and Hösel *et al.*, 2003). The increased transgene transcription efficiency in super-infected CHO cells, relative to super-infected HEK 293 cells, was therefore a consequence of their increased tolerance to adenovirus infection. This was due to the inability of the adenovirus to initiate cell lysis in CHO cells.

4.4.2- Gene expression from different plasmids in CHO cells super-infected with adenovirus at MOI of 10 PFU/cell

Although super-infection with the wild type adenovirus dl309 increased transgene transcription levels in both cell lines, the use of CHO cells was favoured over the use of HEK 293 cells in subsequent super-infection experiments. This decision was made based on the observation that CHO cells were more resistant to rapid lysis initiated by the viral infection, while still allowing complementation with the viral proteins that were required for improved efficiency of exogenous gene expression. The effects of the adenovirus super-infections on the efficiencies of transgene expression were elevated from different constructs, including incomplete and complete TPL sequences as well as the plasmid pE1. These constructs yielded valuable information about the regulation of transgene expression in mammalian cells.

Adenovirus super-infection was unable to improve the intracellular stability of plasmids that were not encoded for the ITRs and the E1. However, a significant increase in the copy number of pE1 (which encoded the ITRs and the E1) was measured 1.5 days post-transfection in super-infected cells (Figure 3.56). This indicated that this episomal vector replicated in the presence of adenoviral proteins. This data agrees with previous findings that show that the replication of circular adenoviral genomes, containing incomplete ligated ITRs, is able to produce linear genome copies and subsequently infectious viral particles (Graham *et al.*, 1989). The circular ITRs used in the construction of the pE1 plasmid were derived from such circular, replication competent adenoviral genomes. Therefore, the adenovirus super-infection should provide the viral proteins required for replication and also induced the S-phase in host cells (Hay *et al.*, 1995). The replication of pE1 coincided with peak adenoviral DNA replication, which occurs five to eight hours post-infection (Berk, 2007). Despite the increase in pE1 copy number in super-infected CHO cells that were measured 1.5 days post-transfection, mRNA transcription did not increase accordingly. This finding reflected the strength of the super-infection, as expression of viral proteins placed an overwhelming demand on the cellular gene expression machinery.

The copy number of pE1 in CHO cells dropped significantly 3.5 days post-transfection (three days after the super-infection). This was accompanied by high levels of cellular detachment from the monolayer. This phenomenon, where the infected cells start to round and then detach from the monolayer, is common at the late stages of viral infection and is a hallmark of the cytopathic effect (CPE) (Flint, 1984). In adenovirus infected CHO cells, the CPE is slower to appear as these cells are not the natural host of

human adenoviruses. This effect was observed about 3 days post-infection. Vital staining showed that the majority of the detached cells were still alive. The investigation of pE1 activity in both attached and detached cells revealed that detached cells contained significantly higher amounts of the plasmid. In addition, there was more GFP mRNA and higher efficiencies of transgene transcription in the detached cells relative to adhered cells.

The adenovirus super-infection did not increase the efficiency of GFP mRNA transcription from the pMGA and pMT_1GA constructs. Both of these constructs lacked the complete TPL sequence. The data suggests that, even in the presence of viral proteins, an incomplete or missing TPL structure negatively affected mRNA stability and subsequently lowered transcription efficiency. The significant improvement of transgene transcription efficiency, measured when the complete TPL was used, indicated that all TPL exons are required for TPL functionality. The TPL sequence must be complete in order to interact with viral proteins E1B 55k and E4 orf6 (Dobbelstein *et al.*, 1997 and Horridge & Leppard, 1998). GFP intensity was used as a direct measurement of transgene expression at the protein level and was also negatively affected by the exclusion of the TPL from the construct. However, even when the complete TPL sequence was part of the transgene expression construct, no significant increase in the intensity was observed relative to transfected but non-super-infected cells. This indicated that translational competition existed between the GFP transgene and the viral genes when the cells were super-infected with wild type adenovirus dl309 at an MOI of 10 PFU/cell.

To summarize, cellular detachment was a characteristic event in all adenoviral infections, including infections of control CHO cells that did not contain plasmid DNA. Therefore, our experiments showed that adenoviral infection of CHO cells caused cellular detachment and not complete cellular lysis, which began two to three days post-infection. Active pE1 replication occurred only in adenovirus infected cells, explaining why pE1 copy numbers were significantly increased in detached cells, relative to monolayer cells. Furthermore, detached cells (from the super-infected pE1) had significantly increased transgene transcription efficiency relative to attached cells. Despite an increase in plasmid pE1 copy number, adenovirus super-infection did not improve transgene expression, relative to transfected but non-super-infected cells. We assumed that the use of an MOI of 10 PFU/cell overloaded the cellular expression machinery and also biased it towards processing other mRNAs that have the TPL sequence. This was indicated by a decrease in GFP intensity when the TPL sequence was excluded from the transgene construct.

4.4.3- Optimization of viral MOI in CHO cells

MOI optimization was performed for infections of CHO cells transfected with pE1. MOI did not have a measurable effect on transgene/plasmid stability. Furthermore, pE1 copy numbers did not increase at any of the used MOIs, including an MOI of 10 PFU/cell. This is an interesting finding since, in the previous experiment, a transient increase in pE1 copies was observed at an MOI of 10 PFU/cell. Although the experiment was not repeated again, these differing results can be explained by a variable efficiency of replication from the circular ITR forms. In particular, replication from the circular ITR

forms appears to be inefficient compared to the linear forms, especially at the early stages of the replication cycle.

The adenovirus replicates its genome through a strand displacement mechanism starting at the ITRs that serve as an origin of replication (Brenkman *et al.*, 2002) (Figure 1.3). Graham *et al.* (1989) proposed a model for viral DNA replication from circular molecules (See the appendix). In their model, replication takes place at the junction of viral ITRs to produce linear forms of the viral DNA. Cellular background may be another factor that affected replication from circular ITRs. The complete circular viral genome can complete the virus life cycle in human cells and produce new infectious viruses. However, in the super-infected CHO cells, replication from circular ITRs may not have been as efficient as replication from the linear viral genome.

Decreasing the MOI caused an enhancement of GFP mRNA levels, transgene transcription efficiency and translation levels (Figures 3.62-3.64). At an MOI of 1 PFU/cell, transgene transcription efficiency and GFP intensity were significantly higher than at an MOI of 10 PFU/cell. These results concurred with our previous observations of cellular vitality and monolayer attachment. The cells remained attached at an MOI of 1 PFU/cell, similarly to the non-infected control cells, but further increases of MOI resulted in proportional detachment of cells from the monolayer.

These findings indicated that the strength of viral infection and expression directly affected transgene expression inside the cells. At higher MOIs, it appears that the competition between viral and transgene mRNA translation lowered transgene expression, while high viral loads severely affected host cells. This was in accordance with previously published data obtained from adenovirus infected HEK 293 cells. The

data showed that further increases of the MOI over 5 PFU/cell did not elevate viral production (Ferreira *et al.*, 2005), as cellular machinery had reached its saturation point and could no longer produce more viruses. Similarly, at an MOI of 10 PFU/cell in our experiment, transgene expression was lowered by competing viral proteins, whose expression overtaxed the cellular expression machinery and affected other cellular processes. Therefore, it was concluded that use of lower MOI is more suitable for both transgene expression and cellular vitality.

4.4.4- Gene expression from different plasmids in CHO cells super-infected with adenovirus at MOI of 1 PFU/cell

The use of an MOI of 1 PFU/cell did not severely affect cellular activity and attachment. Therefore, we were able to extend DNA, RNA and protein collection times which provided us with more detailed results. As expected from the previous optimization experiment, adenovirus super-infection did not affect plasmid stability over time. At low MOIs, it appears that viral proteins were not produced in quantities required to force active replication from the circular ITRs construct. Low viral yield at an MOI of 1 PFU/cell was also reported by Ferreira *et al.* (2005), who showed that viral yield was lower by 10^4 compared to an MOI of 5 PFU/cell.

The presence of viral proteins had a positive effect on transgene transcription from the MLP, as GFP mRNA copy numbers increased after the super-infection (Figure 3.66). The direct effect of the viral infection on MLP activity was clearly demonstrated with the use of the constructs lacking the TPL sequence. However, the gradual increase in transgene transcript copies with the addition of TPL exons in the expression constructs

indicated an additive effect, which was mainly exerted on transgene mRNA stability. Although the inclusion of TPL exons in the expression cassette enhanced transgene mRNA expression in non-infected cells, this effect was more pronounced in adenovirus super-infected cells.

In contrast to the other four plasmids (pMGA, pMT_1GA, $pMT_{1,2}GA$ and pMTGA), transgene transcription efficiency from pE1 was significantly higher after super-infection (Figure 3.67). The only difference between the pE1 and pMTGA plasmids was that pE1 encoded the ITRs-E1 fragment, while pMTGA did not. Therefore, the increased transgene transcription efficiency of pE1, relative to pMTGA, was most likely caused by the inclusion of this fragment. In a previous experiment, it was demonstrated that the ITRs-E1 fragment enhanced transgene transcription efficiency in the absence of viral super-infection. Most notably, the E1A proteins, which were encoded by the ITRs-E1 fragment, play a major role in the transactivation of transcription from the MLP. Although the wild type adenovirus dl309 also encoded the E1 region and the ITRs, enhanced transgene expression from pMTGA did not reach same levels as pE1 after super-infection. This indicated that an excess amount of E1A proteins enhances transgene transcription efficiency. The pE1 plasmid increased the abundance of these proteins by increasing their gene copy number and hence, GFP expression from this construct was significantly higher than from pMTGA.

The translation of GFP mRNA also increased after viral infection, most likely as a result of the viral encoded E1B 55k and E4 orf6 proteins (Babiss *et al.*, 1985; Pilder *et al.*, 1986b; Leppard & Shenk, 1989 and Bridge & Ketner, 1990). The only exception was GFP mRNA translation from the pMGA plasmid, which did not increase after super-

infection. This result was expected, since the TPL sequence was absent from this transgene expression construct. On the other hand, the constructs that contained the complete TPL structure (pMTGA and pE1) showed a significant increase in GFP intensity after super-infection. This demonstrates the importance of the E1B 55k and E4 orf6 viral proteins. In addition, the intensity of GFP expressed from pE1 was significantly higher than that from pMTGA, mainly because of the higher transgene transcription efficiency from pE1.

CONCLUSION

Based on the data presented in this thesis, one can conclude the following:

1- Contaminants have a major negative effect on DNA delivery and gene expression by either affecting transfection efficiency or mutating the transgene coding region. Among the contaminants tested in this study, only EtBr appeared to cause mutations in the DNA sequence. Using a new, ultrasensitive, PCR-based mutation detection method, developed in this study, it was possible to detect very low mutation frequencies.

2- Five plasmids were engineered and contained an expression cassette with a common promoter (MLP) and incomplete or complete TPL exons. The ITRs-E1 fragment was included in one construct. The TPL exons 2 and 3 are essential for the TPL functionality. The incorporation of the Ad5 E1 region or the use of HEK 293 cells enhanced transgene expression.

3- The constructed CHO cell lines showed no expression of the Ad5 E2 genes, neither constitutively nor upon induction, and thus, were unable to facilitate the replication of episomal DNA.

4- Adenovirus super-infection enhanced transgene expression when the MOI was optimized for gene expression and cellular vitality. The MLP, as well as the TPL, showed higher activity under the super-infection. However, there was no conclusive evidence of transgene replication at the optimized MOI.

In summary, this study emphasized the importance of DNA quality for transgene delivery and expression. However, the use of adenoviral elements to enhance exogenous gene expression was successful only when the complementary viral proteins and sequences were present. Active expression of the adenoviral proteins did not depend solely on the presence of a few major regulatory elements, but rather on the specific combination of different elements that work in cis or trans to activate gene expression.

LITERATURE CITED

Abdallah, B.; Hassan, A.; Benoist, C.; Goula, D.; Behr, J. P. and Demeneix, B. A. (1996). A powerful nonviral vector for *in vivo* gene transfer into the adult mammalian brain: polyethylenimine. *Hum. Gene Ther.* 7: 1947-1954.

Acheson, N. (2007). Fundamentals of molecular virology. p 123-133. John Wiley & Sons.

Adam, S. A. and Dreyfuss, G. (1987). Adenovirus proteins associated with mRNA and hnRNA in infected HeLa cells. *J. Virol.* 61: 3276-3283.

Ahn, H. H.; Lee, J. H.; Kim, K. S.; Lee, J. Y.; Kim, M. S.; Khang, G.; Lee, I. W. and Lee, H. B. (2008). Polyethyleneimine-mediated gene delivery into human adipose derived stem cells. *Biomaterials* 29: 2415-2422.

Aiello, L.; Guilfoyle, R.; Huebner, K.; and Weinmann, R. (1979). Adenovirus 5 DNA sequences present and RNA sequences transcribed in transformed human embryonic kidney cells (HEK-Ad-5 or 293). *Virology* 94: 460-469.

Andersen, D. C. and Krummen, L. (2002). Recombinant protein expression for therapeutic applications. *Curr. Opin. Biotechnol.* 13: 117-123

Aslan, H.; Zilberman, Y.; Arbeli, V.; Sheyn, D.; Matan, Y.; Liebergall, M.; Li, J. Z.; Helm, G. A.; Gazit, D. and Gazit, Z. (2006). Nucleofection-based ex vivo nonviral gene delivery to human stem cells as a platform for tissue regeneration. *Tissue Eng.* 12: 877-889.

Atchison, M. L. (1988). Enhancers: mechanisms of action and cell specificity. *Annu. Rev. Cell. Biol.* 4: 127-153.

Babiss, L. E. and Ginsberg, H. S. (1984). Adenovirus type 5 early region 1B gene product is required for efficient shutoff of host protein synthesis. *J. Virol.* 50: 202-212.

Babiss, L. E.; Ginsberg, H. S. and Darnell, J. E. (1985). Adenovirus E1B proteins are required for accumulation of late viral mRNA and for effects on cellular mRNA translation and transport. *Mol. Cell. Biol.* 5: 2552-2558.

Bablanian, R. and Russell, W. C. (1974). Adenovirus polypeptide synthesis in the presence of non-replicating poliovirus. *J. Gen. Virol.* 24: 261-279.

Báez, J.; Olsen, D. and Polarek, J. W. (2005). Recombinant microbial systems for the production of human collagen and gelatin. *Appl. Microbiol. Biotechnol.* 69: 245-252.

Baird, S. D.; Turcotte, M.; Korneluk, R. G. and Holcik, M. (2006). Searching for IRES. *RNA* 12: 1755-1785.

Balaban, A. T. and Ilies, M. A. (2001). Recent developments in cationic lipid-mediated gene delivery and gene therapy. *Expert Opin. Ther. Patents* 11: 1729-1752.

Banerjee, A. K. (1980). 5'-terminal cap structure in eucaryotic messenger ribonucleic acids. *Bacteriol. Rev.* 44: 175-205.

Banerji, J.; Olson, L. and Schaffner, W. (1983). A lymphocyte-specific cellular enhancer is located downstream of the joining region in immunoglobulin heavy chain genes. *Cell* 33: 729-740.

Banerji, J.; Rusconi, S. and Schaffner, W. (1981). Expression of a β-globin gene is enhanced by remote SV40 DNA sequences. *Cell* 27: 299-308.

Barrett, J. W.; Sun, Y.; Nazarian, S. H.; Belsito, T. A.; Brunetti, C. R. and McFadden, G. (2006). Optimization of codon usage of poxvirus genes allows for improved transient expression in mammalian cells. *Virus Genes* 33:15-26.

Basu, J. and Willard, H. F. (2005). Artificial and engineered chromosomes: nonintegrating vectors for gene therapy. *Trends Mol. Med.* 11: 251-258.

Bates, S.; Phillips, A. C.; Clark, P. A.; Stott, F.; Peters, G.; Ludwig, R. L. and Vousden, K. H. (1998). $p14^{ARF}$ links the tumour suppressors RB and p53. *Nature* 395: 124-125.

Beattie, E.; Tartaglia, J. and Paoletti, E. (1991). Vaccinia virus-encoded eIF-2a homolog abrogates the antiviral effect of interferon. *Virology* 183: 419-422.

Bechler, K. (1997). Influence of Capping and Polyadenylation on mRNA Expression and on Antisense RNA Mediated Inhibition of Gene Expression. *Biochem. Biophys. Res. Commun.* 241: 193-199.

Behr, J. P. (1996). The proton sponge, a means to enter cells viruses never thought of. *M/S-Med Sci.* 12: 56-58.

Beltz, G. A. and Flint, S. J. (1979). Inhibition of HeLa cell protein synthesis during adenovirus infection. *J. Mol. Biol.* 131: 353-373.

Benko, M.; Harrach, B. and Russell, W. C. (1999). *Adenoviridae*. In: van Regenmortel, M. H. V.; Fauquet, C. M. and Bishop, D. H. L. (eds.), Virus Taxonomy, Seventh Report of the International Committee on Taxonomy of Viruses. Academic Press, San Diego, pp. 227-238.

Berget, S. M.; Moore, C. and Sharp, P. (1977). Spliced segments at the 5' terminus of Ad2 late mRNA. *Proc. Natl. Acad. Sci. USA* 74: 3171-3175.

Berk, A. J. (2007). Adenoviridae: The Viruses and Their replication. In: Knipe, D. M. David, M., Howley, P. M. and Peter M. (eds.), Fields Virology. Lippincott Williams & Wilkins: Philadelphia, PA, pp. 2356-2394.

Berk, A. J.; Lee, F.; Harrison, T.; Williams, J. and Sharp, P. A. (1979). Pre-early adenovirus 5 gene product regulates synthesis of early viral messenger RNAs. *Cell* 17: 935-944.

Berkner, K. E. and Sharp, P. A. (1985). Effect of tripartite leader on synthesis of a non-viral protein in a adenovirus 5' recombinant. *Nucleic Acids Res.* 13: 841-857.

Bernstein, P. and Ross, J. (1989). Poly(A), poly(A) binding protein and the regulation of mRNA stability.. *Trends Biochem. Sci.* 14: 373-377.

Bernstein, P. L.; Herrick, D. J.; Prokipcak, R. D. and Ross, J. (1992). Control of c-myc mRNA half-life *in vitro* by a protein capable of binding to a coding region stability determinant. *Genes Dev.* 6: 642-654.

Birnstiel, M. L., Busslinger, M. and Strub, K. (1985). Transcription termination and 3' processing: the end is in site!. *Cell* 41: 349-359.

Blasey, H. D.; Aubry, J. -P.; Mazzei, G. J. and Bernard, A. R. (1996). Large scale transient expression with COS cells. *Cytotechnology* 18: 138-142.

Boam, D. S. W.; Davidson, I. and Chambon, P. (1995). A TATAless promoter containing binding sites for ubiquitous transcription factors mediates cell type-specific regulation of the gene for transcription enhancer factor-1 (TEF-1). *J. Biol. Chem.* 270: 19487-19494.

Boettner, M.; Prinz, B.; Holz, C.; Stahl, U. and Lang, C. (2002). High-throughput screening for expression of heterologous proteins in the yeast *Pichia pastoris*. *J. Biotechnol.* 99: 51-62.

Bollag, R. J.; Waldman, A. S. and Liskay, R. M. (1989). Homologous Recombination in mammalian cells. *Annual Reviews of Genetics* 23: 199-225.

Bolster, D. R.; Vary, T. C.; Kimball, S. R. and Jefferson, L. S. (2004). Leucine regulates translation initiation in rat skeletal muscle via enhanced eIF4G phosphorylation. *J. Nutr.* 134: 1704-1710.

Bos, J. L.; Polder, L. J.; Bernards, R.; Schrier, P. I.; van den Elsen, P. J.; van der Eb, A. J. and van Ormondt, H. (1981). The 2.2 kb E1B mRNA of human adenovirus 12 and adenovirus 5 codes for two tumor antigens starting at different AUG triplets. *Cell* 27: 121-131.

Bosher, J.; Robinson, E. C. and Hay, R. T. (1990). Interactions between the adenovirus type 2 DNA polymerase and the DNA binding domain of nuclear factor I. *New Biol.* 2: 1083-1090.

Botting, C. H. and Hay, R. T. (1999). Characterisation of the adenovirus preterminal protein and its interaction with the POU homeodomain of NFIII (Oct-1). *Nucleic Acids Res.* 27: 2799-2805.

Boussif, O.; Lezoualch, F.; Zanta, M. A.; Mergny, M. D.; Scherman, D.; Demeneix, B. and Behr, J. P. (1995). A versatile vector for gene and oligonucleotide transfer into cells in culture and *in vivo*: polyethylenimine. *Proc. Natl. Acad. Sci. USA* 92: 7297-7301.

Brand, S. R.; Kobayashi, R. and Mathews, M. B. (1997). The Tat protein of human immunodeficiency virus type 1 is a substrate and inhibitor of the interferon-induced, virally activated protein kinase, PKR. *J. Biol. Chem.* 272: 8388-8395.

Brawermann, G. (1981). The Role of the poly(A) sequence in mammalian messenger RNA. *Crit. Rev. Biochem.* 10: 1-38.

Brehm, A.; Miska, E. A.; McCance, D. J.; Reid, J. L.; Bannister, A. J. and Kouzarides, T. (1998). Retinoblastoma protein recruits histone deacetylase to repress transcription. *Nature* 391: 597-601.

Brenkman, A. B.; Breure, E. C. and van der Vliet, P. C. (2002). Molecular architecture of adenovirus DNA polymerase and location of the protein primer. *J. Virol.* 76: 8200-8207.

Brenkman, A. B.; Heideman, M. R.; Truniger, V.; Salas, M. and van der Vliet, P. C. (2001). The (I/Y)XGG motif of adenovirus DNA polymerase affects template DNA binding and the transition from initiation to elongation. *J. Biol. Chem.* 276: 29846-29853.

Bridge, E. and Ketner, G. (1990). Interaction of adenoviral E4 and E1b products in late gene expression. *Virology* 174: 345-353.

Brinster, R. L.; Chen, H. Y.; Trumbauer, M. E.; Yagle, M. K.; Palmiter, R. D. (1985). Factors affecting the efficiency of introducing foreign DNA into mice by microinjecting eggs. *Proc. Natl. Acad. Sci. USA* 82: 4438-4442.

Brunner, S.; Sauer, T.; Carotta, S.; Cotton, M.; Saltik. M, and Wagner, E (2000). Cell cycle dependence of gene transfer by lipoplex, polyplex and recombinant adenovirus. *Gene Ther.* 7: 401-407

Burton, E. A.; Fink, D. J. and Glorioso, J. C. (2002). Gene delivery using herpes simplex virus vectors. *DNA Cell Biol.* 21:915-936

Bushell, M. E.; Rowe, M.; Avignone-Rossa, C. A. and Wardell, J. N. (2003). Cyclic fed-batch culture for production of human serum albumin in *Pichia pastoris*. *Biotech. Bioeng.* 82: 678-683.

Butler, M. (2005). Animal cell cultures: recent achievements and perspectives in the production of biopharmaceuticals. *Appl. Microbiol. Biotechnol.* 68: 283-291.

Caput, D.; Beutler, B.; Hartog, K.; Thayer, R.; Brown-Shimer, S. and Cerami, A. (1986). Identification of a common nucleotide sequence in the 39- untranslated regions of mRNA molecules specifying inflammatory mediators. *Proc. Natl. Acad. Sci. USA* 83: 1670-1674.

Carter, K.; Bowman, D.; Carrington, W.; Fogarty, K.; McNeil, A.; Fay, F. S. and Lawrence, J. B. (1993). A three-dimensional view of precursor messenger RNA metabolism within the mammalian nucleus. *Science* 259: 1330-1335.

Cassan, M. and Rousset, J. P. (2001). UAG readthrough in mammalian cells: Effect of upstreamand downstreamstop codon contexts reveal different signals. *BMC Mol. Biol.* 2: 3.

Chang, L. S. and Shenk, T. (1990). The adenovirus DNA-binding protein stimulates the rate of transcription directed by adenovirus and adenoassociated virus promoters. *J. Virol.* 64: 2103-2109.

Chang, W. P. and Little, J. B. (1991). Delayed reproductive death in X-irradiated Chinese hamster ovary cells. *Int. J. Radiat. Biol.* 60: 483-496.

Chao, D. and Korsmeyer, S. (1998). BCL-2 family: regulators of cell death. *Annu. Rev. Immunol.* 16: 395-419.

Chatton, B.; Bocco, J. L.; Gaire, M.; Hauss, C.; Reimund, B.; Goetz, J. and Kedinger, C. (1993). Transcriptional activation by the adenovirus larger E1A product is mediated by members

of the cellular transcription factor ATF family which can directly associate with E1A. *Mol. Cell. Biol.* 13: 561-570.

Chen, C. Y.; Gherzi, R.; Ong, S. E.; Chan, E. L.; Raijmakers, R.; Pruijn, G. J.; Stoecklin, G.; Moroni, C.; Mann, M. and Karin, M. (2001). AU binding proteins recruit the exosome to degrade ARE-containing mRNAs. *Cell* 107: 451-464.

Chen, F.; MacDonald, C. C. and Wilusz, J. (1995). Cleavage site determinants in the mammalian polyadenylation signal. *Nucleic Acids Res.* 23: 2614-2620.

Chen, M.; Mermod, N. and Horwitz, M. S. (1990). Protein-protein interactions between adenovirus DNA polymerase and nuclear factor I mediate formation of the DNA replication preinitiation complex. *J. Biol. Chem.* 265: 18634-18642.

Chou, T. W.; Biswas, S. and Lu, S. (2004). Gene delivery using physical methods, an overview. *Methods in Molecular Biology* 245: 147-165.

Chou, Z. F.; Chen, F. and Wilusz, J. (1994). Sequence and position requirements for uridylate-rich downstream elements of polyadenylation signals. *Nucleic Acids Res.* 22: 2525-2531.

Chow, L. T. and Broker, T. R. (1994). Papillomavirus DNA replication. *Intervirology* 37: 150-158.

Chow, L. T.; Roberts, J. M.; Lewis, J. B. and Broker, T. R. (1977). A map of cytoplasmic RNA transcripts from lytic adenovirus type 2, determined by electron microscopy of RNA:DNA hybrids. *Cell* 11: 819-836.

Chung, J. H.; Whiteley, M. and Felsenfeld, G. (1993). A 50 element of the chicken beta-globin domain serves as an insulator in human erythroid cells and protects against position effects in Drosophila. *Cell* 74: 505-514.

Chung, J.; Ahn, H.; Lim, S.; Sung, Y.; Koh, Y.; Park, S. and Lee, G. (2003). Development of recombinant Chinese *hamster* ovary cell lines producing human thrombopoietin or its analog. *Journal of Microbiology and Biotechnology* 13: 759-766.

Clark, D. P. (2005). Processing of RNA. In: Molecular Biology: Understanding the Genetic Revolution. Elsevier Academic Press, San Diego.

Cleat, P. H. and Hay, R. T. (1989). Co-operative interactions between NFI and the adenovirus DNA binding protein at the adenovirus origin of replication. *EMBO J.* 8: 1841-1848.

Cleghon, V.; Voelkerding, K.; Morin, N.; Delsert, C. and Klessig, D. F. (1989). Isolation and characterization of a viable adenovirus mutant defective in nuclear transport of the DNA-binding protein. *J. Virol.* 63: 2289-2299.

Cohen, S. N.; Chang, A. C. Y. and Hsu, L. (1972). Nonchromosomal antibiotic resistance in bacteria: Genetic transformation of *Escherichia coli* by R-factor DNA. *Proc. Natl. Acad. Sci. USA* 69: 2110-2114.

Coller, J. and Parker, R. (2004). Eukaryotic mRNA decapping. *Annu. Rev. Biochem.* 73: 861-890.

Conese, M.; Auriche, C. and Ascenzioni, F. (2004). Gene therapy progress and prospects: episomally maintained self-replicating systems. *Gene Ther.* 11: 1735-1741.

Conti, E. and Izaurralde, E. (2001). Nucleocytoplasmic transport enters the atomic age. *Curr. Opin. Cell Biol.* 13: 310-319.

Coura Rdos, S. and Nardi, N. B. (2008). The state of the art of adeno-associated virus-based vectors in gene therapy. *Virol. J.* 4: 99.

Crick, F. (1970). Central Dogma of Molecular Biology. *Nature* 227: 561-563.

Crick, F. H. C. (1958). On Protein Synthesis. *Symp. Soc. Exp. Biol.* 12: 138-163.

Cuesta, R.; Xi, Q. and Schneider, R. J. (2000). Adenovirus-specific translation by displacement of kinase Mnk1 from cap-initiation complex eIF4F. *EMBO J.* 19: 3465-3474.

Culp, J. S.; Webster, L. C.; Friedman, D. J.; Smith, C. L.; Huang, W-J.; Wu, F. Y-H.; Rosenberg, M. and Ricciardi, R. P. (1988). The 289-amino acid E1A protein of adenovirus binds zinc in a region that is important for trans-activation. *Proc. Natl. Acad. Sci. USA* 85: 6450-6454.

Dalby, B.; Cates, S.; Harris, A.; Ohki, E. C.; Tilkins, M. L.; Price, P. J. and Ciccarone, V. C. (2004). Advanced transfection with Lipofectamine 2000 reagent: primary neurons, siRNA, and high-throughput applications. *Methods* 33: 95-103.

de Jong, R. N. and van der Vliet, P. C. (1999). Mechanism of DNA replication in eukaryotic cells: cellular host factors stimulating adenovirus DNA replication. *Gene* 236: 1-12.

Debbas, M. and White, E. (1993). Wild-type p53 mediates apoptosis by E1A, which is inhibited by E1B. *Genes Dev.* 7: 546-554.

Dekker, J.; Kanellopoulos, P. N.; Loonstra, A. K.; van Oosterhout, J. A.; Leonard, K.; Tucker, P. A. and van der Vliet, P. C. (1997). Multimerization of the adenovirus DNA-binding protein is the driving force for ATP-independent DNA unwinding during strand displacement synthesis. *EMBO J.* 16: 1455-1463.

Deshpande, M. C. and Prausnitz, M. R. (2007). Synergistic effect of ultrasound and PEI on DNA transfection *in vitro*. *J. Control Release* 118: 126-135.

Dillon, N. (2004). Heterochromatin structure and function. *Biol. Cell.* 96: 631-637.

Dillon, N. and Festenstein, R. (2002). Unravelling heterochromatin: competition between positive and negative factors regulates accessibility. *Trends Genet.* 18: 252-258.

Dinnis, D. M. and James, D. C. (2005). Engineering mammalian cell factories for improved recombinant monoclonal antibody production: Lessons from nature? *Biotechnol. Bioeng.* 91: 180-189.

Disbrow, G. L.; Sunitha, I.; Baker, C. C.; Hanover, J. and Schlegel, R. (2003). Codon optimization of the HPV-16 E5 gene enhances protein expression. *Virology* 311: 105-114.

Dobbelstein, M.; Roth, J.; Kimberly, W. T.; Levine, A. J. and Shenk, T. (1997). Nuclear export of the E1B 55-kDa and E4 34-kDa adenoviral oncoproteins mediated by a rev-like signal sequence. *EMBO J.* 16: 4276-4284.

Dobner, T.; Horikoshi, N.; Rubenwolf, S. and Shenk, T. (1996). Blockage by adenovirus E4orf6 of transcriptional activation by the p53 tumor suppressor. *Science* 272: 1470-1473.

Doerfler, W. (1991). The abortive infection and malignant transformation by adenoviruses: integration of viral DNA and control of viral gene expression by specific patterns of DNA methylation. *Adv. Virus Res.* 39: 89-128.

Dolph, P. J.; Huang, J. and Schneider, R. J. (1990). Translation by the adenovirus tripartite leader: elements which determine independence from cap-binding protein complex. *J. Virol.* 64: 2669-2677.

Dolph, P. J.; Racaniello, V.; Villamarin, A.; Palladino, F. and Schneider, R. J. (1988). The adenovirus tripartite leader eliminates the requirement for cap-binding protein during translation initiation. *J. Virol.* 62: 2059-2066.

Douglas, J. T. (2008). Adenoviral vectors for gene therapy. *Molecular Biotechnology* 36: 71-80.

Du, M.; Ye, L.; Liu, J.; Liu, J. and Yang, L. (2008). Enhancement of GFP expression by Kozak sequence +4G in HEK293 cells. *Chinese Journal of Biotechnology* 24: 491-494.

Edmonds, M. (2002). A history of poly A sequences: from formation to factors to function. *Prog Nucleic Acid Res. Mol. Biol.* 71: 285-389.

Esche, H.; Mathews, M. B. and Lewis, J. B. (1980). Proteins and messenger RNAs of the transforming region of wild-type and mutant adenoviruses. *J. Mol. Biol.* 142: 399-417.

Evans, R. M.; Fraser, N.; Ziff, E.; Weber, J.; Wilson, M. and Darnell, J. E. (1977). The initiation sites for RNA transcription in Ad2 DNA. *Cell* 12: 733-739.

Farr, C. J.; Stevanovic, M.; Thomson, E. J.; Goodfellow, P. N. and Cooke, H. J. (1992). Telomere-associated chromosome fragmentation: applications in genome manipulation and analysis. *Nat. Genet.* 2: 275-282.

Felgner, P. L. and Ringold, G. M. (1998). Cationic liposome-mediated transfection. *Nature* 337: 387-388.

Felgner, P. L.; Gadek, T. R.; Holm, M.; Roman, R.; Chan, H. W.; Wenz, M.; Northrop, J. P.; Ringold, G. M. and Danielsen, M. (1987). Lipofection: a highly efficient, lipid-mediated DNA-transfection procedure. *Proc. Natl. Acad. Sci. USA* 84: 7413-7417.

Ferreira, T. B.; Alves, P. M.; Gonçalves, D. and Carrondo, M. J. T. (2005). Effect of MOI and Medium Composition on Adenovirus Infection Kinetics. In: Gòdia, F. and Fussenegger, M. (eds.), Animal cell technology meets genomics. Springer Netherlands, pp. 329-332.

Field, J.; Gronostajski, R. M. and Hurwitz, J. (1984). Properties of the adenovirus DNA polymerase. *J. Biol. Chem.* 259: 9487-9495.

Flint, J. and Shenk, T. (1997). Viral transactivating proteins. *Annu. Rev. Genet.* 31: 177-212.

Flint, K. J. and Jones, N. C. (1991). Differential regulation of three members of the ATF/CREB family of DNA-binding proteins. *Oncogene* 6: 2019-2026.

Flint, S. J. (1984). Adenovirus cytopathology. *Compr. Virol.* 19: 297-358.

Flint, S. J. and Gonzalez, R. A. (2003). Regulation of mRNA production by the adenoviral E1B 55-kDa and E4 Orf6 proteins. *Curr. Top. Microbiol. Immunol.* 272: 287-330.

Fort, P.; Rech, J.; Vie, A.; Piechaczyk, M.; Bonnieu, A.; Jeanteur, P. and Blanchard, J.-M. (1987). Regulation of c-*fos* gene expression in hamster fibroblasts: initiation and elongation of transcription and mRNA degradation. *Nucleic Acids Res.* 15: 5657-5667.

Francastel, C.; Walters, M. C.; Groudine, M. and Martin, D. I. (1999). A functional enhancer suppresses silencing of a transgene and prevents its localization close to centrometric heterochromatin. *Cell* 99: 259-69.

Frenkel, G. D. and Horan, K. (1983). DNase inhibition by the adenovirus DNA-binding protein exhibits specificity for the enzyme but not for the secondary structure of the DNA. *Biochem. Biophys. Res. Commun.* 110: 443-448.

Frenkel, P. A.; Chen, S.; Thai, T.; Shohet, R. V. and Grayburn, P. A. (2002). DNA-loaded albumin microbubbles enhance ultrasound-mediated transfection *in vitro*. *Ultrasound Med. Biol.* 28: 817-822

Freyer, G. A.; Katoh, Y. and Roberts, R. J. (1984). Characterization of the major mRNAs from adenovirus 2 early region 4 by cDNA cloning and sequencing. *Nucleic Acids Res.* 12: 3503-3519.

Furuichi, Y.; LaFiandra, A. and Shatkin, A. J. (1977). 5'-Terminal structure and mRNA stability. *Nature* 266: 235-239.

Gale, M. Jr., Blakely, C. M.; Kwieciszewski, B.; Tan, S. -L.; Dossett, M.; Korth, M. J.; Polyak, S. J.; Gretch, D. R. and Katze, M. G. (1998). Control of PKR protein kinase by hepatitis C virus nonstructural 5A protein: molecular mechanisms of kinase regulation. *Mol. Cell. Biol.* 18: 5208-5218.

Gale, M. Jr.; Korth, M. J.; Tang, N. M.; Tan, S. -L.; Hopkins, D. A.; Dever, T. E.; Polyak, S. J.; Gretch, D. R. and Katze, M. G. (1997). Evidence that hepatitis C virus resistance to interferon is mediated through repression of the PKR protein kinase by the nonstructural 5A protein. *Virology* 230: 217-227.

Gale, M. Jr.; Kwieciszewski, B.; Dossett, M.; Nakao, H. and Katze, M. G. (1999). Anti-apoptotic and oncogenic potentials of hepatitis C virus are linked to interferon resistance by viral repression of the PKR protein kinase. *J. Virol.* 73: 6506-6516.

Gallie, D. R.; Feder, J. N.; Schimke, R. T. and Walbot, V. (1991). Post-transcriptional regulation in higher eukaryotes: the role of the reporter gene in controlling expression. *Mol. Gen. Genet.* 228: 258-264.

Gao, X. and Huang, L. (1995). Cationic liposome-mediated gene transfer. *Gene Ther.* 2: 710-722.

Garrick, D., Fiering, S., Martin, D. I. and Whitelaw, E. (1998). Repeat-induced gene silencing in mammals. *Nat. Genet.* 18: 56-59.

Gerngross, T. U. (2004). Advances in the production of human therapeutic proteins in yeasts and filamentous fungi. *Nat. Biotechnol.* 22: 1409-1414.

Gilardi, P. and Perricaudet, M. (1986). The E4 promoter of adenovirus type 2 contains an E1A dependent cis-acting element. *Nucleic Acids Res.* 14: 9035-9049.

Glover, D. J.; Lipps, H. J. and Jans, D. A. (2005). Towards safe, non-viral therapeutic gene expression in humans. *Nat. Rev. Genet.* 6: 299-310.

Godbey, W. T.; Wu, K. K. and Mikos, A. G. (1999). Poly(ethylenimine) and its role in gene delivery. *J. Control Release* 60: 149-160.

Goeddel, D.; Kleid, D.; Bolivar, F.; Heyneker, H.; Yansura, D.; Crea, R.; Hirose, T.; Kraszewski, A.; Itakura, K. and Riggs, A. (1979). Expression in Escherichia coli of chemically synthesized genes for human insulin. *Proc. Natl. Acad. Sci. USA* 76: 106-110.

Gonzalez, R. A. and Flint, S. J. (2002). Effects of mutations in the adenoviral E1B 55-kilodalton protein coding sequence on viral late mRNA metabolism. *J. Virol.* 76: 4507-4519.

Goodrich, J. A.; Cutler, G. and Tjian, R. (1996). Contacts in context: Promoter specificity and macromolecular interactions in transcription. *Cell* 84: 825-830.

Görlach, M.; Burd, C. G. and Dreyfuss, G. (1994). The mRNA poly(A)-binding protein: localization, abundance, and RNA-binding specificity. *Exp. Cell Res.* 211: 400-407.

Görlich, D. and Kutay, U. (1999). Transport between the cell nucleus and the cytoplasm. *Annu. Rev. Cell Dev. Biol.* 15: 607-660.

Graber, J. H.; Cantor, C. R.; Mohr, S. C. and Smith, T. F. (1999). *In silico* detection of control signals: mRNA 3'-end-processing sequences in diverse species. *Proc. Natl. Acad. Sci. USA* 96: 14055-14060.

Graessmann, M. and Graessmann, A. (1983). Microinjection of tissue culture cells. *Methods Enzymol.* 101: 482-492.

Graham, F. L. (1984). Covalently closed circles of human adenovirus DNA are infectious. *EMBO J.* 3: 2917-2922.

Graham, F. L. and van der Eb, A. J. (1973). A new technique for the assay of infectivity of human adenovirus 5 DNA. *Virology* 52: 456-467.

Graham, F. L.; Rudy, J. and Brinkley, P. (1989). Infectious circular DNA of human adenovirus type 5: regeneration of viral DNA termini from molecules lacking terminal sequences. *EMBO J.* 8: 2077-2085.

Graham, F. L.; Smiley, J.; Russell, W. C. and Nairn, R. (1977). Characteristics of a human cell line transformed by DNA from human adenovirus type 5. *J. Gen Virol.* 36: 59-72.

Granados, R. R. and Federici, B. A. (1986). The Biology of Baculoviruses. CRC Press, Boca Raton, Florida.

Grand, R. J.; Parkhill, J.; Szestak, T.; Rookes, S. M.; Roberts, S. and Gallimore, P. H. (1999). Definition of a major p53 binding site on Ad2E1B58K protein and a possible nuclear localization signal on the Ad12E1B54K protein. *Oncogene* 18: 955-965.

Gregory, T. R. (2005). Animal Genome Size Database. http://www.genomesize.com.

Griffin, T. J.; Seth, G.; Xie, H.; Bandhakavi, S. and Hu, W. S. (2007). *Advancing mammalian cell culture engineering using genome*-scale technologies Trends in Biotechnology 25: 401-408.

Groner, A. (1986). Specificity and safety of baculoviruses. In: Granados, R. R. and Federici, B. A. (eds.), The Biology of Baculoviruses. CRC Press, Boca Raton, Florida, p. 177.

Grosjean, F.; Batard, P.; Jordan, M. and Wurm, F. (2002). S-phase synchronized CHO cells show elevated transfection efficiency using CaPi. *Cytotechnology* 38: 57-62.

Grosveld, F.; van Assendelft, G. B.; Greaves, D. R. and Kollias, G. (1987). Position-independent, high-level expression of the human beta-globin gene in transgenic mice. *Cell* 51: 975-985.

Halbert, D. N.; Cutt, J. R. and Shenk, T. (1985). Adenovirus early region 4 encodes functions required for efficient DNA replication, late gene expression, and host cell shutoff. *J. Virol.* 56: 250-257.

Hall, T. M. (2002). Poly(A) tail synthesis and regulation: recent structural insights. *Curr. Opin. Struct. Biol.* 12: 82-88.

Hamm, J. and Mattaj, I. W. (1990). A cap binding protein that may mediate nuclear export of RNA polymerase II-transcribed RNAs. *Cell* 63: 109-118.

Han, J.; Sabbatini, P.; Perez, D.; Rao, L.; Mohda, D. and White, E. (1996). The E1B 19K protein blocks apoptosis by interacting with and inhibiting the p53- inducible and death-promoting Bax protein. *Genes Dev.* 10: 461-477.

Hans, H. and Alwine, J. C. (2000). Functionally significant secondary structure of the simian virus 40 late polyadenylation signal. *Mol. Cell Biol.* 20: 2926-2932.

Hardwick, J. M.; von Sprecken, R. S.; Yielding, K. L. and Yielding, L. W. (1984). Ethidium binding sites on plasmid DNA determined by photoaffinity labelling. *J. Biol. Chem.* 259: 11090-11097.

Harrington, J. J.; van Bokkelen, G.; Mays, R. W.; Gustashaw, K. and Willard, H. F. (1997). Formation of de novo centromeres and construction of first-generation human artificial microchromosomes. *Nat. Genet.* 15: 345-355.

Hay, R. T.; Freeman, A.; Leith, I.; Monaghan, A. and Webster, A. (1995). Molecular interactions during adenovirus DNA replication. In: Doerfler, W. and Bohm, P. (eds.), The Molecular Repertoire of Adenoviruses. Berlin: Springer, pp. 31-48.

Hayashi, M. and Harada, Y. (2007). Direct observation of the reversible unwinding of a single DNA molecule caused by the intercalation of ethidium bromide. *Nucleic Acids Res.* 35: e125-e125.

Helin, K. and E. Harlow. (1994). Heterodimerization of the transcription factors E2F-1 and DP-1 is required for binding to the adenovirus E4 (ORF6/7) protein. *J. Virol.* 68: 5027-5035.

Hillemann, M. R. and Werner, J. R. (1954). Recovery of a new agent from patients with acute respiratory illness. *Proceedings of the Society for Experimental Biology and Medicine* 85, 183-188.

Hérissé, J.; Rigolet, M.; de Dinechin, S. D. and Galibert, F. (1981). Nucleotide sequence of adenovirus 2 DNA fragment encoding for the carboxylic region of the fiber protein and the entire E4 region. *Nucleic Acids Res.* 9: 4023-4042.

Hinnebusch, A. G. (2000). Mechanism and regulation of initiator methionyl-tRNA binding to ribosomes. In: Sonenberg, N., Hershey, J. W. B. & Mathews, M. B. (eds.), Translational Control of Gene Expression. Cold Spring Harbor Laboratory Press, Cold Spring Harbor, NY, pp. 185–243.

Horkoshi, N.; Maguire, K. J.; Kralli, A.; Maldonado, E.; Reinberg, D. and Weinmann, R. (1991). Direct interaction between adenovirus E1A protein and the TATA box binding transcription factor IID. *Proc. Natl. Acad. Sci. USA* 88: 5124-5128.

Horridge, J. J. and Leppard, K. N. (1998). RNA-binding activity of the E1B 55-kilodalton protein from human adenovirus type 5. *J. Virol.* 72: 9374-9379.

Horwitz, M. S. (2001). Adenovirus immunoregulatory genes and their cellular targets. *Virology* 279: 1-8.

Hösel, M.; Webb, D.; Schröer, J. and Doerfler, W. (2003). The abortive infection of Syrian hamster cells with human adenovirus type 12. *Curr. Top. Microbiol. Immunol.* 272: 415-440.

Hseih, P. and Robbins, P. W. (1984). Regulation of asparagine-linked oligosaccharide processing: Oligosaccharide processing in *Aedes albopictus* mosquito cells. *J. Biol. Chem.* 259: 2375-2382.

Huang, W. B.; Wong, J. M. and Bateman, E. (1996). TATA elements direct bi-directional transcription by RNA polymerases II and III. *Nucleic Acids Res.* 24: 1158-1163.

Hunt, I. (2005). From gene to protein: a review of new and enabling technologies for multi-parallel protein expression. *Protein Expression and Purification* 40: 1-22.

Hurley, L. H. (2002). DNA and its associated processes as targets for cancer therapy. *Nat. Rev. Cancer* 2: 188-200.

Ikemura, T. (1985). Codon usage and tRNA content in unicellular and multicellular organisms. *Mol. Biol. Evol.* 2: 13-34.

Imperiale, M. J.; Akusjarvi, G. and Leppard, K. N. (1995). Post-transcriptional control of adenovirus gene expression. *Curr. Top. Microbiol. Immunol.* 199: 139-171.

Inoue, H.; Nojima, H. and Okayama, H. (1990). High efficiency transformation of *Escherichia coli* with plasmids. *Gene* 96: 23-28.

Ishikawa, T.; Lee, E. J. and Jameson, J. L. (2004). Nonhomologous end-joining ligation transfers DNA regulatory elements between cointroduced plasmids. *Mol. Cell Biol.* 24: 8323-8331.

Iyer, M.; Wu, L.; Carey, M.; Wang, Y.; Smallwood, A. and Gambhir, S. S. (2001). Two-step transcriptional amplification as a method for imaging reporter gene expression using weak promoters. *Proc. Natl. Acad. Sci. USA* 98: 14595-14600.

Jackson, D. A.; Symons, R. H. and Berg, P. (1972). Biochemical method for inserting new genetic information into DNA of Simian Virus 40: circular SV40 DNA molecules containing lambda phage genes and the galactose operon of Escherichia coli. *Proc. Natl. Acad. Sci. USA* 69: 2904-2909.

Jackson, R. J. and Kaminski, A. (1995). Internal initiation of translation in eukaryotes: the picornavirus paradigm and beyond. *RNA* 1: 985-1000.

Jacobson, A. (1996). Poly(A) metabolism and translation: the closed loop model. In: Hershey, J. W.; Mathews, M. B. and Sonenberg, N. (eds.), Translational Control. Cold Spring Harbor Press, pp. 451-480.

Jang, S. K., Kra¨usslich, H. -G.; Nicklin, M. J. H.; Duke, G. M.; Palmenberg, A. C. and Wimmer, E. (1988). A segment of the 59 nontranslated region of encephalomyocarditis virus RNA directs internal entry of ribosomes during *in vitro* translation. *J. Virol.* 62: 2636-2643.

Jang, S.; Davies, M.; Kaufman, R. and Wimmer, E. (1989). Initiation of protein synthesis by internal entry of ribosomes into the 5' nontranslated region of encephalomyocarditis virus RNA *in vivo*. *J. Virol.* 63: 1651-1660.

Jaśkiewicz, E.; Jedynak, A. and Zioło, E. (2005). Expression of recombinant forms of human 21.5 kDa myelin basic protein and proteolipid protein in CHO cells. *Acta Biochimica Polonica* 52: 863-866.

Jefferson, L. S. and Kimball, S. R. (2003). Amino acids as regulators of gene expression at the level of mRNA translation. *J. Nutr.* 133: 2046S-2051S.

Jenkins, N.; Murphy, L. and Tyther, R. (2008). Post-translational modifications of recombinant proteins: significance for biopharmaceuticals. *Mol. Biotechnol.* 39: 113-118.

Jones, N. and Shenk, T. (1979). Isolation of adenovirus type 5 host range deletion mutants defective for transformation of rat embryo cells. *Cell* 17: 683-689.

Jordan, M.; Köhne, C. and Wurm, F. M. (1998). Calcium-phosphate mediated DNA transfer into HEK-293 cells in suspension: control of physicochemical parameters allows transfection in

stirred media: Transfection and protein expression in mammalian cells. *Cytotechnology* 26: 39-47.

Jordan, M.; Schallhorn, A. and Wurm, F. W. (1996). Transfecting mammalian cells: Optimization of critical parameters affecting calcium-phosphate precipitate formation. *Nucleic Acids Res.* 24: 596-601.

Kabotyanski, E. B.; Gomelsky, L.; Han, J. -O.; Stamato, T. D. and Roth, D. B. (1998). Double-strand break repair in Ku86- and XRCC4-deficient cells. *Nucleic Acids Res.* 26: 5333-5342.

Kaczmarczyk, S. J. and Green, J. E. (2001). A single vector containing modified cre recombinase and LOX recombination sequences for inducible tissue-specific amplification of gene expression. *Nucleic Acids Res.* 29: E56-66.

Kang, C.Y., (1988). Baculovirus for expression of foreign genes. *Adv. Virus Res.* 35: 177-192.

Kaufman, R. J. (1990). Vectors used for expression in mammalian cells. *Methods Enzymol.* 185: 487-511.

Kaufman, R. J. (1999). Double-stranded RNA-activated protein kinase mediates virus-induced apoptosis: a new role for an old actor. *Proc. Natl. Acad. Sci. USA* 96: 11693-11695.

Kaufman, R. J. (2000). Overview of vector design for mammalian gene expression. *Mol. Biotechnol.* 16: 151-160.

Kawagishi-Kobayashi, M.; Silverman, J. B.; Ung, T. L. and Dever, T. E. (1997). Regulation of the protein kinase PKR by the vaccinia virus pseudosubstrate inhibitor K3L is dependent on residues conserved between the K3L protein and the PKR substrate eIF-2a. *Mol. Cell. Biol.* 17: 4146-4158.

Keblusek, P.; Dorsman, J. C.; Teunisse, A. F.; Teunissen, H.; van der Eb, A. J. and Zantema, A. (1999). The adenoviral E1A oncoproteins interfere with the growth-inhibiting effect of the cdk-inhibitor p21CIP"/WAF". *Journal of General Virology* 80: 381-390.

Kichler, A.; Erbacher, P. and Behr, J. P. (1995). Polyethylenimines: a family of potent polymers for nucleic acid delivery. In: Huang, L.; Hung, M. and Wagner, E. (eds.), Non-Viral Vectors for Gene Therapy. San Diego, CA, USA: Academic press.

Kim, C. H.; Oh, Y. and Lee, T. H. (1997). Codon optimization for high-level expression of human erythropoietin (EPO) in mammalian cells. *Gene* 199: 293-301.

King, A. J. and van der Vliet, P. C. (1994). A precursor terminal proteintrinucleotide intermediate during initiation of adenovirus DNA replication: regeneration of molecular ends *in vitro* by a jumping back mechanism. *EMBO J.* 13: 5786-5792.

King, A. J.; Teertstra, W. R. and van der Vliet, P. C. (1997a). Dissociation of the protein primer and DNA polymerase after initiation of adenovirus DNA replication. *J. Biol. Chem.* 272: 24617-24623.

King, A. J.; Teertstra, W. R.; Blanco, L.; Salas, M. and van der Vliet, P. C. (1997b). Processive proofreading by the adenovirus DNA polymerase. Association with the priming protein reduces exonucleolytic degradation. *Nucleic Acids Res.* 25: 1745-1752.

Klann, E. and Dever, T. E. (2004). Biochemical mechanisms for translational regulation in synaptic plasticity. *Nature Reviews Neuroscience* 5: 931-942.

Klimkait, T. and Doerfler, W. (1985). Adenovirus types 2 and 5 functions elicit replication and late expression of adenovirus type 12 DNA in hamster cells. *J. Virol.* 55: 466-474.

Klimkait, T. and Doerfler, W. (1987). E1B functions of type C adenoviruses play a role in the complementation of blocked adenovirus type 12 DNA replication and late gene transcription in hamster cells. *Virology* 161: 109-120.

Koch, S.; Pohl, P.; Cobet, U. and Rainov, N. G. (2000). Ultrasound enhancement of liposome-mediated cell transfection is caused by cavitation effects. *Ultrasound Med. Biol.* 26: 897-903.

Kollmar, R.; Sukow, K. A.; Sponagle, S. K. and Farnham, P. J. (1994). Start site selection at the TATA-less carbamoyl-phosphate synthase (glutamine-hydrolyzing)/aspartate carbamoyltransferase dihydroorotase promoter. *J. Biol. Chem.* 269: 2252-2257.

Kost, T. A.; Condreay, J. P. and Jarvis, D. (2005). Baculovirus as versatile vectors for protein expression in insect and mammalian cells. *Nat. Biotechnol.* 23: 567-575.

Kozak, M. (1987). At least six nucleotides preceding the AUG initiator codon enhance translation in mammalian cells. *J. Mol. Biol.* 196: 947-950.

Kozak, M. (1997). Recognition of AUG and alternative initiator codons is augmented by G in position +4 but is not generally affected by the nucleotides in positins +5 and +6. *EMBO J.* 16: 2482-2492.

Kriegler, M. (1990). Assembly of enhancers, promoters, and splice signals to control expression of transferred genes. *Methods Enzymol.* 185: 512-527.

Krugh, T. R. and Reinhardt, C. G. (1975). Evidence for sequence preferences in the intercalative binding of ethidium bromide to dinucleoside monophosphates. *J. Mol. Biol.* 97: 133-162.

Labatmoleur, F.; Steffan, A. M.; Brisson, C.; Perron, H.; Feugeas, O.; Furstenberger, P.; Oberling, F.; Brambilla, E. and Behr, J. P. (1996). An electron microscopy study into the mechanism of gene transfer with lipopolyamines. *Gene Ther.* 3: 1010-1017.

Lechner, R. L. and Kelly, T. J. J. (1977). The structure of replicating adenovirus 2 DNA molecules. *Cell* 12: 1007-1020.

Lee, T. G.; Tang, N.; Thompson, S.; Miller, J. and Katze, M. G. (1994). The 58,000-dalton cellular inhibitor of the interferon-induced double-stranded RNA-activated protein kinase (PKR) is a member of the tetratricopeptide repeat family of proteins. *Mol. Cell. Biol.* 14: 2331-2342.

Lee, T. I. and Young, R. A. (2000). Transcription of eukaryotic protein-coding genes. *Annu. Rev. Genet.* 34: 77-137

Lee, W. S.; Kao, C.; Bryant, G. O.; Liu, X. and Berk, A. J. (1991). Adenovirus E1A activation domain binds the basic repeat in the TATA box transcription factor. *Cell* 67: 365-376.

Lemkine, G. F. and Demeneix, B. A. (2001). Polyethylenimines for *in vivo* gene delivery, *Curr. Opin. Mol. Ther.* 3: 178-182.

Leppard, K. N. and Shenk, T. (1989). The adenovirus E1B 55 kD protein influences mRNA transport via an intranuclear effect on RNA metabolism. *EMBO J.* 8: 2329-2336.

Lichtenstein, D. L. and Wold W. S. M. (2004). Experimental infections of humans with wild-type adenoviruses and with replication-competent adenovirus vectors: replication, safety, and transmission. *Cancer Gene Ther.* 11: 819-829.

Lichy, J. H.; Horwitz, M. S. and Hurwitz, J. (1981). Formation of a covalent complex between the 80,000-dalton adenovirus terminal protein and 5'-dCMP *in vitro*. *Proc. Natl. Acad. Sci. USA* 78: 2678-2682.

Lieberman, A. P.; Pitha, P. M. and Shin, M. L. (1992). Poly(A) removal is the kinase-regulated step in tumor necrosis factor mRNA decay. *J. Biol. Chem.* 267: 2123-2126.

Lipps, H. J.; Jenke, A. C.; Nehlsen, K.; Scinteie, M. F.; Stehle, I. M. and Bode, J. (2003). Chromosome-based vectors for gene therapy. *Gene* 304: 23-33.

Liu, C.; Dalby, B.; Chen, W.; Kilzer, J. M. and Chiou, H. C. (2008). Transient transfection factors for high-level recombinant protein production in suspension cultured mammalian cell. *Mol. Biotechnol.* 39: 141-153.

Liu, D.; Chiao, E. F. and Tian, H. (2004). Chemical methods for DNA delivery: an overview. *Methods Mol. Biol.* 245: 3-24.

Liu, F. and Green, M. R., (1994). Promoter Targeting by Adenovirus-E1a through Interaction with Different Cellular DNA-Binding Domains. *Nature* 368: 520-525.

Lodish, H.; Berk, A.; Kaiser, C. A.; Krieger, M.; Scott, M. P.; Bretscher, A.; Ploegh, H. and Matsudaira, P. (2007). Molecular Cell Biology, 6th edition. W.H. Freeman and Company, New York.

Logan, J. and Shenk, T. (1984). Adenovirus tripartite leader sequence enhances translation of mRNAs late after infection. *Proc. Natl. Acad. Sci. USA* 81: 3655-3659.

Longiaru, M. and Horwitz, M. S. (1981). Chinese hamster ovary cells replicate adenovirus deoxyribonucleic acid. *Mol. Cell Biol.* 1: 208-215.

Lowe, S. W. and Ruley, H. E. (1993). Stabilization of the p53 tumor suppressor is induced by adenovirus 5 E1A and accompanies apoptosis. *Genes Dev.* 7: 535-545.

Loyter, A.; Scangos, G.; Juricek, D.; Keene, D. and Ruddle, F. H. (1982). Mechanisms of DNA entry into mammalian cells. II. Phagocytosis of calcium phosphate DNA co-precipitate visualized by electron microscopy. *Exp. Cell Res.* 139: 223234.

Lucas, B.; Giere, L.; DeMarco, R.; Shen, A.; Chisholm, V. and Crowley, C. (1996). High-level production of recombinant proteins in CHO cells using a dicistronic DHFR intron expression vector. *Nucleic Acids Res.* 24: 1774-1779.

Luckow, V. A. and Summers, M. D. (1988). Trends in the development of baculovirus expression systems. *Bio/Technology (NY)* 6: 47-55.

Lutz, P. and Kendinger, C. (1996). Properties of the adenovirus IVa2 gene product, an effector of late-phase-dependent activation of the major late promoter. *J. Virol.* 70: 1396-1405.

Lutz, P.; Rosa-Calatrava, M. and Kedinger, C. (1997). The product of the adenovirus intermediate gene IX is a transcriptional activator. *J. Virol.* 71: 5102-5109.

Macauley-Patrick, S.; Fazenda, M. L.; McNeil, B. and Harvey, L. M. (2005). Heterologous protein production using the *Pichia pastoris* expression system. *Yeast* 22: 249-270.

Maeda, S. (1989). Expression of foreign genes in insects using baculovirus vectors. *Annu. Rev. Entomol.* 34: 351-372.

Makrides, S. C. (1999). Components of vectors for gene transfer and expression in mammalian cells. *Protein Expr. Purif.* 17: 183-202.

Malone, R. W.; Felgner, P. L.; Verma, I. M. (1989). Cationic liposome-mediated RNA transfection. *Proc. Natl. Acad. Sci. USA* 86: 6077-6081.

Mansour, S. L.; Grodzicker, T. and Tjian, R. (1986). Downstream sequences affect transcription initiation from the adenovirus major late promoter. *Mol. Cell Biol.* 6: 2684-2694.

Markrides, S.C. (1999). Components of vectors for gene transfer and expression in mammalian cells. *Protein Expression and Purification.* 17: 183-202.

Martínez-Salas, E.; Pacheco, A.; Serrano, P. and Fernandez, N. (2008). New insights into internal ribosome entry site elements relevant for viral gene expression. *J. Gen. Virol.* 89: 611-626.

Marzluff, W. F. and Pandey, N. B. (1988). Multiple regulatory steps control histone mRNA concentrations. *Trends Biochem. Sci.* 13: 49-52.

Maston, G. A.; Evans, S. K. and Green, M. R. (2006). Transcriptional Regulatory Elements in the Human Genome. *Annu. Rev. Genomics Hum. Genet.* 7: 29-59.

Matsuki, N.; Ishikawa, T.; Imai, Y. and Yamaguchi, T. (2008). Low voltage pulses can induce apoptosis. *Cancer Lett.* 269: 93-100.

Mattaj, I. W. and Englmeier, L. (1998). Nucleocytoplasmic transport: The soluble phase. *Annu. Rev. Biochem.* 67: 265-306.

McCrae, M. A. and Woodland, H. R. (1981). Stability of non-polyadenylated viral mRNAs injected into frog oocytes. *Eur. J. Biochem.* 116: 467-470.

McMillan, N. A. J.; Chun, R. F.; Siderovski, D. P.; Galabru, J.; Toone, W. M.; Samuel, C. E.; Mak, T. W.; Hovanessian, A. G.; Jeang, K. -T. and Williams, B. R. G. (1995). HIV-1 Tat directly interacts with the interferon-induced, double-stranded RNA-dependent kinase, PKR. *Virology* 213: 413-424.

Michael, S. F. (1994). Mutagenesis by incorporation of a phosphorylated oligo during PCR amplification. *Biotechniques* 16: 410-412.

Miller, L.K. (1988). Baculoviruses as gene expression vectors. *Annu. Rev. Microbiol.* 42: 177-199.

Miyamoto, N. G.; Moncolin, V.; Egly, J. M. and Chambon, P. (1985). Specific interaction between a transcription factor and the upstream element of the adenovirus-2 major late promoter. *The EMBO Journal* 4: 3563-3570.

Mockey, M.; Gonçalves, C.; Dupuy, F. P.; Lemoine, F. M.; Pichon, C. and Midoux, P. (2006). mRNA transfection of dendritic cells: synergistic effect of ARCA mRNA capping with Poly(A) chains in cis and in trans for a high protein expression level. *Biochem. Biophys. Res. Commun.* 340: 1062-1068.

Moghimi, S. M.; Symonds, P.; Murray, J. C.; Hunter, A. C.; Debska, G. and Szewczyk, A. (2005). A two-stage poly(ethylenimine)-mediated cytotoxicity: implications for gene transfer/therapy. *Mol. Ther.* 11: 990-995.

Molla, A.; Jang, S.; Paul, A.; Reuer, Q. and Wimmer, E. (1992). Cardioviral internal ribosomal entry site is functional in a genetically engineered dicistronic poliovirus. *Nature* 356: 255-257.

Monaco, L.; Tagliabue, R.; Giovanazzi, S.; Bragonzi, A. and Soria, M. (1996). Expression of recombinant human granulocyte colony-stimulating factor in CHO *dhfr*$^-$ cells: new insights into the *in vitro* amplification expression system. *Gene* 180: 145-150.

Montell, C.; Fisher, E. F.; Caruthers, M. H. and Berk, A. J. (1984). Control of adenovirus E1B mRNA synthesis by a shift in the activation of RNA splice sites. *Mol. Cell. Biol.* 4: 966-972.

Moore, M. A. and T. Shenk. (1988). The adenovirus tripartite leader sequence can alter nuclear and cytoplasmic metabolism of a non-adenovirus mRNA within infected cells. *Nucleic Acids Res.* 16: 2247-2262.

Mossadegh, N.; Gissmann, L.; Muller, M.; Zentgraf, H.; Alonso, A. and Tomakidi, P. (2004). Codon optimization of the human papillomavirus 11 (HPV 11) L1 gene leads to increased gene expression and formation of virus-like particles in mammalian epithelial cells. *Virology* 326: 57-66.

Mukherjee, D.; Gao, M.; O'Connor, J. P.; Raijmakers, R.; Pruijn, G.; Lutz, C. S. and Wilusz, J. (2002). The mammalian exosome mediates the efficient degradation of mRNAs that contain AU-rich elements. *EMBO J.* 21: 165-174.

Mul, Y. M. and van der Vliet, P. C. (1992). Nuclear factor I enhances adenovirus DNA replication by increasing the stability of a preinitiation complex. *EMBO J.* 11: 751-760.

Mul, Y. M.; Verrijzer, C. P. and van der Vliet, P. C. (1990). Transcription factors NFI and NFIII/oct-1 function independently, employing different mechanisms to enhance adenovirus DNA replication. *J. Virol.* 64: 5510-5518.

Mullis, K.; Faloona, F.; Scharf, S.; Saiki, R.; Horn, G. and Erlich, H. (1986). Specific enzymatic amplification of DNA *in vitro*: the polymerase chain reaction. *Cold Spring Harbor Symposium on Quantitative Biology* 51 Part 1: 263-273.

Nadeau, I. and Kamen, A. (2003). Production of adenovirus vectors for gene therapy. *Biotechnology advances* 20: 475-489.

Nadeau, I.; Jacob, D.; Perrier, M. and Kamen, A. (2000a). 293SF metabolic flux analysis during cell growth and infection with an adenoviral vector. *Biotechnol. Prog.* 16: 872-884.

Nadeau, I.; Sabatie, J.; Koehl, M.; Perrier, M. and Kamen, A. (2000b). Human 293 cell metabolism in low glutamine-supplied culture: interpretation of metabolic changes through metabolic flux analysis. *Metab. Eng.* 2: 277-292.

Nadeau, I.; Seanez, G. and Wu, F. (2001). Adenovirus production in 293 cells: a comparative study between a suspension cell and an adherent cell process. The 17th ESACT Meeting, Tylosand, Sweden, June 10-14.

Nagata, T.; Uchijima, M.; Yoshida, A.; Kawashima, M. and Koide, Y. (1999). Codon optimization effect on translational efficiency of DNA vaccine in mammalian cells: analysis of plasmid DNA encoding a CTL epitope derived from microorganisms. *Biochem. Biophys. Res. Comm.* 261: 445-451.

Nagy, A.; Gertsenstein, M.; Vintersten, K. and Behringer, R. (2003). Manipulating the mouse embryo, a laboratory manual: Production of transgenic mice. pp. 289-358, cold spring harbour laboratory press.

Najjar, S. M., and Lewis, R. E. (1999). Persistent expression of foreign genes in cultured hepatocytes: Expression vectors. *Gene* 230: 41-45.

Nakamura, S.; Watanabe, S.; Ohtsuka, M.; Maehara, T.; Ishihara, M.; Yokomine, T. and Sato, M. (2008). Cre-loxP system as a versatile tool for conferring increased levels of tissue-specific gene expression from a weak promoter. *Mol. Reprod. Dev.* 75: 1085-1093.

Namy, O.; Hatin I. and Rousset J. P. (2001). Impact of the six nucleotides downstreamof the stop codon on translation termination. *EMBO Rep.* 2: 787-793.

Nass, K. and Frenkel, G. D. (1978). Adenovirus-induced inhibition of cellular DNase. *J. Virol.* 26: 540-543.

Nass, K. and Frenkel, G. D. (1980). Adenovirus-specific DNA-binding protein inhibits the hydrolysis of DNA by DNase *in vitro*. *J. Virol.* 35: 314-319.

Neill, S. D.; Hemstrom, C.; Virtanen, A. and Nevins, J. R. (1990). An adenovirus E4 gene product trans-activates E2 transcription and stimulates stable E2F binding through a direct association with E2F. *Proc. Natl. Acad. Sci. USA* 87: 2008-2012.

Nettelbeck, D. M.; Jerome, V. and Müller, R. (1998). Astrategy for enhancing the transcriptional activity of weak cell type-specific promoters. *Gene Ther.* 5: 1656-1664.

Nevels, M.; Rubenwolf, S.; Spruss, T.; Wolf, H. and Dobner, T. (1997). The adenovirus E4orf6 protein can promote E1A/E1B-induced focus formation by interfering with p53 tumor suppressor function. *Proc. Natl. Acad. Sci. USA* 94: 1206-1211.

Nevins, J. R. and Darnell, J. E. (1978). Groups of adenovirus type 2 mRNAs derived from a large primary transcript: probable nuclear origin and possible common 3' ends. *J. Virol.* 25: 811-823.

Nevins, J. R., and Wilson, M. C. (1981). Regulation of adenovirus-2 gene expression at the level of transcriptional termination and RNA processing. Nature 290: 113-118.

Nicolas, J. C.; Sarnow, P.; Girard, M. and Levine, A. J. (1983). Host range temperature-conditional mutants in the adenovirus DNA binding protein are defective in the assembly of infectious virus. *Virology* 126: 228-239.

Novina, C. D. and Roy, A. L. (1996). Core promoters and transcriptional control. *Trends Genet.* 12: 351-355.

Nuno-Gonzalez, P.; Chao, H. and Oka, K. (2005). Targeting site-specific chromosome integration. *Acta Biochimica Polonica* 52: 285-291.

O'Neill, E. A.; Fletcher, C.; Burrow, C. R.; Heintz, N.; Roeder, R. G. and Kelly, T. J. (1988). Transcription factor OTF-1 is functionally identical to the DNA replication factor NF-III. *Science* 241: 1210-1213.

Oker-Blom, C.; Petersson, R. F. and Summers, M. D. (1989). Baculovirus polyhedrion promoter directed expression of rubella virus envelope glycoproteins, E1 and E2, in *Spodoptera frugiperda* cells. *Virology* 172: 82-91.

Olafsdottir, G.; Svansson, V.; Ingvarsson, S.; Marti, E. and Torsteinsdottir, S. (2008). *In vitro* analysis of expression vectors for DNA vaccination of horses: the effect of a Kozak sequence. *Acta Vet. Scand.* 50: 44.

Olofsson, J.; Levin, M.; Strömberg, A.; Weber, S. G.; Ryttsén, F. and Orwar, O. (2007). Scanning electroporation of selected areas of adherent cell cultures. *Anal. Chem.* 79: 4410-4418.

Olofsson, J.; Nolkrantz, K.; Ryttsén, F.; Lambie, B. A.; Weber, S. G. and Orwar, O. (2003). Single-cell electroporation. *Curr. Opin. Biotechnol.* 14: 29-34.

Onishi, Y. and Kikuchi, Y. (2003). Study of the complex between DNA and DEAEdextran. *Kobunshi Ronbunshu* 60: 359-364.

Onishi, Y. and Kikuchi, Y. (2004). Study of the complex between RNA and DEAEdextran. *Kobunshi Ronbunshu* 61: 139-143.

Oosterom-Dragon, E. A. and Ginsberg, H. S. (1980). Purification and preliminary immunological characterization of the type 5 adenovirus, non-structural 100,000-dalton protein. *J. Virol.* 33: 1203–1207.

Ornelles, D. A. and Shenk, T. (1991). Localization of the adenovirus early region 1B 55-kilodalton protein during lytic infection: association with nuclear viral inclusions requires the early region 4 34-kilodalton protein. *J. Virol.* 65: 424-429.

Orrantia, E. and Chang, P. L. (1990). Intracellular distribution of DNA internalized through calcium phosphate precipitation. *Exp. Cell Res.* 190: 170-174.

Papadakis, E. D.; Nicklin, S. A.; Baker, A. H. and White, S. J. (2004). Promoters and control elements: designing expression cassettes for gene therapy. *Curr. Gene Ther.* 4: 89-113.

Parham, J. H.; Iannone, M. A.; Overton, L. K. and Hutchins, J. T. (1998).Optimization of transient gene expression in mammalian cells and potential for scale-up using flow electroporation. *Cytotechnology* 28: 147-155.

Parker, E. J.; Botting, C. H.; Webster, A. and Hay, R. T. (1998). Adenovirus DNA polymerase: domain organisation and interaction with preterminal protein. *Nucleic Acids Res.* 26:1240-1247.

Parker, R. and Song, H. (2004). The enzymes and control of eukaryotic mRNA turnover. *Nat. Struct. Mol. Biol.* 11: 121-127.

Parks, C. L. and Shenk, T. (1997). Activation of the adenovirus major late promoter by transcription factors MAZ and Sp1. *J. Virol.* 71: 9600-9607.

Patel, D. and Butler, J. S. (1992). Conditional defect in mRNA 39 end processing caused by a mutation in the gene for poly(A) polymerase. *Mol. Cell. Biol.* 12: 3297-3304.

Patnaik, P. (2003). Handbook of inorganic chemicals. The McGraw-Hill Companies, Inc., NY.

Pauletti, G.; Lai, E. and Attardi, G. (1990). Early appearance and long-term persistence of the submicroscopic extrachromosomal elements (amplisomes) containing the amplified *DHFR* genes in human cell lines. *Proc. Natl. Acad. Sci. USA* 87: 2955-2959.

Pautz, G. E.; Yang, Z. Y.; Wu, B. Y.; Gao, X.; Huang, L. and Nabel, G. J. (1993). Immunotherapy of malignancy by *in vivo* gene transfer into tumors. *Proc. Natl. Acad. Sci. USA* 90: 4645-4649.

Pelletier, J. and Sonenberg, N. (1988). Internal initiation of translation of eukaryotic mRNA directed by a sequence derived from poliovirus RNA. *Nature* 334: 320-325.

Peltz, S. W., and Jacobson, A. (1992). mRNA stability: in trans-it. *Curr. Opin. Cell Biol.* 4: 979-983.

Peltz, S. W.; Brewer, G.; Kobs, G. and Ross, J. (1987). Substrate specificity of the exonuclease activity that degrades H4 histone mRNA. *J. Biol. Chem.* 262: 9382-9388.

Peppel, K. and Baglioni, C. (1991). Deadenylation and turnover of interferon-b mRNA. *J. Biol. Chem.* 266: 6663-6666.

Peroni, C.; Soares, C.; Gimbo, E.; Morganti, L.; Ribela, M. and Bartolini, P. (2002). High-level expression of human thyroid-stimulating hormone in Chinese *hamster* ovary cells by co-transfection of dicistronic expression vectors followed by a dual-marker amplification strategy. *Biotechnology and Applied Biochemistry* 35: 19-26.

Pesole, G., Mignone, F., Gissi, C., Grillo, G., Licciulli, F. and Liuni, S. (2001). Structural and functional features of eukaryotic mRNA untranslated regions. *Gene* 276: 73-81.

Philpott, N. J. and Thrasher, A. J. (2008). Use of nonintegrating lentiviral vectors for gene therapy. *Hum. Gene Ther.* 18: 483-489.

Phi-Van, L. von Kries, J. P.; Ostertag, W. and Strätling, W. H. (1990). The chicken lysozyme 50 matrix attachment region increases transcription from a heterologous promoter in heterologous cells and dampens position effects on the expression of transfected genes. *Mol. Cell. Biol.* 10: 2302-2307.

Pilder, S.; Leppard, K.; Logan, J. and Shenk, T. (1986a). Functional analysis of the adenovirus E1B 55K polypeptide. *Cancer Cells* 4: 285-290.

Pilder, S.; Logan, J. and Shenk, T. (1984). Deletion of the gene encoding the adenovirus 5 early region 1b 21,000-molecular-weight polypeptide leads to degradation of viral and host cell DNA. *J. Virol.* 52: 664-671.

Pilder, S.; Moore, M.; Logan, J. and Shenk, T. (1986b). The adenovirus E1B- 55K transforming polypeptide modulates transport or cytoplasmic stabilization of viral and host cell mRNAs. *Mol. Cell. Biol.* 6: 470-476.

Preuss, A. K.; Connor, J. A. and Vogel, H. (2000). Transient transfection induces diVerent intracellular calcium signaling in CHOK1 versus HEK293 cells. *Cytotechnology* 33: 139-145.

Preuss, A. K.; Pick, H. M.; Wurm, F. and Vogel, H. (1999). Transient transfection induces early cytosolic calcium signaling in CHO-K1 cells. In: Ikura, K.; Nagao, M.; Masuda, S. and Sasaki, R. (eds.), Animal Cell Technology: Challenges for the 21st Century. Kluwer Academic Publishers, Dordrecht, pp. 17-21.

Prives, C. (1998). Signaling to p53: breaking the MDM2-p53 circuit. *Cell* 95: 5-8.

Ptushkina, M.; von der Haar, T.; Karim, M. M.; Hughes, J. M. X. and McCarthy, J. E. G. (1999). Repressor binding to a dorsal regulatory site traps human eIF4E in a high cap-affinity state. *EMBO J.* 18: 4068-4075.

Puck, T. T.; Cieciura, S. J. and Robinson, A. (1958). Genetics of somatic mammalian cells: iii. Long-term cultivation of euploid cells from human and animal subjects. *J. Exp. Med.* 108: 945-956.

Querido, E.; Marcellus, R. C.; Lai, A.; Charbonneau, R.; Teodoro, J. G.; Ketner, G. and Branton, P. E. (1997a). Regulation of p53 levels by the E1B 55-kilodalton protein and E4orf6 in adenovirus-infected cells. *J. Virol.* 71: 3788-3798.

Querido, E.; Teodoro J. G. and Branton, P. E. (1997b). Accumulation of p53 induced by the adenovirus E1A protein requires regions involved in the stimulation of DNA synthesis. *J. Virol.* 71: 3526-3533.

Rabussay D. (2008). Applicator and electrode design for *in vivo* DNA delivery by electroporation. *Methods Mol. Biol.* 423: 35-59.

Rao, L.; Debbas, M.; Sabbatini, P.; Hockenbery, D.; Korsmeyer, S. and White, E. (1992). The adenovirus E1A proteins induce apoptosis, which is inhibited by the E1B 19-kDa and Bcl-2 proteins. *Proc. Natl. Acad. Sci. USA* 89: 7742-7746, Erratum in: 89: 9974.

Recillas-Targa, F. (2004). Gene transfer and expression in mammalian cell lines and transgenic animals. *Methods Mol. Biol.* 267: 417-433.

Reed, R. and Hurt, E. A. (2002). Conserved mRNA export machinery coupled to pre-mRNA splicing. *Cell* 108: 523-531.

Reed, R. and Magni, K. A. (2001). A new view of mRNA export: Separating the wheat from the chaff. *Nat. Cell Biol.* 3: E201-E204.

Rekosh, D. M.; Russell, W. C.; Bellet, A. J. and Robinson, A. J. (1977). Identification of a protein linked to the ends of adenovirus DNA. *Cell* 11: 283-295.

Rhoads, R. E. (1988). Cap recognition and the entry of mRNA into the protein synthesis initiation cycle. *Trends Biochem. Sci.* 13: 52-56.

Ridgway, P. J.; Hall, A. R.; Myers, C. J. and Braithwaite, A. W. (1997). p53/E1b58kDa complex regulates adenovirus replication. *Virology* 237: 404-413.

Riley, D. and S. J. Flint. (1993). RNA-binding properties of a translational activator, the adenovirus L4 100-kilodalton protein. *J. Virol.* 67: 3586-3595.

Ross, J. (1995). mRNA stability in mammalian cells. *Microbiological Reviews* 59: 423-450.

Roth, J.; König, C.; Wienzek, S.; Weigel, S.; Ristea, S. and Dobbelstein, M. (1998). Inactivation of p53 but not p73 by adenovirus type 5 E1B 55-kilodalton and E4 34-kilodalton oncoproteins. *J. Virol.* 72: 8510-8516.

Rowe, W. P.; Huebner, R. J.; Gilmore, L. K.; Parrot, R. H. and Ward, T. G. (1953). Isolation of a cytopathic agent from human adenoids undergoing spontaneous degradation in tissue culture. *Proceedings of the Society for Experimental Biology and Medicine* 84: 570-573.

Rowlett, R. M.; Chrestensen, C. A.; Schroeder, M. J.; Harp, M. G.; Pelo, J. W.; Shabanowitz, J.; DeRose, R.; Hunt, D. F.; Sturgill, T. W. and Worthington, M. T. (2008). Inhibition of tristetraprolin deadenylation by poly(A) binding protein. *Am. J. Physiol. Gastrointest Liver Physiol.* 295: G421-G430.

Ruben, M.; Bacchetti, S. and Graham, F. (1983). Covalently closed circles of adenovirus 5 DNA. *Nature* 301: 172-174.

Russell WC. (2000). Update on adenovirus and its vectors. *J. Gen. Virol.* 81: 2573-2604.

Sabbattini, P.; Han, J. H.; Chiou, S. -K..; Nicholson, D. and White, E. (1997). Interleukin 1b converting enzyme-like proteases are essential for p53-mediated transcriptionally dependent apoptosis. *Cell Growth Diff.* 8: 643-653.

Sachs, A. (1990). The role of poly(A) in the translation and stability of mRNA. *Curr. Opin. Cell Biol.* 2: 1092-1098.

Sachs, A. B. (1993). Messenger RNA degradation in eukaryotes. *Cell* 74: 413-421.

Sambrook, J.; Fritsch, E. F. and Maniatis, T. (1989). Molecular Cloning: A Laboratory Manual, 2nd ed. Cold Spring Harbor Laboratory Press, Cold Spring Harbor, NY.

Sarnow, P.; Ho, Y.; Williams, J. and Levine, A. (1982). Adenovirus E1b-58kd tumor antigen and SV40 large tumor antigen are physically associated with the same 54 kd cellular protein in transformed cells. *Cell* 28: 387-394.

Schatzlein, A. G. (2001). Non-viral vectors in cancer gene therapy principles and progress. *Anticancer Drugs* 12: 275-304.

Schiedner, G.; Schmitz, B. and Doerfler, W. (1994). Late transcripts of adenovirus type 12 DNA are not translated in hamster cells expressing the E1 region of adenovirus type 5. *J. Virol.* 68: 5476-5482.

Schumperli, D. (1988). Multilevel regulation of replication-dependent histone genes. *Trends Genet.* 4: 187-191.

Shatkin, A. J. (1985). mRNA cap binding proteins: essential factors for initiating translation. *Cell* 40: 223-224.

Shaw, A. R. and Ziff, E. B. (1980). Transcripts from the adenovirus-2 major late promoter yield a single early family of 3' coterminal mRNAs and five late families. *Cell* 22: 905-916.

Shaw, G. and Kamen, R. (1986). A conserved AU sequence from the 39 untranslated region of GM-CSF mRNA mediates selective mRNA degradation. *Cell* 46: 659-667.

Shaw-Jackson, C. and Michiels, T. (1999). Absence of internal ribosome entry site-mediated tissue specificity in the translation of a bicistronic transgene. *J. Virol.* 73: 2729-2738.

Shenk, T. and Flint, J. (1991). Transcriptional and transforming activities of the adenovirus E1A proteins. *Adv. Cancer Res.* 57: 47-85.

Shenk, T. (2001). *Adenoviridae*: the virus and their replication. In: Knipe, D. M. and Howley, P. M. (eds.), Fundamental Virology, 4th ed. Philadelphia: Lippincott Williams and Wilkins, pp. 1053-1088.

Shenk, T.; Jones, N.; Colby, W. and Fowlkes, D. (1980). Functional analysis of adenovirus-5 host-range deletion mutants defective for transformation of rat embryo cells. *Cold Spring Harb. Symp. Quant. Biol.* 44: 367-375.

Shimotohno, K.; Kodama, Y.; Hashimoto, J. and Miura, K. (1977). Importance of 59-terminal blocking structure to stabilize mRNA in eukaryotic protein synthesis. *Proc. Natl. Acad. Sci. USA* 74: 2734-2738.

Shyu, A. -B.; Belasco, J. G. and Greenberg, M. E. (1991). Two distinct destabilizing elements in the c-*fos* message trigger deadenylation as a first step in rapid mRNA decay. *Genes Dev.* 5: 221-231.

Smart, J. E. and Stillman, B. W. (1982). Adenovirus terminal protein precursor. Partial amino acid sequence and the site of covalent linkage to virus DNA. *J. Biol. Chem.* 257: 13499-13506.

Smith, J., Riballo, E.; Kysela, B.; Baldeyron, C.; Manolis, K.; Masson, C.; Lieber, M. R.; Papadopoulo, D. and Jeggo, P. (2003). Impact of DNA ligase IV on the fidelty of end joining in human cells. *Nucleic Acids Res.* 31: 2157-2167.

Song, B.; Hu, S. -L.; Darai, G.; Spindler, K. R. and Young, C. S. H. (1996). Conservation of DNA sequences in the predicted major late promoter region of selected mastadenoviruses. *Virology* 220: 390-401.

Steegenga, W. T.; Riteco, N.; Jochemsen, A. G.; Fallaux, F. J. and Bos, J. L. (1998). The large E1B protein together with the E4orf6 protein target p53 for active degradation in adenovirus infected cells. *Oncogene* 16: 349-357.

Stein, R. W.; Corrigan, M.; Yaciuk, P.; Whelan, P. and Moran, E. (1990). Analysis of E1A-mediated growth regulation functions: binding of the 300-kilodalton cellular product correlates with E1A enhancer repression function and DNBA synthesis-inducing activity. *J. Virol.* 64: 4421-4427.

Stephens, C. and Harlow, E. (1987). Differential splicing yields novel adenovirus 5 E1A mRNAs that encode 30 kd and 35 kd proteins. *EMBO J.* 6: 2027-2035.

Stepinski, J.; Waddell, C.; Stolarski, R.; Darzynkiewicz, E. and Rhoads, R. E. (2001). Synthesis and properties of mRNAs containing the novel "anti-reverse" cap analogs 7-methyl(3'-O-methyl)GpppG and 7-methyl (3'-deoxy)GpppG. *RNA* 7: 1486-1495.

Stillman, B. (2005). Origin recognition and the chromosome cycle. *FEBS Lett.* 579: 877-884.

Stuiver, M. H. and van der Vliet, P. C. (1990). Adenovirus DNA-binding protein forms a multimeric protein complex with double-stranded DNA and enhances binding of nuclear factor I. *J. Virol.* 64: 379-386.

Sun, J.; Chen, M.; Xu, J. and Luo, J. (2005). Relationships among stop codon usage bias, its context, isochores, and gene expression level in various eukaryotes. *J. Mol. Evol.* 61: 437-444.

Sutherland, H. G.; Martin, D. I. and Whitelaw, E. (1997). A globin enhancer acts by increasing the proportion of erythrocytes expressing a linked transgene. *Mol. Cell. Biol.* 17: 1607-1614.

Swaminathan, S. and Thimmapaya, B. (1995). Regulation of adenovirus E2 transcription unit. In: Doerfler, W. and Böhm, P. (eds.), The Molecular Repertoire of Adenoviruses, vol. III. Springer-Verlag, Berlin, Germany, pp. 177-194.

Szutorisz, H.; Dillon, N. and Tora, L. (2005). The role of enhancers as centres for general transcription factor recruitment. *Trends Biochem. Sci.* 30: 593-99.

Tai, C. K. and Kasahara N. (2008). Replication-competent retrovirus vectors for cancer gene therapy. *Front Biosci.* 13: 3083-3095.

Tang, Y. M.; Ning, B. T.; Cao, J.; Shen, H. Q. and Qian, B. Q. (2007). Construction and expression of single-chain antibody derived from a new clone of monoclonal antibody against human CD14 in CHO cells. *Immunopharmacol Immunotoxicol.* 29: 375-386.

Temperley, S. M. and Hay, R. T. (1992). Recognition of the adenovirus type 2 origin of DNA replication by the virally encoded DNA polymerase and preterminal proteins. *The EMBO J.* 11: 761-768.

Tripathi, A. K. and Kumar, H. D. (1986). Mutagenesis by *ethidium bromide*, proflavine and mitomycin C in the *cyanobacterium Nostoc sp. Mutation Research Letters* 174: 175-178.

Ulfendahl, P. J.; Linder, S.; Kreivi, J. P.; Nordqvist, K.; Sevensson, C.; Hultberg, H. and Akusjärvi, G. (1987). A novel adenovirus-2 E1A mRNA encoding a protein with transcription activation properties. *EMBO J.* 6: 2037-2044.

Ullu, E. and Tschudi, C. (1991). Trans splicing in trypanosomes requires methylation of the 5' end of the spliced leader RNA. *Proc. Natl. Acad. Sci. USA* 88: 10074-10078.

Unger, E. C.; McCreery, T. and Sweitzer, R. H. (1997). Ultrasound enhances gene expression of liposomal transfection. *Invest. Radiol.* 32: 723-727.

van Breukelen, B.; Brenkman, A. B.; Holthuizen, P. E. and van der Vliet, P. C. (2003). Adenovirus Type 5 DNA Binding Protein Stimulates Binding of DNA Polymerase to the Replication Origin. *J. Virol.* 77: 915-922.

van Breukelen, B.; Kanellopoulos, P. N.; Tucker, P. A. and van der Vliet, P. C. (2000). The formation of a flexible DNA-binding protein chain is required for efficient DNA unwinding and adenovirus DNA chain elongation. *J. Biol. Chem.* 275: 40897-40903.

van der Vliet, P. C. (1995). Adenovirus DNA replication. *Curr. Top. Microbiol. Immunol.* 199:1-30.

van Leeuwen, H. C.; Rensen, M. and van der Vliet, P. C. (1997). The Oct-1 POU homeodomain stabilizes the adenovirus preinitiation complex via a direct interaction with the priming protein and is displaced when the replication fork passes. *J. Biol. Chem.* 272: 3398-3405.

Verma, R.; Boleti, E. and George, A. (1998). Antibody engineering: comparison of bacterial, yeast, insect and mammalian expression systems. *Journal of Immunological Methods* 216: 165-181.

Vilar, J. M. and Saiz, L. (2005). DNA looping in gene regulation: from the assembly of macromolecular complexes to the control of transcriptional noise. *Curr. Opin. Genet. Dev.* 15: 136-44.

Virtanen, A.; Gilardi, P.; Näslund, A.; LeMoullec, J. M.; Pettersson, U. and Perricaudet, M. (1984). mRNAs from human adenovirus 2 early region 4. *J. Virol.* 51: 822-831.

Waggoner, S. A. and Liebhaber, S. A. (2003). Regulation of alpha-globin mRNA stability. *Exp. Biol. Med. (Maywood)* 228: 387-395.

Wahle, E. and Ruegsegger, U. (1999). 3'-end processing of pre-mRNA in eukaryotes. *FEMS Microbiol. Rev.* 23: 277-295.

Wake, C. T.; Gudewicz, T.; Porter, T.; White, A. and Wilson, J. H. (1984). How damaged is the biologically active subpopulation of transfected DNA? *Mol. Cell Biol.* 4: 387-398.

Walsh, G. and Jefferis, R. (2006). Post-translational modifications in the context of therapeutic proteins. *Nature Biotechnology* 24: 1241-1252.

Walters, M. C.; Fiering, S.; Eidemiller, J.; Magis, W.; Groudine, M. and Martin, D. I. (1995). Enhancers increase the probability but not the level of gene expression. *Proc. Natl. Acad. Sci. USA* 92: 7125-7129.

Walters, M. C.; Magis, W.; Fiering, S.; Eidemiller, J.; Scalzo, D.; Groudine, M. and Martin, D. I. (1996). Transcriptional enhancers act in cis to suppress position-effect variegation. *Genes Dev.* 10: 185-195.

Wang, X.; Kiledjian, M.; Weiss, I. M. and Liebhaber, S. A. (1995). Detection and characterization of a 3_ untranslated region ribonucleoprotein complex associated with human alpha-globin mRNA stability. *Mol. Cell. Biol.* 15: 1769-1777.

Wang, Z. R. and Kiledjian, M. (2001). Functional link between the mammalian exosome and mRNA decapping. *Cell* 107:751-762.

Watanabe, H.; Imai, T.; Sharp, P. A. and Handa, H. (1988). Identification of two transcription factors that bind to specific elements in the promoter of the adenovirus early-region 4. *Mol. Cell. Biol.* 8: 1290-1300.

Weaver, F. R. and Hedrick, P. W. (1992). Genetics, 2nd edition. Wm. C. Brown, Dubuque.

Webster, L. C. and Ricciardi, R. P. (1991). trans-dominant mutants of E1A provide genetic evidence that the zinc finger of the trans-activating domain binds a transcription factor. *Mol. Cell. Biol.* 11: 4287-4296.

Webster, L. C.; Zhang, K.; Chance, B.; Ayene, I.; Culp, J. S.; Huang, W. -J.; Wu, F. Y. -H. and Ricciardi, R. P. (1991). Conversion of the E1A Cys4 zinc finger to a nonfunctional

His2,Cys2 zinc finger by a single point mutation. *Proc. Natl. Acad. Sci. USA* 88: 9989-9993.

Weiss, I. M. and Liebhaber, S. A. (1995). Erythroid cell-specific mRNA stability elements in the alpha 2-globin 3_ nontranslated region. *Mol. Cell. Biol.* 15: 2457-2465.

White, E.; Grodzicker, T. and Stillman, B. W. (1984). Mutations in the gene encoding the adenovirus early region 1B 19,000-molecular-weight tumor antigen cause the degradation of chromosomal DNA. *J. Virol.* 52: 410-419.

Whyte, P.; Williamson, N. M. and Harlow, E. (1989). Cellular targets for transformation by the adenovirus E1A proteins. *Cell* 56: 67-75.

Williams, J.; Karger, B. D.; Ho, Y. S.; Castaglia, C. L.; Mann, T. and Flint, S. J. (1986). The adenovirus E1B 495R protein plays a role in regulating the transport and stability of the viral late messages. *Cancer Cells* 4: 275-284.

Wilson, J. M.; Grossman, M.; Cabrera, J. A.; Wu, C. H. and Wu, G. Y. (1992). A novel mechanism for achieving transgene persistence *in vivo* after somatic gene transfer into hepatocytes. *J. Biol. Chem.* 267: 11483-11489.

Wimmer, E.; Hellen, C. U. and Cao, X. (1993). Genetics of poliovirus. *Annu. Rev. Genet.* 27: 353-436.

Woodcock, D. M.; Cowther, P. J.; Doherty, J.; Jefferson, S.; DeCruz, E.; Noyer-Weidner, M.; Smith, S. S.; Michael, M. Z. and Graham, M. W. (1989). Quantitative evaluation of *Escherichia coli* host strains for tolerance to cytosine methylation in plasmid and phage recombinants. *Nucleic Acids Res.* 17: 3469-3478.

Worgall, S. (2005). A realistic chance for gene therapy in the near future. *Pediatr. Nephrol.* 20: 118-124.

Wright, J. L.; Jordan, M. and Wurm, F. M. (2003). Transfection of partially purified plasmid DNA for high-level transient protein expression in HEK293-EBNA cells. *J. Biotechnol.* 102: 211-221.

Wu, C. and Alwine, J. C. (2004). Secondary structure as a functional feature in the downstream region of mammalian polyadenylation signals. *Mol. Cell Biol.* 24: 2789-2796.

Wu, J. M.; Lin, J. C.; Chieng, L. L.; Lee, C. K. and Hsu, T. A. (2003). Combined use of *GAP* and *AOX1* promoter to enhance the expression of human granulocyte-macrophage colony-stimulating factor in *Pichia pastoris*. *Enz. Microb. Technol.* 33: 453-459.

Wurm, F. M. (2004). Production of recombinant protein therapeutics in cultivated mammalian cells. *Nat. Biotechnol.* 22: 1393-1398.

Wurm, F. M. and Bernard, A. (1999). Large-scale transient expression in mammalian cells for recombinant protein production. *Curr. Opin. Biotechnol.* 313: 156-159.

Xi, Q.; Cuesta, R. and Schneider, R. J. (2004). Tethering of eIF4G to adenoviral mRNAs by 100k protein drives ribosome shunting. *Genes Dev.* 18: 1997-2009.

Xi, Q.; Cuesta, R. and Schneider, R. J. (2005). Regulation of translation by ribosome shunting through phosphotyrosine-dependent coupling of adenovirus protein 100k to viral mRNAs. *J. Virol.* 79: 5676-5683.

Xia, X. (2007). The +4G site in Kozak consensus is not related to the efficiency of translation initiation. *PLoS ONE* 2: e188.

Xiang, W. K.; Paul, A. V. and Wimmer, E. (1997). RNA signals in entero- and rhinovirus genome replication. *Semin. Virol.* 8: 256-273.

Yang, G.; Zhou, H.; Lu, Y.; Lin, Y. and Zhou, S. (2004). Comparing expression of different forms of human DNA topoisomerase I in *Pichia pastoris*. *Enz. Microb. Technol.* 34: 139-146.

Yang, N. S.; Burkholder, J.; McCabe, D.; Neumann, V. and Fuller, D. (2001). Particle-mediated gene delivery *in vivo* and *in vitro*. *Curr. Protoc. Hum. Genet.* Chapter 12: Unit 12.6.

Yang, T. -T.; Cheng, L. and Kain, S. R. (1996). Optimized codon usage and chromophore mutations provide enhanced sensitivity with the green fluorescent protein. *Nucleic Acids Res.* 24: 4592-4593.

Yew, N. S.; Wysokenski, D. M.; Wang, K. X.; Ziegler, R. J.; Marshall, J.; McNeilly, D.; Cherry, M.; Osbum, W. and Cheng, S. H. (1997). Optimization of plasmid vectors for high-level expression in lung epithelial cells. *Hum. Gene Ther.* 8: 575-584.

Young, C. S. H. (2003). The structure and function of the adenovirus major late promoter. *Current Topics in Microbiology and Immunology* 272: 213-249.

Yueh, A. and Schneider, R. J. (1996). Selective translation initiation by ribosome jumping in adenovirus-infected and heat-shocked cells. *Genes Dev.* 10: 1557-1567.

Yueh, A. and Schneider, R. J. (2000). Translation by ribosome shunting on adenovirus and hsp70 mRNAs facilitated by complementarity to 18S rRNA. *Genes Dev.* 14: 414-421.

Zhang, D. Y.; Yang, S.; Lü, S. J.; Yan, J. D. and Zhu, T. H. (2006). Expression, characterization and biological activity analysis of recombinant human bone morphogenetic protein 2 in CHO cells. *Sheng Wu Gong Cheng Xue Bao.* 22: 968-972.

Zhang, G.; Budker, V. G.; Ludtke, J. J. and Wolff, J. A. (2004). Naked DNA Gene Transfer in Mammalian Cells. *Methods Mol Biol.* 245: 251-264.

Zhang, Y. and Yu, L. C. (2008). Single-cell microinjection technology in cell biology. *Bioessays* 30: 606-610.

Zhang, Y.; Dolph, P. J. and Schneider, R. J. (1989). Secondary Structure Analysis of Adenovirus Tripartite Leader. *J. Biol Chem.* 264: 10679-10684.

Zhang, Y.; Feigenblum, D. and Schneider, R. J. (1994). A late adenovirus factor induces eIF-4E dephosphorylation and inhibition of cell protein synthesis. *J. Virol.* 68: 7040-7050.

Zhang, Y.; Xiong, Y. and Yarbrough, W. G. (1998). ARF promotes mdm2 degradation and stabilises p53: ARF-INK4a locus deletion impairs both the Rb and p53 tumor suppression pathways. *Cell* 92: 725-734.

Zhao, J.; Hyman, L. and Moore, C. (1999). Formation of mRNA 3' ends in eukaryotes: mechanism, regulation, and interrelationships with other steps in mRNA synthesis. *Microbiol. Mol. Biol. Rev.* 63: 405-445.

Ziff, E. and Fraser, N. (1978). Adenovirus type 2 late mRNAs: structural evidence for 3'-coterminal species. *J. Virol.* 25: 897-906.

Ziff, E. B. and Evans, R. M. (1978). Coincidence of the promoter and capped 5' terminus of RNA from the adenovirus 2 major late transcription unit. *Cell* 15: 1463-1475.

Zijderveld, D. C.; d'Adda di Fagagna, F.; Giacca, M.; Timmers, H. T. and van der Vliet, P. C. (1994). Stimulation of the adenovirus major late promoter *in vitro* by transcription factor USF is enhanced by the adenovirus DNA binding protein. *J. Virol.* 68: 8288-8295.

Zolotukhin, S.; Potter, M.; Hauswirth, W. W.; Guy, J. and Muzyczka, N. (1996). A "humanized" green fluorescent protein cDNA adapted for high-level expression in mammalian cells. *J. Virol.* 70: 4646-4654.

APPENDIX

A- Effect of CsCl, EtBr/CsCl, endotoxin and EtOH on mutation frequency

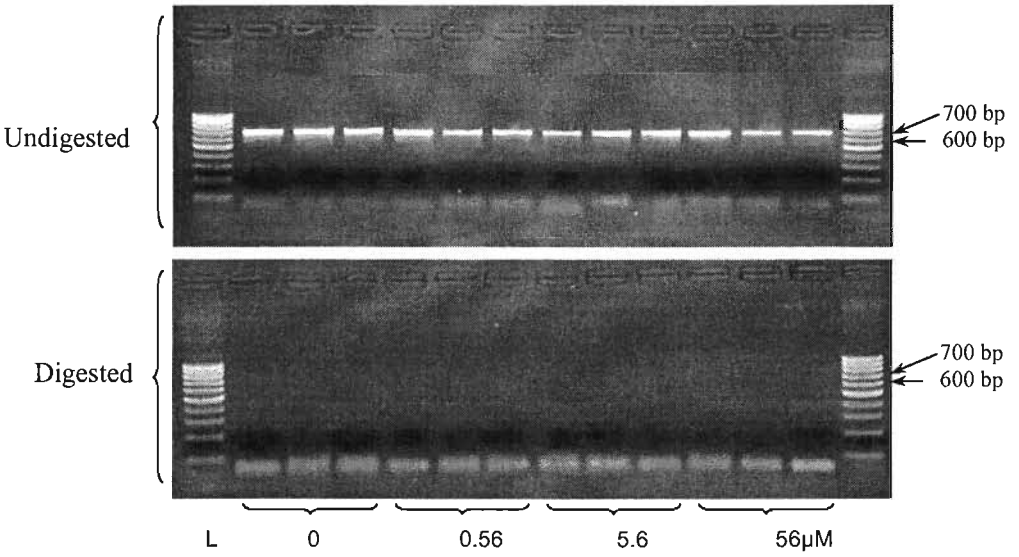

Figure A.1: PCR amplification before and after *Hind*III digestion of DNA isolated from cells transfected with pCMVβ spiked with CsCl. The amplicon size of 677 bp and CsCl spiking concentrations are shown on the Figure. The DNA ladder (L) used is Norgen's PCRSizer.

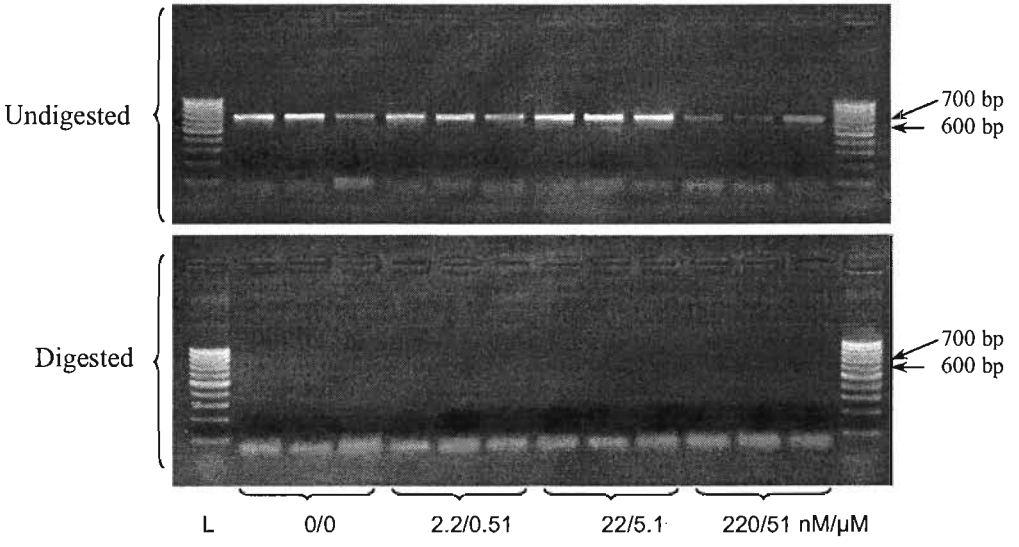

Figure A.2: PCR amplification before and after *Hind*III digestion of DNA isolated from cells transfected with pCMVβ spiked with EtBr/CsCl. The amplicon size of 677 bp and EtBr/CsCl spiking concentrations are shown on the Figure. The DNA ladder (L) used is Norgen's PCRSizer.

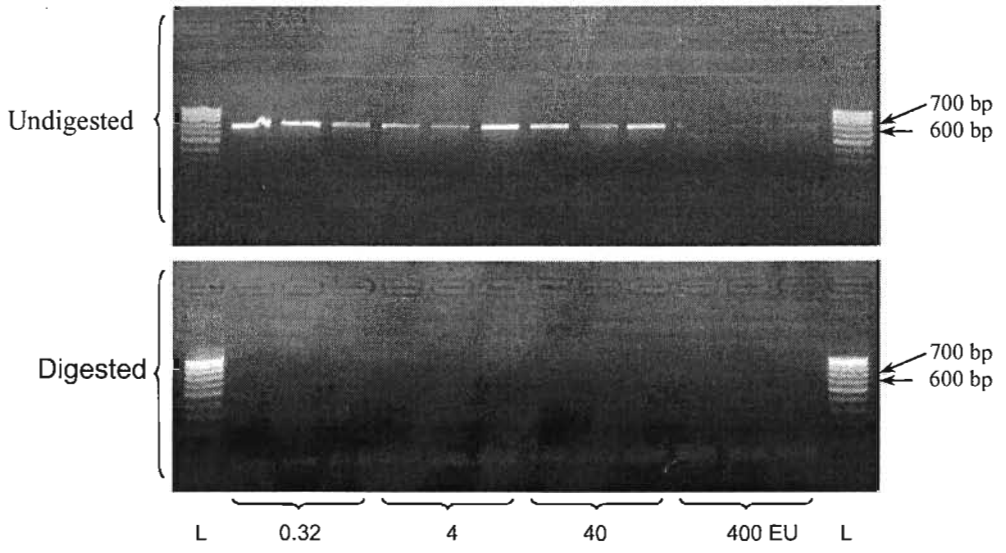

Figure A.3: PCR amplification before and after *Hind*III digestion of DNA isolated from cells transfected with pCMVβ spiked with endotoxin. The amplicon size of 677 bp and endotoxin spiking concentrations are shown on the Figure. The DNA ladder (L) used is Norgen's PCRSizer.

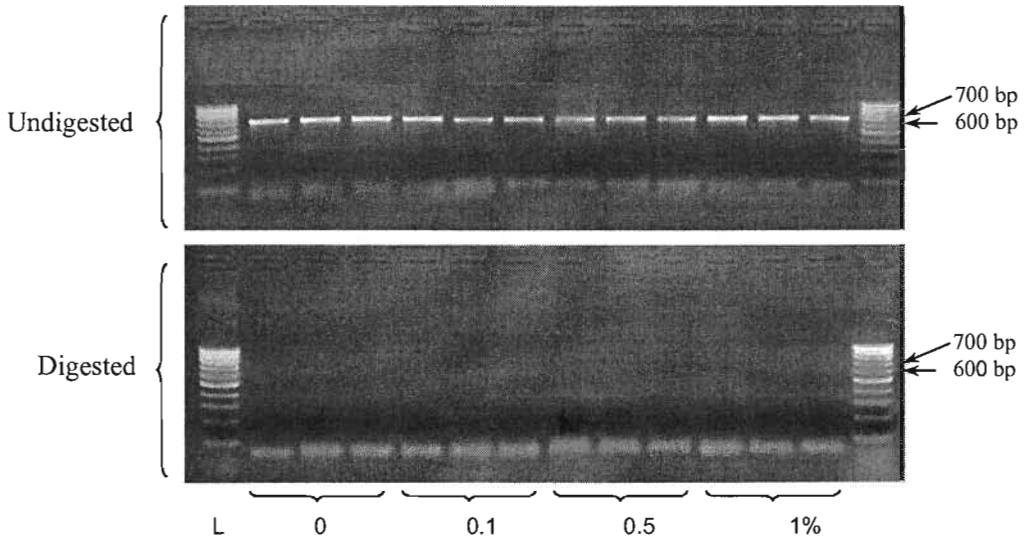

Figure A.4: PCR amplification before and after *Hind*III digestion of DNA isolated from cells transfected with pCMVβ spiked with EtOH. The amplicon size of 677 bp and EtOH spiking concentrations are shown on the Figure. The DNA ladder (L) used is Norgen's PCRSizer.

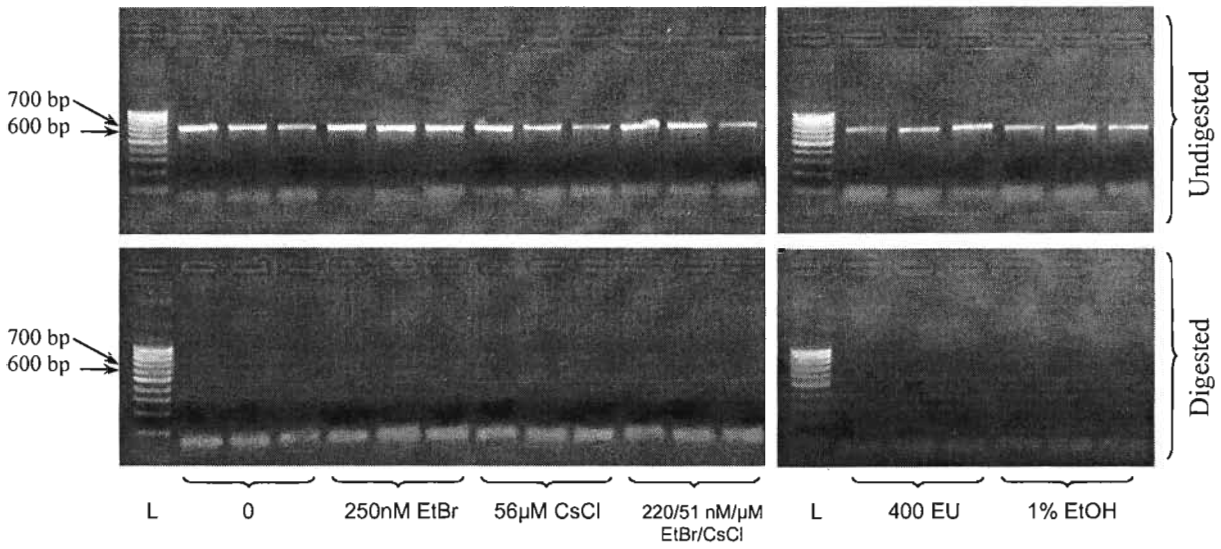

Figure A.5: PCR amplification before and after *Hind*III digestion of DNA isolated from cells transfected with pCMVβ spiked with the highest contaminant concentrations and cleaned before transfection. The amplicon size of 677 bp and the spiking conditions and concentrations are shown on the Figure. The DNA ladder (L) used is Norgen's PCRSizer.

B- Construction of pE1

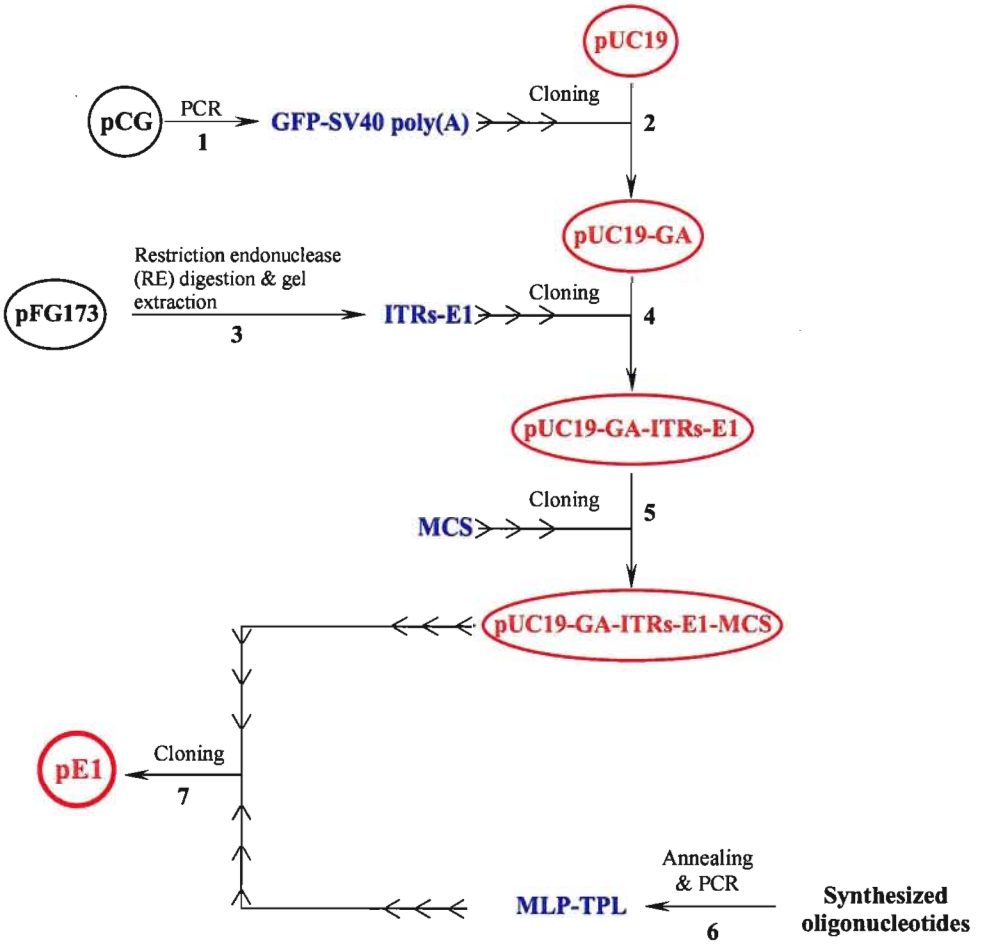

Figure A6: Overall construction strategy of pE1 plasmid. Numbers shows the flow of the construction steps.

3.2.1.1- Construction of pUC19-GA

The plasmid pCG contains GFP (AcGFP1: derived from the jellyfish *Aequorea coerulescens*) and SV40 poly(A). It was used as a template in a PCR reaction to amplify a fragment of 969 bp and contains the gene and poly(A) using the GA specific primer set. The reaction was performed using the *Pfu* DNA polymerase enzyme to reduce the mutation probability and also to create a product with blunt ends needed for downstream

cloning. An agarose gel was used to run the reaction product and the amplified DNA fragment was extracted from the gel. The amplification strategy and the gel picture of the amplification are shown in Figures A7 and A8, respectively.

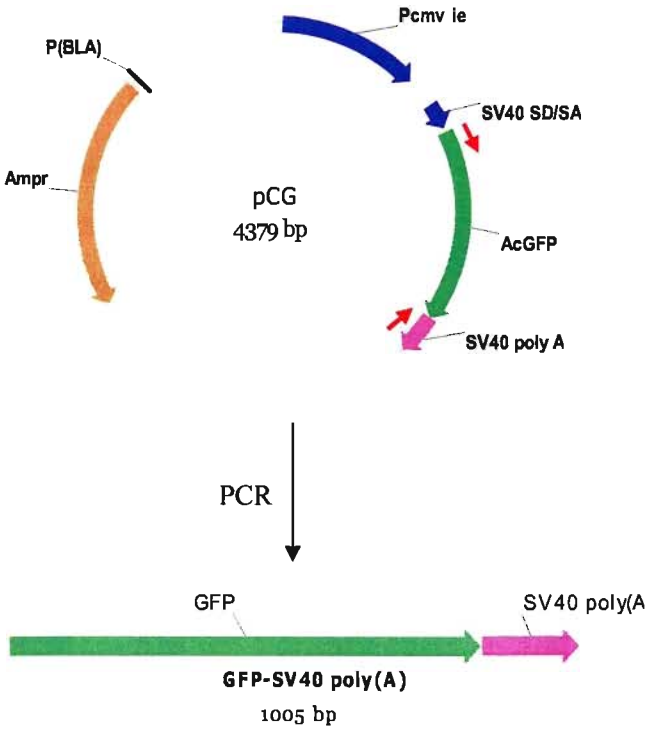

Figure A7: Strategy of PCR amplification of GFP-SV40 poly(A) from pCMV-GFP. Red arrows represent the annealing sites of the two PCR primers.

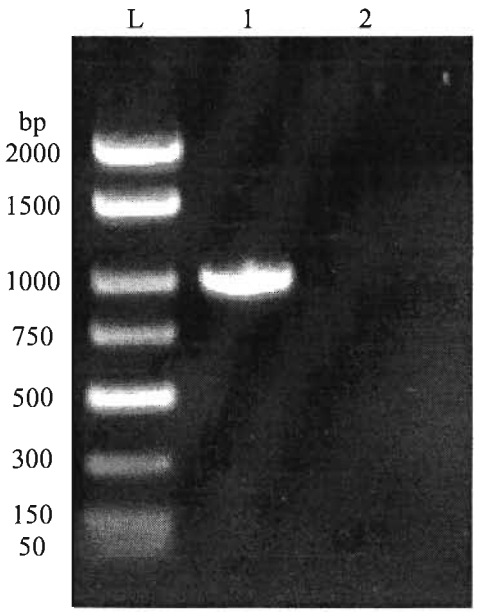

Figure A8: PCR amplification of GFP-SV40 poly(A) using pCMV-GFP as a template. Lane 1 shows the amplification product of 969 bp, lane 2 is the negative control and lane L is Norgen's FastRunner DNA ladder. The bp sizes of the ladder bands are shown on the left side.

pUC19 was digested with the restriction enzyme *Hinc*II (blunt ends) and subsequently cleaned to remove salts and enzymatic residuals. The cleaned GFP-SV40 poly(A) fragment was then cloned into the *Hinc*II digested and cleaned pUC19 using T4 DNA ligase and later transformed into DH5α cells. The obtained plasmid was designated pUC19-GA. The construction strategy is seen in Figure A9 and the restriction enzyme digestion pattern and the digestion picture are shown in Table A1 and Figure A10, respectively.

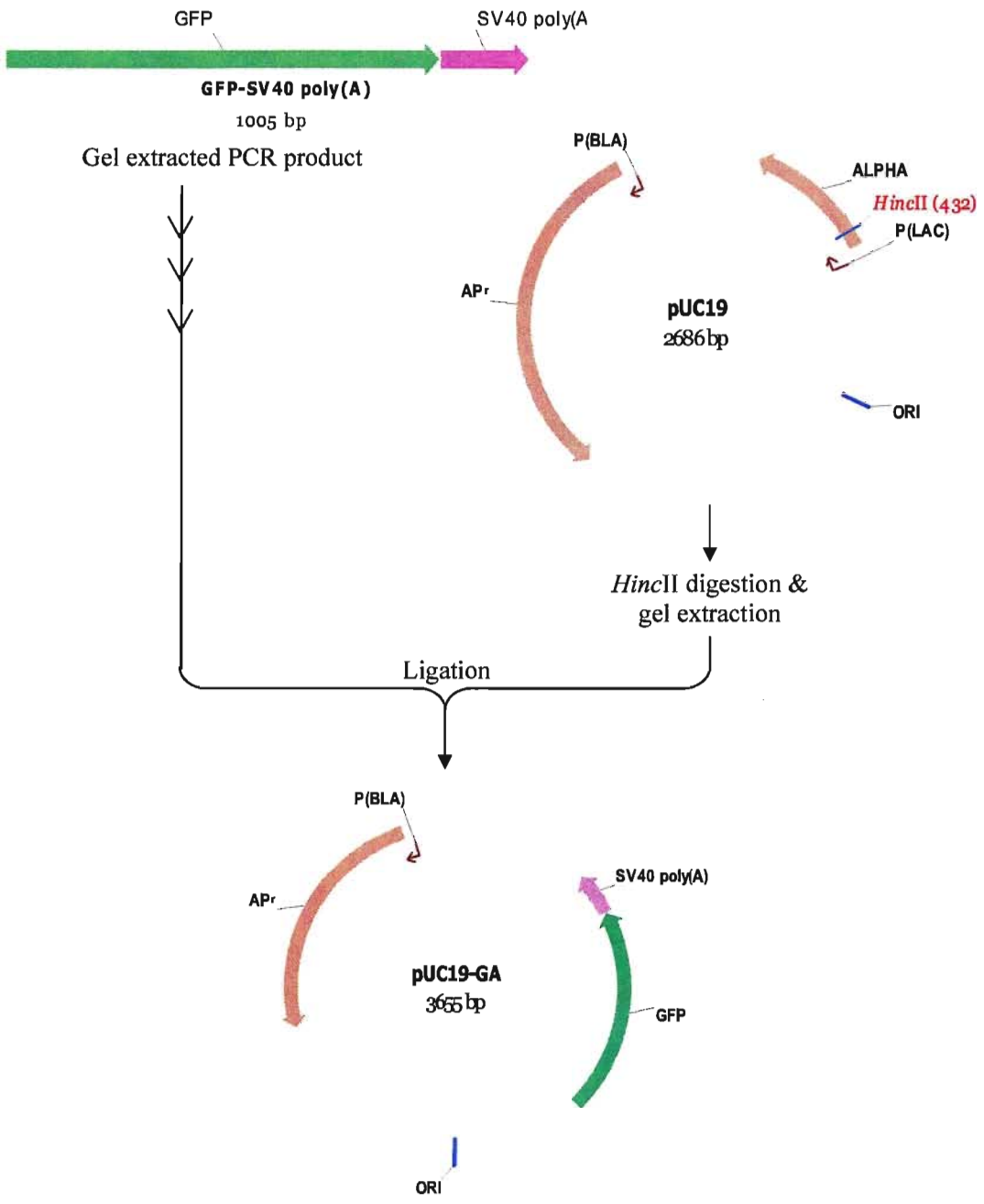

Figure A9: pUC19-GA construction strategy. The PCR product was extracted from the gel and cloned into the *Hinc*II site of pUC19.

Table A1: Restriction enzyme analysis of pUC19-GA.

Restriction enzyme	*Hind*III	*Apa*I	*Bam*HI	*Eco*O109I
Fragment size(s) (bp)	3655	3655	3449 206	2249 736 670

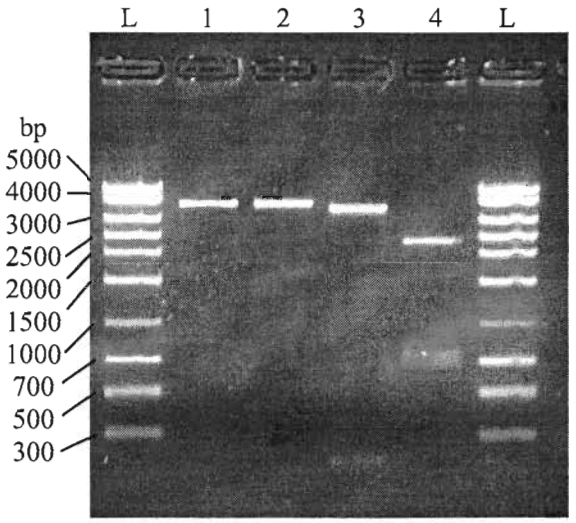

Figure A10: Restriction enzyme analysis of pUC19-GA. Lanes 1-4: plasmid DNA digested with *Hind*III, *Apa*I, *Bam*HI and *Eco*O109I, respectively. Lanes L: Norgen's MidRanger DNA ladder. The bp sizes of the ladder bands are shown on the left side.

3.2.1.2- Construction of pUC19-GA-ITRs-E1

The adenoviral backbone plasmid pFG173 (36731 bp) was digested with *Avr*II and *Mfe*I to obtain the ITRs-E1 fragment (4384 bp). The fragment was extracted from the gel and it has the two sticky ends of *Avr*II and *Mfe*I. On the other hand, pUC19GA was digested with *Eco*RI and *Xba*I to produce two fragments of 27 bp and 3628 bp. Gel extraction was used to obtain the large fragment of 3628 bp which has *Eco*RI and *Mfe*I sticky ends. *Mfe*I and *Eco*RI have complementary sticky ends and since the sticky ends of *Avr*II and *Xba*I can complement with each other, it was possible to clone the ITRs-E1 fragment into the pUC19-GA. The resulting plasmid was designated pUC19-GA-ITRs-E1. The construction strategy is seen in Figure A11 and the restriction enzyme digestion pattern and picture are shown in Table A2 and Figure A12, respectively.

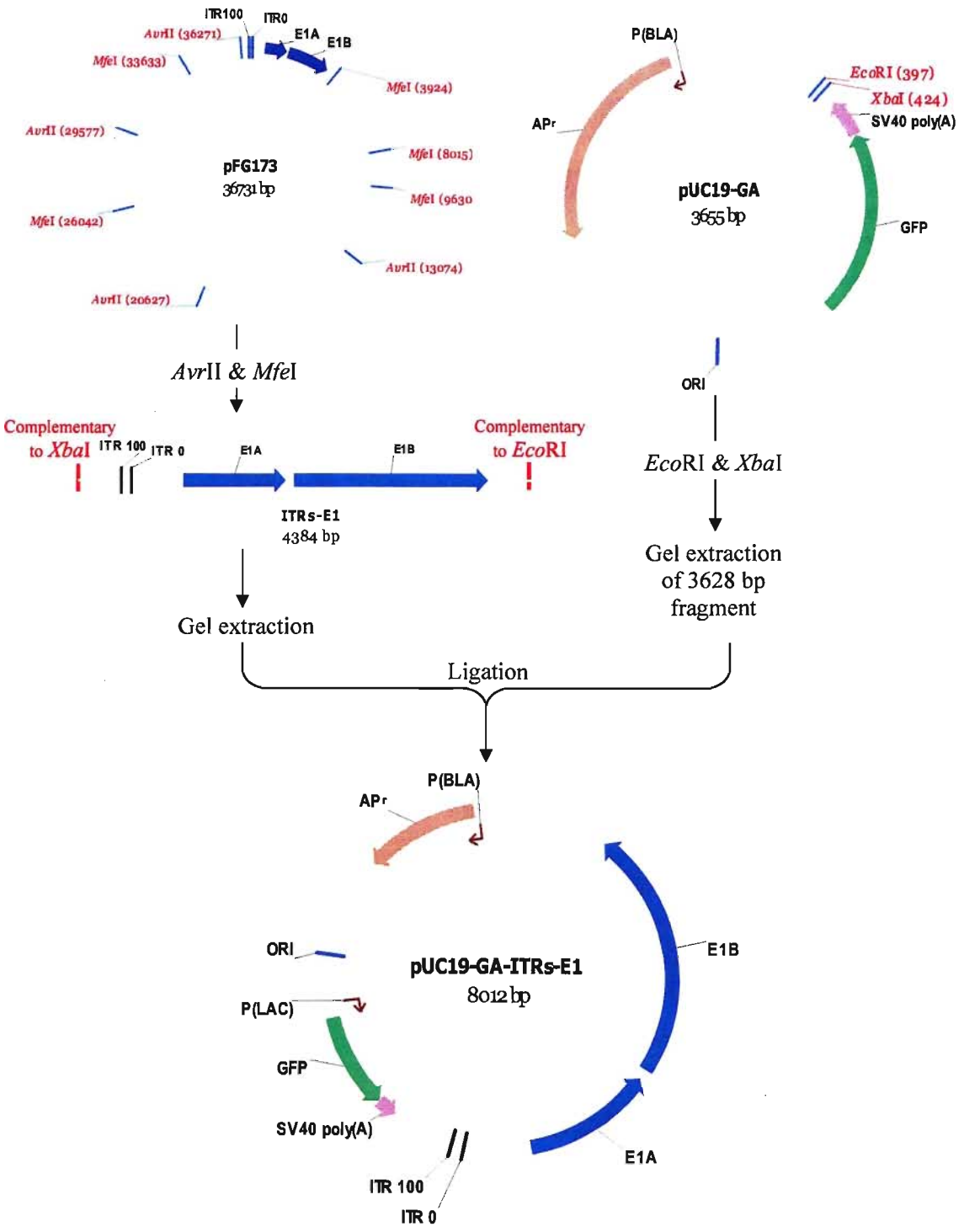

Figure A11: pUC19-GA-ITRs-E1 construction strategy.

Table A2: Restriction enzyme analysis of pUC19-GA-ITRs-E1.

Restriction enzyme	*Xba*I	*Sph*I	*Nco*I	*Pvu*II
Fragment size(s) (bp)	8012	5108 2904	3598 2951 1463	2364 1862 1530 1310 775 171

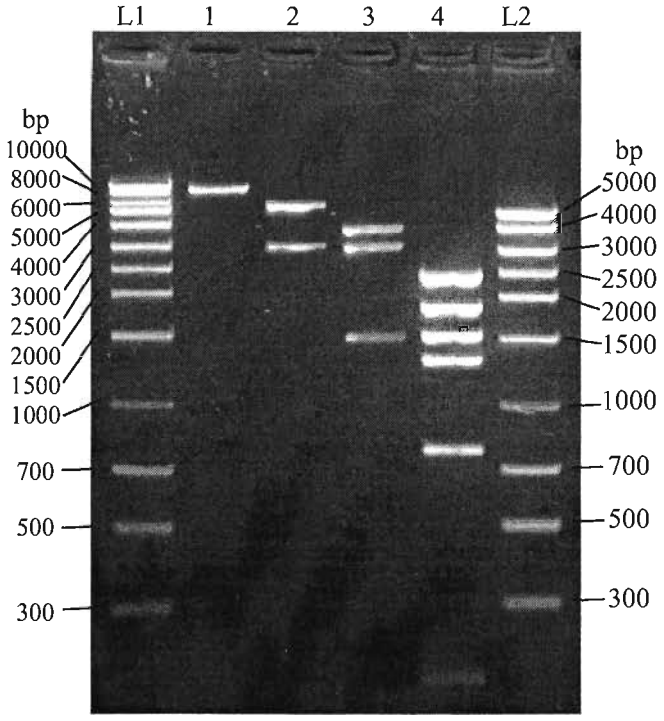

Figure A12: Restriction enzyme analysis of pUC19-GA-ITRs-E1. Lanes 1-4: plasmid DNA digested with *Xba*I, *Sph*I, *Nco*I and *Pvu*II, respectively. Lane L1: Norgen's HighRanger DNA ladder and lane L2: Norgen's MidRanger DNA ladder. The bp sizes of the ladder bands are shown on the side of the picture.

3.2.1.3- Construction of pUC19-GA-ITRs-E1-MCS

The cloning of the MLP-TPL fragment into the pUC19-GA-ITRs-E1 plasmid will require additional restriction enzyme sites. In this step, a multi-cloning site (MCS) containing all the necessary sites for the downstream cloning was designed to have a sticky complementary ends to *Eco*RI and *Age*I. This was created by the annealing of two synthesized oligonucleotides. pUC19-GA-ITRs-E1 was digested with *Sbf*I and *Age*I, yielding two fragments of 7970 bp and 42 bp in size. An agarose gel was run to separate the two fragments and the large fragment was extracted. The MCS is then ligated to the pUC19-GA-ITRs-E1 backbone since *Eco*RI and *Sbf*I have complementary sticky ends. The resulting plasmid was designated pUC19-GA-ITRs-E1-MCS. The construction strategy is shown in Figure A13. Table A3 contains the restriction enzyme digestion pattern and Figure A14 shows the digestion picture.

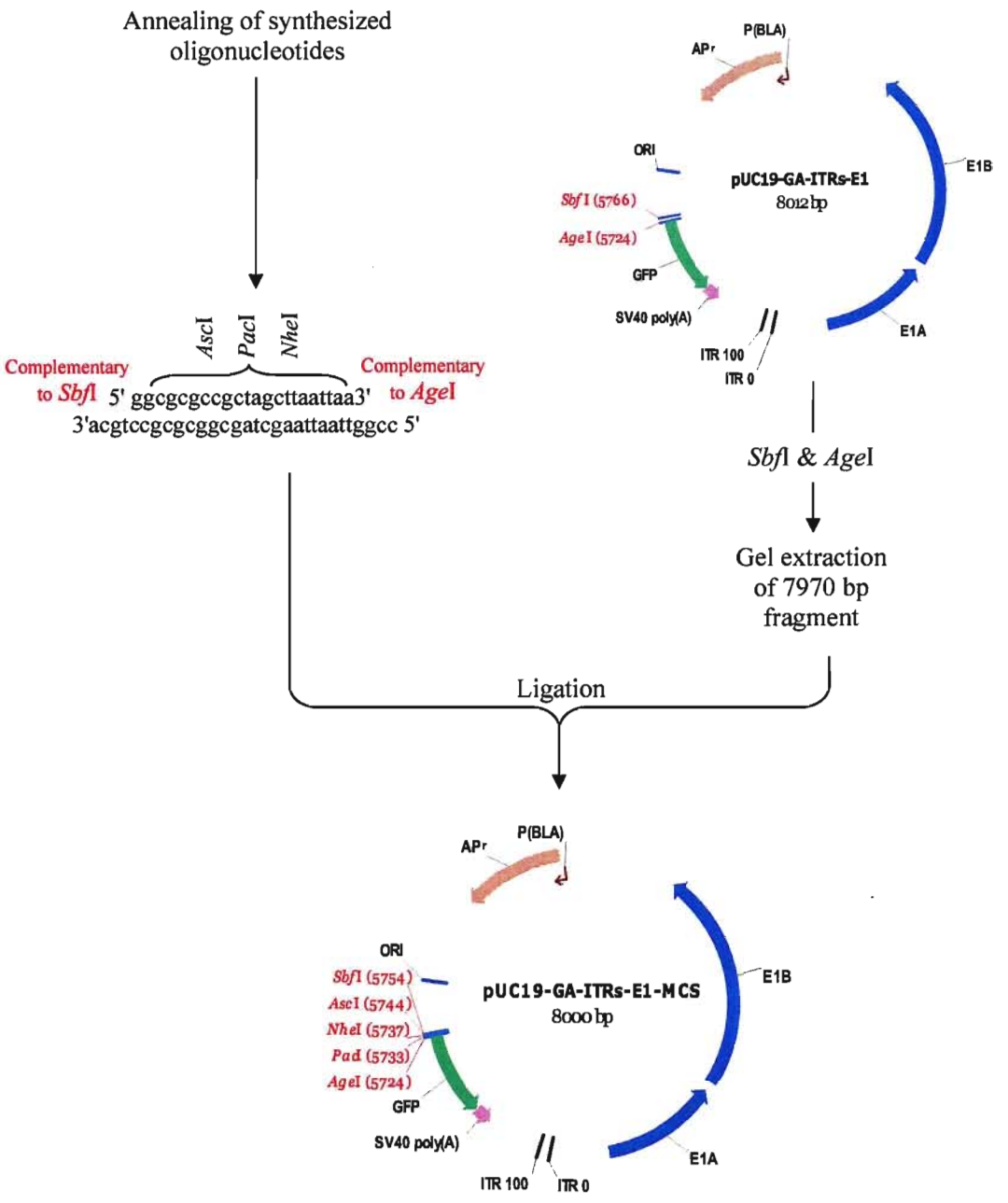

Figure A13: pUC19-GA-ITRs-E1-MCS construction strategy.

Table A3: Restriction enzyme analysis of pUC19-GA-ITRs-E1-MCS.

Restriction enzyme	*Nhe*I	*Hind*III	*Pvu*II
Fragment size(s) (bp)	8012	4245 3755	2364 1862 1530 1310 763 171

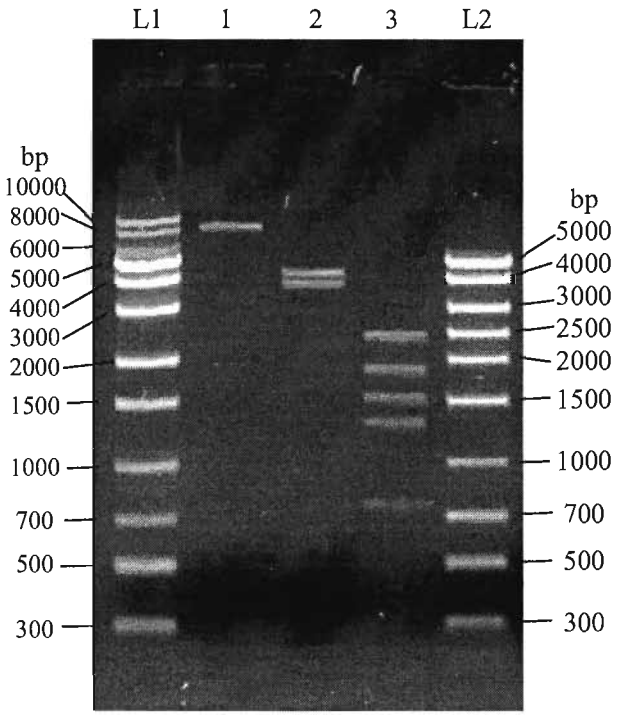

Figure A14: Restriction enzyme analysis of pUC19-GA-ITRs-E1-MCS. Lanes 1-3: plasmid DNA digested with *Nhe*I, *Hind*III and *Pvu*II, respectively. Lane L1: Norgen's HighRanger-2500 DNA ladder and lane L2: Norgen's MidRanger DNA ladder. The bp sizes of each ladder band are shown on the sides of the picture.

3.2.1.4- Construction of MLP-TPL fragment

The MLP sequence was obtained from the work done by Parks & Shenk (1997). The sequence was aligned to the adenovirus 5 genome obtained from the National Center for Biotechnology Information (NCBI) genome browser (http://www.ncbi.nlm.nih.gov/sites/entrez?Db=genome&Cmd=ShowDetailView&TermToSearch=2000008). Alignment of the adenovirus 5 genome to the TPL exon sequences obtained by Zhang *et al.* (1989) was used to determine the exact TPL sequence.

The MLP-TPL fragment (493 bp) was then built up by gene construction procedures. The fragment contains the MLP and TPL in addition to restriction enzyme linkers for downstream cloning. The reverse and forward strands were divided into oligonucleotides of 47 bases in length, except for the terminal 5' oligonucleotides that have a size of 23 bases and can be used as primers in PCR amplification of the whole fragment. Oligonucleotides were designed so that they will have a 23 bp and 24 bp overlap with the complementary oligonucleotides with a single strand break in between (Table A4).

First, the 22 oligonucleotides were phosphorylated using T4 polynucleotide kinase, which adds a phosphate group to the hydroxyl of the 5' end. Next, the phosphorylated oligonucleotides were annealed together to form the primary non-ligated MLP-TPL fragment containing single strand breaks between the adjacent oligonucleotides. *Taq* DNA ligase was then used to ligate the neighbouring oligonucleotides followed by PCR amplification of the whole fragment using *Pfu* DNA polymerase and the terminal primers MT-F1 and MT-R1. The construction strategy and the gel picture of the amplified

constructed fragment are shown in Figures A15 and A16, respectively. The fragment was gene cleaned and cloned into the *Hinc*II site of pUC19 to construct pUC19-MLP-TPL.

Table A4: Nucleotide Sequences of oligonucleotides used in MLP-TPL DNA fragment construction.

Name	Nucleotide sequence
Forward oligonucleotides:	
MT-F1	5'ATAAGAGCCAAGTTCCAGCGTCC3'
MT-F2	5'TGCAGGGCCCACTCTGAGACAAAGGCTCGCGTCCAGGCCAGCACGAA3'
MT-F3	5'GGAGGCTAAGTGGGAGGGGTAGCGGTCGTTGTCCACTAGGGGGTCCA3'
MT-F4	5'CTCGCTCCAGGGTGTGAAGACACATGTCGCCCTCTTCGGCATCAAGG3'
MT-F5	5'AAGGTGATTGGTTTGTAGGTGTAGGCCACGTGACCGGGTGTTCCTGA3'
MT-F6	5'AGGGGGGCTATAAAAGGGGGTGGGGGCGCGTTCGTCCTCACTCTCTT3'
MT-F7	5'CCGCATCGCTGTCTGCGAGGGCCAGCTGTTGGGCTCGCGGTTGAGGA3'
MT-F8	5'CAAACTCTTCGCGGTCTTTCCAGTACTCTTGGATCGGAAACCCGTCG3'
MT-F9	5'GCCTCCGAACGGTACTCCGCCGCCGAGGGACCTGAGCGAGTCCGCAT3'
MT-F10	5'CGACCGGATCGGAAAACCTCTCGAGAAAGGCGTCTAACCAGTCACAG3'
MT-F11	5'TCGCACTAGTGAATTCGGGCCCACCGGTATCGCAAGCCACAGGTATT3'
Reverse oligonucleotides:	
MT-R1	5'AATACCTGTGGCTTGCGATACCG3'
MT-R2	5'GTGGGCCCGAATTCACTAGTGCGACTGTGACTGGTTAGACGCCTTTC3'
MT-R3	5'TCGAGAGGTTTTCCGATCCGGTCGATGCGGACTCGCTCAGGTCCCTC3'
MT-R4	5'GGCGGCGGAGTACCGTTCGGAGGCCGACGGGTTTCCGATCCAAGAGT3'
MT-R5	5'ACTGGAAAGACCGCGAAGAGTTTGTCCTCAACCGCGAGCCCAACAGC3'
MT-R6	5'TGGCCCTCGCAGACAGCGATGCGGAAGAGAGTGAGGACGAACGCGCC3'
MT-R7	5'CCCACCCCCTTTTATAGCCCCCCTTCAGGAACACCCGGTCACGTGGC3'
MT-R8	5'CTACACCTACAAACCAATCACCTTCCTTGATGCCGAAGAGGGCGACA3'
MT-R9	5'TGTGTCTTCACACCCTGGAGCGAGTGGACCCCCTAGTGGACAACGAC3'
MT-R10	5'CGCTACCCCTCCCACTTAGCCTCCTTCGTGCTGGCCTGGACGCGAGC3'
MT-R11	5'CTTTGTCTCAGAGTGGGCCCTGCAGGACGCTGGAACTTGGCTCTTAT3'

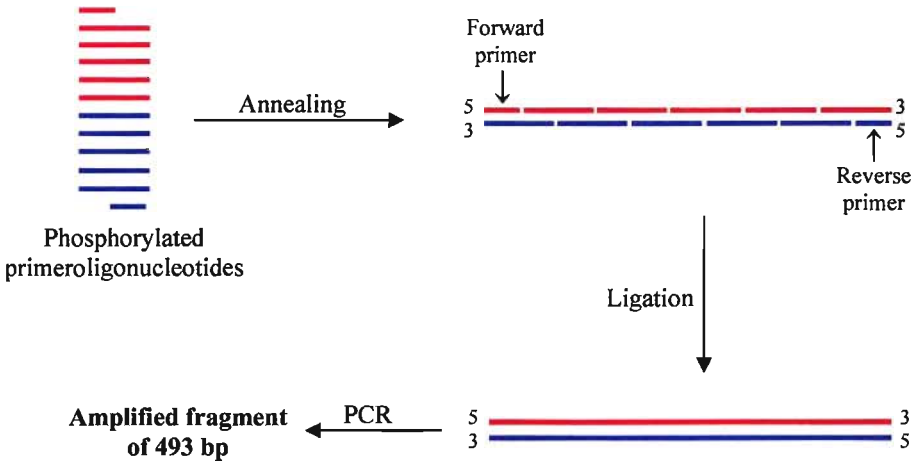

Figure A15: Strategy of MLP-TPL DNA fragment construction.

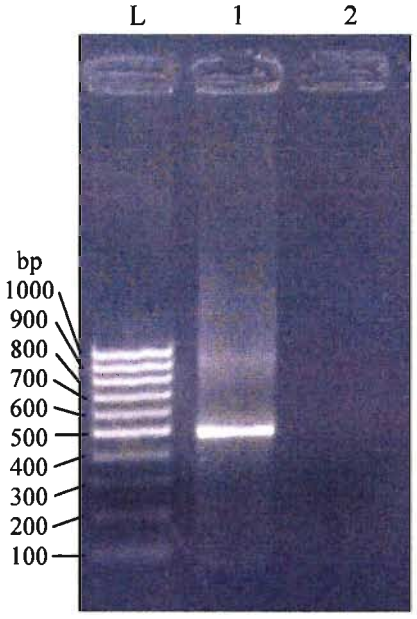

Figure A16: PCR amplification of MLP-TPL fragment after annealing and ligation of the different oligonucleotides. Lane 1 shows the amplification product of 493 bp, lane 2 is the negative control and lane L is Norgen's PCRSizer DNA ladder with its band sizes on the left side of the picture.

3.2.1.5- Cloning of MLP-TPL into pUC19-GA-ITRs-E1-MCS

This is the final step in the construction of the pE1 plasmid. In this step, the 494 bp fragment containing MLP-TPL was obtained from pUC19-MLP-TPL by *Xba*I and *Age*I digestion and subsequently extracted from an agarose gel. The fragment was then ligated to the *Nhe*I and *Age*I-digested pUC19-GA-ITRs-E1-MCS, since *Xba*I and *Nhe*I have complementary sticky ends. The resulting plasmid was named pE1 (8481 bp) and it contains the complete expression cassette (MLP-TPL-GFP-SV40 poly(A)) in addition to the adenoviral ITRs and E1 region. The strategy of this step is shown in Figure A17 and the restriction enzyme digestion pattern is listed in Table A5 with the agarose gel picture visualized in Figure A18.

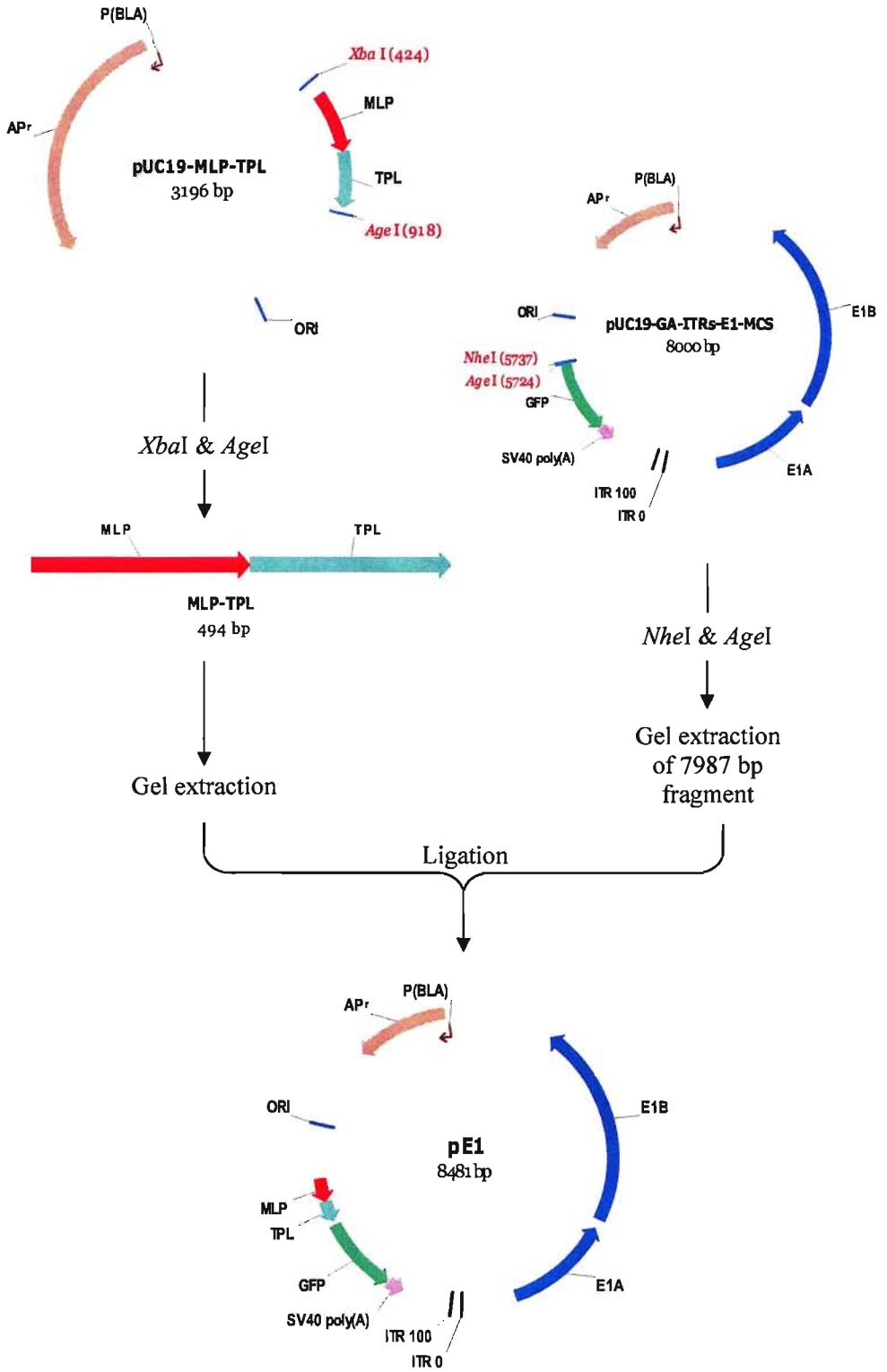

Figure A17: pE1 construction strategy.

Table A5: Restriction enzyme analysis of pE1.

Restriction enzyme	*Eco*RI	*Sca*I	*Hind*III	*Hinc*II	*Pvu*II
Fragment size(s) (bp)	8481	6374 2107	4726 3755	4049 2334 2037 61	2364 1862 1530 1310 732 512 171

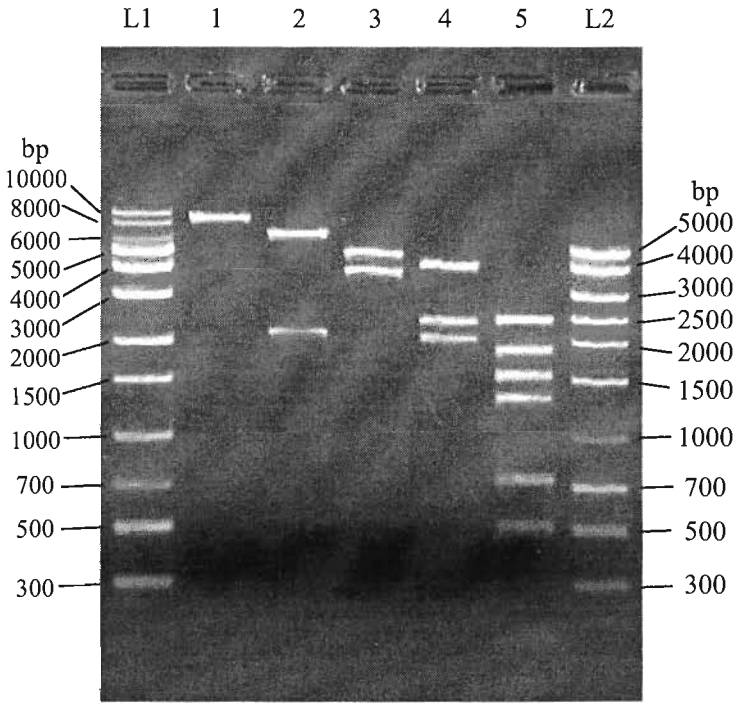

Figure A18: Restriction enzyme analysis of pE1. Lanes 1-5: plasmid DNA digested with *Eco*RI, *Sca*I, *Hind*III, *Hinc*II and *Pvu*II, respectively. Lanes L1 is Norgen's HighRanger-2500 DNA ladder and L2 is Norgen's MidRanger DNA ladder. The bp size of each ladder band is shown on the sides of the picture.

C- Construction of plasmids with incomplete and complete TPL exons

The effect of the complete and incomplete TPL on mRNA transport and stability was investigated using four different plasmids. pE1 was the backbone plasmid in the construction of all the four plasmids which share the same promoter and reporter gene (GFP) in addition to SV40 poly(A). The four plasmids contain either: no TPL exons (pMGA), TPL exon 1 (pMT_1GA), TPL exons 1,2 ($pMT_{1,2}GA$) or the entire TPL (pMTGA). The overall construction strategy is shown in Figure A19.

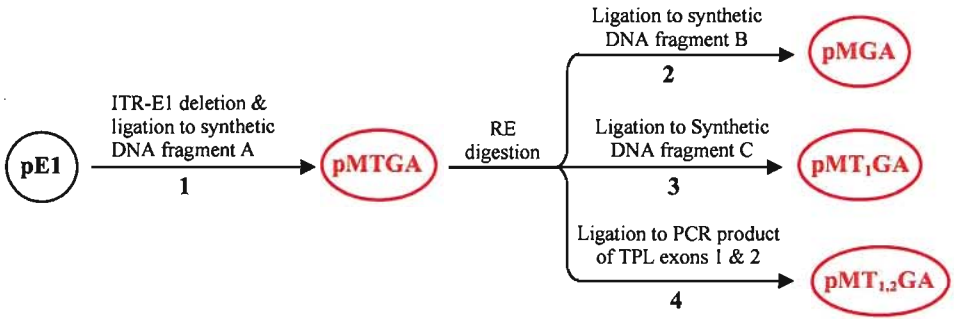

Figure A19: Overall construction strategy of the complete and incomplete TPL exons plasmids. Numbers show the flow of the construction steps. RE: Restriction endonuclease.

3.2.3.1.1- Construction of pMTGA

pMTGA contains the complete TPL sequence and it was constructed from pE1 by the deletion of the ITRs-E1 fragment. First, pE1 was digested with *Nde*I and *Mfe*I to split the plasmid into two fragments of 4652 bp and 3829 bp in size. The smaller fragment contains the MLP, the complete TPL, GFP, SV40 poly(A), the ampicillin resistant gene and the origin of bacterial replication. An agarose gel was used to separate the two fragments and the smaller one was extracted from the gel. Two synthesized oligonucleotides were annealed to produce a short DNA fragment (synthetic DNA fragment A) with *Nde*I and *Mfe*I sticky ends, and then ligated to the extracted DNA fragment. The obtained plasmid was designated pMTGA (3716 bp) and was used to construct the other three plasmids by deleting a part from the MLP and the entire TPL. Different DNA fragments, either oligonucleotides or PCR amplification products, were used to complement the MLP and introduce the desired TPL exons. The construction strategy of pMTGA is shown in Figure A20. Sequences of the two oligonucleotides that forms the DNA fragment A and the restriction enzyme digestion pattern are contained in Tables A6 and A7, respectively. The agarose gel picture is displayed in Figure A21.

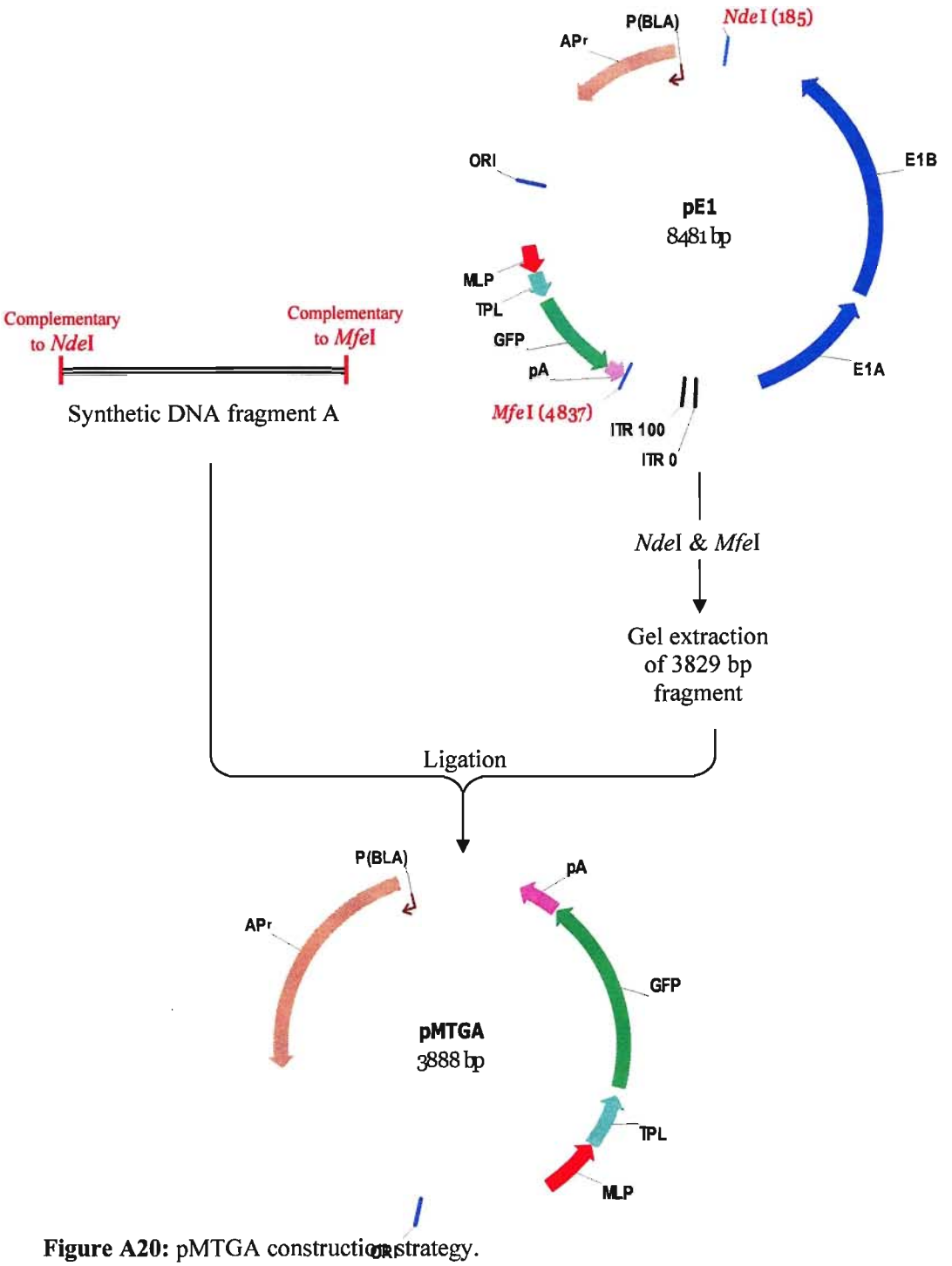

Figure A20: pMTGA construction strategy.

Table A6: Sequences of the oligonucleotides forming the synthetic DNA fragment A.

Sticky end	Sequences	Sticky end
*Nde*I	5' tatcgaattctagcatcgatcattactagtcattggcgcgccacgaatttaaatcttac 3' 3' agcttaagatcgtagctagtaatgatcagtaaccgcgcggtgcttaaatttagaatgttaa 5'	*Mfe*I

Table A7: Restriction enzyme analysis of pMTGA.

Restriction enzyme	*Eco*RI	*Nco*I & *Hind*III	*Pvu*II
Fragment size(s) (bp)	2935 953	3358 530	2644 732 512

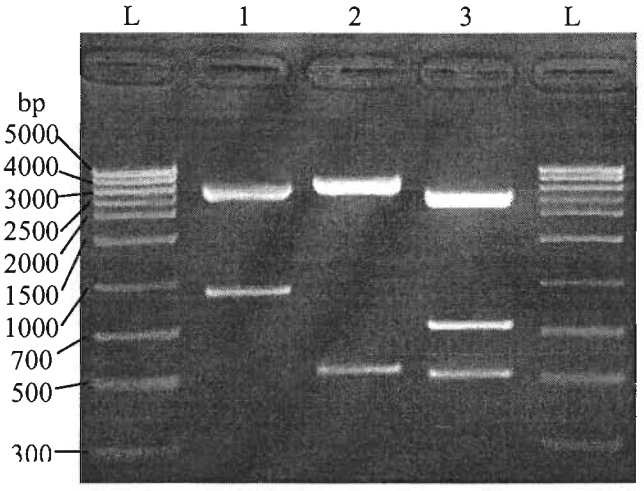

Figure A21: Restriction enzyme analysis of pMTGA. Lanes 1-3: plasmid DNA digested with *Eco*RI, double digestion with *Nco*I & *Hind*III and *Pvu*II, respectively. Lanes L are Norgen's MidRanger DNA ladder. The bp size of each ladder band is shown on the left side of the picture.

3.2.3.1.2- Construction of pMGA and pMT_1GA

pMTGA was used to construct the TPL-free plasmid as well as a plasmid with only the first TPL exon. First, pMTGA was digested with *PmlI* (blunt end) and *Age*I to erase a 280 bp fragment containing the entire TPL with some of the MLP. The rest of the plasmid (3608 bp) was then cleaned by gel extraction and used to construct pMGA and pMT_1GA plasmids by cloning synthetic DNA fragments obtained by annealing two oligonucleotides having both the *PmlI* and *Age*I complementary ends. DNA fragment B contains part of the MLP however fragment C contains part of the MLP plus the first TPL exon. The ligation of fragments B to the 3608 bp fragment resulted in the plasmid designated pMGA (Figure A22) and pMT_1GA resulted from fragment C being ligated to the 3608 bp fragment (Figure A24). Sequences of the oligonucleotides that form DNA fragments B and C are listed in Tables A8 and A10, respectively. The pMGA restriction enzyme digestion patterns and agarose gel picture are shown in is shown in Table A9 and Figure A23, respectively. The digestion pattern of pMT_1GA and its agarose gel picture are shown in Table A11 and Figure A25, respectively.

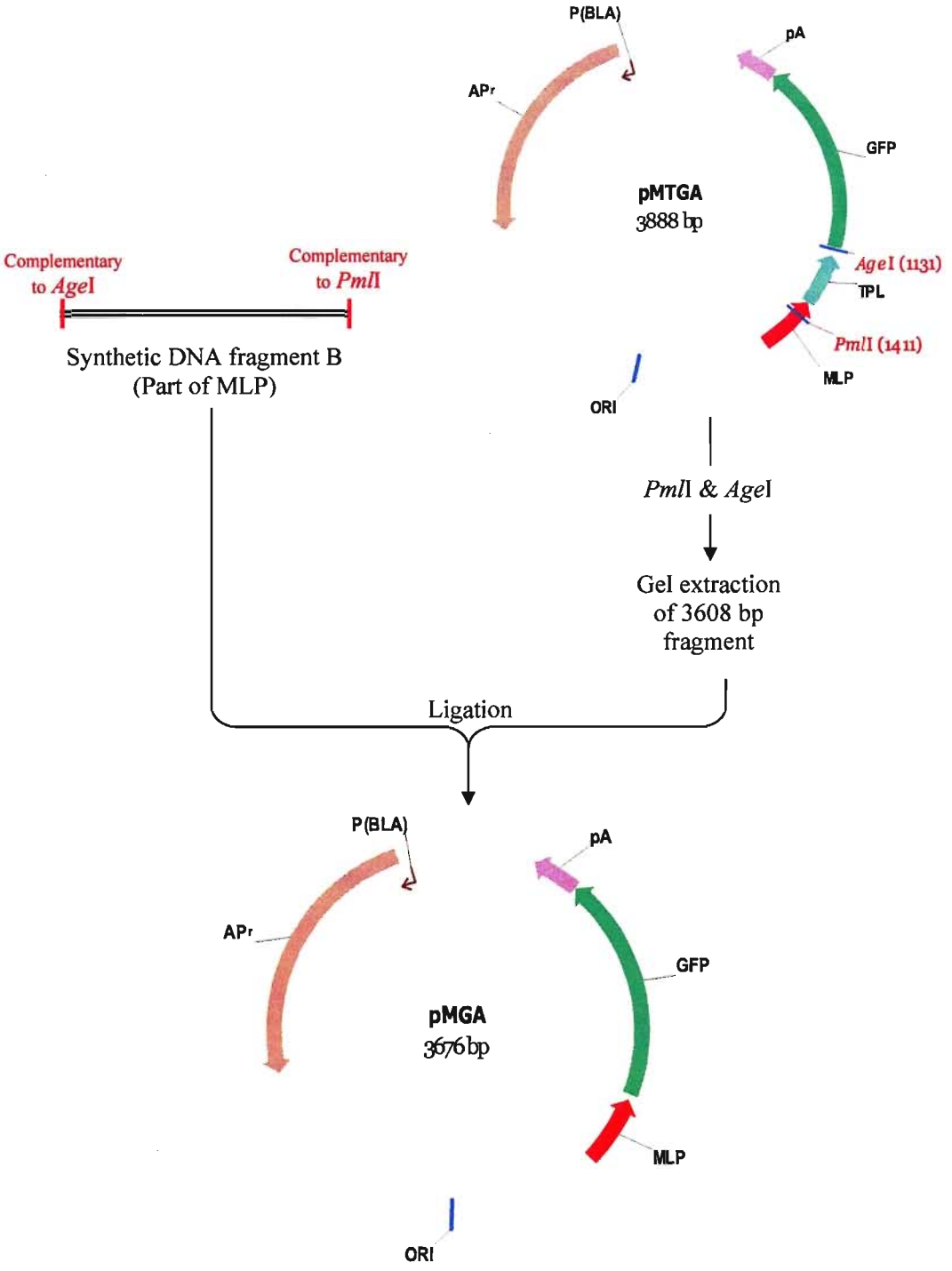

Figure A22: pMGA construction strategy.

Table A8: Sequences of the oligonucleotides forming the synthetic DNA fragment B.

Sticky end	Sequences	Blunt end
*Age*I	5' ccggatctagagaggacgaacgcgcccccaccccctttatagccccccttcaggaacacccggtcac 3' 3' tagatctctcctgcttgcgcgggggtgggggaaaatatcgggggggaagtccttgtgggccagtg 5'	*Pml*I

Table A9: Restriction enzyme analysis of pMGA.

Restriction enzyme	*Eco*RI	*Nco*I & *Hind*III	*Pvu*II
Fragment size(s) (bp)	3676	3358 318	2644 1023

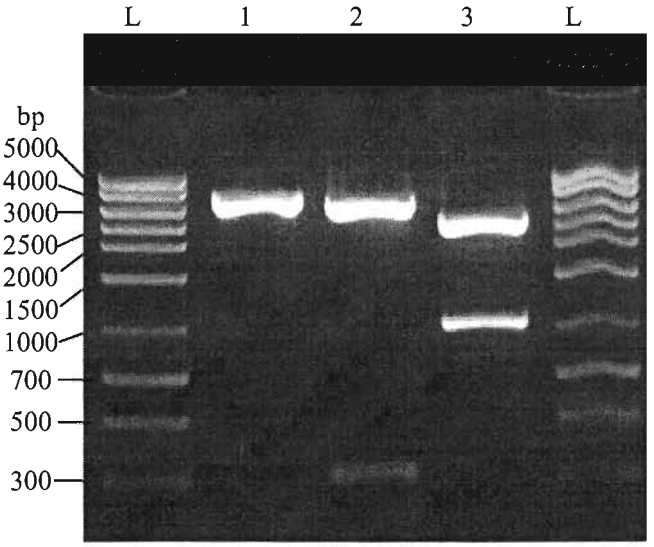

Figure A23: Restriction enzyme analysis of pMGA. Lanes 1-3: plasmid DNA digested with *Eco*RI, double digestion with *Nco*I & *Hind*III and *Pvu*II, respectively. Lanes L are Norgen's MidRanger DNA ladder. The bp size of each ladder band is shown on the left side of the picture.

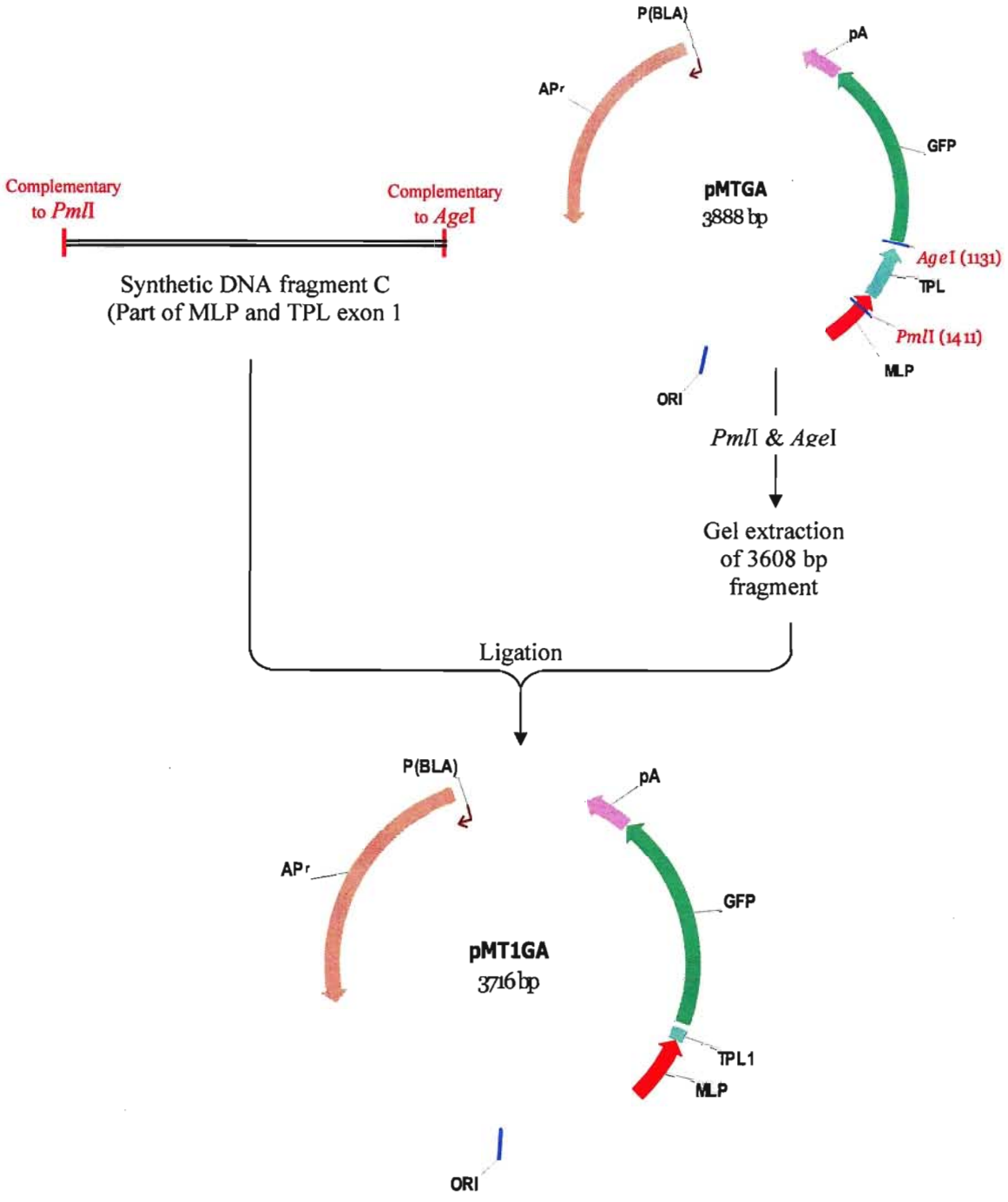

Figure A24: pMT$_1$GA construction strategy.

Table A10: Sequences of the oligonucleotides forming the synthetic DNA fragment C.

Sticky end	Sequences	Blunt end
*Age*I	5' ccggatctagaccaacagctggccctcgcagacagcgatgcggaagagagtgaggacgaacgcg ccccacccccttttatagccccccttcaggaacacccggtcac 3' 3' tagatctggttgtcgaccgggagcgtctgtcgctacgccttctctcactcctgcttgcgcgggggtggg ggaaaatatcgggggggaagtccttgtgggccagtg 5'	*Pml*I

Table A11: Restriction enzyme analysis of pMT_1GA.

Restriction enzyme	*Eco*RI	*Nco*I & *Hind*III	*Pvu*II
Fragment size(s) (bp)	3716	3358 358	2644 560 512

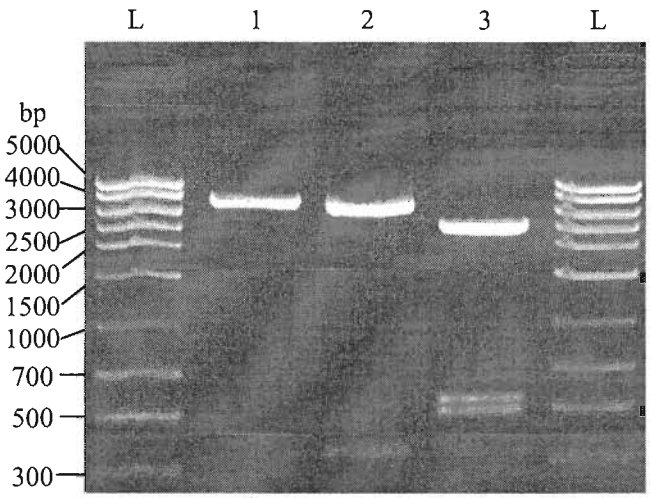

Figure A25: Restriction enzyme analysis of pMT_1GA. Lanes 1-3: plasmid DNA digested with *Eco*RI, double digestion with *Nco*I & *Hind*III and *Pvu*II, respectively. Lanes L are Norgen's MidRanger DNA ladder. The bp size of each ladder band is shown on the left side of the picture.

3.2.3.1.3- Construction of $pMT_{1,2}GA$

We performed PCR amplification using specific primers and pMTGA as a template to obtain the DNA fragment that contains part of MLP and the first two exons of the TPL. The two primers were named TPL1,2-F and TPL1,2-R; the later contains extra nucleotides to introduce the *Nco*I restriction enzyme site into the PCR product. *Pfu* DNA polymerase was used to amplify the fragment because it produces a blunt ended product. After that, the PCR product was cleaned and digested with *Nco*I and the DNA was cleaned again. The digested PCR product was then ligated to a 3597 bp fragment obtained from *Pml*I and *Nco*I-digested pMTGA and extracted from an agarose gel. The resulting plasmid was sequenced to verify the accuracy of its nucleotide sequence and was designated $pMT_{1,2}GA$. The construction strategy of this plasmid is displayed in Figure A26 and the restriction enzyme digestion pattern is shown in Table A12 with the agarose gel picture in Figure A27.

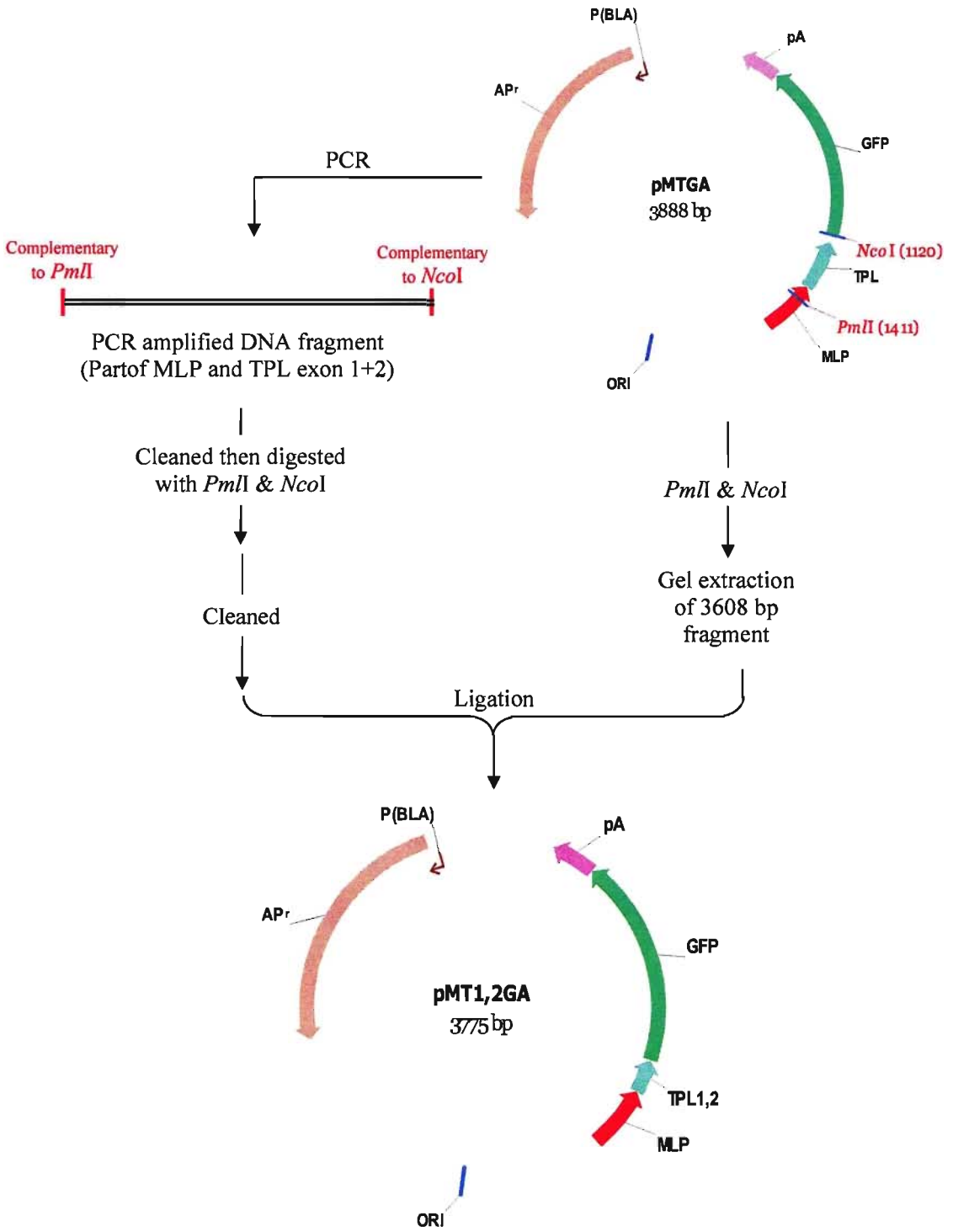

Figure A26: $pMT_{1,2}GA$ construction strategy.

Table A12: Restriction enzyme analysis of pMT_1GA.

Restriction enzyme	*Eco*RI	*Nco*I & *Hind*III	*Pvu*II
Fragment size(s) (bp)	3775	3358 417	2644 619 512

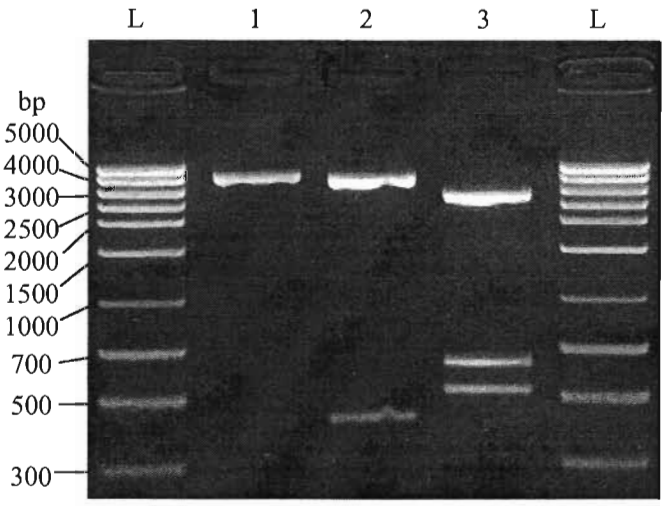

Figure A27: Restriction enzyme analysis of $pMT_{1,2}GA$. Lanes 1-3: plasmid DNA digested with *Eco*RI, double digestion with *Nco*I & *Hind*III and *Pvu*II, respectively. Lanes L are Norgen's MidRanger DNA ladder. The bp size of each ladder band is shown on the left side of the picture.

D- Construction of pE2

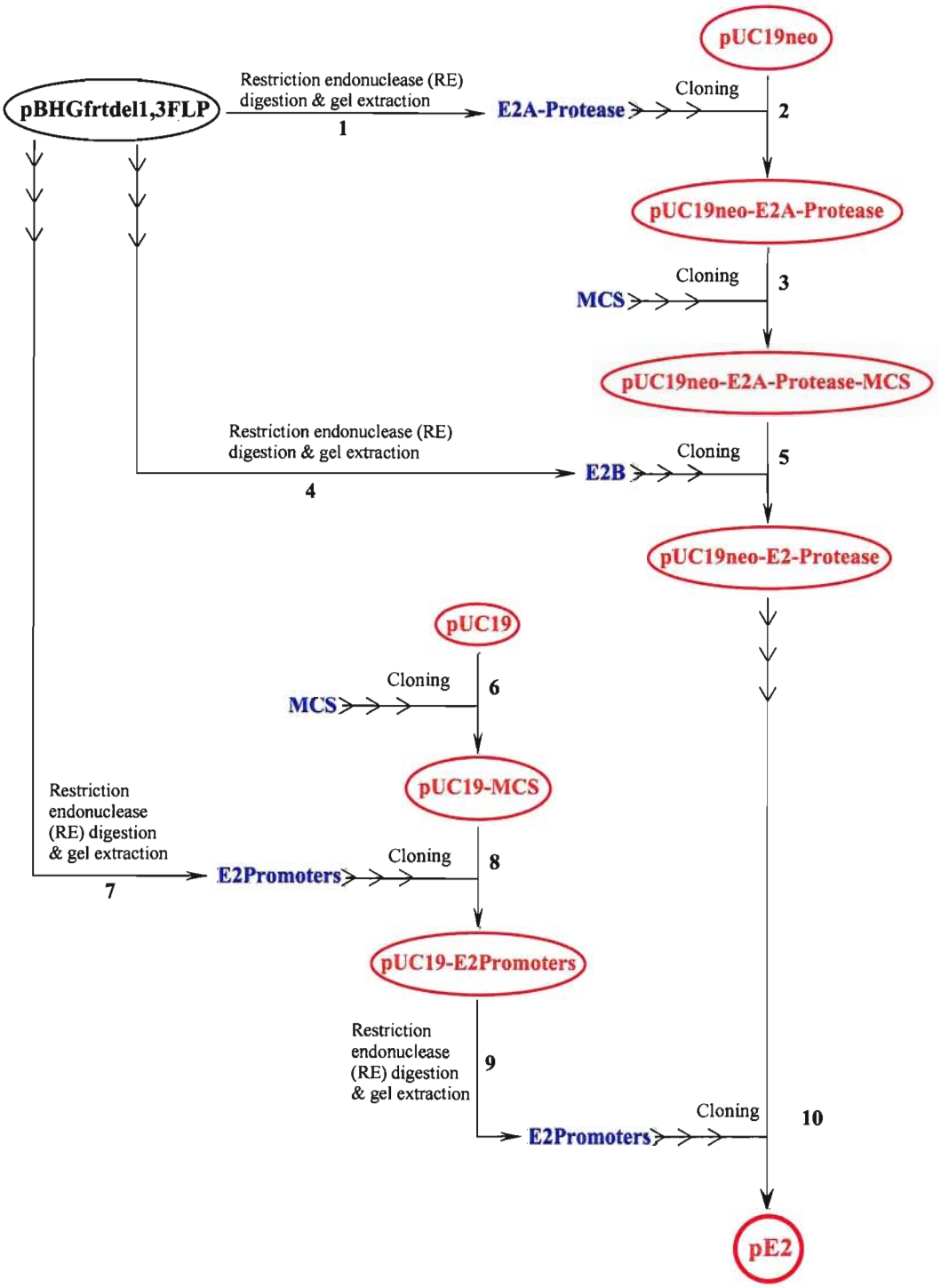

Figure A28: Overall construction strategy of pE2 plasmid. Numbers shows the flow of the construction steps.

3.3.1.1- Cloning of E2A and viral protease into pUC19neo

The backbone plasmid of this construction step is pUC19neo which contains the neomycin resistant cassette cloned in pUC19. The neomycin cassette provides resistance to neomycin and its chemical synthetic form, G418, in mammalian cells. First, E2A and viral protease are obtained from pBHGfrtdel1,3FLP by *Sac*I digestion. The subsequent gel extraction of the 4581 bp fragment took place which contains both E2A and the viral protease. This fragment was then cloned into pUC19neo previously digested with the same enzyme. The resulted plasmid was designated pUC19neo-E2A-protease. The construction strategy is outlined in Figure A29 and the restriction enzyme digestion pattern and picture are shown in Table A13 and Figure A30, respectively.

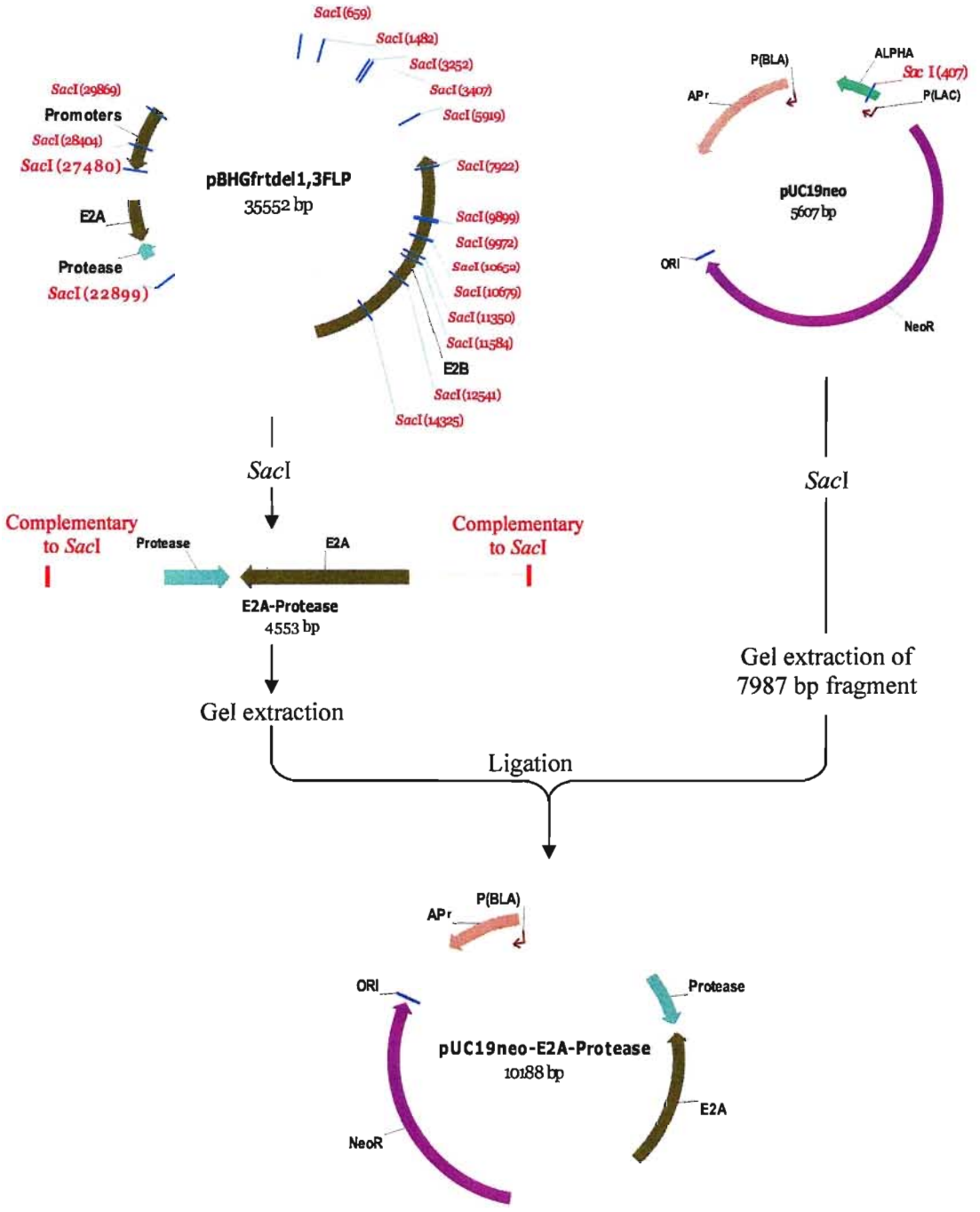

Figure A29: pUC19neo-E2A-Protease construction strategy.

Table A13: Restriction enzyme analysis of pUC19neo-E2A-Protease.

Restriction enzyme	*Eco*RI	*Sca*I	*Drd*I	*Eco*O109I
Fragment size(s) (bp)	10188	5607 4581	4721 1942 1869 951 705	5426 1868 1444 771 561 118

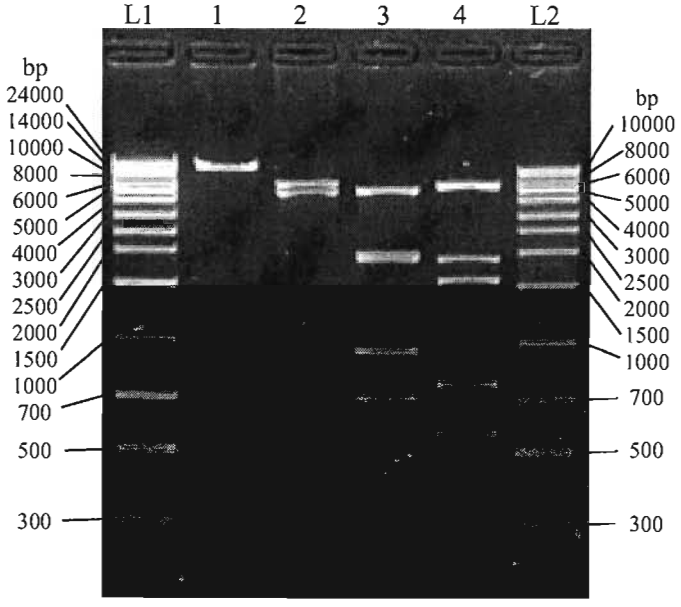

Figure A30: Restriction enzyme analysis of pUC19neo-E2A-Protease. Lanes 1-4: plasmid DNA digested with *Eco*RI, *Sac*I, *Drd*I and *Eco*O109I, respectively. Lane L1: Norgen's UltraRanger DNA ladder and lane L2: Norgen's HighRanger DNA ladder. The bp size of each ladder band is shown on the picture.

3.3.1.2- Cloning of MCS into pUC19neo-E2A-Protease

The downstream cloning of E2B required restriction enzymes that are not present in pUC19neo-E2-Protease. Hence, we cloned an MCS in between the *Nde*I site and *Eco*RI site of the plasmid. The inserted MCS was designed so that the original *Nde*I and *Eco*RI sites of the plasmid were removed and replaced with a new *Eco*RI site inside the MCS to control the orientation during the subsequent E2B cloning. Another four enzymes were incorporated in the MCS including *Cla*I, *Spe*I, *Asc*I and *Swa*I. The MCS was synthesized as two DNA oligonucleotides and was then annealed together. The annealed MSC contained complementary ends, just in the overhanging nucleotides but not in the entire sequence, to *Nde*I and *Eco*RI. The MCS was then ligated to pUC19neo-E2A-Protease previously digested with *Nde*I and *Eco*RI and extracted from an agarose gel. The resulting plasmid was designated pUC19neo-E2A-Protease-MCS. The construction strategy and the gel picture of the digested plasmid are shown in Figures A31 and A32, respectively. The restriction enzyme digestion pattern is listed in Table A14.

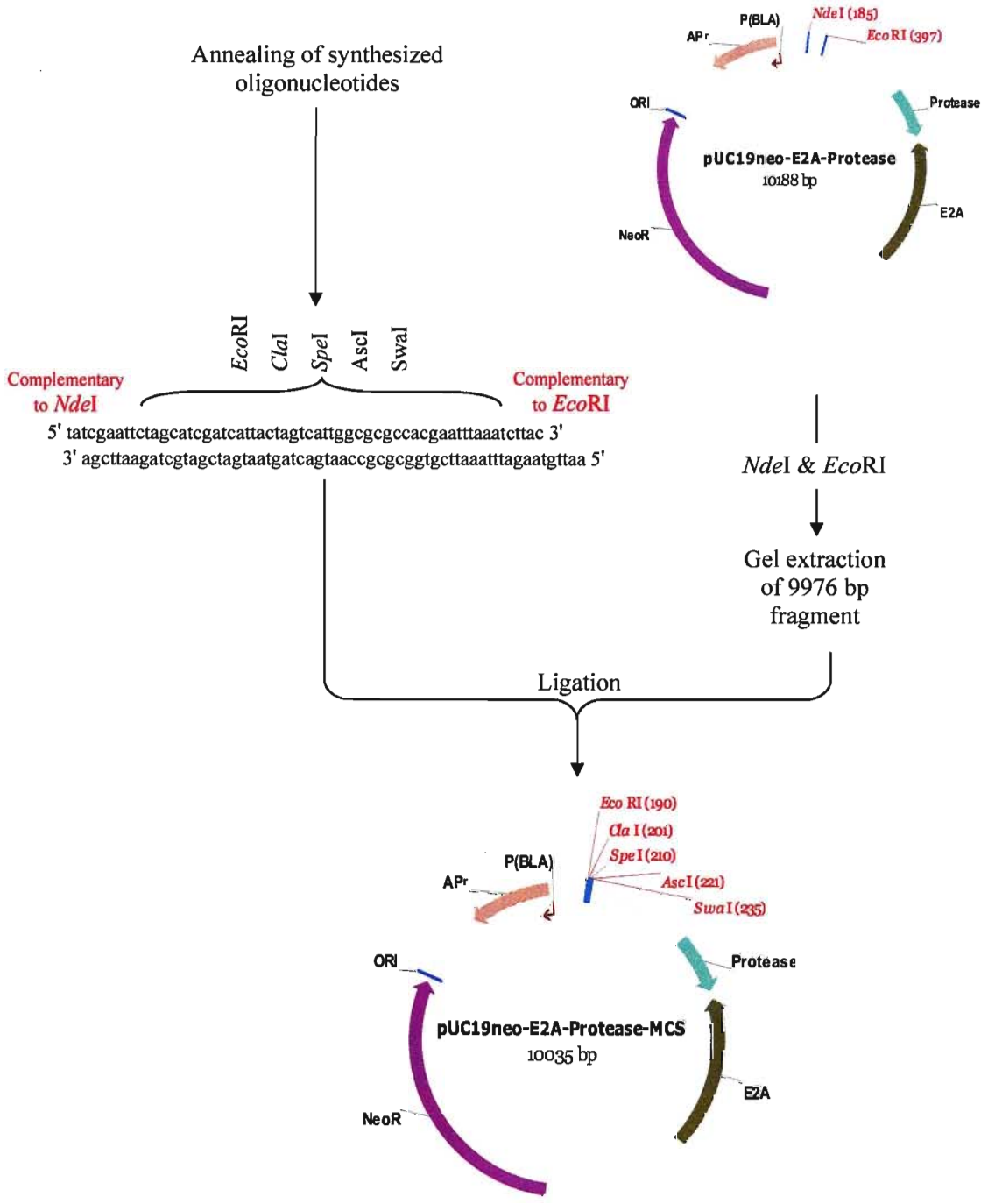

Figure A31: pUC19neo-E2A-Protease-MCS construction strategy.

Table A14: Restriction enzyme analysis of pUC19neo-E2A-Protease-MCS.

Restriction enzyme	*Eco*RI	*Asc*I	*Sac*I	*Drd*I
Fragment size(s) (bp)	10035	10035	5454 4581	4721 1942 1869 951 552

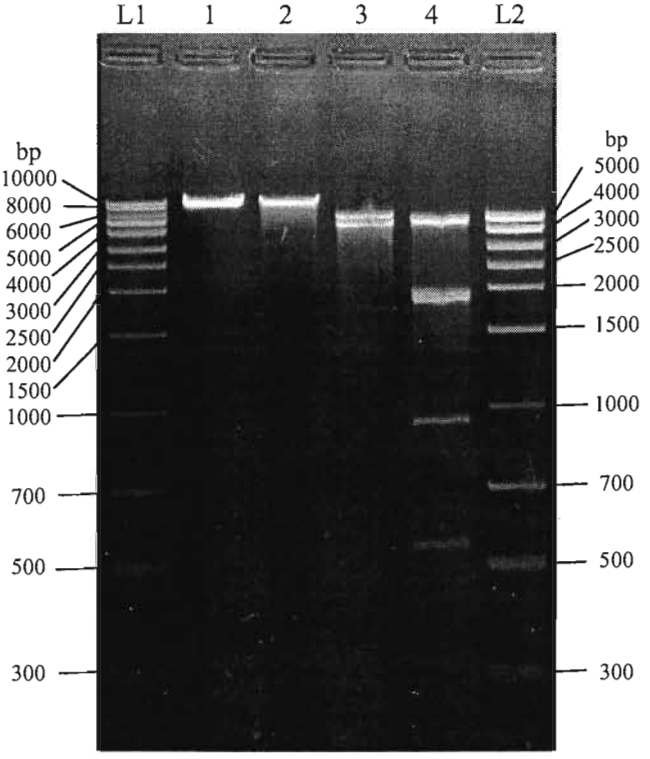

Figure A32: Restriction enzyme analysis of pUC19neo-E2A-Protease-MCS. Lanes 1-4: plasmid DNA digested with *Eco*RI, *Asc*I, *Sac*I and *Drd*I, respectively. Lane L1: Norgen's HighRanger DNA ladder and lane L2: Norgen's UltraRanger DNA ladder. The bp size of each ladder band is shown on the picture.

3.3.1.3- Construction of pUC19neo-E2-Protease

The MCS of the pUC19neo-E2A-Protease-MCS plasmid was used to clone the E2B. The plasmid was digested with *Eco*RI and *Asc*I, and then the 10004 bp fragment was extracted from an agarose gel. Meanwhile, the adenoviral E2B was obtained from the pBHGfrtdel1,3FLP plasmid by *Eco*RI and *Asc*I digestion. The 12154 bp fragment that contains E2B was extracted from an agarose gel and cloned into the pre-digested pUC19neo-E2A-Protease-MCS to create a plasmid that contains the entire viral E2 region and named pUC19neo-E2-Protease. The construction strategy of this plasmid is illustrated is Figure A33 and the restriction enzyme digestion pattern and the agarose gel picture are shown in Table A15 and Figure A34, respectively.

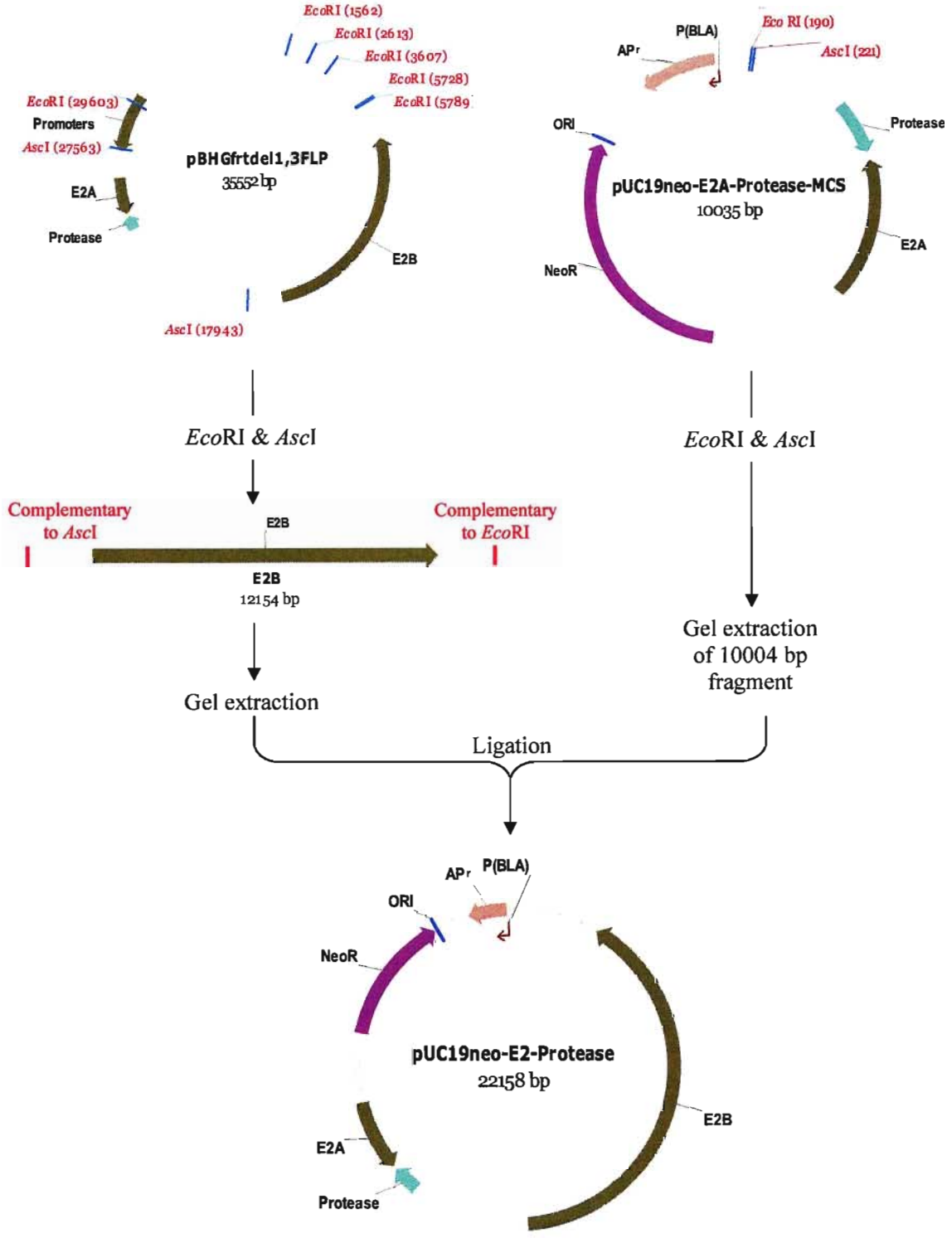

Figure A33: pUC19neo-E2-Protease construction strategy.

Table A15: Restriction enzyme analysis of pUC19neo-E2-Protease.

Restriction enzyme	*Eco*RI	*Asc*I	*Hind*III	*Sac*I	*Drd*I
Fragment size(s) (bp)	22158	22158	7140 6605 5322 2081 935 75	5520 4581 3651 2003 1977 1784 957 680 671 234 73 27	6963 4721 2035 1942 1869 1589 1581 951 506

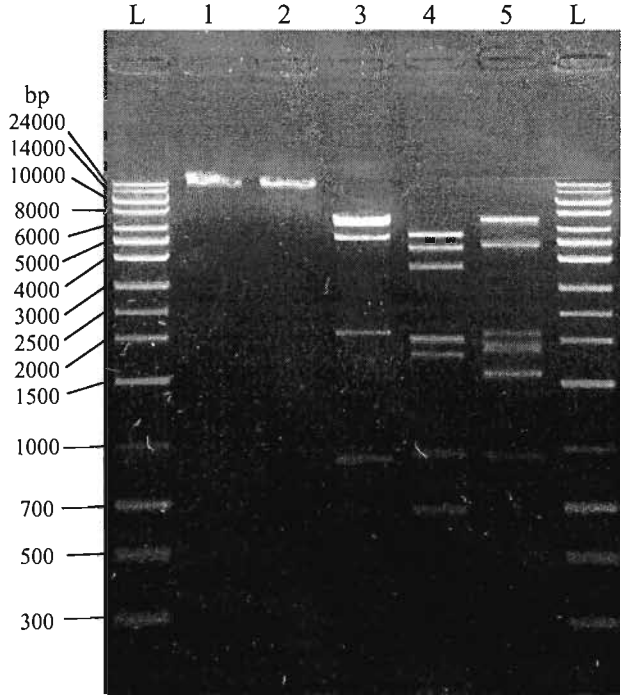

Figure A34: Restriction enzyme analysis of pUC19neo-E2-Protease. Lanes 1-5: plasmid DNA digested with *Eco*RI, *Asc*I, *Hind*III, *Sac*I and *Drd*I, respectively. Lanes L: Norgen's UltraRanger DNA ladder. The bp size of each ladder band is shown on the picture.

3.3.1.4- Construction of pUC19-MCS

The final part that is missing in the pE2 construction is the E2 promoters (early and late). Due to the relatively long size of the promoter fragment (2512 bp), we decided to use multistep cloning procedures rather than PCR to lower the probability of creating mutation within the sequence. First, pUC19 was modified by the insertion of a MCS containing restriction enzymes needed for the downstream cloning of the E2 promoter. In addition, the MCS contained more enzymes to add new restriction sites to the terminal ends of the fragment suitable for its subsequent cloning into pUC19neo-E2-protease. The MCS was synthesized through the annealing of two oligonucleotides. The resulting MCS contained complementary terminal ends, just in the overhanging nucleotides but not in the entire sequence, to *Nde*I and *Sph*I. Meanwhile, pUC19 was digested with *Nde*I and *Sph*I and the 2425 bp fragment was extracted from an agarose gel. The MCS and the pUC19 fragment were ligated to generate the pUC19-MCS plasmid. The construction strategy of this plasmid is illustrated is Figure A35, and the restriction enzyme digestion pattern and the agarose gel picture are shown in Table A16 and Figure A36, respectively.

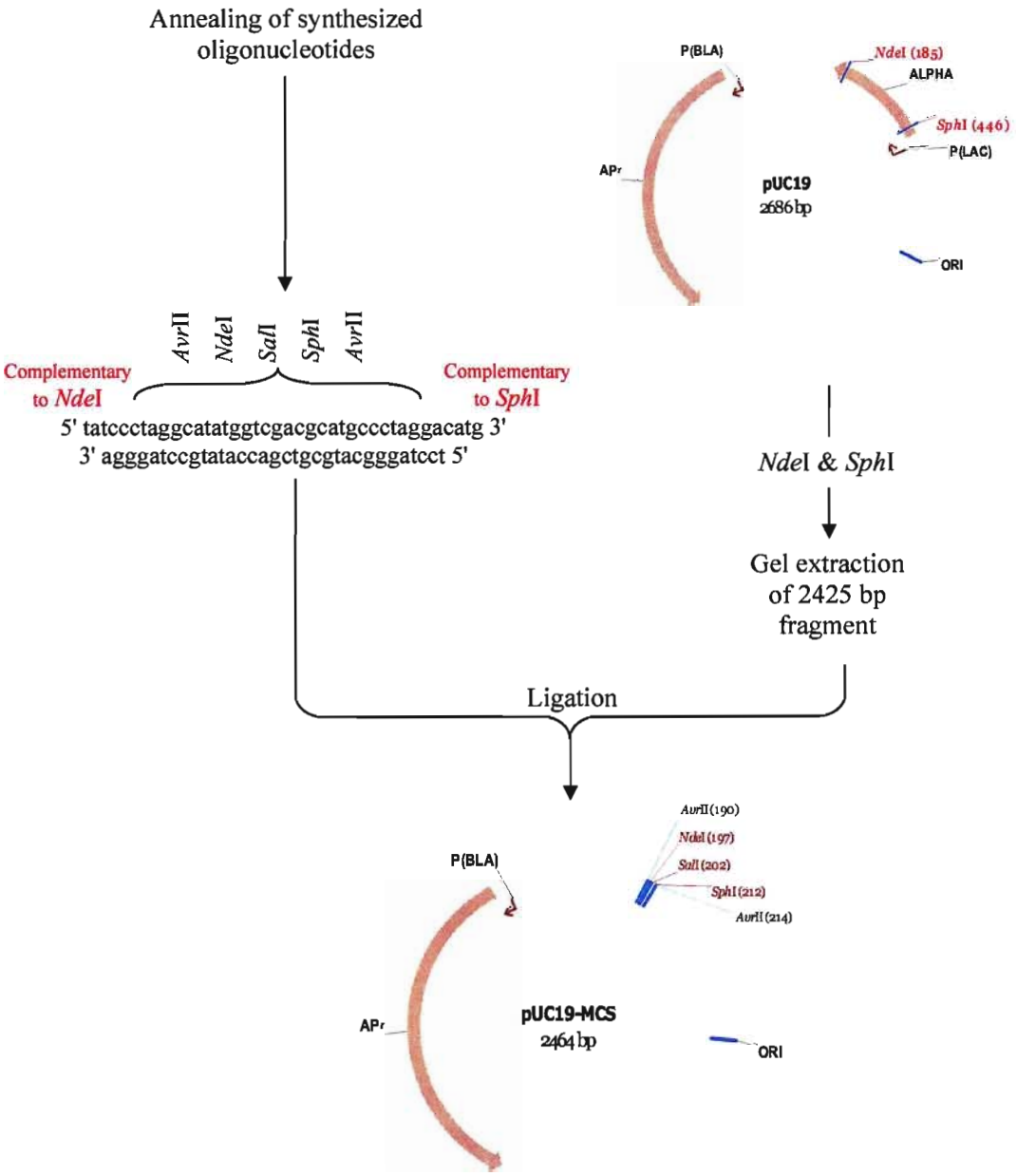

Figure A35: pUC19-MCS construction strategy.

Table A16: Restriction enzyme analysis of pUC19-MCS.

Restriction enzyme	*Sal*I	*Drd*I
Fragment size(s) (bp)	2464	1896 595

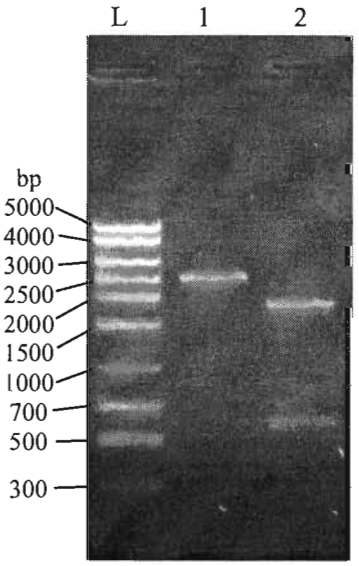

Figure A36: Restriction enzyme analysis of pUC19-MCS. Lanes 1 and 2: plasmid DNA digested with *Sal*I and *Drd*I, respectively. Lane L: Norgen's MidRanger DNA ladder. The bp size of each ladder band is shown on the left side of the picture.

3.3.1.5- Construction of pUC19-E2promoters

The adenoviral E2 genes are driven by different promoters during the early and late phases of the life cycle and both promoters were cloned in our construction. The E2 promoter fragment of 3338 bp was obtained from pBHGfrtdel1,3FLP by *Nde*I and *Sph*I digestion and extracted from an agarose gel. Since both terminal restriction enzyme sites are not suitable for cloning the fragment into pUC19neo-E2-Protease, the fragment needed new restriction enzyme sites that are suitable for the subsequent cloning to form the final plasmid pE2. For this purpose, we cloned the fragment into pUC19-MCS after its digestion with *Nde*I and *Sph*I and extraction from an agarose gel. The resulting plasmid was designated pUC19-E2promoters. The construction strategy of this plasmid is illustrated in Figure A37 and the restriction enzyme digestion pattern and the agarose gel picture are shown in Table A17 and Figure A38, respectively.

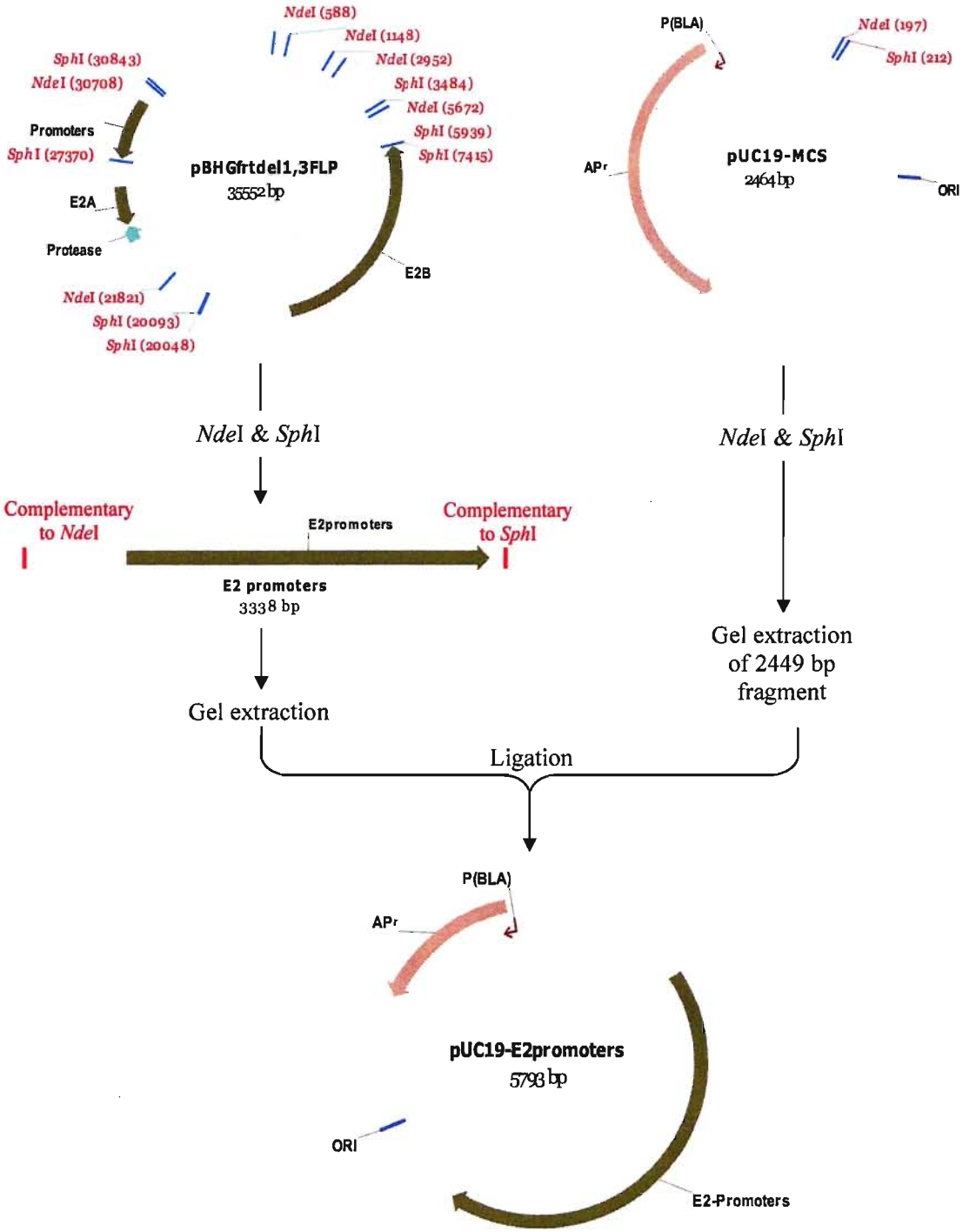

Figure A37: pUC19-E2promoters construction strategy.

Table A17: Restriction enzyme analysis of pUC19-E2promoters.

Restriction enzyme	*Nde*I	*Hind*III	*Sac*I
Fragment size(s) (bp)	5793	4541 1252	3404 1465 924

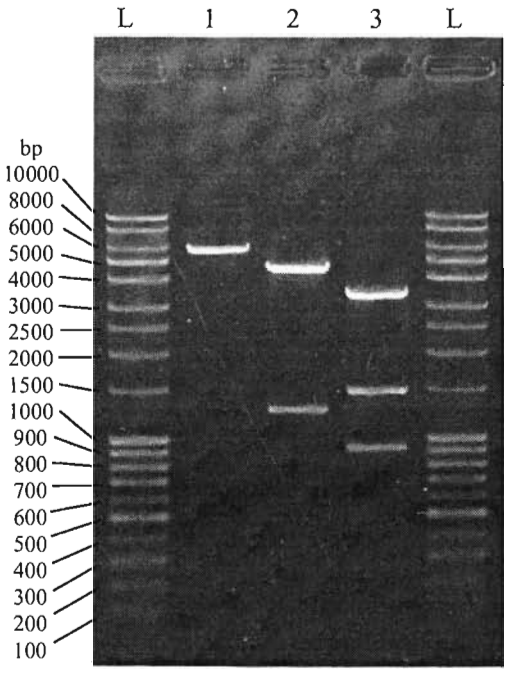

Figure A38: Restriction enzyme analysis of pUC19-E2promoters. Lanes 1-3: plasmid DNA digested with *Nde*I. *Hind*III and *Sac*I, respectively. Lanes L: Norgen's HighRanger Plus DNA ladder. The bp size of each ladder band is shown on the left side of the picture.

3.3.1.6- Construction of pE2

The cloned E2 promoters fragment in pUC19-E2promoters was digested by *Avr*II and extracted from an agarose gel. Meanwhile, pUC19neo-E2-Protease was cut open by *Xba*I and cleaned afterwards through agarose gel extraction. Since *Avr*II and *Xba*I have combatable sticky ends, it was possible to ligate both fragments. The orientation of the cloned E2 promoter fragment was then screened for through colony picking. When the proper orientation upstream from the E2A region was found, the plasmid was designated pE2. The construction strategy of this plasmid is illustrated in Figure A39 and the restriction enzyme digestion pattern and the agarose gel picture are shown in Table A18 and Figure A40, respectively.

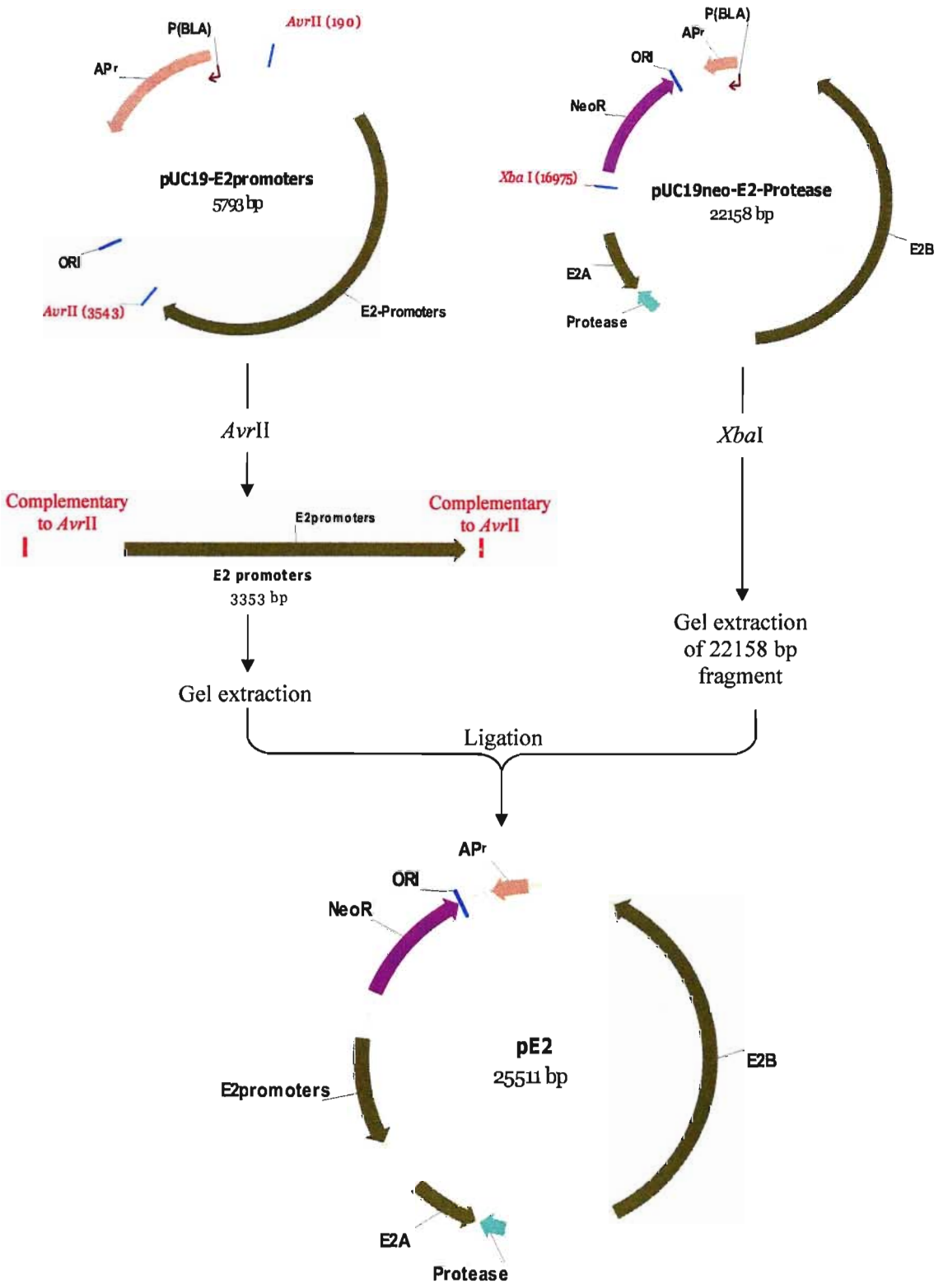

Figure A39: pE2 construction strategy.

Table A18: Restriction enzyme analysis of pE2.

Restriction enzyme	*Nde*I	*Mfe*I	*Hind*III	*Sac*I
Fragment size(s) (bp)	25511	11626 5553 4091 2626 1615	7821 7140 5322 2137 2081 935 75	6347 4581 3651 2003 1977 1784 1465 957 924 680 671 234 137 73 27

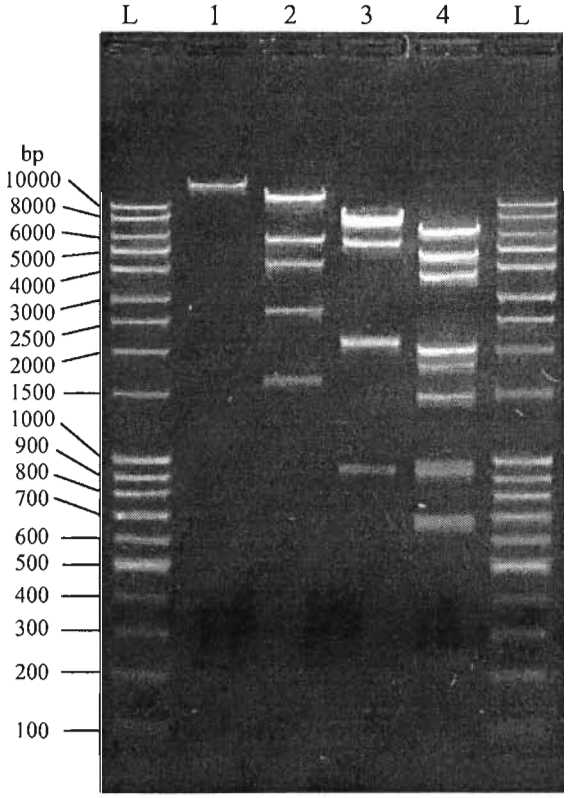

Figure A40: Restriction enzyme analysis of pE2. Lanes 1-4: plasmid DNA digested with *Nde*I, *Mfe*I, *Hind*III and *Sac*I, respectively. Lanes L: Norgen's HighRanger Plus DNA ladder. The bp size of each ladder band is shown on the left side of the picture.

E- Replication mechanism from circular adenoviral plasmids

The replication mechanism of viral DNA from circular molecules was proposed by Graham *et al.* (1989):

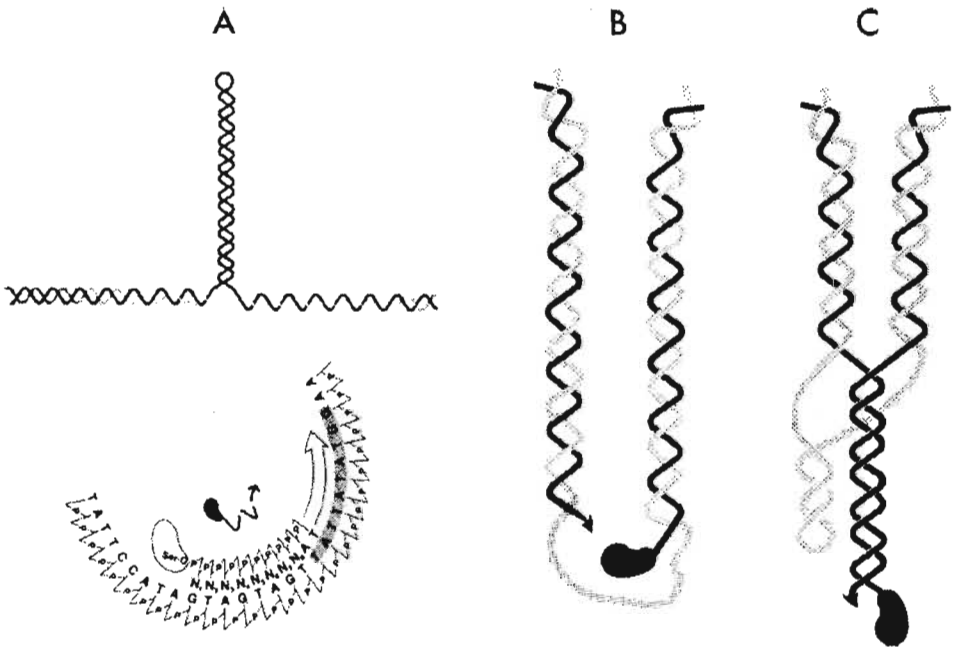

"Model for replication of viral DNA from circular molecules. (A) Initiation of replication by protein priming. DNA at the junction of viral ITRs is assumed to form a cruciform with readily denaturable regions which facilitate initiation of viral DNA replication. The sequence of the template strand shown below is that determined for a hypothetical plasmid with one intact ITR (e.g. p141 or 142) and the shaded segment identifies the conserved decamer present near the ends of all human adenovirus genomes. See text for details. (B) Completion of the first round of viral DNA replication off a circular template. Synthesis (DNA indicated in black) has initiated as in (A) proceeded all the way around the circular genome by strand displacement replication, reaching the junction region (from the left in A) and terminating near the 5' pTP-blocked end of the newly made strand. (C) Generation of a panhandle. Annealing of newly made ITR sequences, or template switching as the 3' end of the growing chain progresses down the 'right' ITR, generates a duplex terminus similar in structure to the ends of viral DNA. If the ITR sequences at the 3' end of the newly synthesized strand are incomplete they can be repaired using the 5' sequences as a template." (Graham *et al.*, 1989).